INTERMEDIATES AND ENZYMES INVOLVED IN FLUOROMETABOLITE BIOSYNTHESIS IN STREPTOMYCES CATTLEYA

Ryan McGlinchey

A Thesis Submitted for the Degree of PhD
at the
University of St Andrews

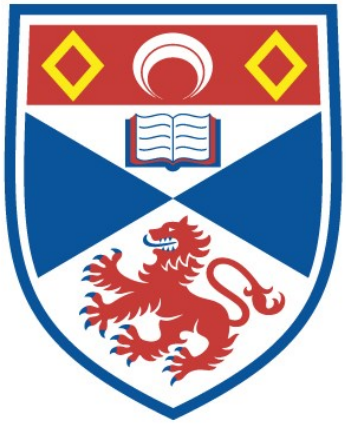

2006

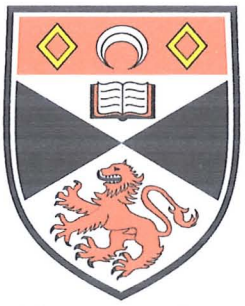

University
of
St Andrews

Intermediates and enzymes involved in fluorometabolite biosynthesis in *Streptomyces cattleya*

by
Ryan McGlinchey

A thesis presented for the degree of
Doctor of Philosophy
in the
School of Chemistry
University of St Andrews

January 2006

Declaration

I, Ryan Patrick McGlinchey, hereby certify that this thesis, which is approximately 41,000 words in length, has been written by me, that it is the record of work carried out by me and that it has not been submitted in any previous application for a higher degree.

Date.....17/3/06.....Signature of Candidate.....[redacted].....

I was admitted as a research student in October 2002 and as a candidate for the degree of Doctor of Philosophy in October 2002; the higher study for which this is a record was carried out at the University of St Andrews between October 2002 and August 2005.

Date.....17/3/06.....Signature of Candidate.....[redacted].....

I hereby certify that the candidate has fulfilled the conditions of the Resolution and Regulations appropriate for the Degree of Doctor of Philosophy in the University of St Andrews and that the candidate is qualified to submit this thesis in application for that degree.

Date..17/03/06.....Signature of Supervisor..[redacted]

Declaration

Copyright

In submission of this thesis to the University of St. Andrews I understand that I am giving permission for it to be made available for use in accordance with the regulation of the University Library for the time being in force, subject to any copyright vested in the work not being affected thereby. I understand that the title and abstract will be published and a copy of the work may be made and supplied to any *bona fide* library or research worker.

Date....17/3/06.....Signature of Candidate.....[redacted].....

This work is dedicated to my family and my close friends.

Acknowledgements

Firstly, I would like to thank my supervisor Professor David O'Hagan for all of his help, support and guidance over the last three years. I am also grateful to GlaxoSmithKline (GSK) and EPSRC for financial support. Special thanks must go to the GSK team based at the PET centre, Addenbrooks hospital, Cambridge. In particular Dr Andrew Lockhart.

I would like to next thank Dr. Hai Deng, Dr Steven L. Cobb (now at the University of Alberta, Canada) and (Dr) Mayca Onega for all their help and endless discussions relating to this work. It has been a pleasure and a thorough enjoyment working with you. On the same note, special thanks must go to the O'Hagan group, both past and present for making this an enjoyable place to work.

I am extremely grateful to the following people at the University of St. Andrews for technical support. Dr Douglas Philp, Mrs Melanja Smith and Dr Tomas Lebl for the NMR service, Dr Graham Kemp and Mr Paul Talbot for N-terminus sequencing and finally Dr Catherine Botting and Mr Alex Houston for MALDI TOF analysis. Sincere thanks also go to Dr. Jack T. G. Hamilton (University of Belfast) for GC-MS analysis. My gratitude also extends to both Andy McEwan and Gareth Williams, from Professor Jim Naismith's group, for being great house mates.

I would like to thank Dr Vicki Bamford and (Dr) Natalie Gooseman for proof reading the thesis. I would also like to say a special thank you to Miss Amy Clark for much support and help during the last three years.

Finally, and most importantly, I would like to thank my family. Without their encouragement and support I would never have gotten this far.

Contents

List of abbreviations

~	Approximately
μg	Microgram
μl	Microlitre
μM	Micromolar
Å	Ångstrom
amu	Atomic mass unit
ATP	Adenosine tri-phosphate
5'-BrDA	5'-Bromo-5'-deoxyadenosine
BSA	Bovine serum albumin
CFE	Cell free extract
CI	Chemical ionisation
5'-ClDA	5'-Chloro-5'-deoxyadenosine
5'-ClDI	5'-Chloro-5'-deoxyinosine
Cma	1-Amino-1-carboxy-2-ethylcyclopropane
CoA	Coenzyme A
conc.	Concentration
d	Doublet
ddd	Doublet of doublet of doublets
DHAP	Dihydroxyacetone phosphate
DHKMTPene	1,2-Dihydroxy-3-keto-5-methylthiopentene
DK-MTP-1-P	2,3-Diketo-5-methylthiopentyl-1-phosphate
EDTA	Ethylenediaminetetraacetic acid
ES-MS	Electrospray mass spectrometry

Abbreviations

Exp	Experiment
FAD	Flavin adenine dinucleotide (oxidised form)
$FADH_2$	Flavin adenine dinucleotide (reduced form)
5'-FDA	5'-Fluoro-5'-deoxyadenosine
5'-FDI	5'-Fluoro-5'-deoxyinosine
5-FDR	5-Fluoro-5-deoxy-D-ribose
5-FDRP	5-Fluoro-5-deoxy-D-ribose-1-phosphate
5-FDRibP	5-Fluoro-5-deoxy-D-ribulose-1-phosphate
5-FDRib	5-Fluoro-5-deoxy-D-ribulose
5-FDX	5-Fluoro-5-deoxy-D-xylose
5-FDXyu	5-Fluoro-5-deoxy-D-xylulose
5-FDXyuP	5-Fluoro-5-deoxy-D-xylulose-1-phosphate
FF	Fast flow
FPLC	Fast protein liquid chromatography
Fr-1,6-P_2	Fructose-1,6-bisphosphate
L-FruA	L-Fructose-1,6-bisphosphate aldolase
L-FucA	L-Fuculose-1-phosphate aldolase
GC-MS	Gas chromatography mass spectrometry
g	Gram
GDP	Guanosine diphosphate
GTP	Guanosine triphosphate
HIC	Hydrophobic interaction chromatography
HK-MTPenyl-1-P	2-Hydroxy-3-keto-5-methylthiopentenyl-1-phosphate
HPLC	High pressure liquid chromatography
HP	High performance

Abbreviations

hrs	Hours
Hz	Hertz
J	Coupling constant
kDa	Kilo dalton
KMTB	2-Keto-4-methylthiobutyrate
L	Litre
M	Molar
mA	Milliamp
m/z	Mass over charge ratio
MALDI	Matrix assisted laser desorption ionisation
MES	2-Morpholinoethanesulfonic acid
MeCN	Acetonitrile
mg	Milligram
min	Minutes
ml	Millilitre
mM	Millimolar
MSTFA	*N*-Methyl-*N*-(trimethylsilyl)-trifluoroacetamide
MTA	5'-Methylthio-5'-deoxyadenosine
MTAP	Methylthioadenosine phosphorylase
MTR	5-Methylthio-5-deoxy-D-ribose
MTRP	5-Methylthio-5-deoxy-D-ribose-1-phosphate
MTRibP	5-Methylthio-5-deoxy-D-ribulose-1-phosphate
NAD^+	Nicotinamide adenine dinucleotide (oxidised form)
NADH	Nicotinamide adenine dinucleotide (reduced form)
NADPH	Nicotinamide adenine dinucleotide phosphate (reduced form)

Abbreviations

NMR	Nuclear magnetic resonance
O.D.	Optical density
PET	Positron emission tomography
PLP	Pyridoxal 5'-phosphate
PNP	Purine nucleoside phosphorylase
ppm	Parts per million
Prn	Pyrrolnitrin
SDS-PAGE	Sodium dodecyl sulfate-polyacrylamide gel electrophoresis
Reb	Rebeccamycin
RCY	Radiochemical yield
rpm	Revolutions per minute
s	Singlet
SAH	*S*-Adenosyl-L-homocysteine
SAM	*S*-Adenosyl-L-methionine
sp.	Species
t	triplet
td	triplet of doublets
TOF	Time of flight
TMS	Trimethylsilyl
Tris	Tris(hydroxymethyl)aminoethane
UV	Ultra-violet
V	Volt
V_e	Elution volume
V_o	Void volume

Abstract

Enzymatic halogenation occurs during the biosynthesis of more than 4,000 natural products. The presence of fluorinated natural products is much less common, with only 13 reported to date. The bacterium *Streptomyces cattleya* is known to biosynthesise two fluorinated secondary metabolites, fluoroacetate and 4-fluorothreonine. The precursor to these secondary metabolites is known to be fluoroacetaldehyde. It had previously been shown that a fluorination enzyme mediates a reaction between *S*-adenosyl-L-methionine (SAM) and F^- to generate 5'-fluoro-5'-deoxyadenosine (5'-FDA). This is the first committed step on the biosynthetic pathway. The pathway between 5'-FDA and fluoroacetaldehyde had not been investigated in detail prior to the work carried out in this thesis.

A purine nucleoside phosphorylase has been partially purified from cell-free extracts which catalyses the phosphorolytic cleavage of 5'-FDA to 5-fluoro-5-deoxy-D-ribose-1-phosphate (5-FDRP). Substrate specificity shows a profile which shares a close similarity to bacterial 5'-methylthioadenosine phosphorylases (MTAP's). The identification of a gene cluster encoding enzymes responsible for fluorometabolite biosynthesis shows the PNP gene located adjacent to the fluorinase gene, reinforcing the involvement of this enzyme in the fluorometabolite pathway.

It is shown that 5-FDRP is converted to 5-fluoro-5-deoxy-D-ribulose-1-phosphate (5-FDRibP) *via* an isomerase activity. The enzyme responsible for this transformation has been partially purified from cell free extracts (CFE's). Another metabolite was identified as 5-fluoro-5-deoxy-D-xylulose-1-phosphate (5-FDXyuP), a diastereoisomer of 5-FDRibP, which appears to be an adventitious product in CFE's of *S. cattleya*.

Two DHAP dependent aldolases have been identified, one of which is a putative L-fuculose-1-phosphate aldolase which catalyses conversion of 5-FDRibP to fluoroacetaldehyde. The other, an L-fructose 1,6-bisphosphate aldolase has been purified to homogeneity and catalyses an aldol reaction between DHAP and fluoroacetaldehyde to generate 5-FDXyuP. This enzyme is most probably one of primary metabolism.

1 Introduction

Throughout the ages plant natural products have been used in traditional medicine.[1] Today, with marine organisms and other living creatures as additional sources of active compounds, the biosynthesis of natural products represents a major avenue to drug discovery and development. Indeed, a large portion of today's major drugs have their origins in nature. Over 25 % of all drugs have originated from natural products, and more than 80 % of the world's total population rely on natural extracts for primary healthcare.[2] It is therefore, not surprising that one of the most flourishing and rewarding frontiers in modern science is the study of the chemistry and biology of natural products.

Natural products arise from routes other than normal metabolic pathways, mostly after a phase of active growth and under conditions of nutrient deficiency. Although plants are the best known source of secondary metabolites, bacteria, fungi and marine organisms are also sources of natural product synthesis. Most low molecular weight natural products fall into the categories; alkaloids, terpenoids, polyketides, glycosides and phenolic compounds. Large natural product molecules include the ribosomal and non-ribosomal peptides.[3] The study of these natural products has played a major part in the development of organic and medicinal chemistry and has provided an understanding of the ecological role that these compounds have. Examples of biologically active natural products which have had significant medicinal applications include taxol **1**,[4] camptothecin **2**,[5] artemisinin **3**[6] and shikonin **4**.[7] These are among the most powerful anticancer and antimalaria compounds to date (Figure 1.1).

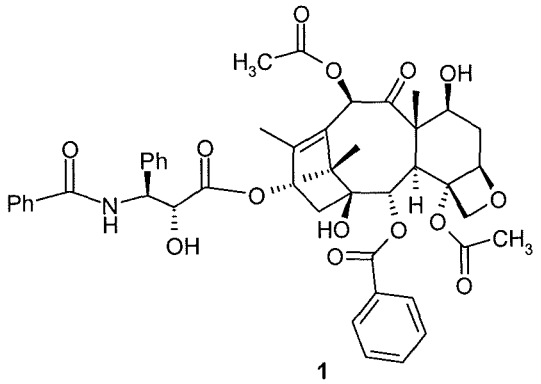

1

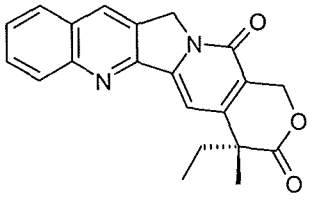

2

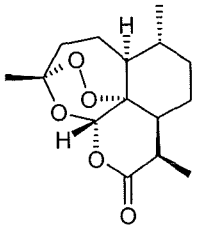

3

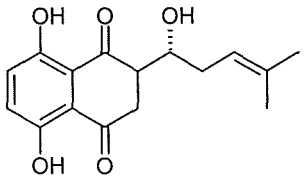

4

Figure 1.1 Selected natural products; taxol **1**, camptothecin **2**, artemisinin **3**, shikonin **4**,

A potent subset of natural products are the organo-halogen compounds which are diverse and have attracted interest both from manufacturers and researchers. By way of introduction, the occurrence and biosynthesis of the halogenated natural products are reviewed.

1.1 Biological halogenation of natural products

Enzymatic incorporation of chlorine, bromine or iodine atoms occurs during the biosynthesis of more than 4,000 natural products (Gribble *et al.* 2004).[8] These have been isolated from a variety of organisms such as bacteria, fungi, marine algae, litchens, higher plants, mammals and insects. Brominated metabolites are the most prevalent in the marine environment, whereas chlorine-containing metabolites are more predominant in terrestrial organisms. The presence of fluorinated and iodinated natural products is much less common. The presence of halogen atoms in organic compounds has been shown to be important for biological activity. For example, it is shown that the de-chloro derivative of

the anti-tumour compound rebeccamycin **24** (see page 10) showed no antimicrobial activity towards different micro-organisms tested, in contrast to the chlorinated compound **24**.[9] Figure 1.2 shows several examples of naturally occurring halogenated products. The structural diversity is considerable, ranging from poly-chlorinated products such as nordysidenin **5**[10,11] to the highly toxic compound fluoroacetate **8**.[12]

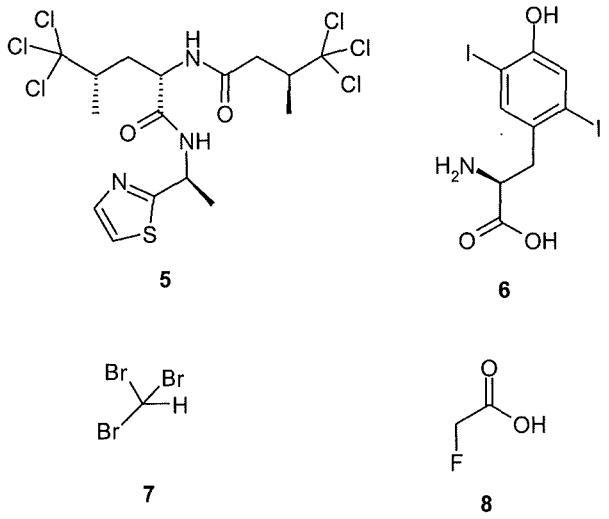

5 **6** **7** **8**

Figure 1.2 Examples of halogenated natural products; nordysidenin **5**, diiodotyrosine **6** (*G. cavolinii*),[8] bromoform **7** (marine algae) and fluoroacetate **8** (*S. cattleya*).

Although a large number of halogenated natural products have been isolated, it is only very recently that details have emerged on the mechanism by which the halogens, F^-, Cl^-, Br^- and I^- are incorporated into organic compounds. For the past 35 years haloperoxidases were thought to catalyse all halogenation reactions. There is some evidence supporting the involvement of haloperoxidases in the production of some organohalogens, such as bromoform **7** biosynthesis in the algae *Penicillus capitatus*. The biosynthetic pathway appears to involve a bromoperoxidase.[13] However, elucidation of the reaction mechanism shows that these enzymes lack substrate specificity and regioselectivity.[14,15] A re-

evaluation of enzymatic halogenation has occured in recent years with the discovery of different types of halogenating enzymes.

1.1.1 Haloperoxidases

Haloperoxidases are a group of enzymes that are able to catalyse the halogenation of organic compounds in the presence of halide ions and peroxides such as H_2O_2. The first halogenating enzyme was discovered while investigating the biosynthesis of the chlorinated metabolite caldariomycin **9** from *Caldariomyces fumago*.[16] It was observed that the enzyme required a chloride ion and hydrogen peroxide and was thus named a 'chloroperoxidase'.[17] In order to assay this enzyme, a spectrophotometric method was adopted which employed the synthetic substrate, monochlorodimedone **10**, which is structurally similar to 2-chloro-1,3-cyclopentanedione **11,** a late intermediate in caldariomycin **9** biosynthesis (Figure 1.3).

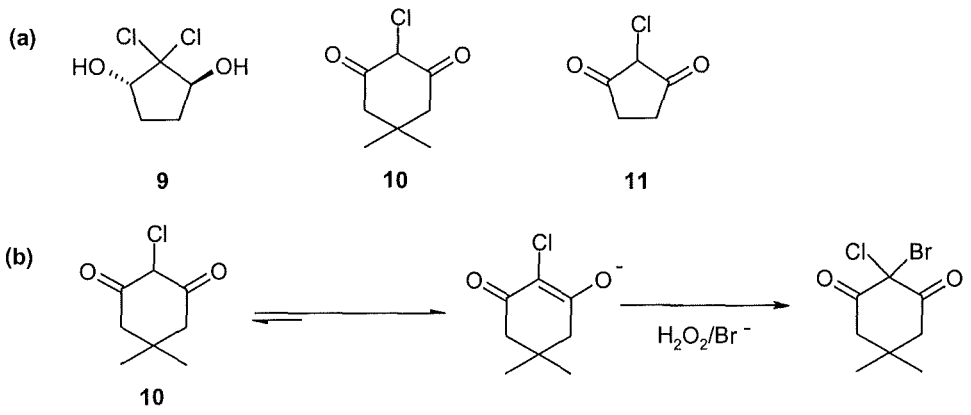

Figure 1.3 **(a)** Chlorinated compounds; caldariomycin **9**, monochlorodimedone **10** and 2-chloro-1,3-cyclopentanedione **11**. **(b)**, Dimedone assay for the haloperoxidase reaction.

The assay has been used to identify haloperoxidases from a wide range of prokaryotes and eukaryotes,[18] which have been further classified according to the halide source.

Chloroperoxidases can use chloride, bromide and iodide whereas bromoperoxidases use only bromide and iodide; and iodoperoxidases only iodide. Haloperoxidases are unable to utilise fluoride as a halide source.[17] These enzymes can be further characterised into three distinct classes, based on their catalytic mechanism, those which contain a haem group, those which contain vanadium and those which do not contain metal ions, namely perhydrolases.

Haem and vanadium containing haloperoxidases

The chloroperoxidase from *Caldariomyces fumago* was shown to contain a haem group. During the catalytic cycle hypohalous acid (HOCl) is generated as the halogenating agent in the presence of H_2O_2 and halide ions. A different type of haloperoxidase was isolated from a marine algae and was found to require vanadium instead of iron for its halogenating activity.[19] The reaction also produces hypohalous acid as the halogenating agent (Scheme 1.1). Vanadium-dependent chloro- and bromo-peroxidases have subsequently been isolated from lichen, algae and fungi.[20]

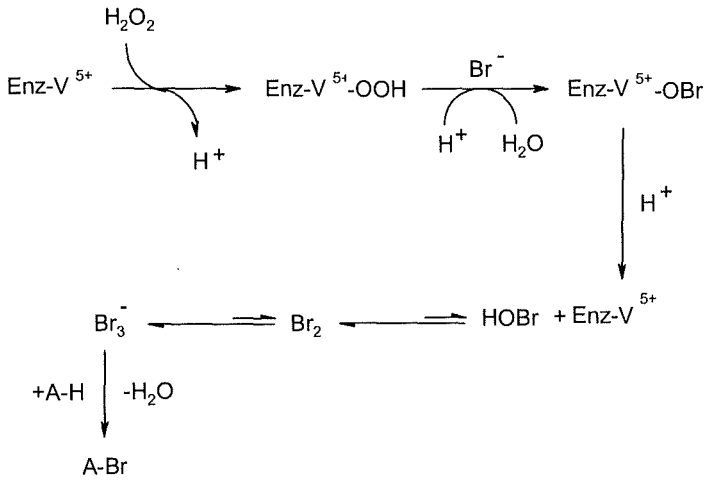

Scheme 1.1 Enzymatic mechanism of vanadium containing haloperoxidases.

Perhydrolases

Further types of halogenating enzymes are those that contain neither a haem group nor any metal ion. Although they require hydrogen peroxide for their halogenating activity, they are not peroxidases. These have been isolated from *Streptomyces lividans* and *Pseudomonas fluorescens*.[21] The protein structure shows a catalytic triad consisting of a serine, an aspartate and a histidine residue, indicating that they belong to the α/β hydrolase family. The reaction mechanism proceeds whereby an acyl-enzyme intermediate is formed from the reaction of a short-chained carboxylic acid with the serine residue at the active site.[22] The addition of H_2O_2 causes the perhydrolysis of the acyl-enzyme intermediate which results in the formation of peracids. These peracids oxidise halide ions to hypohalous acids which then act as the halogenating agent (Scheme 1.2).[23]

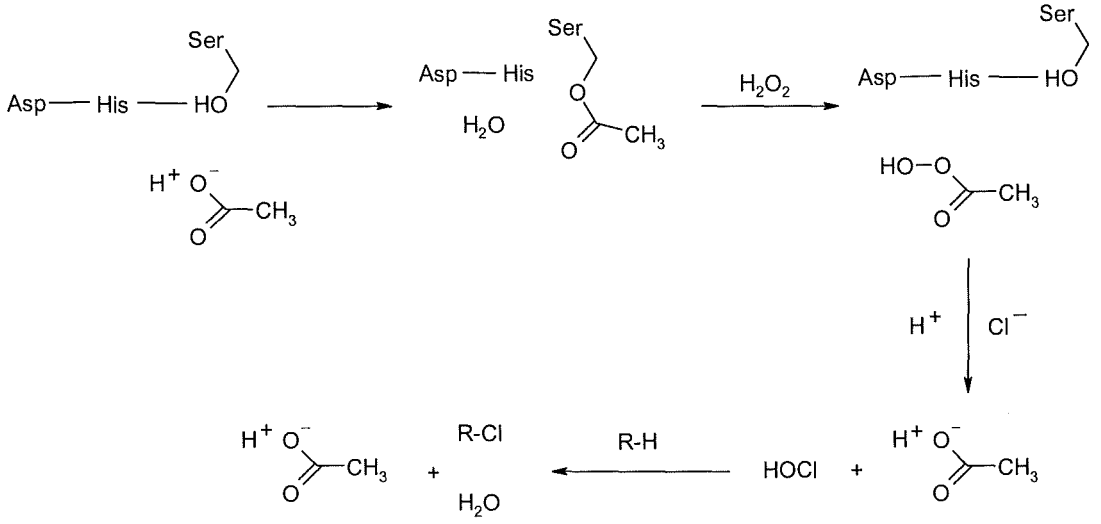

Scheme 1.2 Enzymatic mechanism of a perhydrolase.[23]

Overall, the lack of substrate specificity and regioselectivity of these enzymes makes it unlikely that haloperoxidases and perhydrolases are involved in more regulated biosynthetic pathways for halometabolite formation.

1.1.2 $FADH_2$-dependent halogenases

Examination of the gene cluster involved in 7-chlorotetracycline **13** biosynthesis identified a gene coding for a halogenation enzyme.[24] The deduced amino acid sequence showed no similarity to haloperoxidases or perhydrolases, suggesting a different type of halogenating enzyme. Studies on the biosynthesis of the anti-fungal compound pyrrolnitrin **19** (page 8) from *Pseudomonas fluorescens* have shown two related genes coding for two halogenase enzymes.[25] These two halogenating enzymes were shown to be flavin-dependent with one of them having a sequence similarity to the halogenation enzyme involved in 7-chlorotetracycline **13** biosynthesis. Members of this family have since been identified in vancomycin **12**,[26] calicheamicin,[27] balhimycin,[28] as well as pyoluteorin **14**[29] biosynthesis. Figure 1.4 shows several of these halogenated natural products in which regiospecific halogenation is most probably carried out by flavin dependent halogenases.

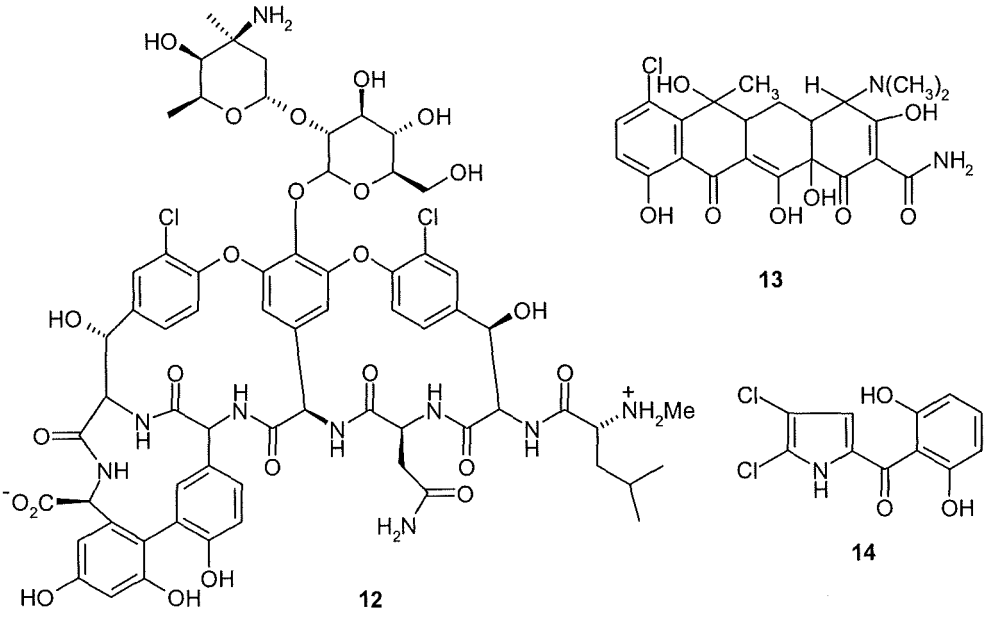

Figure 1.4 Examples of halogenated natural products involving $FADH_2$-dependent halogenases.

During the elucidation of pyrrolnitrin **19** biosynthesis, it was shown that there are two halogenating enzymes present which require $FADH_2$ for catalytic activity.[30] Both of these enzymes were shown to exhibit low sequence homology to flavin dependent monooxygenase enzymes.[31] The first of these, a tryptophan-7-halogenase (PrnA) was shown to be responsible for the regioselective chlorination of tryptophan **15** to generate 7-chlorotryptophan **16**. The second halogenase (PrnC) catalyses the regioselective chlorination of monodechloroaminopyrrolnitrin **17** in the 3-position of the pyrrole ring, generating aminopyrrolnitrin **18** (Scheme 1.3).

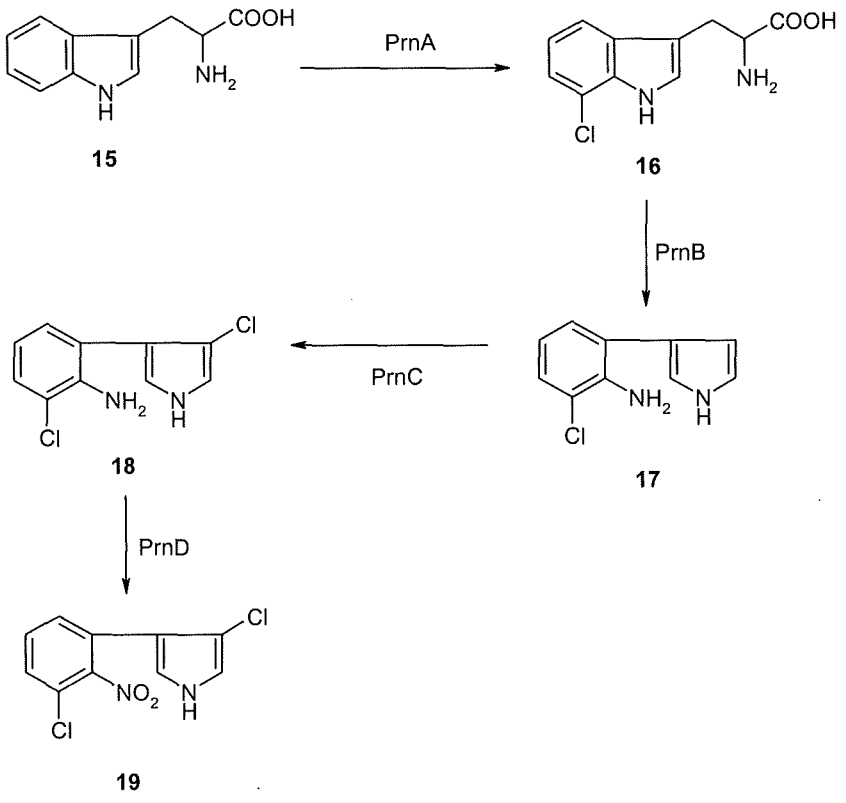

Scheme 1.3 Biosynthetic steps to pyrrolnitrin **19** in *Pseudomonas fluorescens*.

Recently, J. Naismith and co-workers[32] at St Andrews University reported the crystal structure of tryptophan 7-halogenase (PrnA) along with further biochemical studies which suggested a mechanism for regioselective chlorination. It was shown from crystallographic data that the Cl^- ion binding site is over 10 Å from 7-chlorotryptophan **16**. Furthermore,

there was no indication of large conformational changes which could bring tryptophan and flavin together. It is proposed that the Cl^- is positioned to make a nucleophilic attack on the flavin peroxide **21**. This results in the formation of FAD-OH **22** and HOCl (Scheme 1.4).

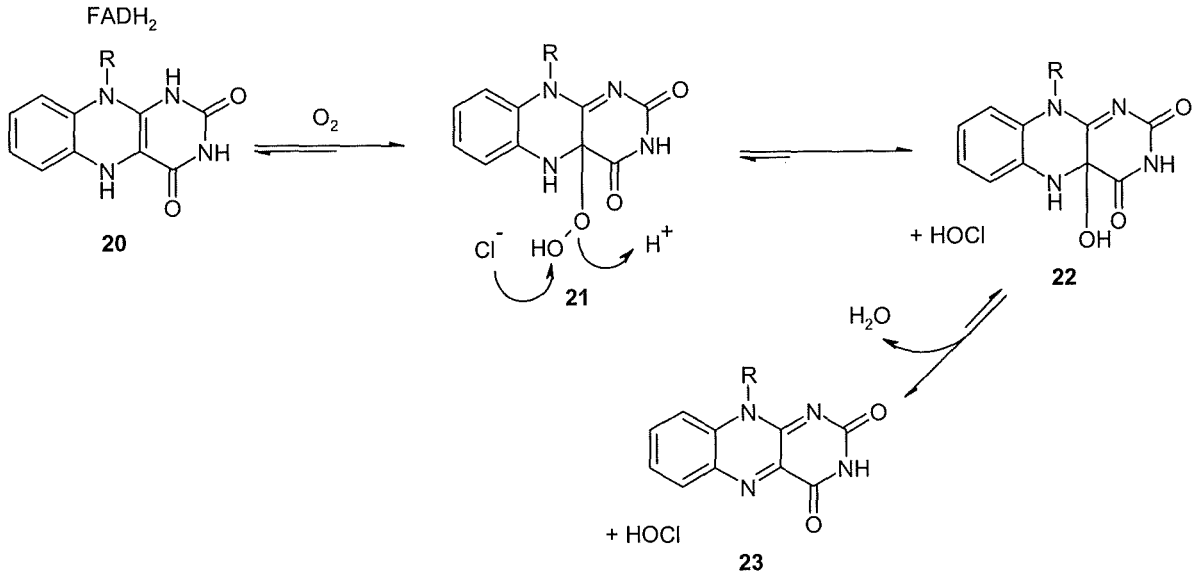

Scheme 1.4 Predicted mechanism for the generation of HOCl.[32]

The generated hypohalous acid (HOCl) is positioned in the active site where it travels along a 10 Å tunnel towards tryptophan **15** to undergo an electrophilic aromatic substitution in a controlled regioselective manner (Scheme 1.5).

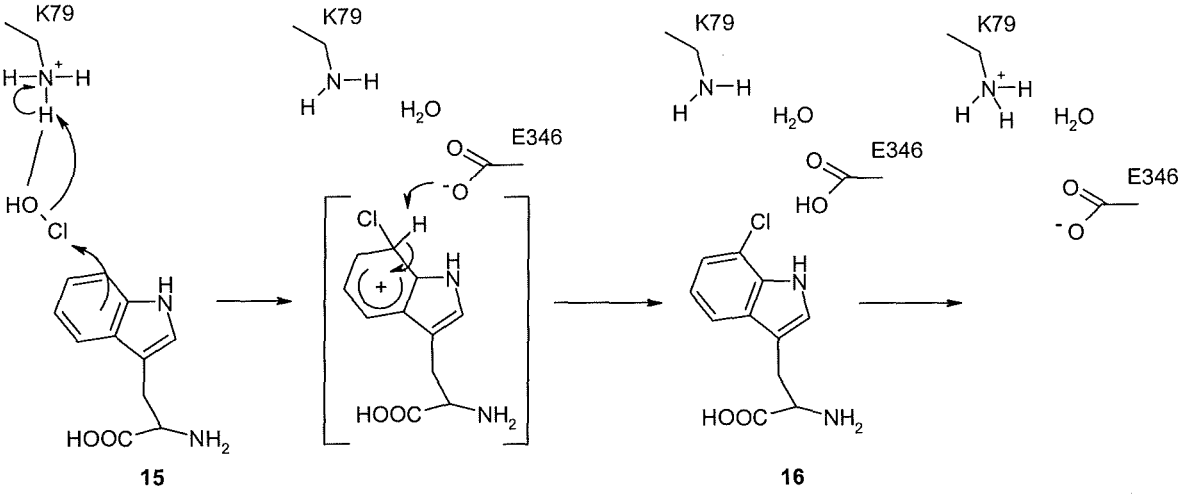

Scheme 1.5 Proposed mechanism of halogenation of tryptophan **15** at the 7 position.[32]

It is conceivable that the hypohalous acid mechanism applies to all flavin-dependent halogenases. For example in rebeccamycin **24** biosynthesis the halogenation reactions occur early in rebeccamycin **24** biosynthesis involving two genes (*reb*F) and (*reb*H), which encode a NADPH dependent flavin reductase and an $FADH_2$–dependent halogenase respectively[33] (Scheme 1.6). This halogenation is of biological significance.[34]

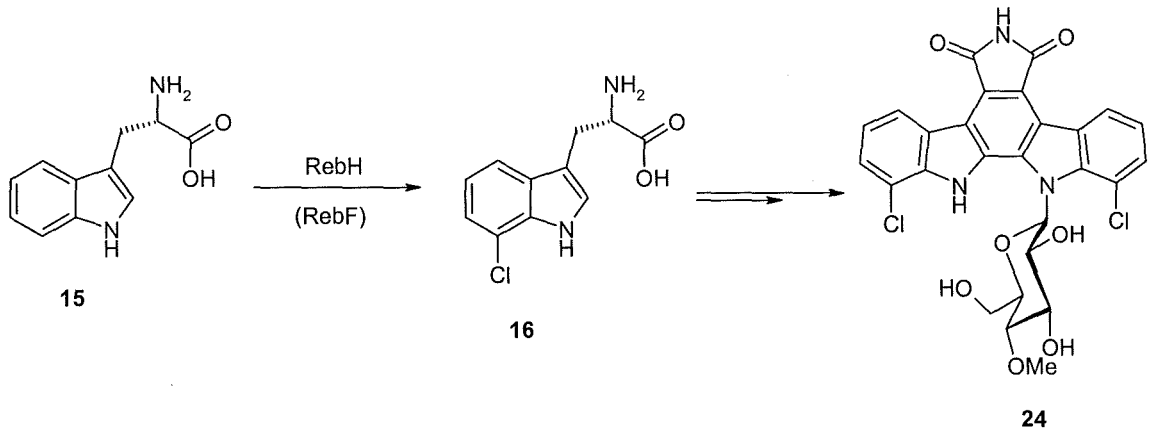

Scheme 1.6 Chlorination of tryptophan **15** as the initial step in rebeccamycin **24** biosynthesis.

The protein rebH was shown to share a 55 % identity with the protein prnA involved in pyrrolnitrin **19** biosynthesis. It appears that RebF/RebH catalyses the regioselective chlorination of tryptophan **15** to 7-chlorotryptophan **16** in a similar manner to that shown in Scheme 1.4 and 1.5.

Overall, $FADH_2$-dependent halogenases appear to be responsible for the halogenation of aromatic substrates in secondary metabolite biosynthesis. However, for chlorinated natural products such as barbamide **25**[35] and syringomycin E **26**,[36] a separate mechanism exists for the chlorination of the un-activated aliphatic carbon centres (Figure 1.5). This is discussed in the next section.

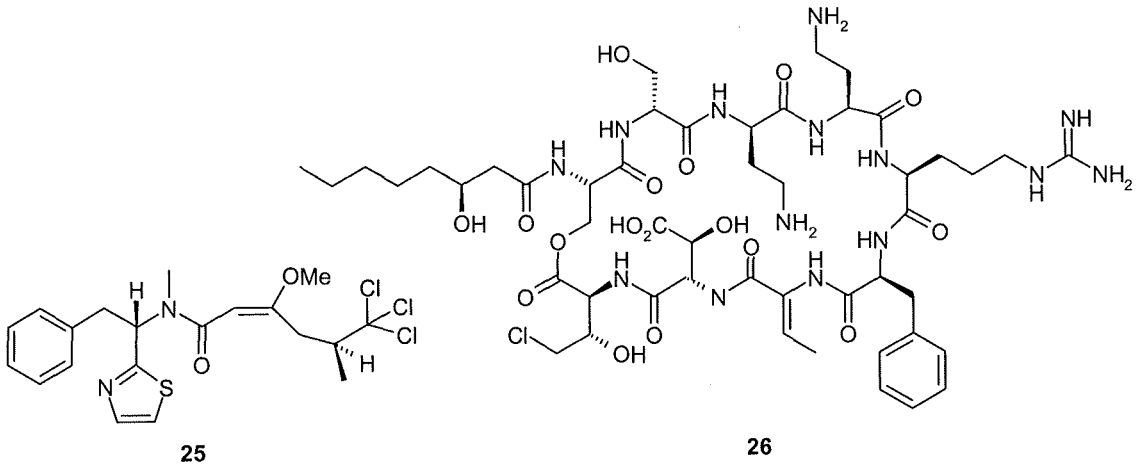

25 26

Figure 1.5 Chlorinated natural products barbamide **25** and syringomycin E **26**.

1.1.3 Chlorination by a non-haem α-ketoglutamate dependent enzyme[37]

There is a chlorination step during the biosynthesis of the natural product coronatine **30**, a leaf toxin synthesised by the phytopathogenic bacterium *Pseudomonas syringae.* Walsh and co-workers[37] have recently identified a halogenase, CmaB in which chlorination occurs at the unactivated methyl group during the biosynthesis of this natural product (Scheme 1.7).

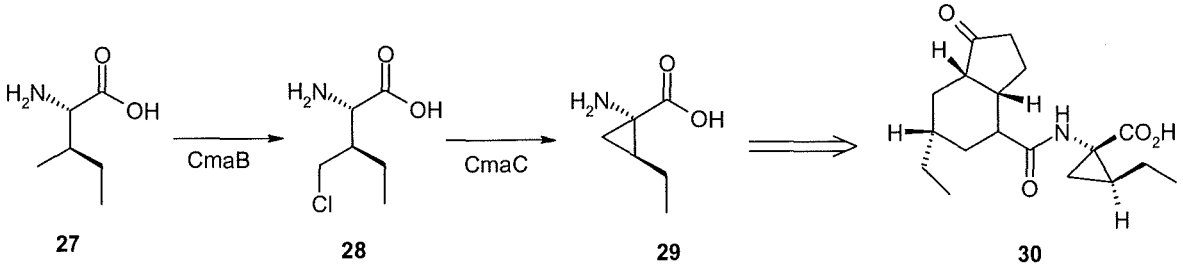

27 28 29 30

Scheme 1.7 The biosynthesis of coronatine **30**, a leaf toxin. Coronatine **30** does not have a chlorine atom but it is chlorinated during the biotransformation of L-*allo*-isoleucine **27**.

The halogenase, CmaB is shown to catalyse the chlorination of the γ-position of L-allo-isoleucine **27** followed by a second enzyme (CmaC) which then catalyses the formation of

a cyclopropyl ring in **29** from **28**. Together, both enzymes execute γ-halogenation followed by intramolecular γ-elimination. The generated cyclopropyl ring in **29** then undergoes several further reactions before the generation of coronatine **30**.

The enzyme, CmaB is shown to have sequence similarity to α-ketoglutarate (α-KG) dependent enzymes that contain non haem iron and use one Asp/Glu and two His side chains as ligands to oxygen-labile Fe^{2+}.[38,39] These enzymes typically perform oxygenation reactions, however CmaB performs chlorination rather than oxygenation at the unactivated γ position of the amino acid substrate **27**. Analogous genes have since been identified, involved in the biosynthesis of barbamide **25** and syringomycin **26** (Figure 1.5).[35,36]

A mechanism has recently been proposed by Walsh and co-workers in which CmaB mediates a radical pathway involving the prototypic high-valent oxo-iron[40,41] (Fe^{IV} = O) (Scheme 1.8).

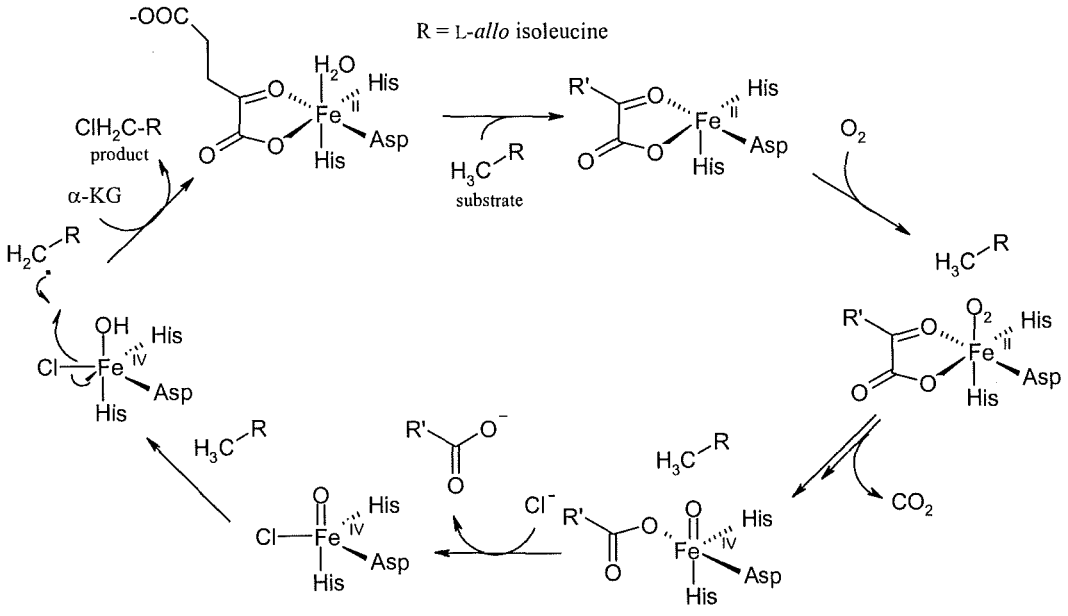

Scheme 1.8 Proposed mechanism of halogenation catalysed by CmaB.[37]

It appears that nature uses both $FADH_2$-dependent (Section 1.1.2) and non haem Fe^{2+} dependent enzymes to mediate halogenation reactions. For electron rich aromatic

substrates, $FADH_2$-dependent halogenases are used, which generate HOCl to undergo an electrophilic aromatic substitution in a controlled regioselective manner. For unactivated carbon centres halogenation is carried out by a radical mechanism using highly reactive iron-oxo species (Scheme 1.8).

1.2 Biological fluorination

Fluorine is the most abundant halogen in the Earth's crust with fluoride ion concentrations ranging from 270-740 ppm, compared to that of chlorine of 10-180 ppm.[42] Although ranked the 13th most abundant of all the elements,[43] only 13 fluorinated secondary metabolites have been identified to date. These have been found in both tropical plants and microorganisms. The absence of fluorinated natural products can be attributed to fluoride residing in an insoluble form and therefore being biologically unavailable.[43] Fluoride exists predominantly as insoluble minerals (e.g fluorospar) and consequently fluoride levels in sea water are low at 1.3 ppm.[42] This can be compared to chloride which is present at 19,000 ppm. Other reasons for the paucity of fluorinated natural products reside in the unique properties of fluorine (Table 1.1).[44-45] Fluorine is the smallest of all of the halogens with an atomic radius only slightly larger than hydrogen. Probably the most important factor restricting participation of fluoride in biochemical processes is the large heat of hydration of the fluoride ion.[43] In the aqueous environment, fluoride is heavily solvated precluding it as a potent nucleophile for biochemical processes. The high heat of hydration is largely responsible for the substantial differences in redox potential between fluoride and other halogen ions and this excludes any type of haloperoxidase mechanism.[43]

Halogen, X^-	Heat of hydration, X^- [KJ mol^{-1}]	Standard redox potential (E^0)
F^-	490	-3.06
Cl^-	351	-1.36
Br^-	326	-1.07
I^-	285	-0.54

Table 1.1 Heat of hydration and standard redox potential for the halogens.[44-45]

1.2.1 Fluorinated natural products from plants

1.2.1.1 Fluoroacetate

Fluoroacetate **8** was first isolated in 1943 by Marais[46,47] from the South African plant *Dichapetalum cymosum*.

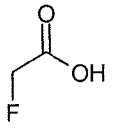

8

The inhabitants of the South African province 'Transvaal' had long recognised this plant as a hazard to livestock and had consequently named it 'gifblaar' (poison leaf). The young leaves of the *Dichapetalum* genus were reported to contain on average up to 2500 mg kg^{-1} dry wt of fluoroacetate **8**, with those from *Dichapetalum braunii* containing a staggering 8000 mg kg^{-1} dry wt. After the original discovery, many other species of the *Dichapetalum* genus have been shown to contain high levels of fluoroacetate **8** in their leaves, such as *D. heudelotti*,[48] *D. stuhlmannii*[49] and *D. toxicarium*.[50] In Australia more than forty plant species from the *Leguminosae* genus have been shown to contain traces of fluoroacetate **8**.

1.2.1.2 Fluorocitrate

The high toxicity of fluoroacetate **8** is attributed to its *in vivo* conversion to (2*R*, 3*R*)-fluorocitrate **31**.

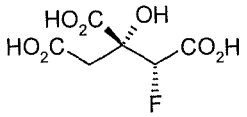

31

This transformation has be termed the 'lethal synthesis' (Peters *et al*).[51] Many plants which accumulate low levels of fluoroacetate **8** have also been shown to contain trace levels of fluorocitrate **31**.[52,53] Fluorocitrate **31** is biosynthesised after *in vivo* activation of fluoroacetate **8** to fluoroacetyl-CoA **32**.[53] This then combines with oxaloacetate **33** catalysed by the citric acid cycle enzyme, citrate synthase.[53] It emerges that the enzymatic reaction is highly stereospecific and generates the only toxic stereoisomer, (2*R*, 3*R*)-fluorocitrate **31**.[53] The metabolic product **35** is a competitive inhibitor of aconitase, the enzyme after citrate synthase on the citric acid cycle (Scheme 1.9).

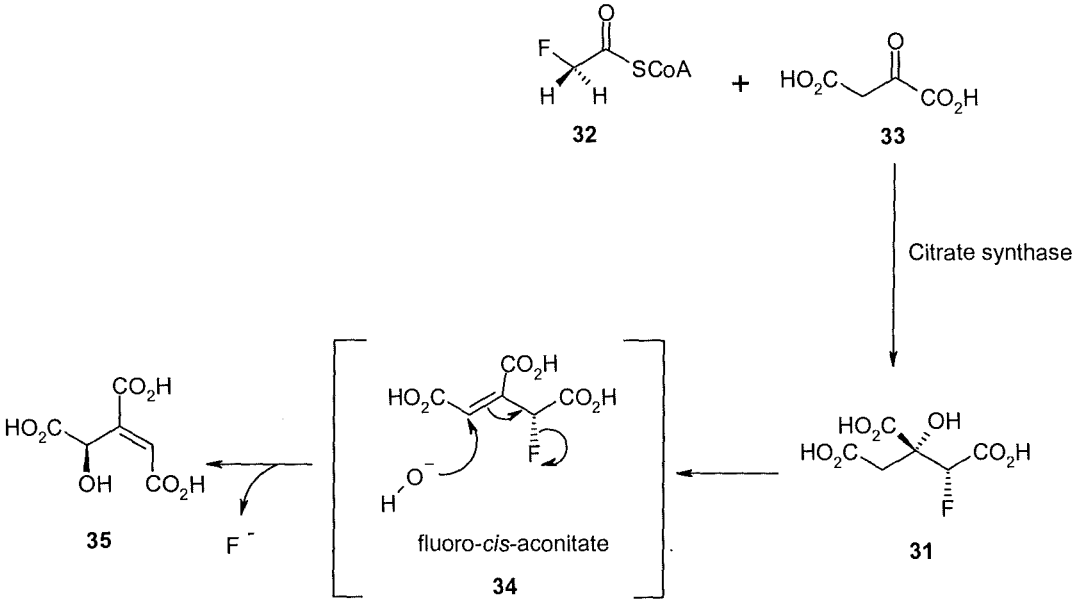

Scheme 1.9 The metabolic fate of fluoroacetyl-CoA **32** with oxaloacetate **33**.

The mechanism for aconitase inhibition involves a dehydration to give fluoro-cis-aconitate **34**, followed by an S_N2' addition of hydroxide with loss of fluoride ion to form 4-hydroxy-trans-aconitate **35**.[54] This product is a potent competitive inhibitor of the enzyme. [54] Additionally, it has been suggested that fluorocitrate **31** covalently binds to proteins involved in citrate transport across the mitochondrial membrane.[55] The toxicity attributed to this latter process has been estimated to be 10^4 times more significant than aconitase inhibition alone.[55]

1.2.1.3 Fluoroacetone

Fluoroacetone **36** was first identified by Peters and Shorthouse[56,57] after a series of experiments in the late 1960's exploring fluoride metabolism in the Australian plant *Acacia georginae.*

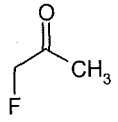

36

These experiments showed up to a 34 % loss of the total fluoride ion (1 mM) originally present.[56,57] This was attributed to the biosynthesis of volatile organofluorine compounds.[57] Derivatisation with 2,4-dinitrophenylhydrazine gave a product which had an identical retention time on paper chromatography to that of fluoroacetone **36**.[57] However, as pointed out in the report, the derivatisation method could not distinguish between fluoroacetone **36** and fluoroacetaldehyde **48**.[57] Based on the subsequently identified role of fluoroacetaldehyde **48** in fluorometabolite biosynthesis in *S. cattleya* (Section 1.4),[78] it is plausible that the hydrazone derivative was actually that of fluoroacetaldehyde **48**.

1.2.1.4 Fluorinated fatty acids

ω-Fluorooleic acid **37** was first identified and isolated by Peters and co-workers[58- 60] in 1959 from the seeds of the West African shrub *D. toxicarium.*

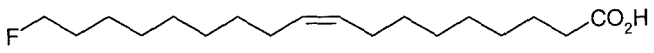

37

It was shown that ~80 % of the organic fluorine present in the seed oil was ω-fluorooleic acid **37**, with minor traces of ω-fluoropalmitic acid ($C_{16:0F}$). Re-analysis by Hamilton and coworkers[61] using GC-MS has established a further five additional fluorinated acids, ω-fluoropalmitoleic ($C_{16:1F}$), ω-fluorostearic ($C_{18:0F}$), ω-fluorolinoleic ($C_{18:2F}$), ω-fluoroarachidic ($C_{20:0F}$) and ω-fluoroeicosenoic acid ($C_{18:1F}$). *Threo*-18-Fluoro-9,10-dihydroxystearic acid has also been isolated from *D. toxicarium,* which is presumably a metabolite of ω-fluorooleic acid **37**. Scheme 1.10 shows the hypothetical pathway to these fluorinated fatty acids.

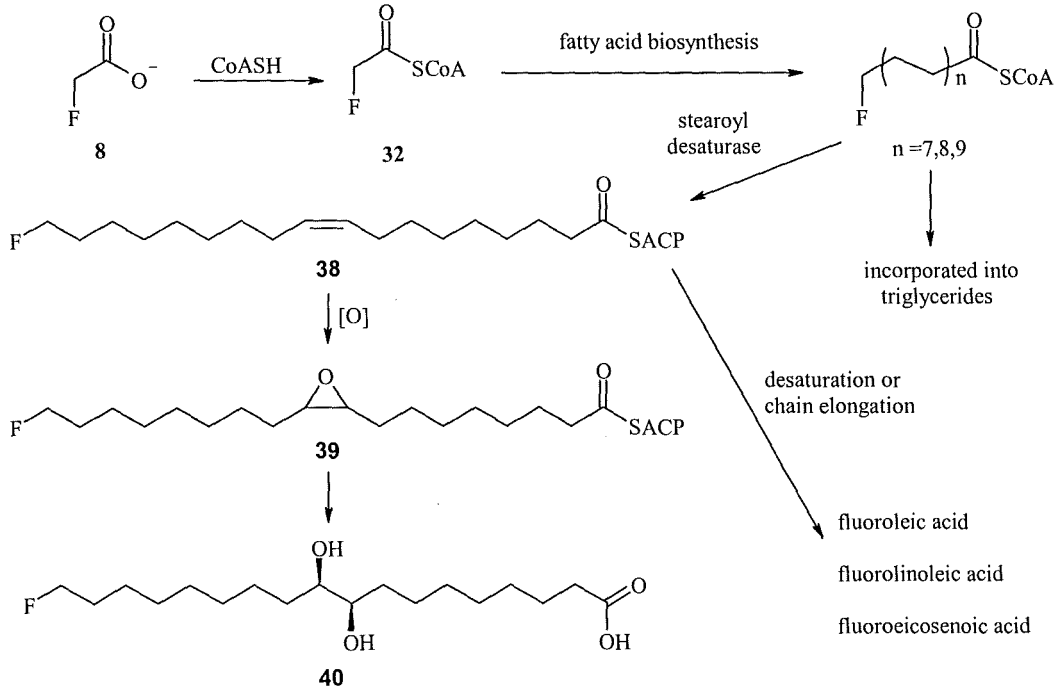

Scheme 1.10 Putative biosynthetic pathway to ω-fluorofatty acids in *D. toxicarium.*

If the plant has the ability to generate and utilise fluoroacetyl-CoA **32** then it is envisaged that the biosynthetic pathway would follow conventional fatty acid biosynthesis. It is worth noting that the fluorine atom is only ever located on the terminal carbon (ω), implying that a fluorinated analogue of a malonyl acyl carrier protein cannot be biosynthesised in this system.

1.2.2 Fluorinated natural products from marine sources

1.2.2.1 5'-Fluorouracil derivatives from the sponge *Phakellia fusca*

Chlorine and bromine containing natural products are common from marine sources.[62] Recently, the first case of fluorine containing natural products from a marine source was reported by Xu and co-workers.[63] Extracts of the marine sponge *Phakellia fusca* Schmidt, which had previously been reported to yield various alkaloids,[64,65] were shown to contain 5-fluorouracil alkaloids **41**-**45** (Figure 1.6).

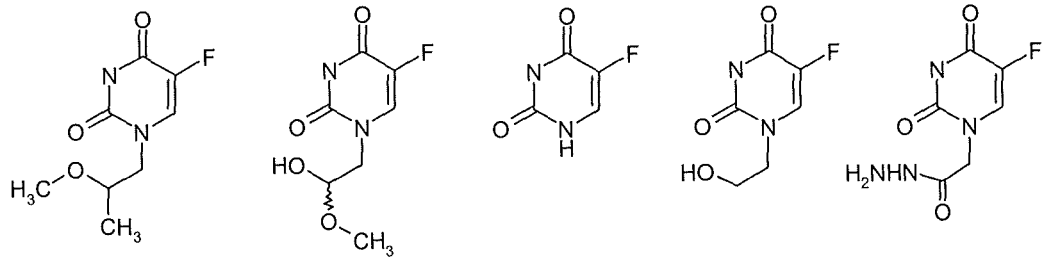

41 **42** **43** **44** **45**

Figure 1.6 Fluorinated natural products from the sponge *Phakellia fusca*.[63]

Two of these, **43**[64] and **44**[65] are known to possess anti-tumour activity.[66] The other three derivatives were shown to be novel compounds, however there is some ambiguity about

the accumulation of these compounds in the sponge, suggesting the possibility that these compounds arise as a result of industrial contamination rather than *de novo* biosynthesis.

1.2.3 Fluorinated natural products from bacteria

1.2.3.1 Nucleocidin from *Streptomyces calvus*

The fluorinated natural product nucleocidin **46** was the first organo-fluorine compound to be isolated from a bacterial source. This anti-trypanosomal antibiotic was originally isolated in 1957 from the fermentation broth of an actinomycete, *Streptomyces calvus*.[67] The isolated compound was initially identified as an adenine glycoside esterified with sulfamic acid,[68] however it was not until 1969 that a re-analysis of the structure showed the presence of a fluorine atom at the 4'-position of the ribosyl ring system.[69]

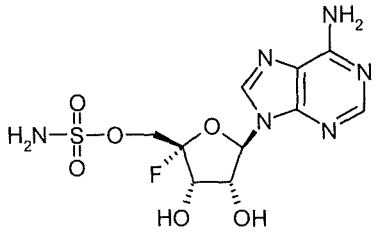

46

In 1976 the structure of nucleocidin **46** was confirmed unambiguously by total chemical synthesis.[70] The site of fluorination at the C-4-position of the ribose ring makes this fluorometabolite an attractive source for a novel C-F bond forming enzyme. Unfortunately, attempts in recent years to re-isolate nucleocidin **46** from *S. calvus* have failed, possibly due to the repeated subculturing of stock strains of *S. calvus* and loss of the biosynthetic genes from the subcultured strains.[71] It appears that we have lost the capacity to explore the biosynthesis of this natural product.

1.2.3.2 Fluoroacetate and 4-fluorothreonine from *Streptomyces cattleya*

The actinomycete *Streptomyces cattleya* is recognised for its biosynthesis of the β-lactam antibiotic thienamycin.[72] This was the first naturally occurring β-lactam antibiotic to be discovered what has a carbapenem ring system.[73] In 1986, Sanada and co-workers[12] noticed that during the optimisation of thienamycin production, extracts of *S. cattleya* biosynthesised fluoroacetate **8** and 4-fluorothreonine **47**.

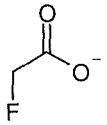

8

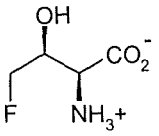

47

Further examination showed that the media containing soy-bean casein had 0.7 % inorganic fluoride present. This was reinforced with control experiments in the absence of soy bean casein which showed no fluorometabolite biosynthesis. However, addition of fluoride (2 mM) restored the biosynthetic activity, showing a controlled production of fluoroacetate **8** and 4-fluorothreonine **47**. During batch culturing of *S. cattleya*, fluorometabolite production was restricted to the stationary phase signifying fluoroacetate **8** and 4-fluorothreonine **47** are secondary metabolites. This observation raised the possibility of a convenient biological system for exploring enzymatic C-F bond formation.

1.3 Techniques used for studying the biosynthesis of natural products

A number of techniques have been used to study biosynthetic pathways, which comprise of both biochemical and biological approaches. The biochemical approach can be differentiated into two main categories. Firstly, biosynthesis of secondary metabolites can be blocked at different stages on the pathway by using various chemical reagents which

inhibit the enzymatic steps of interest. This in turn, leads to the accumulation of the desired metabolic intermediate. Additionally, chemically prepared compounds can be added to cell-free-extracts (CFE's) to study substrate specificity and co-factor requirements for a particular enzyme. Alternatively, the synthesis of potential metabolic precursors which carry an isotopic label (e.g stable isotopes ^{13}C and ^{2}H) can be administered to an organism in order to examine the isotopic incorporation of the desired metabolite, usually by NMR spectroscopy.

A second method to elucidate secondary metabolic pathways involves mutational analysis. Here, mutants unable to express a particular gene on a pathway accumulate biosynthetic intermediates. Mutations can be induced by chemical mutagenesis, UV radiation and transposon insertion. The disadvantage with this approach is the random nature of mutagenesis. In the genomic age, one can use targeted mutagenesis to overcome the randomness (provided the DNA sequence of genes directing biosynthesis is known).

1.3.1 Isotopic labelling

Isotopic labelling has proven to be a very powerful technique for exploring biochemical pathways. Pioneering work by Schoenheimer and co-workers[74] demonstrated the first use of a stable isotope (^{2}H) in fatty acid biosynthesis. The incorporation of stable isotopes can be analysed by NMR spectroscopy and mass spectrometry, techniques which provide sensitive tools with which to resolve regiochemical and stereochemical incorporation patterns. Previously, radio-isotopic techniques had been employed. This has been demonstrated e.g. by Cowie and co-workers[75] and in the extensive work of Roberts and co-workers.[76] The main stable and radio isotopes used to study biosynthetic pathways are summarised in Table 1.2.

Isotope	Relative natural abundance %	Radiation emitted	Half-life
^{2}H	0.015		stable
^{3}H	<0.001	β	12.1 years
^{13}C	1.1		stable
^{14}C	<0.001	β	5700 years
^{15}N	0.37		stable
^{18}O	0.2		stable
^{32}P	<0.001	β	14.3 days

Table 1.2 Isotopes used in biological studies

Detection of radioisotopes is traditionally performed by decay-counting, in which radiation detection instruments can detect a β particle ejected from an atomic nucleus. However, a high degree of chemical purity is required in order to avoid errors from cross-contamination. Furthermore, this approach offers limited regiochemical information. With the improved sophistication of NMR and MS methods, stable isotopes (^{2}H, ^{13}C) are much more commonly used in biosynthesis studies. For example, the incorporation of a ^{13}C label into a secondary metabolite can be detected by enhancement of the resonances in the ^{13}C NMR spectrum. In early studies on fluoroacetate **8** biosynthesis in *S. cattleya*, incorporations with ^{13}C and ^{2}H labelled glycine, glycerol, pyruvate and succinate were explored by Hamilton and co-workers.[77] These labelling studies indicated that the glycolytic intermediates play a crucial role in fluorometabolite biosynthesis in *S. cattleya*.

1.3.2 ^{19}F NMR spectroscopy

^{19}F NMR is used in this thesis as a powerful analytical tool in facilitating the assay of fluorometabolite production in *Streptomyces cattleya*. The identity of fluorinated natural products (see Section 1.2.3.2) can be analysed by ^{19}F NMR spectroscopy without the need of isolating the metabolite. The coupling of fluorine (^{19}F) with hydrogen (^{1}H) allows the chemical environment of the fluorine to be determined. This can clearly be seen in Figure 1.7, which shows the two fluorinated secondary metabolites, fluoroacetate **8** and 4-fluorothreonine **47** from *S. cattleya*.

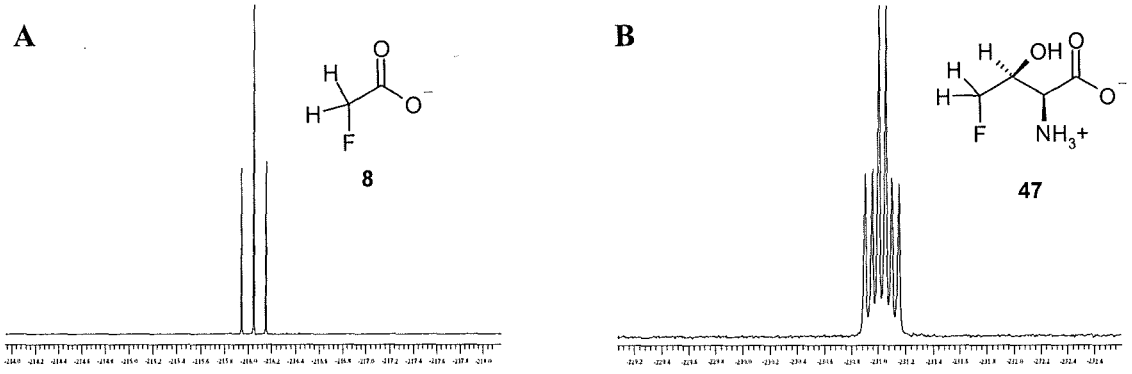

Figure 1.7 ^{19}F NMR spectra of (**A**), fluoroacetate **8** and (**B**), 4-fluorothreonine **47**.

In the case of fluoroacetate **8**, the fluorine of the fluoromethyl group is a triplet in the ^{19}F NMR spectrum. The corresponding spectrum **B** for 4-fluorothreonine **47** is a doublet of doublet of doublets arising from coupling to the β proton. The chemical shifts of fluoroacetate **8** (-216.9 ppm) and 4-fluorothreonine **47** (-231.5 ppm) are quite distinct from one another, making it possible to distinguish between these two, and other fluorinated metabolites. Furthermore, isotopic labelling of compounds can be identified by isotope induced shifts by proton decoupled ^{19}F{^{1}H} NMR analysis.

1.4 Fluoroacetaldehyde as a biosynthetic intermediate in *S. cattleya*

The discovery of 4-fluorothreonine **47** and fluoroacetate **8** production in *S. cattleya* prompted investigations into the biosynthesis of the C-F bond. Appropriate isotopic labelling studies carried out in the mid 1990's by Reid and co-workers[78] led to the conclusion that fluoroacetate **8** was not a precursor of 4-fluorothreonine **47** and *visa versa*. This prompted further investigations which showed that a two-carbon fluorinated intermediate was the precursor to the fluorometabolites **8** and **47**. Later, through additional isotopic labelling studies carried out by Moss and co-workers,[79] it emerged that fluoroacetaldehyde **48** was the precursor to both of the secondary metabolites (Scheme 1.11).

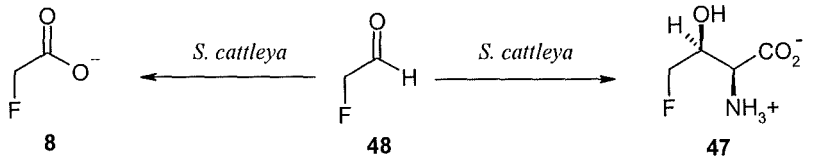

Scheme 1.11 Metabolic fate of fluoroacetaldehyde **48** in *S. cattleya*

1.4.1 Fluoroacetaldehyde dehydrogenase from *S. cattleya*

When fluoroacetaldehyde **48** and NAD^+ were incubated in cell-free extracts of *S. cattleya*, fluoroacetate **8** was formed indicating an aldehyde dehydrogenase responsible for the final oxidative step.[80] This was the first enzyme to be identified and purified in fluorometabolite biosynthesis (Scheme 1.12).

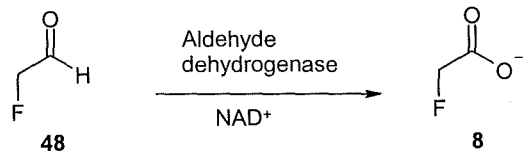

Scheme 1.12 Biotransformation of fluoroacetaldehyde **48** to fluoroacetate **8**.

Purification and characterisation of the enzyme revealed a tetramer with a native mass of 200 kDa and a pH optimum of 9.[80] The enzyme was inhibited by iodoacetamide.[80] The fact that this enzyme is expressed during the late exponential growth phase further suggests its involvement in metabolite biosynthesis.[80] A substrate specificity study of this enzyme showed a high affinity for fluoroacetaldehyde **48** (K_m of 0.08 mM) and interestingly acetaldehyde is a poor substrate.[80]

1.4.2 PLP dependent threonine transaldolase from *S. cattleya*

Labelling studies and incubation experiments with CFE's showed that [^{2}H]-fluoroacetaldehyde **48** is a direct precursor of 4-fluorothreonine **47**.[79] Furthermore, the incubation of L-threonine, fluoroacetaldehyde **48** and PLP in a CFE of *S. cattleya* showed 4-fluorothreonine **47** production by ^{19}F NMR (Figure 1.8).[81]

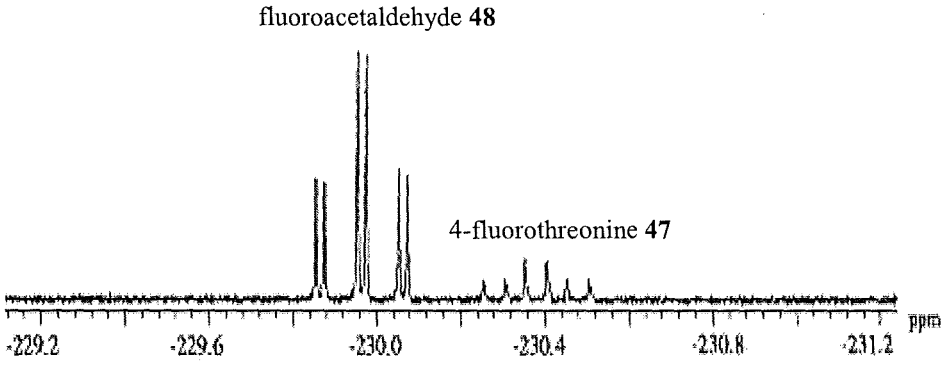

Figure 1.8 ^{19}F NMR spectrum recorded after a CFE was incubated with PLP, L-threonine and fluoroacetaldehyde **48**.[81]

Purification of the enzyme led to the identification of a PLP-dependent threonine transaldolase.[82] A study on substrate specificity showed an absolute requirement for L-threonine and fluoroacetaldehyde **48** with L-serine, L-cysteine, L-aspartate, L-*allo*-

threonine and glycine showing no activity. The absolute requirement for PLP and L-threonine indicates a novel threonine transaldolase. A proposed transaldolase type mechanism based on the requirement for PLP and L-threonine is shown in Scheme 1.13.

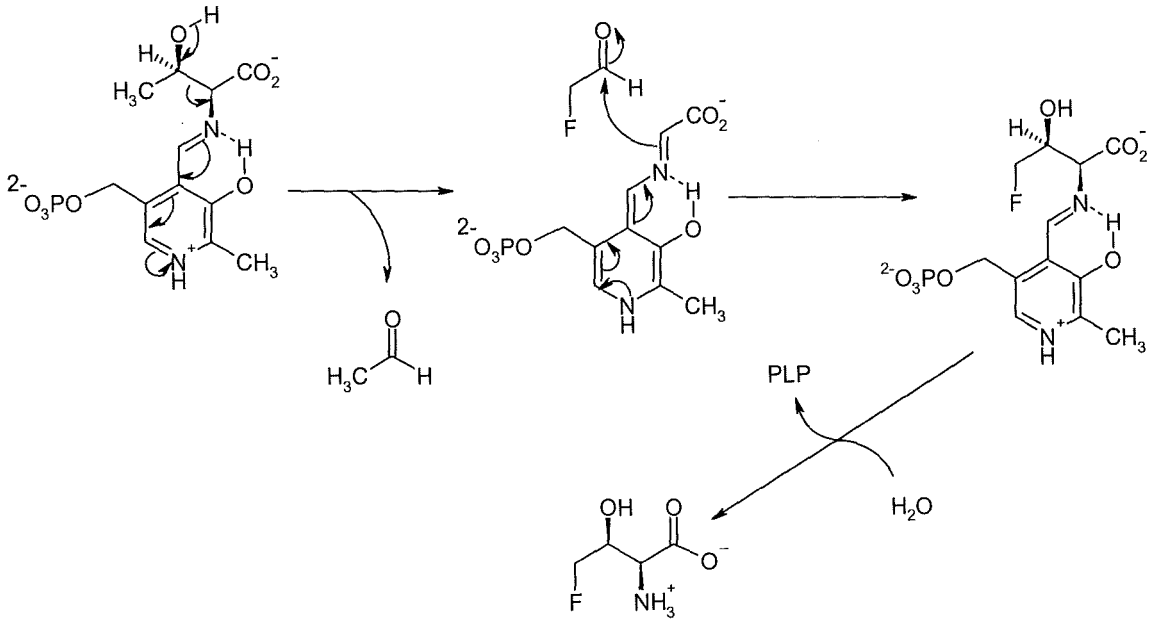

47

Scheme 1.13 Proposed mechanism of 4-fluorothreonine **47** production by a PLP dependent threonine transaldolase from *S. cattleya.*[82]

It is interesting to note from the mechanism that for every 4-fluorothreonine **47** molecule generated, a molecule of L-threonine is forfeited. This unusual occurrence poses the possibility that 4-fluorothreonine **47** may incorporate into a protein in place of L-threonine under metabolic stress. Studies on the biosynthesis of the chlorinated amino acid 4-chlorothreonine in *Pseudomonas syringae*[83] indicated L-threonine as a precursor. Clearly a common biosynthetic pathway may occur here, however for the *S. cattleya* enzyme, although chloroacetaldehyde was a substrate, it was also a time dependent inhibitor.

1.5 Enzymatic synthesis of Carbon-Fluorine bond

1.5.1 Introduction

To date several types of C-X bond forming enzymes (X = Cl, Br, I), operating by different mechanisms, have been identified. Most notably haloperoxidases (Section 1.1.1), $FADH_2$-dependent halogenases (Section 1.1.2) and non-haem iron(II) and α-keto-glutarate dependent halogenases (Section 1.1.3). These halogenating enzymes catalyse electrophilic or radical reactions. In order to understand enzymatic fluorination, the nature of the fluorinating species must be addressed. Firstly, the redox potential for the oxidation of fluoride (-3.06 V) to F^+ renders it thermodynamically impossible for activation to F^+ by a haloperoxidase. Additionally, the unique properties of fluorine, in comparison to other halogens, prevent the possibility of a radical fluorination process occurring. This leaves a possible nucleophilic halogenation reaction. Despite the weak nucleophilicity of fluoride ion in an aqueous environment, a desolvated fluoride ion is a good nucleophile and would be a potent nucleophile for enzymatic C-F bond formation.

1.5.2 Nucleophilic Fluorination

Nucleophilic halogenation reactions are rare, having only been demonstrated for the methylation of Br^-, Cl^- and I^- by *S*-adenosyl-L-methionine methyl transferase.[84] Withers and co-workers[85] reported the first enzymatic C-F bond formation using mutant β-glucosidases and β-mannosidases. The mutants were generated by site directed mutagenesis after replacing the catalytic glutamate residue in *Agrobacterium sp.* β-glucosidase with alanine, glycine or serine. This in turn, arrested any possible glycosidic bond cleavage. However, when assayed with the appropriate 2,4-dinitrophenyl β-glycoside **49** substrate in the presence of a high fluoride conc. (2 M), it was shown that

substantial glycosidic bond activity was restored. This was rationalised by fluoride ion preventing the intermediate oxocarbenium ion, which is normally stabilised by the missing carboxylate residue in the wild type enzyme. This generated an intermediate α-glycosyl fluoride **50** (Scheme 1.14).

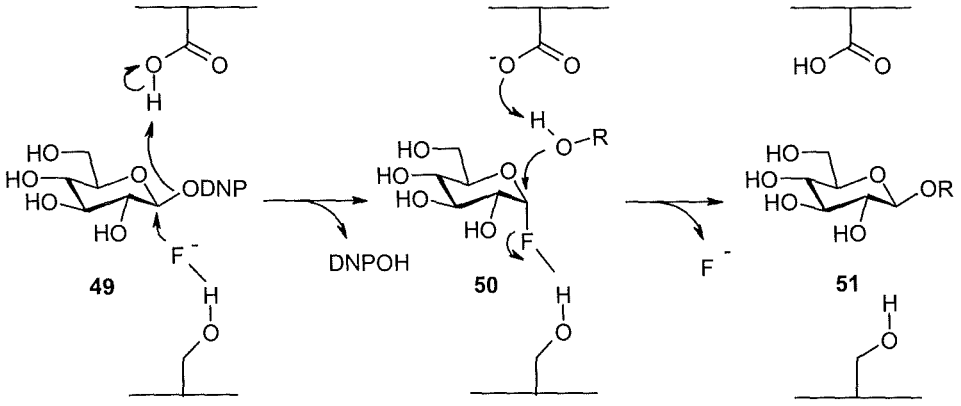

Scheme 1.14 Nucleophilic fluorination of 2,4-dinitrophenyl β-glucoside **49**.[85]

The glycosidase mutants also catalysed nucleophilic halogenation of 2,4-dinitrophenyl β-glucoside **49** with chloride and bromide (2 M). The order of halide reactivity was shown to be opposite to that expected. A comparison of k_{cat}/k_m values for mutated *β*-glucosidase showed a reactivity order of $F^- > Cl^- > Br^-$, opposite to that expected in aqueous solution. Therefore, it is possible that desolvation occurs in the active site of the enzyme. The catalysis of C-F bond formation by mutants of glycosidases, demonstrates the feasibility of a nucleophilic fluorination mechanism.

1.6 The fluorinase

1.6.1 Identification of a fluorination enzyme from *S. cattleya*

In 2002, a series of experiments was carried out by C. Schaffrath,[86] (University of St Andrews), incubating whole cells, prepared under a variety of conditions with various co-factors and fluoride ion. It was found that whole cell incubations when supplemented with glycerol and KF showed low levels of fluorophosphates in the culture medium after 5 days at 28 °C (Figure 1.9).

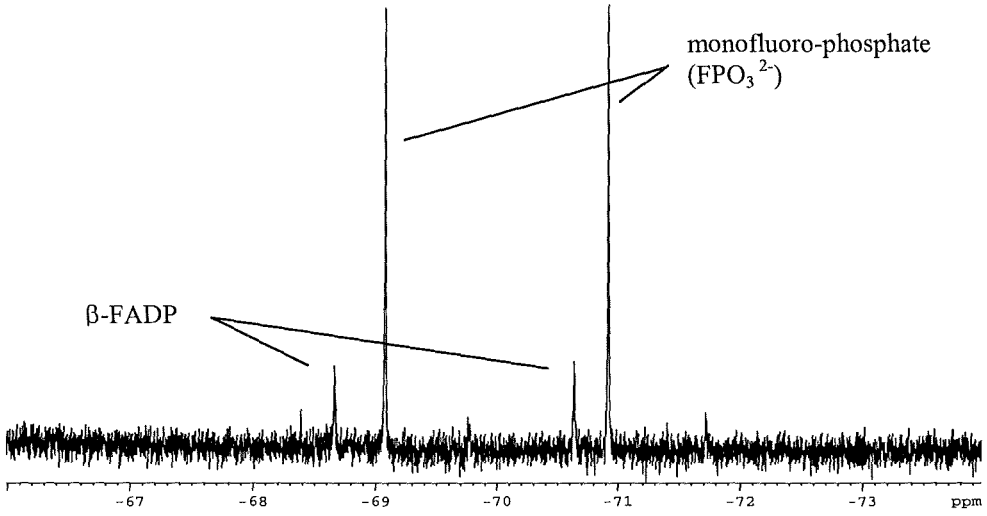

Figure 1.9 ^{19}F NMR spectrum of fluorophosphate production in resting cells of *S. cattleya*.[86]

Work by Ochoa[87] in 1957 first described the enzymatic synthesis of fluorophosphates in mammalian cells when purified pyruvate kinase was incubated with ATP and fluoride ion in the presence of magnesium ions. Clearly a similar enzyme could participate in fluorophosphate formation, which may play a pivotal role in fluoroacetate **8** and 4-fluorothreonine **47** biosynthesis. Although this was a tentative proposal, it was considered that the production of fluorophosphates could overcome some of the problems associated with water solvation of fluoride and provide an activated form of fluoride ion for transport into the cell and further metabolism.

Additional experiments were carried out which involved the incubation of ATP **52** and several other analogues (e.g UTP, GTP and CTP) with fluoride ion in a CFE of *S. cattleya.* It was found that only ATP gave rise to the production of fluoroacetate **8** indicating the CFE converted inorganic fluoride to organo-fluorine in a novel biotransformation (Figure 1.10).

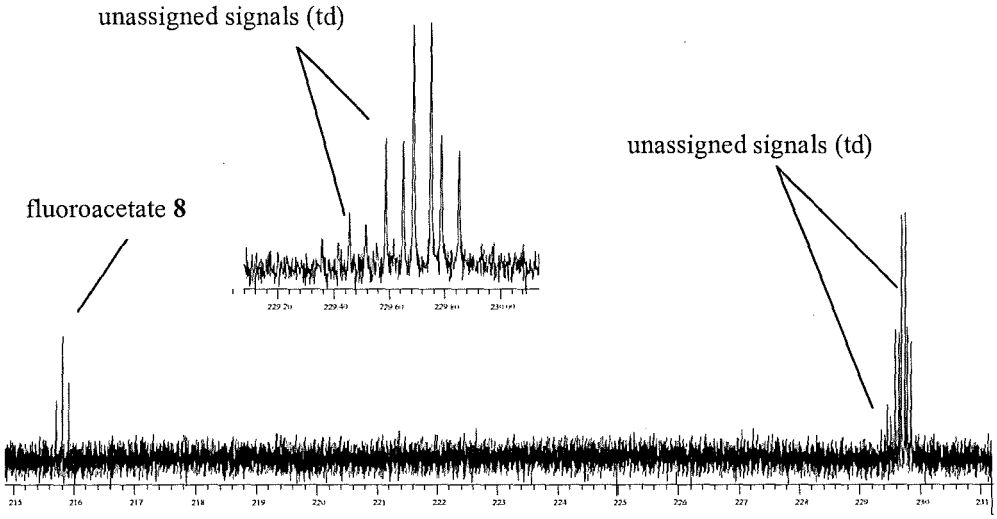

Figure 1.10 ^{19}F NMR spectrum of CFE incubation with ATP **52** and fluoride ion.[86]

The triplet (t) at -216 ppm was assigned as fluoroacetate **8** but the two remaining signals at -229.5 ppm and -229.7 ppm had never been observed in previous experiments. It was clearly possible that the first organo-fluoro compound formed is represented by one of the two unassigned fluorine signals. Both signals were shown to be triplets of doublets with coupling constants of $^{2}J_{H,F}$ 47 and $^{3}J_{H,F}$ 29 Hz, implying similar structures. Previous experiments with isotopically labelled [2-$^{2}H_1$, 2-^{18}O]-glycerol showed that the C-O bond is retained during fluoroacetate **8** and 4-fluorothreonine **48** biosynthesis. With these combined experimental observations a minimal structure for the two unassigned fluorine signals was established (Figure 1.11).

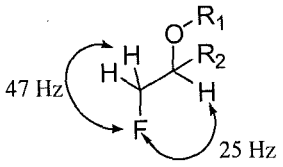

Figure 1.11 Minimal structure to account for the unassigned organofluorine compounds

At this stage it appeared most reasonable that ATP **52** was converted to 5'-fluoro-5'-deoxyadenosine (5'-FDA) **54** by the action of a fluorination enzyme which could represent one of the unassigned fluorine signals. Subsequent cell free investigations showed that the amino acid L-methionine **56** enhanced fluorometabolite biosynthesis, especially the accumulation of the two unassigned fluorine signals. These results suggested that *S*-adenosyl-L-methionine (SAM) **53** and not ATP **52** is involved in fluorometabolite biosynthesis.

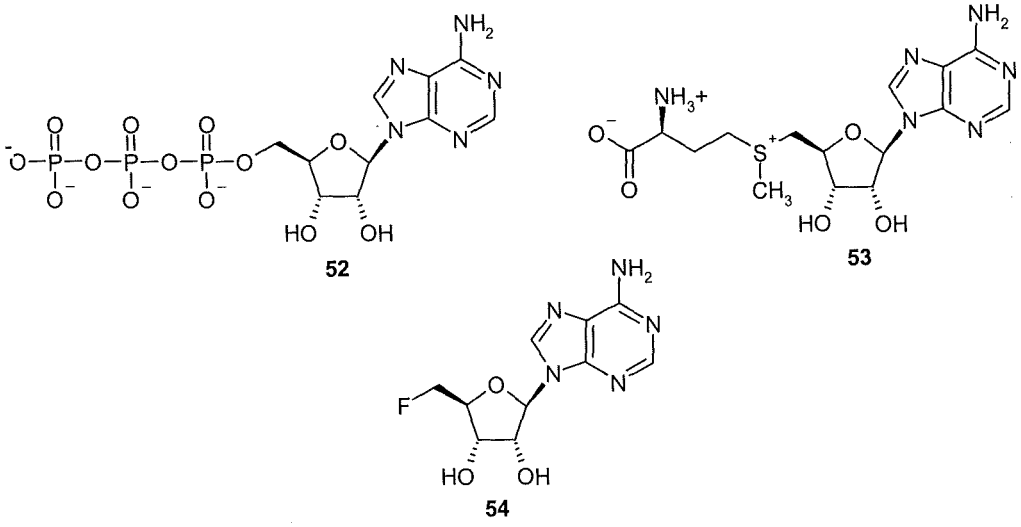

The correlation between **52** and **53** to promote cell-free biosynthesis of fluorometabolites could be rationalised by the presence of the ubiquitous enzyme SAM synthetase which mediates a reaction between ATP **52** and L-methionine **56** to generate SAM **53**.[88] Subsequent incubations involving SAM **53** and fluoride ion were conducted, which resulted in the biosynthesis of fluoroacetate **8** (Figure 1.12).[89]

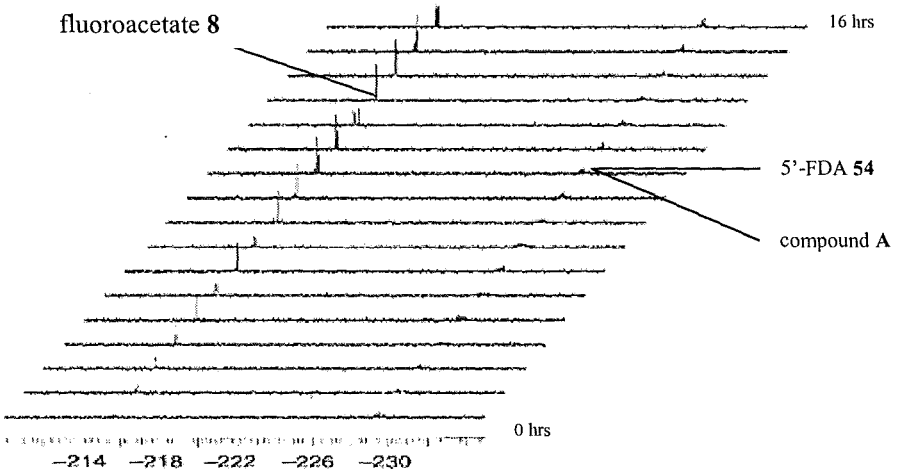

Figure 1.12 A ^{19}F NMR time course showing fluoroacetate biosynthesis and two additional products, 5'-FDA **54** and compound **A**.[89]

The preparation of a synthetic sample of 5'-FDA **54** for analytical comparison with the product of the enzyme reaction confirmed unambiguously that the product of the fluorination enzyme was 5'-FDA **54**. The identity of the other fluorine signal (compound **A**) was determined by further incubations of CFE's with SAM **53** and KF in the presence of iodoacetamide (Figure 1.13). Iodoacetamide inhibited one of the enzymes on the pathway preventing fluoroacetate **8** biosynthesis, and promoting the accumulation of compound **A.**

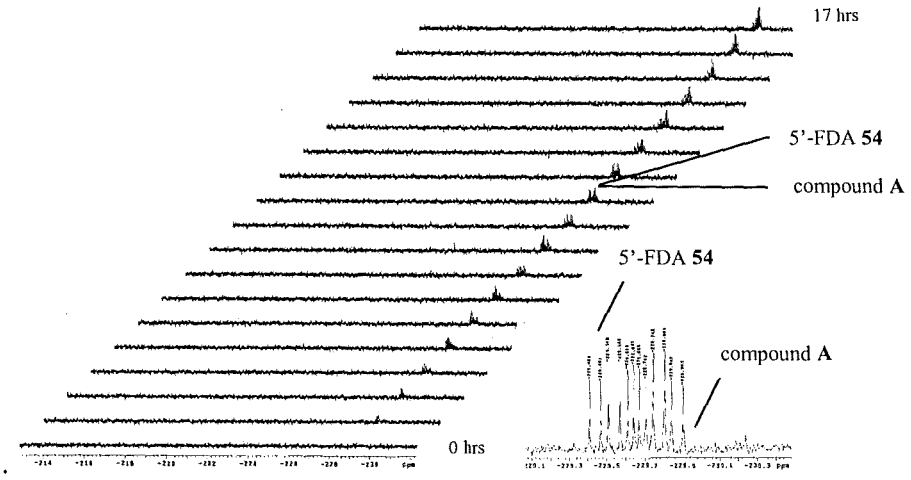

Figure 1.13 A ^{19}F NMR time course showing CFE incubated with SAM **53** and fluoride ion in the presence of iodoacetamide.[86]

It was therefore possible by preparative HPLC using UV detection to obtain a purified sample of compound **A**. Analysis by ^{19}F NMR and ^{1}H NMR confirmed all of the NMR characteristics of 5'-FDA **54**, and that compound **A** was clearly a 5'-fluoro-5'-deoxyribo-nucleoside. However, ES-MS gave a parent ion for compound **A** that was *one atomic mass unit* higher than 5'-FDA **54**. This raised the possibility of an irreversible adventitious deaminase activity responsible for the transformation of 5'-FDA **54** to 5'-fluoro-5'-deoxyinosine (5'-FDI) **55**. Confirmation of this was achieved by an experiment carried out in labelled water ($H_2{}^{18}O$) which gave a product which was now *three atomic mass units* higher than 5'-FDA **54** by ES-MS, showing 18-oxygen incorporation to generate [^{18}O]-5'-FDI **55** from 5'-FDA **54**. Also GC-MS analysis, after derivatisation with MSTFA, confirmed this unambiguously (Figure 1.14).[90]

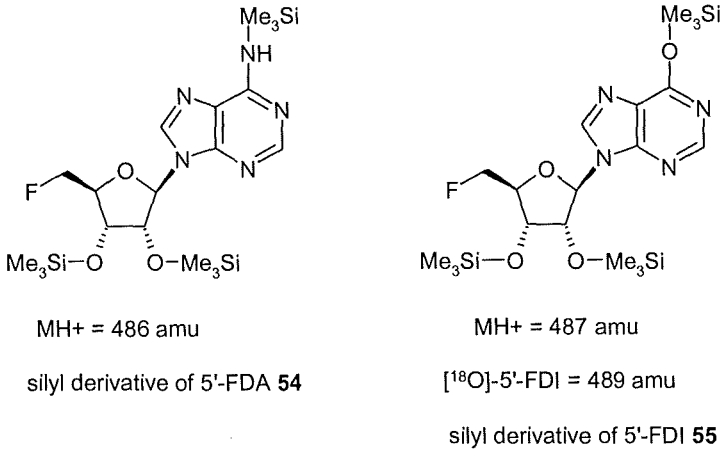

Figure 1. 14 Silyl derivatives analysed by GC-MS (CI) of 5'-FDA **54** and 5'-FDI **55**.

Furthermore, it was found that when 5'-FDI **55** was re-incubated in an active CFE of *S. cattleya* it remained metabolically inert with no sign of fluoroacetate **8** biosynthesis. Thus 5'-FDA **54** is an intermediate on the biosynthetic pathway, but 5'-FDI **55** is a shunt

product which cannot enter the pathway again. Scheme 1.15 shows a working hypothesis from the experiments carried out.

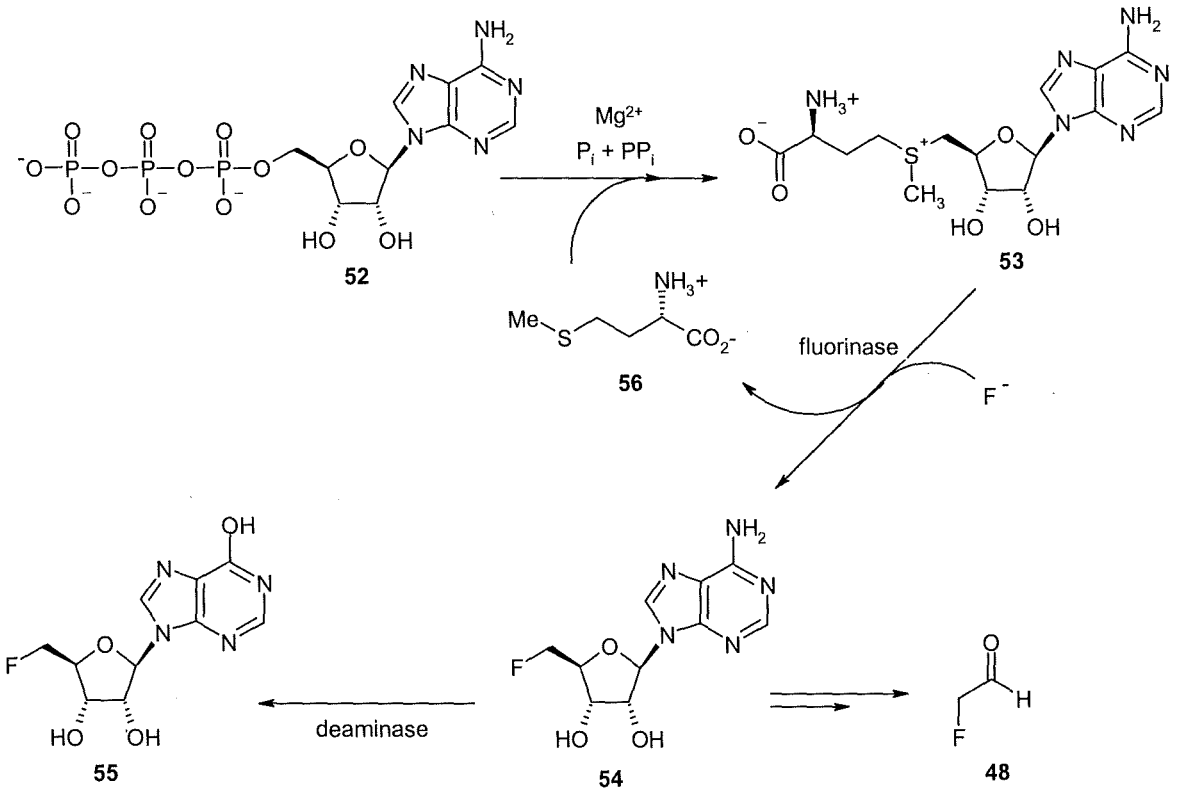

Scheme 1.15 Working hypothesis for enzymatic fluorination in a CFE of *S. cattleya*.

1.6.2 Purification, crystal structure and properties of the fluorinase

Having established a fluorination activity in *S. cattleya*,[91] purification of the fluorinase was carried out by C. Schaffrath at the University of St Andrews.[92] The enzyme was shown by gel filtration to have a native mass of 180 kDa and a subunit mass of 32 kDa as judged by SDS-PAGE. The identity and characterisation of the wild-type fluorinase on the basis of N-terminus amino acid analysis and trypsin digest led to the cloning of the fluorinase (*fl*A) gene. Purification and over-expression of the fluorinase has allowed a fuller characterisation of the activity. Kinetic analysis of the fluorinase was carried out by H. Deng, University of St Andrews[93] which showed a catalytic rate constant (k_{cat}) of 0.07

min^{-1}, a Michaelis constant (K_m) for F^- of 2 mM and a K_m for SAM **53** of 74 μM. The low affinity of fluoride ion for the enzyme indicated by its high K_m presumably reflects the difficulty of the enzyme securing desolvated fluoride ion in the active site due to the high heat of hydration. Inhibitors of SAM-dependent enzymes such as *S*-adenosyl-L-homocysteine (SAH) **57**[94] and sinefungin **58**[95] were explored as inhibitors of the fluorinase which showed a K_i of 29 μM for SAH **57** and sinefungin **58** showed weak inhibition (Figure 1.15).

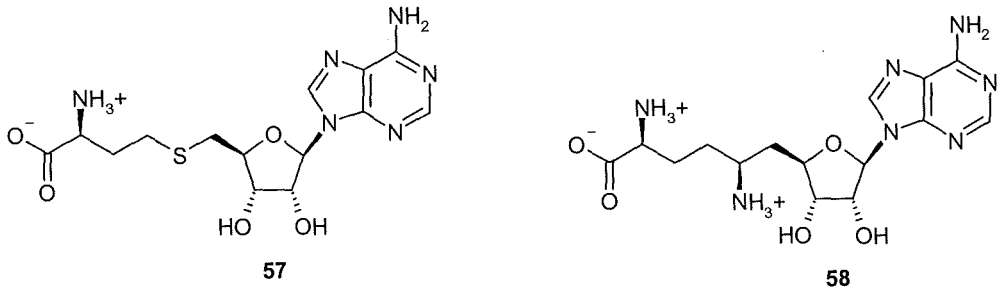

Figure 1.15 Inhibitors of the fluorinase, SAH **57** and Sinefungin **58**.

The cloning and over-expression of the enzyme allowed crystals to be obtained that were suitable for X-ray crystallography which subsequently led to a crystal structure (J. Naismith and C. J. Dong).[93,96]

The fluorinase structure revealed a homohexamer composed of a dimer of trimers (Figure 1.16). The monomeric fold of the trimer was shown to have a unique quaternary structure with no obvious relationship to other protein superfamilies. The crystallised enzyme had SAM **53** bound and indicated that SAM **53** does not dissociate readily from the protein during purification. The structure also revealed that each of the trimers had three SAM **53** molecules bound at the interface between each monomer. The recognition of SAM **53** is shown to be highly specific with each of the components (adenine ring, ribose ring and methionine) forming various hydrogen bonding contacts. It seems reasonable that these

contacts between SAM **53** and both monomers would drive closure of the protein domains to form the enveloped binding site.

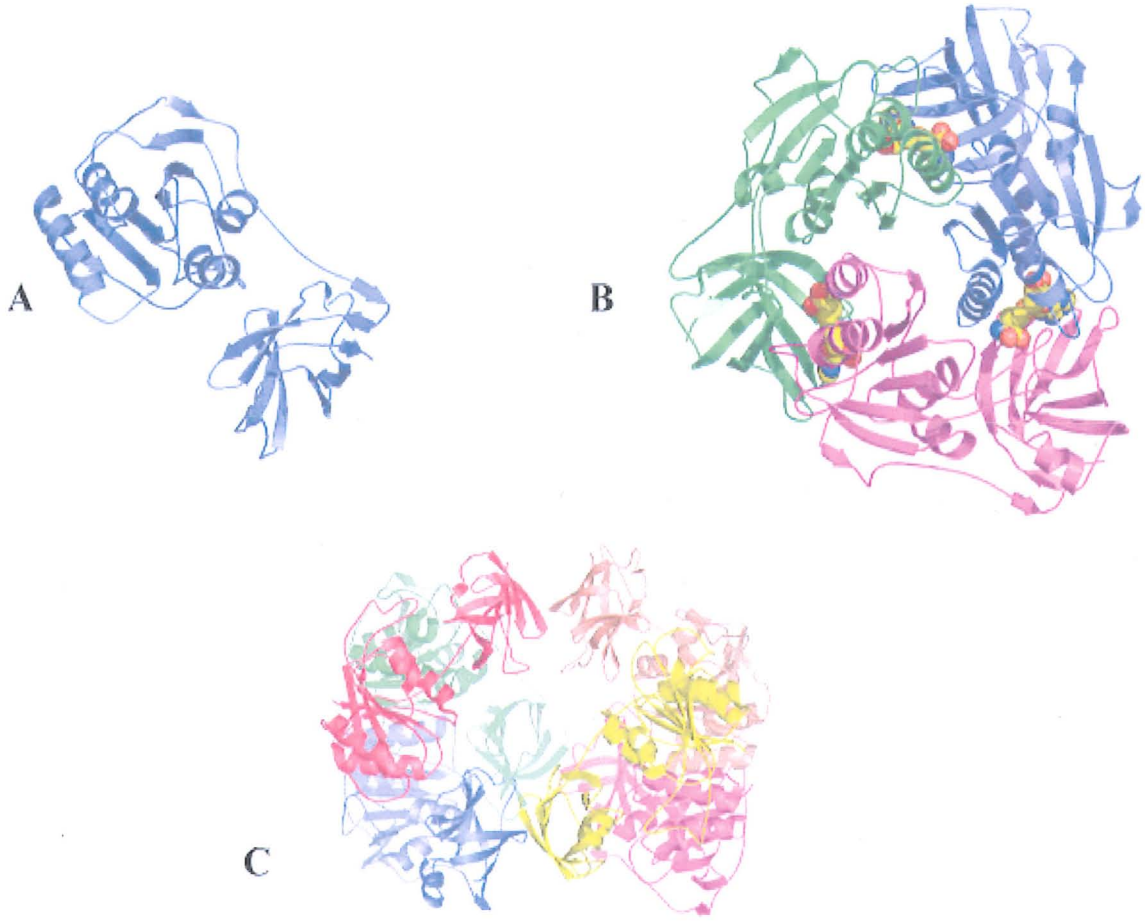

Figure 1.16 Structure of the fluorinase; **A**, monomer. **B**, trimer with SAM bound at the interfaces. **C**, native hexameric structure as a dimer of trimers.[93]

The ribose ring of SAM **53** is held in an unusually planar conformation with hydrogen bonding between the 2' and 3'-hydroxyl groups and the carboxylate side group of Asp-16 (Figure 1.17).

Co-crystallisation of the fluorinase with SAM **53** and fluoride ion resulted in a trapped product complex with 5'-FDA **54** and L-methionine **56** at the active site. Comparisons of diffraction data before and after the fluorination reaction showed little difference in the binding of both structures except in the bond breaking/forming region. The sulfur atom is

displaced with the new C-F bond antiperiplanar to the old C-S bond. This suggests a substitution reaction (S_N2) occurring with inversion of configuration. This stereochemical inversion was confirmed unambiguously by stereochemical studies.[97,98]

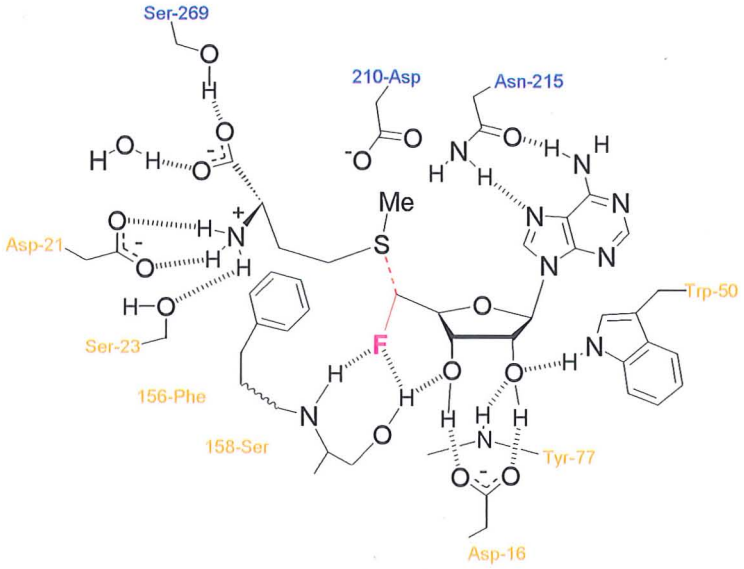

Figure 1.17 5'-FDA **54** and L-methionine **56** bound to the active site of fluorinase showing hydrogen bonding to the fluoromethyl group from Ser 158, and the *anti* relationship between the C-F bond (red) and the disconnected C-S bond (dotted red) of SAM **53** that is indicative of an S_N2 reaction.[93]

Further analysis of the co-crystallised product structure showed the fluorine atom forming two short hydrogen bonds to the Ser158 residue. It is also of interest to note that no water molecules are detected in the vicinity of the fluorine atom, suggesting that fluoride incorporation into the active site must mean that the enzyme was able to strip the hydration sphere from fluoride as it progressed towards the reaction centre. Dehydrated fluoride ion is a potent nucleophile, the most nucleophilic of the halides, and therefore the enzyme has attained a balance between generating a sufficiently nucleophilic fluoride, and paying the full energy cost of dehydration.

Another feature of the product structure is the 3'-hydroxyl position on the ribose ring, which appears to have a role in directing fluoride ion towards the electrophilic C5' site by a hydrogen bonding interaction as illustrated in Figure 1.17. Insights into enzymatic C-F bond formation from QM and QM/MM calculations[99] have recently shown that the fluorinase lowers the barrier for C-F bond formation by 39 kJ mol^{-1}. The major contributing factor to this energy reduction is related to pre-organisation of the substrates in the active site.

Further investigations on the fluorination enzyme led to the realisation that the enzyme works in reverse and that it could catalyse the conversion of 2'-deoxy-5'-FDA **59** substrates to 2'-deoxy SAM **60** (Scheme 1.16).

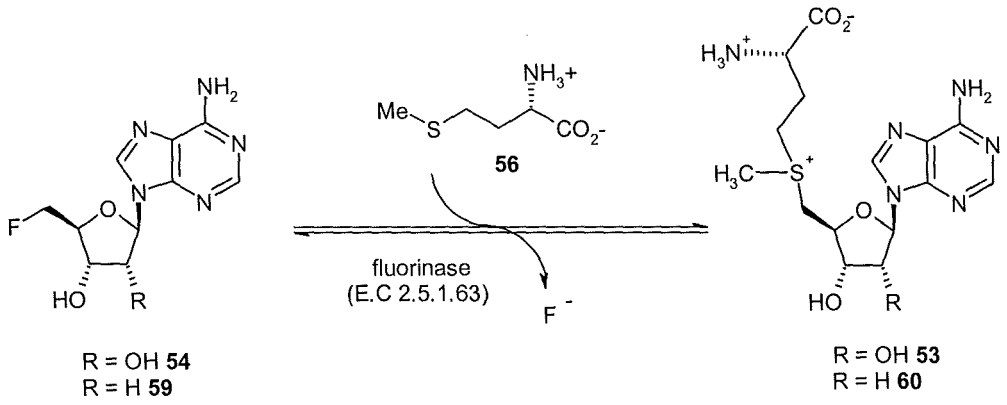

Scheme 1.16 Reversibility of the fluorinase.

Intuitively the reverse reaction appears a less achievable prospect as fluoride forms the strongest covalent bond to carbon. However, V_{max} calculations, at saturating kinetics indicate a reaction at 1/3 of the rate of the forward reaction.

The enzyme is very specific and not amenable to much structural variation in the substrate. However, the 2'-deoxy substitute **59** showed a ten-fold rate decrease by comparison with 5'-FDA **54**. This confirmed that the 2'-OH position is not absolutely essential for catalytic activity, however, the rate decrease does suggest the importance of hydrogen bonding

contacts (see Figure 1.17). In recent unpublished work the structure of the co-crystallised 2-deoxy-5'-FDA-fluorinase complex shows that 2'-deoxy-5'-FDA **59** adopts a slightly different conformation to that exhibited by 5'-FDA **54** (Figure 1.18).

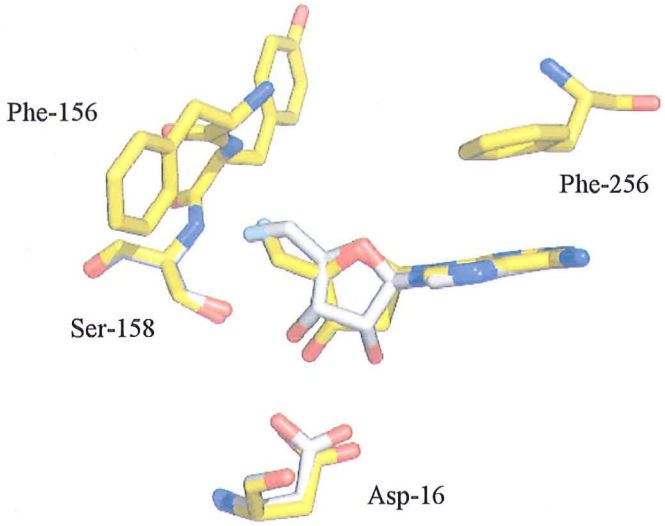

Figure 1.18 Structure of the 2'-deoxy-5'-FDA-fluorinase co-complex. Shown superimposed with 5'-FDA **53**. 2-deoxy-5'-FDA **59** is coloured, C yellow, N blue, O red and F light blue. Shown superimposed is 5'-FDA **54** (C white, F light blue, N blue, O red).

Additional experiments with L-selenomethionine (L-Se-met) **63** and 5'-FDA **54** show a six fold rate increase on comparison with L-methionine **56** and 5'-FDA **54**. This rate increase is consistent with the increased nucleophilicity of selenium over sulfur.

1.6.3 Chlorination by the fluorinase

An interesting feature of the fluorinase is that it will accept chloride ion as a substrate also in a reversible reaction.[100] This novel enzymatic chlorination operates by nucleophilic substitution rather than the reported electrophilic or radical mechanisms proposed for other halogenases (Section 1.1.2, 1.1.3). Early attempts to replace fluoride by chloride as a substrate with SAM **53** in the presence of the fluorinase failed to identify the product 5'-

chloro-5'-deoxyadenosine (5'-ClDA) **61**. Most recently, it was found that the inability to detect the chlorinated product was due to the equilibrium of the chlorination reaction lying extensively in favour of the substrate over the product. This was finally shown by adopting a coupled enzymatic strategy in order to drive the equilibrium in favour of the product. Scheme 1.17 shows two enzymatic routes which indicate that the fluorinase can process chloride ion as a substrate. Firstly, the fluorinase was coupled with an L-amino acid oxidase to remove the generated L-methionine **56** during the halide substitution reaction. This in turn led to the identification of the product 5'-ClDA **61**, while inhibiting the reverse reaction. A second experiment involved the addition of adenyl acid deaminase in the presence of the fluorinase which resulted in the product 5'-chloro-5'-deoxyinosine (5'-ClDI) **62**.

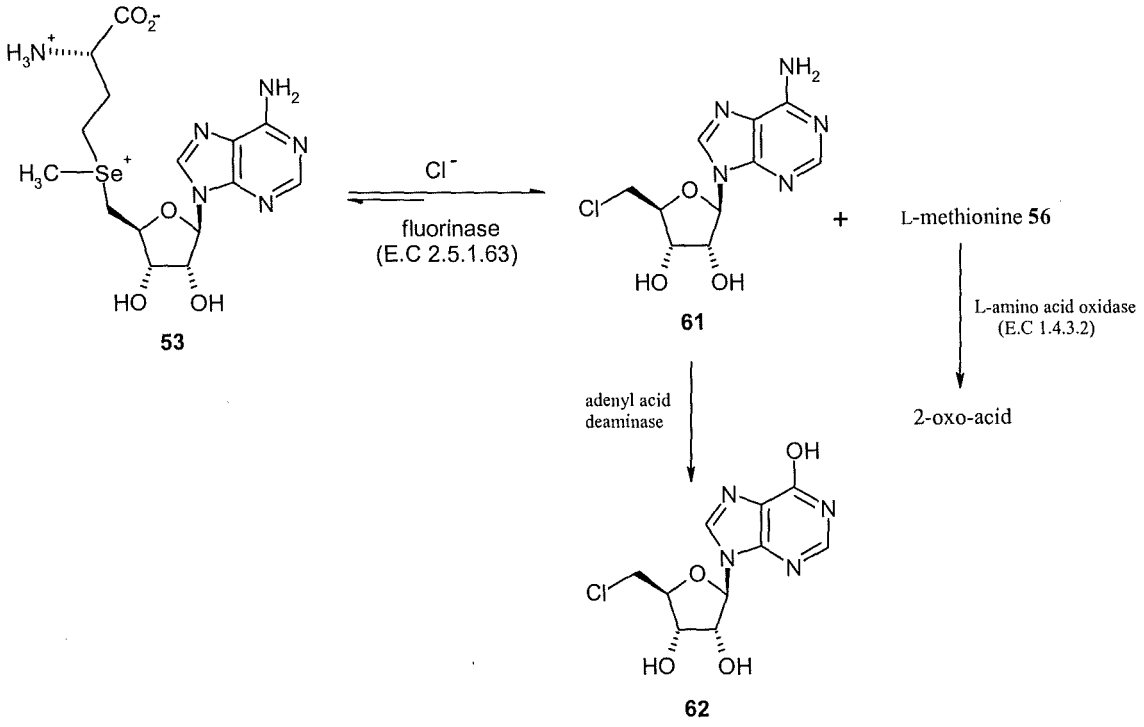

Scheme 1.17 Coupled enzymatic assay towards C-Cl bond formation.

Rates at saturating kinetics have indicated a preference for F^- over Cl^- by a factor of 120. 5'-ClDA **61** also emerged as a better substrate over 5'-FDA **54** in the reverse direction

with an eight fold rate increase. This rate enhancement is consistent with the C-Cl bond being weaker than the C-F bond, and Cl^- being a better leaving group.

It was also demonstrated that incubation of 5'-ClDA **61** with fluoride ion and L-selenomethionine **63** in the presence of the fluorinase resulted in the biotransformation of 5'-ClDA **61** to 5'-FDA **54** (Scheme 1.18). This trans-halogenation reaction was monitored by analytical HPLC. It is interesting to note that Se-SAM **64** is shown to be transient during the experiment (Figure 1.19).

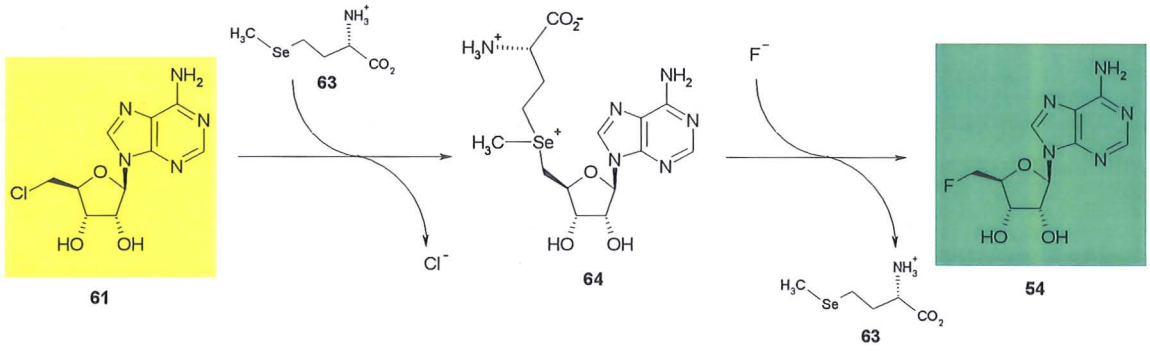

Scheme 1.18 *Trans*-halogenation reaction mediated by the fluorinase.

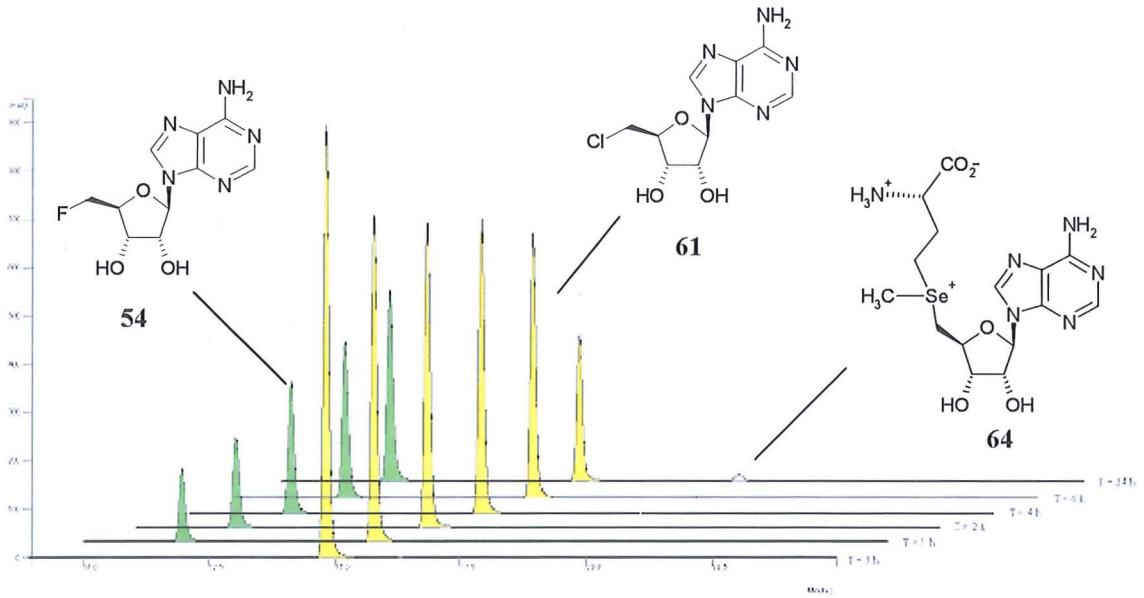

Figure 1.19 Trans-halogenation reactions catalysed by the fluorinase.[100]

The substrate 5'-ClDA **61** was co-crystallised (J. H. Naismith and A. McEwan, St Andrews University) with over-expressed fluorinase in the absence of L-methionine **56**.[100] Figure 1.20 shows 5'-ClDA **61** bound to the active site superimposed with the 5'-FDA **54** structure. The conformation shows that the chlorine atom is displaced by 1.3 Å relative to fluorine in 5'-FDA **54**, consistent with its larger atomic radius. No significant conformational changes of the protein occurred upon 5'-ClDA **61** binding, with only the substrate adjusting its position to accommodate the larger halogen.

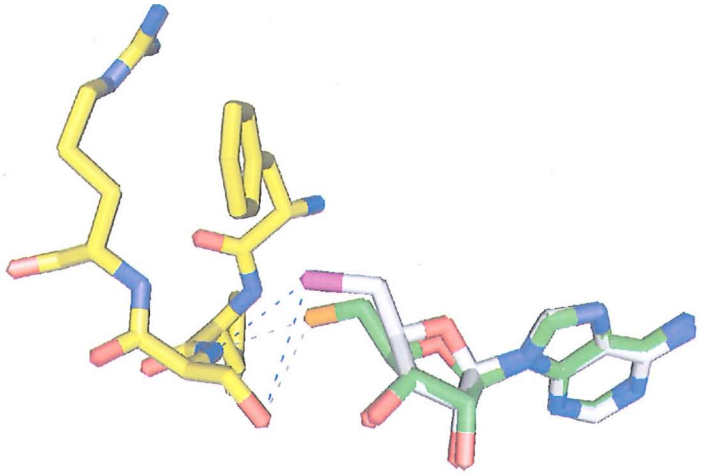

Figure 1.20 Structure of the 5'-ClDA-fluorinase co-complex with hydrogen bonds and polar contacts to the protein shown. 5'-ClDA **61** is coloured, C white, N blue, O red and Cl purple. The protein is coloured as the ligand except C is yellow. Shown superimposed is 5'-FDA **54** (C green, F orange, N blue) where the Cl atom lies further away from the backbone amide of Ser 156.[100]

This study also revealed a second conformation for 5'-ClDA **61** on the enzyme where the chlorine has rotated out of the halogen binding pocket and adopted a conformation where it is accommodated in the empty L-methionine **56** sulfur binding site (Figure 1.21). Of course this second conformation is prohibited in the catalytic reaction when L-methionine **56** is present.

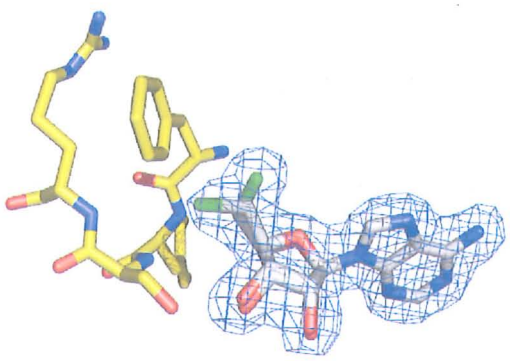

Figure 1.21 The structure of 5'-ClDA **61** bound to the fluorinase showing both conformations of the chlorine atom.

1.7 Positron Emission Tomography (PET)

1.7.1 Introduction

PET is a non-invasive imaging technique used to image metabolic activities in living tissues.[101] The technique uses radiotracers labelled with positron emitting radionuclides with various *in vivo* properties which permit imaging of the distributions of ligands in metabolising tissues. The most common PET radionuclides are ^{11}C, ^{18}F, ^{15}O and ^{13}N which have half lives of 20, 110, 2 and 10 minutes respectively. ^{18}F offers a number of advantages over the other radionuclides, due to its longer half-life (110 min). This in turn permits more time for radiochemical synthesis and purification for use in *in vivo* experiments.

The most widely used radiotracer is [^{18}F]-labelled 2-fluorodeoxyglucose (FDG) which has been routinely used in brain and tumour imaging.[102] Other PET labelled probes which could have potential for the imaging of tumours or adenosine receptors in the brain etc. are the adenosine derivatives which are products of the fluorinase reaction. The adenosine analogue 2'-fluoro-2'-deoxyadenosine has shown promising results in the evaluation of tumour cell proliferation.[103] Other adenosine analogues such as [^{18}F]-5'-fluoro-5'-

deoxyadenosine ([^{18}F]-5'-FDA) **65** have been synthesised, however reported radiochemical yields were found to be less than 1 %.[104]

1.7.2 Enzymatic methods for fluorine-18 labelling

The recent isolation of the fluorinase from *S. cattleya* led to the exploration of this enzyme as a biocatalyst for potential fluorine-18 labelled 5'-FDA **65** studies. This may be advantageous as enzymes are chemospecific with very few side products generated, unlike chemical approaches. However, there are limited examples in the literature where biocatalysts have been used to incorporate radionuclides for PET applications.

H. Deng and L. Martarello[105] (GSK and Aarhus hospital, Denmark) reported the first enzymatic synthesis of [^{18}F]-5'-FDA **65** using purified wild-type fluorinase (Scheme 1.19).

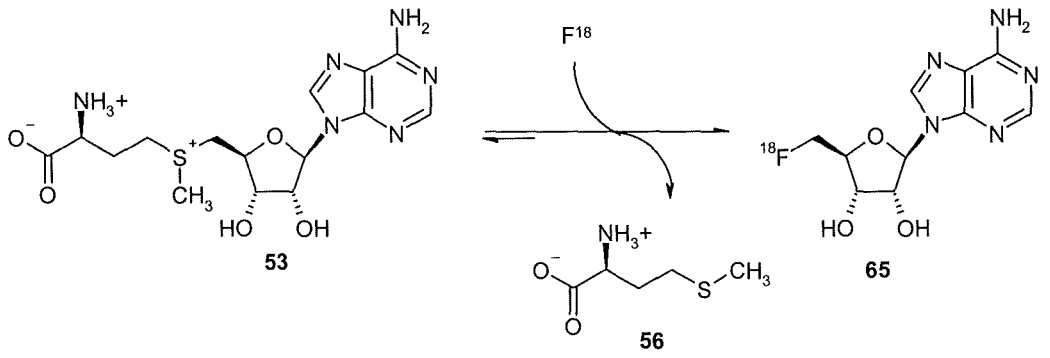

Scheme 1.19 Enzymatic radio-labelling of 5'-[^{18}F]-fluoro-5'-deoxyadenosine **65**.

It was shown that using mg / ml quantities of wild-type fluorinase that a total radio-chemical yield of ~ 1 % could be achieved. Although this is a low yield, it has been demonstrated more recently that use of more protein gives better yields. In recent unpublished work, the over-expressed fluorinase available now in mg's, gave radiochemical yields (RCY) of [^{18}F]-5'-FDA **65** up to 95 %. A key development in optimising the efficiency of [^{18}F]-5'-FDA **65** production was the positioning of the

equilibrium in favour of product over substrate. Two coupled enzymatic strategies were achieved in driving the reaction towards [^{18}F]-5'-FDA **65** synthesis, similar to that shown in Scheme 1.17. The first approach was the coupling of the fluorinase to an L-amino acid oxidase which removed the co-produced L-methionine and therefore suppresses the reverse reaction. The second approach involved the coupling of the fluorinase to an adenosine deaminase to generate [^{18}F]-5'-FDI **66** (Scheme 1.20). This second approach also provided access to another labelled purine nucleoside [^{18}F]-5'-FDI **66**. With this type of coupled enzyme methodology other ^{18}F-labelled products were prepared. This included the enzymatic synthesis of [^{18}F]-5-FDR **68**, a monosaccharide. The biotransformation of SAM **53** to [^{18}F]-5-FDR **68** was accomplished using a coupled enzyme strategy consisting of fluorinase, an immobilised PNP (donated by GSK) and a phytase (Scheme 1.20) giving an overall RCY of 40 %.

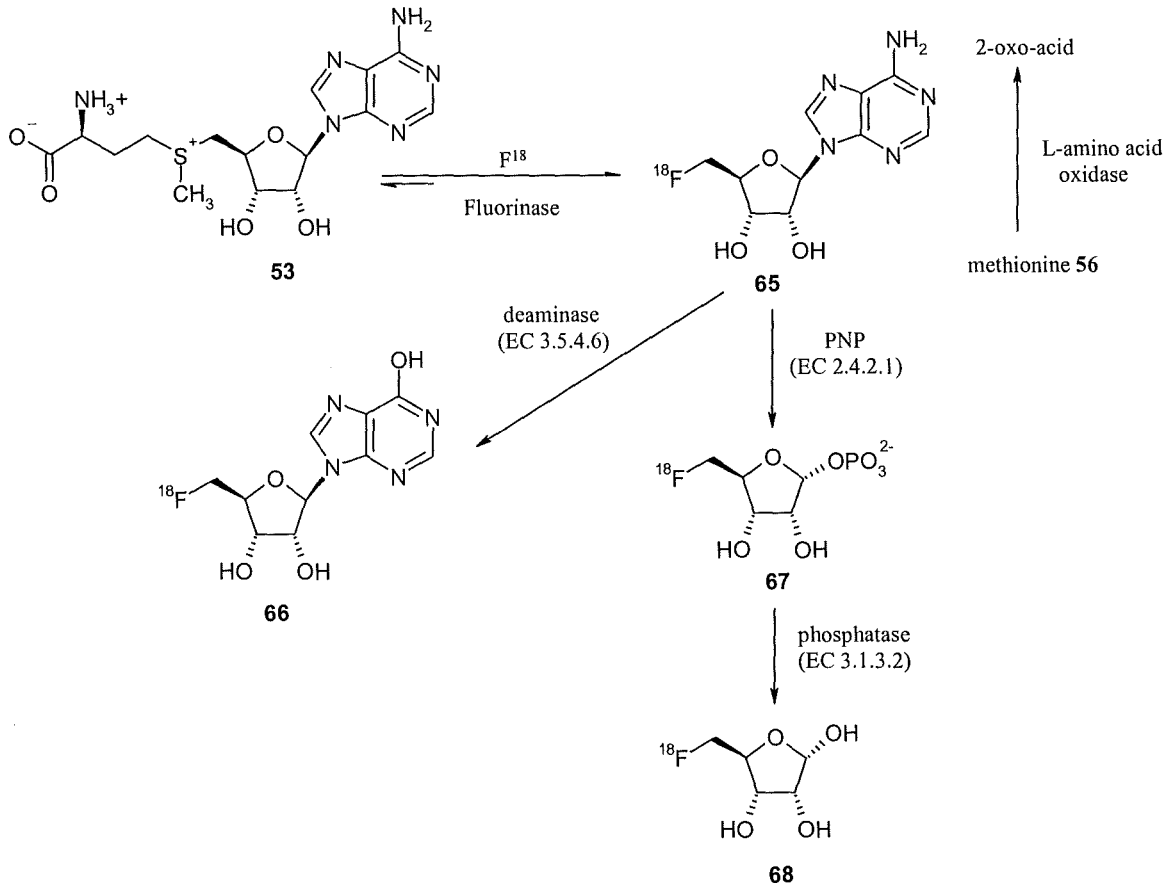

Scheme 1.20 Potential PET labelled probes synthesised by the fluorinase mediated methods.

The enzymatic approach towards the synthesis of PET labelled probes extends the use of the fluorinase as a biocatalyst.

1.8 Metabolic fate of 5'-FDA in *S. cattleya*

Work carried out by C. Schaffrath[89] (University of St Andrews) investigated the metabolic fate of 5'-FDA **54** in *S. cattleya*. It was shown that the incubation of 5'-FDA **54** in a CFE resulted in the biotransformation to several fluorinated intermediates including fluoroacetate **8** and 4-fluorothreonine **47** (Figure 1.22).

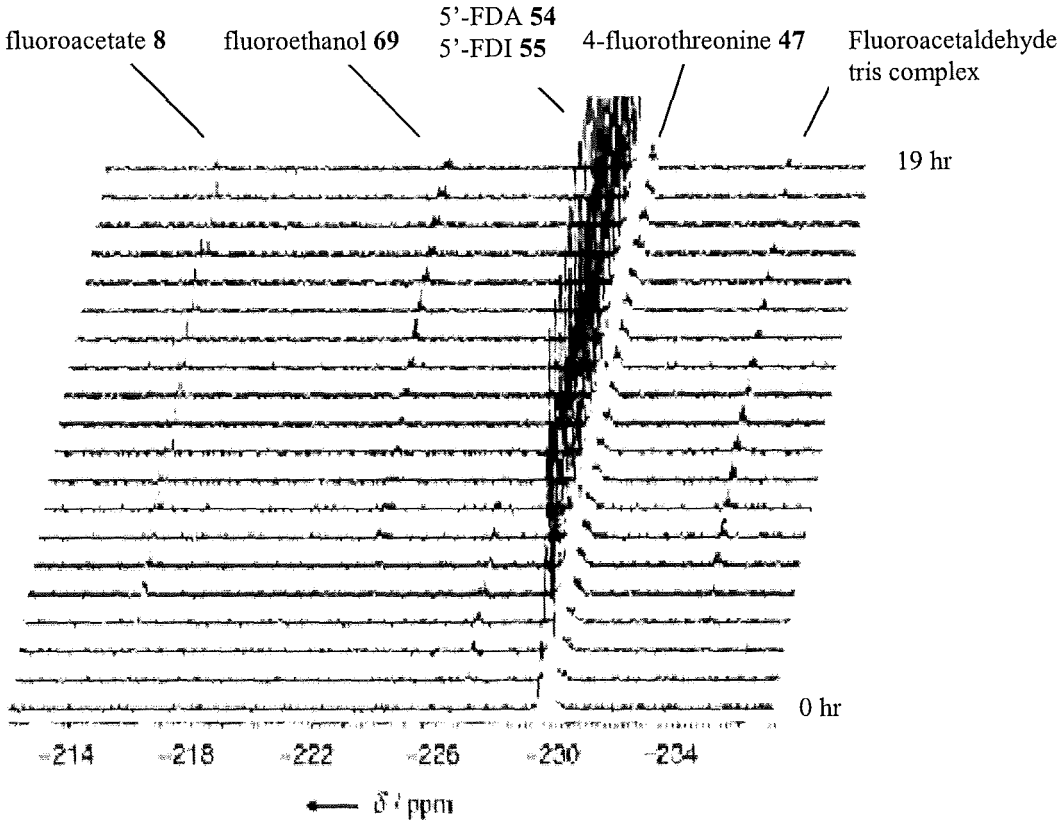

Figure 1. 22 ^{19}F NMR time course of CFE incubated with 5'-FDA **54** at hourly intervals for 19 hrs at 25 °C.[89]

A ^{19}F NMR time course profile of an incubation of 5'-FDA **54** in a CFE showed a complex between fluoroacetaldehyde **48** and tris(hydroxymethyl)aminoethane **70**, the constituent of Tris buffer.

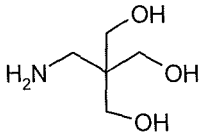

70

In addition it was shown that the CFE had the capacity to reduce fluoroacetaldehyde **48** to fluoroethanol **69** (Scheme 1.21).

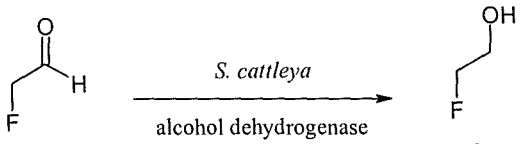

48 **69**

Scheme 1.21 Biotransformation of fluoroacetaldehyde **48** to fluoroethanol **69**.

The presence of fluoroethanol **69** is attributed to an adventitious alcohol dehydrogenase that reduces fluoroacetaldehyde **48**. The conversion of 5'-FDA **54** to the shunt product 5'-FDI **55** arises from the action of a deaminase activity in *S. cattleya*. Some transient fluorinated intermediates are also visible in these experiments. For example, the unassigned signal at -227.2 ppm maybe an intermediate on the pathway beyond 5'-FDA **54**. The elucidation of the pathway between 5'-FDA **54** and fluoroacetaldehyde **48** constitutes the major focus of this thesis. Scheme 1.22 shows the metabolites and enzymes involved in fluoroacetate **8** and 4-fluorothreonine **47** biosynthesis, prior to the work carried out in this thesis.

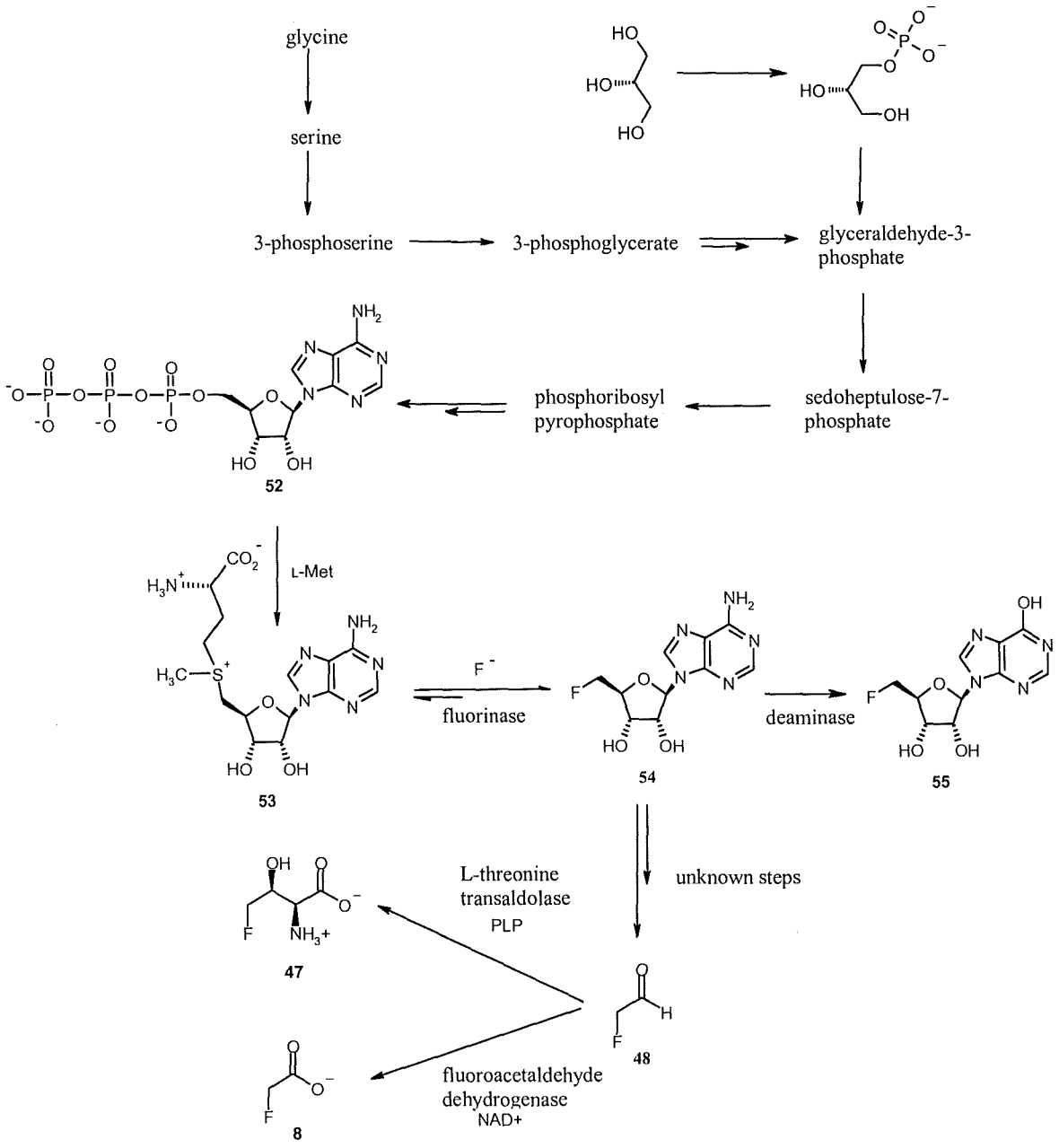

Scheme 1.22 Overview of known metabolites and enzymes involved in fluoroacetate **8** and 4-fluorothreonine **47** biosynthesis.

2 Identification of a purine nucleoside phosphorylase (PNP) involved in fluorometabolite biosynthesis in *S. cattleya*

The fluorinase which catalyses the formation of the metabolic intermediate 5'-fluoro-5'-deoxyadenosine (5'-FDA) **54**, has been identified as the first committed step on the biosynthetic pathway towards the formation of the secondary metabolites fluoroacetate **8** and 4-fluorothreonine **47**.[89] Fluoroacetaldehyde **48** was already known to be a precursor to both of these fluorinated secondary metabolites[79] however, the fluorinated metabolites that exist between 5'-FDA **54** and fluoroacetaldehyde **48** remained to be characterised. The results described in this chapter indicate that 5-fluoro-5-deoxy-D-ribose-1-phosphate (5-FDRP) **81** is the next formed fluorometabolite after 5'-FDA **54** on the biosynthetic pathway.[106] The enzyme responsible for the conversion of 5'-FDA **54** to 5-FDRP **81** has been identified as a purine nucleoside phosphorylase (PNP). In order to understand the metabolic fate of 5'-FDA **54**, a short overview on biochemical processes involving nucleosides is given below.

2.1 Nucleoside metabolism in biological systems

The nucleoside, adenosine is an important intermediate in several metabolic pathways, where it arises not only from the catabolism of nucleic acids and nucleoside co-factors, but also from *S*-adenosyl-L-methionine (SAM) **53** after transmethylation reactions.[107] Activities of enzymes involved in adenosine metabolism have been well characterised in various organisms. Scheme 2.1 shows a selection of enzymes which contribute towards the metabolic fate of adenosine **71**.

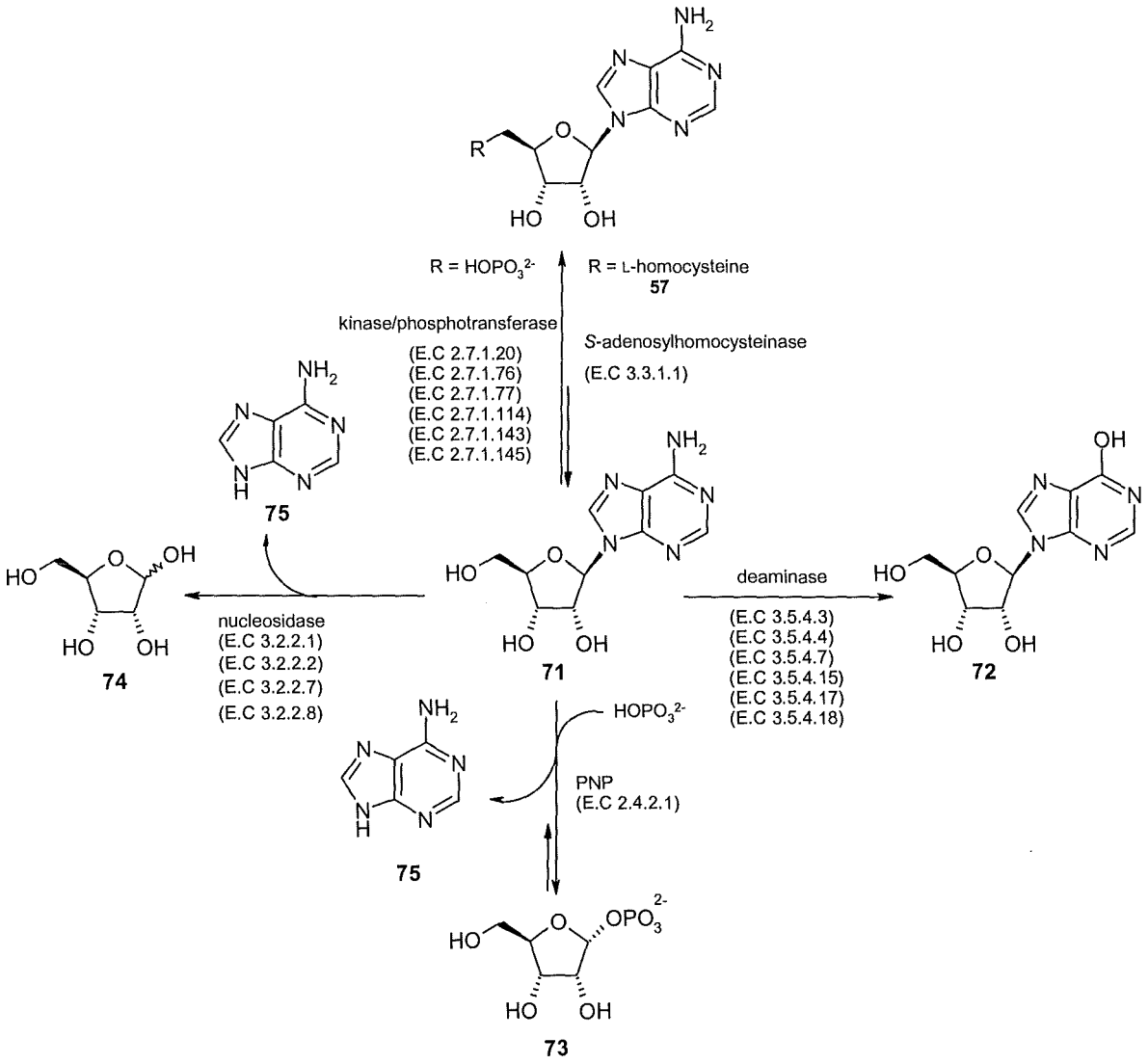

Scheme 2.1 Metabolic routes involving the biotransformation of adenosine **71**.

Hydrolase enzymes such as adenosine deaminase (E.C 3.5.4.3) participate in purine metabolism where they hydrolyse either adenosine **71** or 2'-deoxyadenosine to generate inosine **72** or 2'-deoxyinosine respectively.[108] These enzymes are ubiquitous in all purine catabolic pathways. Other hydrolytic enzymes such as *S*-adenosylhomocysteinase catalyse the reversible addition of L-homocysteine and adenosine **71** to give *S*-adenosyl-L-homocysteine (SAH) **57**. These enzymes play a key role in regulating the intracellular levels of SAH **57** and homocysteine.[109] Another degradation route involves the phosphorylation of ribofuranosyl-containing nucleoside analogues at the 5'-hydroxyl

position using ATP **52** or GTP as the phosphate donor. Such examples include the ubiquitous enzyme, adenosine kinase which functions as a salvage mechanism for returning adenosine to nucleic acids.[110] Other routes lead to the hydrolysis of the C-N glycosidic bond, for example *via* adenosine phosphorolysis which yields ribose-1-phosphate **73** and adenine **75** by the action of a purine nucleoside phosphorylase (PNP).[111,112] This is a common enzyme which contributes to the catabolism and recycling of nucleosides. The enzymatic reaction is specific for β-nucleosides and the catalytic mechanism proceeds in a stereospecific manner to give only the α-ribose-1-phosphate **73**. Hydrolysis of adenosine **71** to ribose **74** and adenine **75** by the action of a nucleosidase represents an alternative degradative pathway.[113]

If the metabolism of 5'-FDA **54** proceeds along a similar pathway to that of adenosine **71**, then it follows that there are four possible biotransformations that could represent the next enzymatic step on the fluorometabolite pathway. The deamination of 5'-FDA **54** is inconsistent with our experimental observation to give 5'-FDI **55**. This is due to the fact that, as discussed in Section 1.6 and 1.8, the formation of the adventitious side product 5'-FDI **55** remains metabolically inert in a CFE of *S. cattleya*. The phosphorylation of 5'-FDA **54** at the 5'-position by a kinase activity is clearly redundant due to the C-F bond replacing C-OH in 5'-FDA **54**. This leaves two alternative routes, both involving the C-N glycosidic bond cleavage. The first of these is a phosphorolysis reaction involving a PNP enzyme to yield 5-FDRP **81** and adenine **75**. The other is a hydrolysis reaction with nucleosidase activity to yield 5-FDR **80** and adenine **75**. In order to delineate these metabolic routes, it is instructive to review the L-methionine salvage pathway which is known to utilise both of these enzyme activities in two independent pathways.

2.1.1 L-Methionine salvage pathway

The L-methionine salvage cycle is a ubiquitous biochemical pathway that maintains methionine **56** levels *in vivo*. It involves the recycling of the thiomethyl moiety of L-methionine **56** through a degradation pathway that leads from *S*-adenosyl-L-methionine (SAM) **53** through methylthioadenosine (MTA) **76**.[113] Scheme 2.2 outlines part of the pathway showing the two alternative routes involved in MTA **76** recycling.

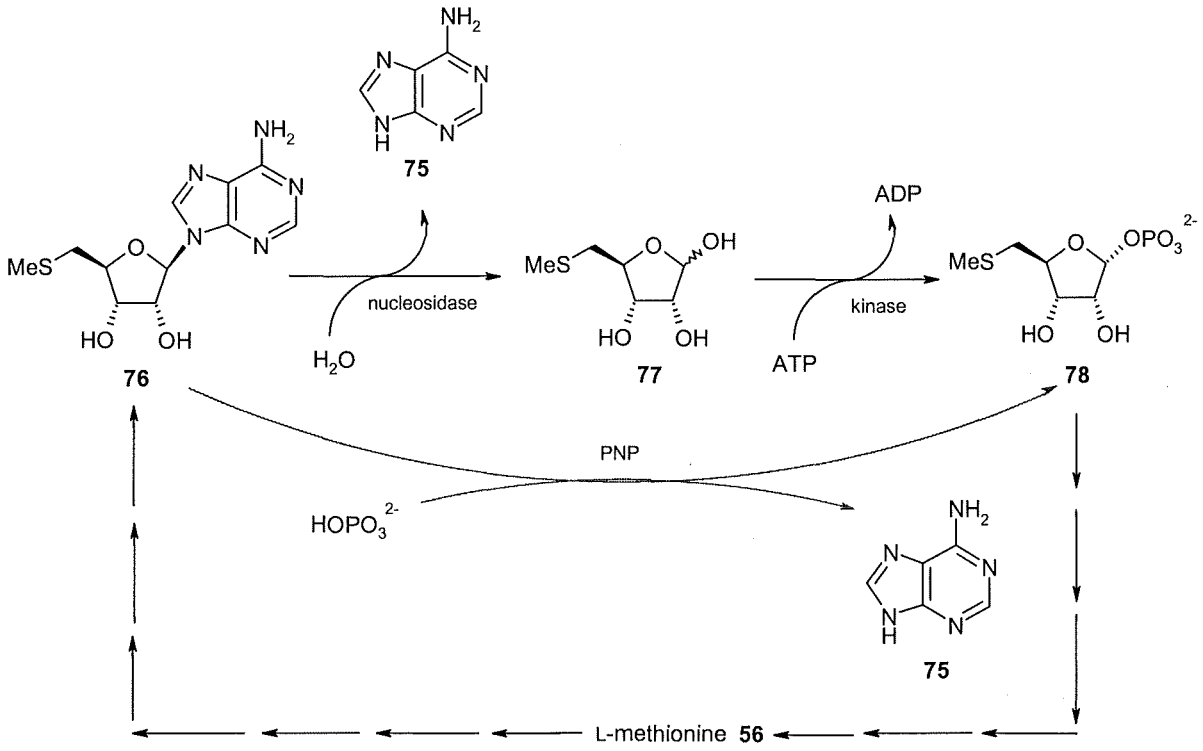

Scheme 2.2 Section of the L-methionine salvage pathway showing two routes for the generation of MTRP **78** from MTA **76**.

The more energy efficient pathway involves the phosphorolysis of MTA **78** to yield methylthioribose-1-phosphate (MTRP) **78** and adenine **75**, catalysed by the enzyme 5'-methylthio-5'-deoxyadenosine phosphorylase (MTAP). The existence of this metabolic route has been shown in mammals, as well as in bacteria and plants.[113] The second pathway splits this direct transformation into two steps; the first involves MTA **76** being

hydrolysed by the action of a nucleosidase to form adenine **75** and 5-methylthioribose (MTR) **77**. The free sugar is then phosphorylated at the expense of ATP by a specific kinase to generate MTRP **78**. This pathway has been characterised in the bacteria, *Klebsiella pneumoniae*[114] and *Bacillus subtilis*.[115] The product of both of these salvage routes, MTRP **78**, is recycled back to L-methionine **56** (see detail in Section 3.1).

2.2 Metabolic fate of 5'-FDA in *S. cattleya*

The metabolism of 5'-FDA **54** by either of the routes outlined in Scheme 2.2, can be followed by UV, monitoring the release of adenine **75**, in an HPLC assay. The method described below has been used throughout this chapter for detecting nucleosides and their corresponding bases. For the analysis of adenine **75** by HPLC, a C18 column was eluted with a gradient starting from 50 mM KH_2PO_4 : MeCN (95:5) to 50 mM KH_2PO_4 : MeCN (80:20) over 30 min and monitored at 254 nm[116,117] (see Section 5.1.17). Using this method; it is also possible to detect 5'-FDA **54** and the shunt product 5'-FDI **55** concurrently by HPLC.

In order to detect the release of adenine **75**, two key experiments were performed. Firstly, a CFE (500 μl) was prepared according to the method described in Section 5.1.6, which was incubated with synthetic 5'-FDA **54** (100 μl, 18.6 mM) at 37 °C for 16 hrs, and the assay solution was subsequently analysed by ^{19}F NMR spectroscopy. The presence of fluoroacetate **8** and 4-fluorothreonine **47** in successful biotransformations confirmed that the CFE retained all of the biosynthetic activities. In supporting experiments, the CFE was incubated with 5'-FDA **54** at a lower concentration (1 mM) compared to the previous experiment. In these experiments the CFE (500 μl) was incubated with 5'-FDA **54** (final conc. 1 mM) for only 1 hr at 37 °C and subsequently analysed by HPLC. The chromatogram for such an analysis is shown in Figure 2.1.

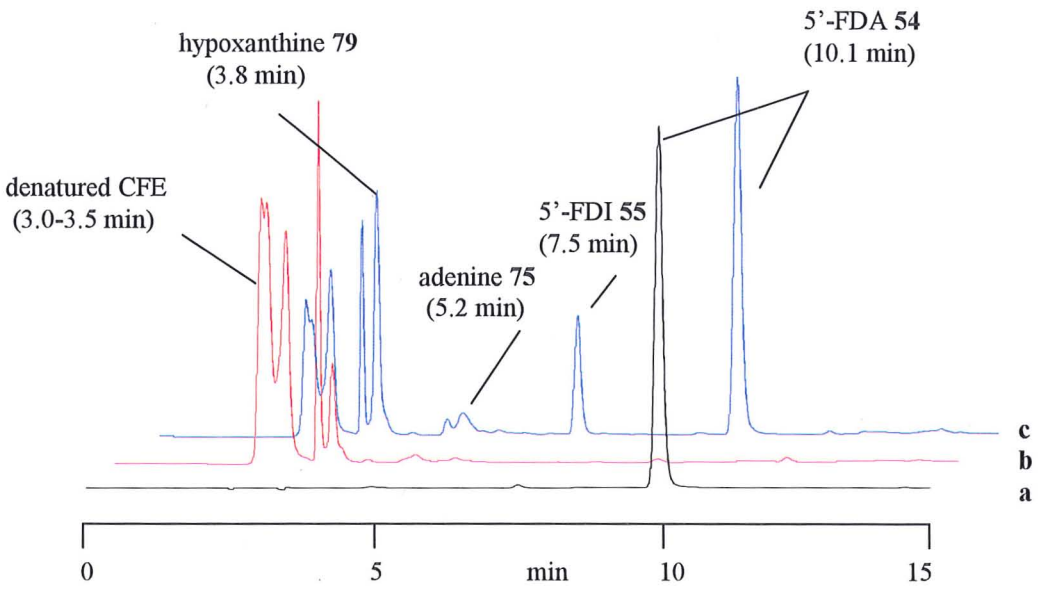

Figure 2.1 HPLC chromatogram showing **(a)**, synthetic 5'-FDA **54** (control), **(b)**, denatured CFE (control), **(c)**, CFE incubated with 5'-FDA **54** for 1 hr at 37 °C.

The two chromatograms corresponding to **a** and **b** represent control experiments of a synthetic sample of 5'-FDA **54** and a denatured CFE respectively. The outcome of an incubation of the CFE with 5'-FDA **54** is reported by chromatogram **c**. The presence of 5'-FDI **55** can clearly be seen from the incubation of 5'-FDA **54** due to a deaminase activity in the CFE. This was confirmed by co-injection experiments using a synthetic sample of 5'-FDI **55**. The presence of adenine **75** from the incubation of 5'-FDA **54** in the CFE confirmed that C-N glycosidic bond of 5'-FDA **54** is cleaved. This was confirmed by co-injection using a synthetic sample. Also, the presence of the purine, hypoxanthine **79** was observed, which can be attributed to deamination of adenine **75** by the presence of a possible adenine deaminase activity in *S. cattleya*. This was also confirmed by co-injection using a synthetic sample of hypoxanthine **79**. Scheme 2.3 summarises the proposed metabolic fate of 5'-FDA **54** in the light of these experimental observations.

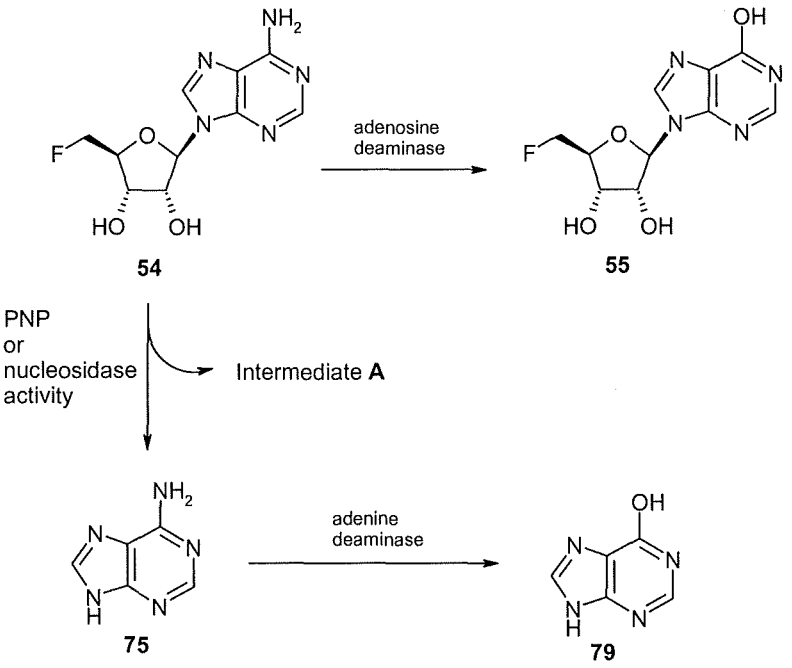

Scheme 2.3 The metabolism of 5'-FDA **54** in a CFE of *S. cattleya*. Intermediate **A** corresponds to the next fluorinated metabolite on the pathway.

It is concluded that the next intermediate after 5'-FDA **54** arises as a consequence of C-N glycosidic cleavage of 5'-FDA **54**. No further intermediates were detected by HPLC, suggesting that the next fluorinated metabolite is not UV active. With this background it became necessary to determine the identity of intermediate **A**.

2.2.1 The role of 5-fluoro-5-deoxy-D-ribose (5-FDR)

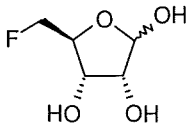

80

At the outset it appeared appropriate to explore a role for 5-FDR **80,** a potential hydrolysis product of 5'-FDA **54** as a possible intermediate in fluorometabolite biosynthesis in *S. cattleya*. The CFE was first assayed by ^{19}F NMR using synthetic 5'-FDA **54** to confirm the production of fluoroacetate **8** and 4-fluorothreonine **47**. This ensured all of the

biosynthetic enzymes on the pathway were active. A synthetic sample of 5-FDR **80** was prepared by S. L. Cobb,[118] University of St Andrews. This compound was tested as a biosynthetic intermediate by incubating it with an active CFE (500 μl) of *S. cattleya* at a final concentration of 5.5 mM for 16 hrs at 37 °C (Section 5.1.8). Figure 2.2 shows two ^{19}F NMR spectra at zero-time and after 16 hrs, with the first showing the 5-FDR **80** control with two characteristic fluorine signals, each a doublet of triplets corresponding to the β-anomer (-228.55 ppm, $^{2}J_{F,H}$ 47.0 and $^{3}J_{F,H}$ 26.4) and the α-anomer (-230.86 ppm, $^{2}J_{F,H}$ 46.9 and $^{3}J_{F,H}$ 26.3). The second spectrum shows the outcome after incubating 5-FDR **80** with the CFE for 16 hrs at 37 °C.

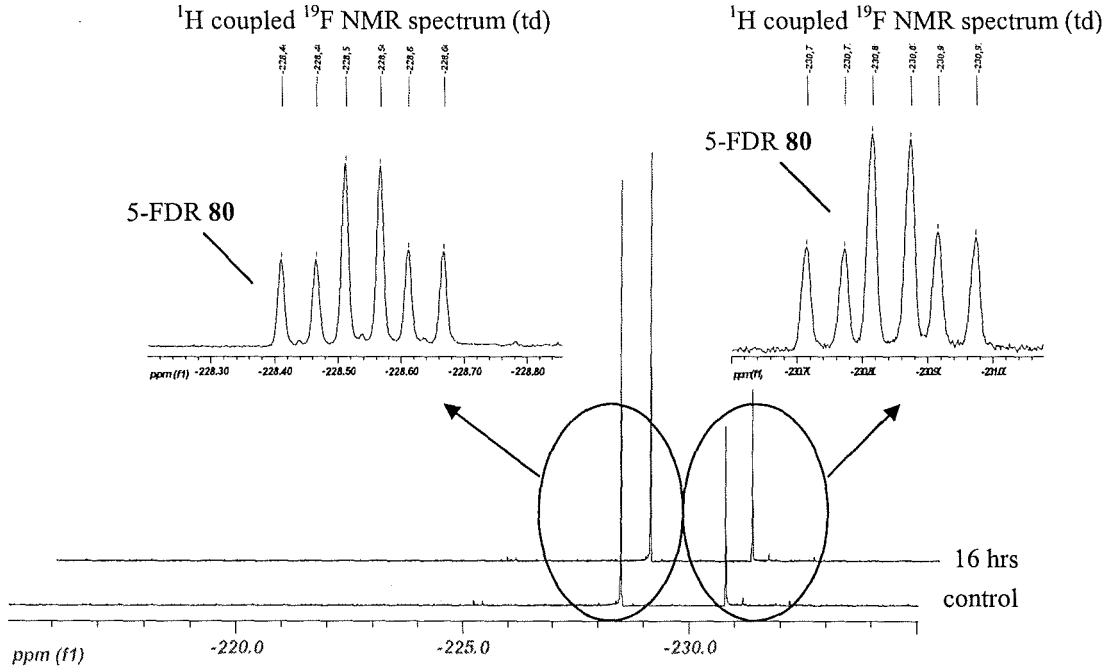

Figure 2.2 ^{19}F {^{1}H} NMR showing 5-FDR **80** (control), overlaid with 5-FDR **80** incubated in a CFE of *S. cattleya* for 16 hrs at 37 °C. Expansions are ^{1}H coupled ^{19}F NMR spectra.

This result clearly suggests that 5-FDR **80** is not metabolised in an active CFE of *S. cattleya*. No new fluorinated metabolites emerged and therefore 5-FDR **80** was not able to support the biosynthesis of fluoroacetate **8** and 4-fluorothreonine **47**. It is therefore

concluded that 5-FDR **80** is not an intermediate on the fluorometabolite biosynthetic pathway in *S. cattleya*. The presence of a nucleosidase activity responsible for the release of adenine **75** from 5'-FDA **54** can clearly be ruled out. The alternative route which facilitates the cleavage of the C-N glycosidic bond of 5'-FDA **54** involving a phosphorolysis reaction was thus investigated.

2.2.2 The role of 5-fluoro-5-deoxy-D-ribose-1-phosphate (5-FDRP)

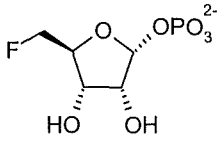

81

In order to explore 5-FDRP **81** as a possible biosynthetic intermediate on the fluorometabolite pathway, a reference sample was required. The chemical synthesis of ribose-1-phosphates is well documented in the literature.[119] However, a more convenient strategy towards the preparation of 5-FDRP **81** involved a chemo-enzymatic method using two commercially available enzymes. Firstly, an adenosine deaminase (EC 3.5.4.4, from *Aspergillus species*) was used for the conversion of 5'-FDA **54** to 5'-FDI **55** and then a bacterial PNP (EC 2.4.2.1 from *E. coli*) specific for 6-oxo nucleosides was used to generate the products 5-FDRP **81** and hypoxanthine **79**. This enzyme showed sufficiently lax substrate specificity and could utilise 5'-FDI **55**. Scheme 2.4 outlines the chemo-enzymatic route used to prepare a sample of 5-FDRP **81**.

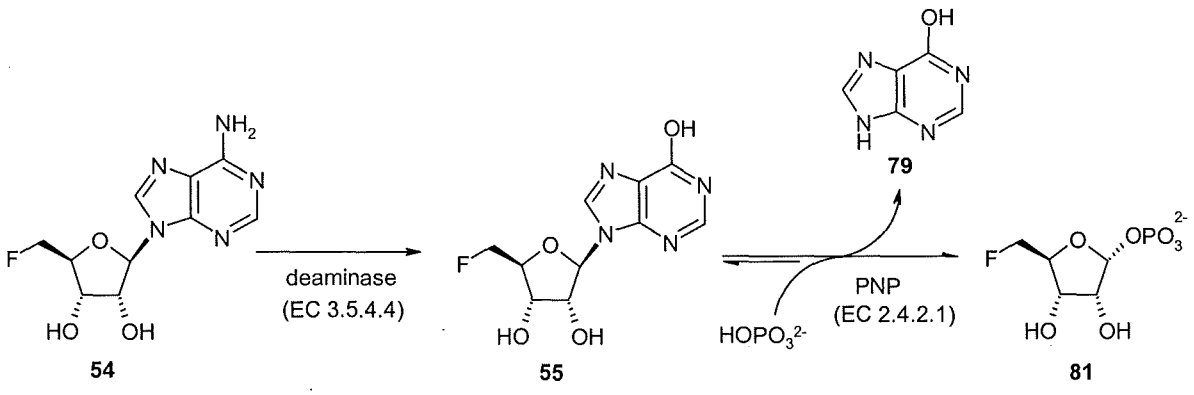

Scheme 2.4 Chemo-enzymatic preparation of 5-FDRP **81**

In order to monitor each enzymatic step, a HPLC method was established for the detection of 5'-FDI **55** and hypoxanthine **79**. The HPLC assay is outlined in detail in Section 5.1.17. Accordingly, the deamination of 5'-FDA **54** (18.6 mM) to 5'-FDI **55** using a commercial adenosine deaminase from *Aspergillus species* in phosphate buffer (50 mM, pH 6.8) was monitored until 100 % biotransformation was achieved. Typical chromatograms (**a**) to (**b**), are shown in Figure 2.3. The product 5'-FDI **55** was then incubated in the presence of an immobilised PNP (EC 2.4.2.1, *E. coli*) in phosphate buffer (50 mM, pH 6.8). Because the enzymatic preparation of 5-FDRP **81** using a PNP enzyme is a reversible process, it was not possible to obtain 100 % conversion to 5-FDRP **81**. Extended incubations at 37 °C generally achieved a maximum conversion of ~40-50 % (chromatogram (**c**), Figure 2.3). The product of this incubation was subsequently analysed by ^{19}F NMR spectroscopy.[118]

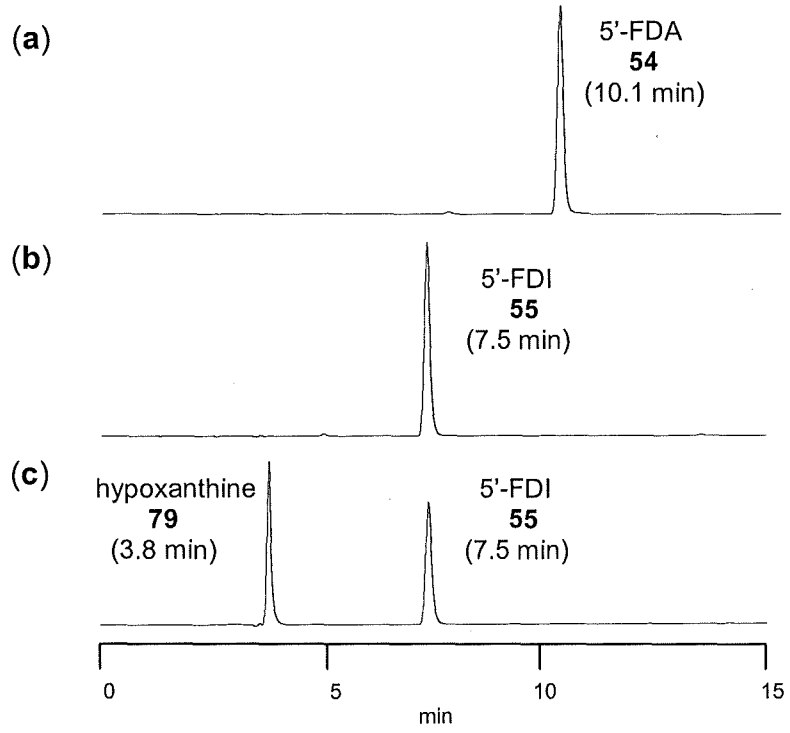

Figure 2.3 HPLC traces illustrating (**a**) synthetic 5'-FDA **54**, (**b**) 5'-FDA **54** incubated with adenosine deaminase and (**c**) 5'-FDI **55** incubated with immobilised PNP.

2.2.3 Incubation of 5-FDRP in a CFE of *S. cattleya*

5-FDRP **81** prepared as described in detail in Section 5.1.9 was used to explore its role as an intermediate on the fluorometabolite pathway by incubating this preparation with an active CFE of *S. cattleya.* As a consequence of its preparation, the 5-FDRP **81** sample also contained an excess of 5'-FDI **55** due to the reversibility of the PNP. However, from the control experiments it was already established that 5'-FDI **55** is not metabolised in the CFE. Accordingly, a sample of 5-FDRP **81** (200 μl) was incubated with the CFE (500 μl) for 16 hrs at 37 ^{o}C and the product subsequently analysed by ^{19}F NMR to establish if organofluorine metabolism had occurred. The resultant spectrum is shown in Figure 2.4.

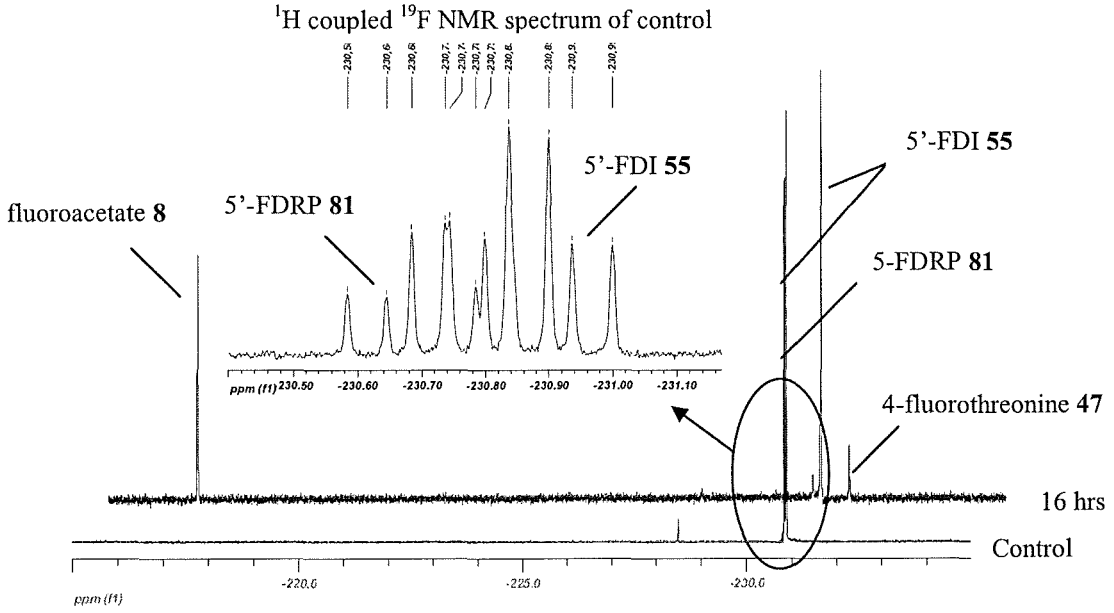

Figure 2.4 ^{19}F {^{1}H} NMR spectra indicating fluorometabolite production after incubation of 5-FDRP **81** (+5'-FDI **55**) in a CFE of *S. cattleya*.

The ^{19}F NMR spectrum of the control experiment (zero time) shows the 5-FRDP **81**, 5'-FDI **55** mixture in the presence of a denatured CFE with their characteristic chemical shifts corresponding to 5-FDRP **81** (-230.78 ppm) and 5'-FDI **55** (-230.85 ppm) respectively. It is clear that under such control conditions both fluorinated compounds are stable indicating that no chemical degradation has occurred. In the second ^{19}F NMR spectrum, the production of the two fluorinated secondary metabolites, fluoroacetate **8** and 4-fluorothreonine **47** is obvious, confirming that 5-FDRP **81** supports the biosynthesis of these secondary metabolites in *S. cattleya*. The biosynthetic intermediates that exist between 5-FDRP **81** and fluoroacetaldehyde **48** are not observed by ^{19}F NMR, suggesting that incubation for 16 hrs is sufficiently long to metabolise the remaining intermediates through to the end products, or that they are transient.

In order to reinforce this result, another experiment was conducted to show that 5-FDRP **81** is biosynthesised in *S. cattleya.* This involved the exogenous addition of an alkaline

phosphatase (EC 3.1.3.1 from bovine intestinal mucosa) to the CFE incubation. This phosphatase should hydrolyse any 5-FDRP **81** and result in the accumulation of the free sugar, 5-FDR **80**. Synthetic 5-FDR **80** has already been shown to be metabolically inert in CFE's of *S. cattleya*. Therefore, the accumulation of 5-FDR **80** as a biotransformation product of 5-FDA **54** after addition of a commercial phosphatase activity, would clearly support the intermediacy of 5-FDRP **81** (Scheme 2.5).

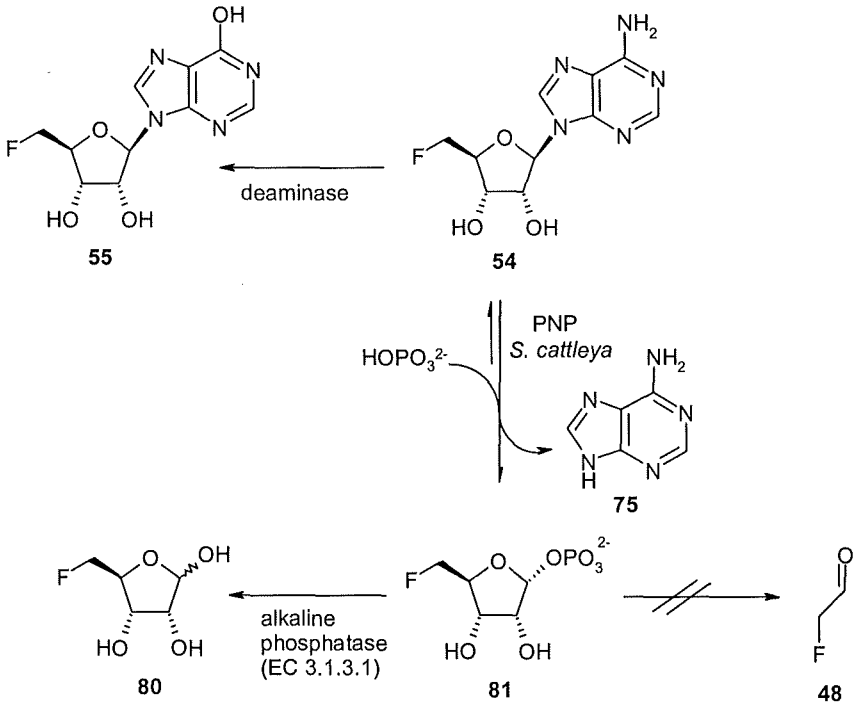

Scheme 2.5 Summary of 5'-FDA **54** biotransformation in CFE's of *S. cattleya* with an 'added' alkaline phosphatase.

Control experiments were first performed in order to show that phosphorolytic cleavage of 5-FDRP **81** occurred using a commercial alkaline phosphatase from bovine intestinal mucosa. Accordingly, 5-FDRP **81** was prepared as outlined in Section 5.1.9 and the solution was supplemented with the alkaline phosphatase (20 μl, 2 mg / ml) in phosphate buffer (50 mM, pH 6.8) and incubated at 37 °C for 16 hrs.

The analysis by ^{19}F NMR spectroscopy showed a complete conversion of 5-FDRP **81** to 5-FDR **80** with the two characteristic fluorine signals corresponding to the β-anomer (-228.54 ppm, $^{2}J_{F,H}$ 47.3 and $^{3}J_{F,H}$ 25.6) and the α-anomer (-230.85 ppm, $^{2}J_{F,H}$ 47.3 and $^{3}J_{F,H}$ 26.8). With this control established, a reaction was then performed in which an active CFE (500 μl) was incubated with 5'-FDA **54** (100 μl, 18.6 mM) in phosphate buffer (50 mM, pH 6.8) but now supplemented with the phosphatase (20 μl, 2 mg / ml). The incubation was carried out at 37 °C for 16 hrs. (Figure 2.5**b**).

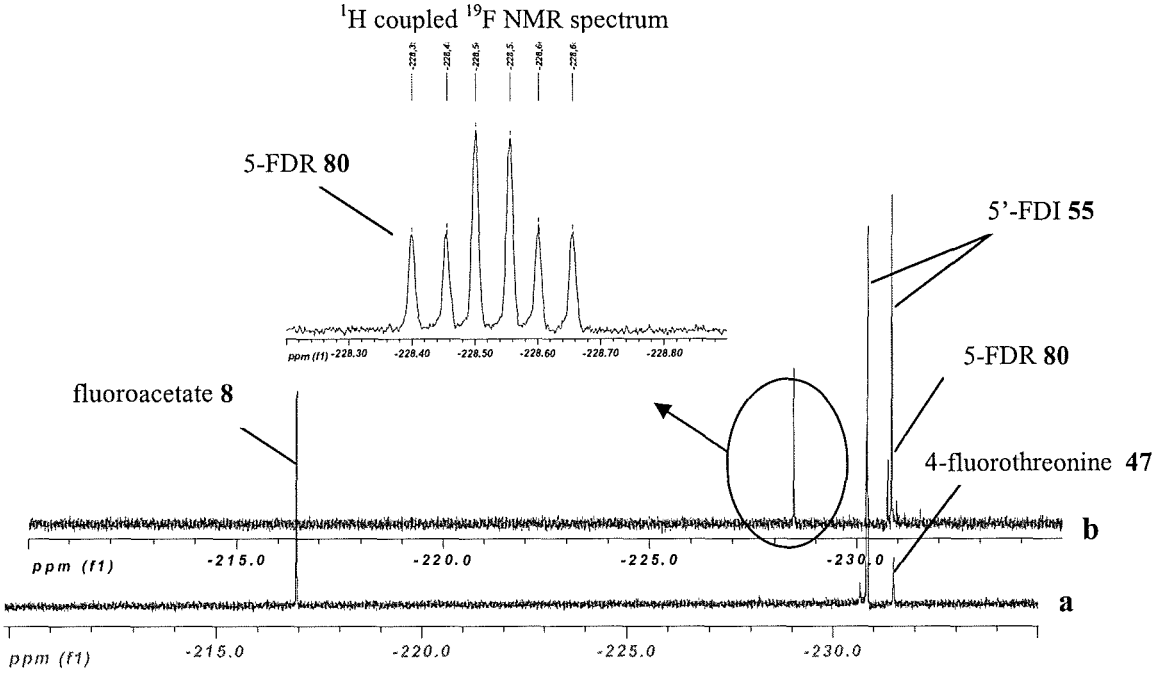

Figure 2.5 ^{19}F {^{1}H} NMR spectra after incubation of (**a**) 5'-FDA **54** in a CFE of *S. cattleya* for 16 hrs at 37 °C, (**b**) 5'-FDA **54** in a CFE supplemented with alkaline phosphatase for 16 hrs at 37 °C.

The ^{19}F NMR spectroscopy analysis (Figure 2.5**b**) resulted in three signals indicating the presence of three organo-fluorine compounds. Two of these signals corresponded to the two anomers of 5-FDR **80**. No fluoroacetate **8** or 4-fluorothreonine **47** was produced during this biotransformation. Their biosynthesis had been arrested. This clearly

confirmed the phosphorolytic cleavage of 5-FDRP **81** by the added alkaline phosphatase. In order to assign the remaining organo-fluorine signal (-230.88 ppm), HPLC analysis was carried out. This analysis indicated the presence of 5'-FDI **55** and the ^{19}F NMR was consistent with this assignment. The presence of 5'-FDI **55** can be attributed again to adventitious deaminase activity in the CFE.

In conclusion, the results from this section have demonstrated that 5'-FDA **54** is metabolised to 5-FDRP **81** by the action of a PNP activity in a CFE of *S. cattleya*.

2.2.4 Incubation of 2'-deoxy-5'-FDA in a CFE of *S. cattleya.*

To explore the substrate specificity of the PNP in *S. cattleya*, 2'-deoxy-5'-FDA **59** was explored as a substrate to see if it is converted to 2-deoxy-5-FDRP **82**. From previous literature it is known that 2-deoxy nucleosides can act as PNP substrates.[120] An active CFE (500 μl) was incubated with synthetic 2'-deoxy-5'-FDA **59** (100 μl, 18.6 mM) (prepared by S. L. Cobb)[118] for 16 hrs at 37 °C. The resultant ^{19}F NMR spectrum is shown in Figure 2.6.

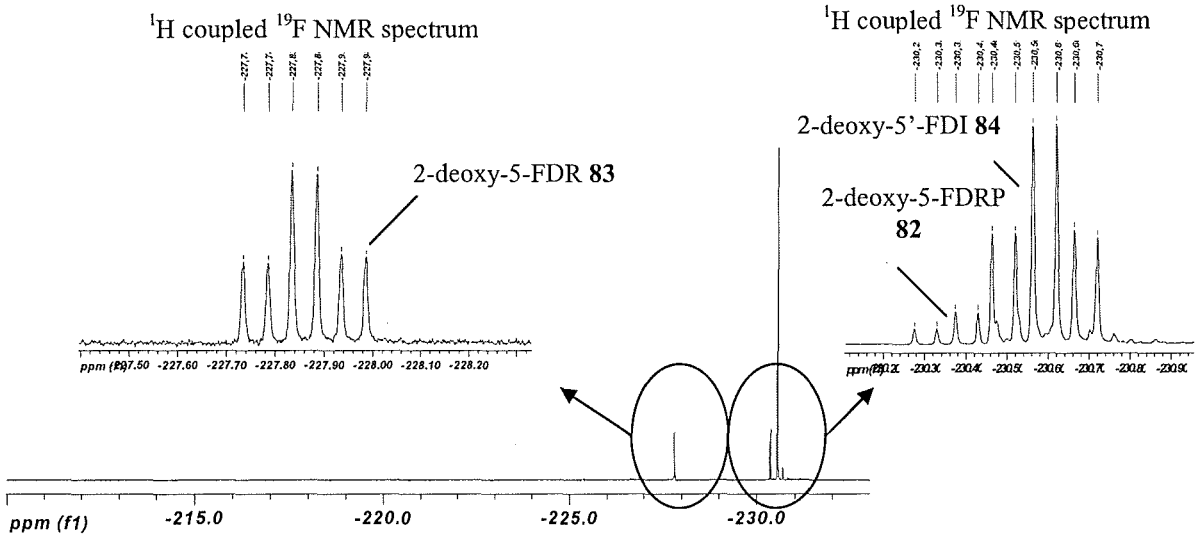

Figure 2.6 ^{19}F {^{1}H} NMR of a CFE incubated with 2-deoxy-5'-FDA **59**. Expansions are ^{1}H coupled ^{19}F NMR spectrum.

Incubation of 2'-deoxy-5'-FDA **59** did not support secondary metabolite production deduced by the absence of fluoroacetate **8** and 4-fluorothreonine **47**. From results obtained in Section 2.3.8, 2-deoxy-5-FDRP **82** is formed from the phosphorolytic cleavage of 2'-deoxy-5'-FDA **59** by the action of a PNP. The fluorine signal at -230.60 ppm was confirmed as 5'-fluoro-2',5'-dideoxy-inosine (2'-deoxy-5'-FDI) **84** by HPLC analysis against a reference sample of 2'-deoxy-5'-FDI **84** prepared independently by the direct deamination of 2'-deoxy-5'-FDA **59** using a commercial adenosine deaminase from *Aspergillus species*. The final fluorine signal at -227.81 ppm was identified as 5-fluoro-2,5-dideoxy-D-ribose (2-deoxy-5-FDR) **83** by comparison to a synthetic sample. Production of 2-deoxy-5-FDR **83** could arise from the presence of a phosphatase activity operating within the CFE. This adventitious activity is not present on the fluorometabolite pathway, as discussed in earlier experiments.

In order to confirm this assumption, a sample of 2-deoxy-5-FDRP **82** was prepared by incubating a synthetic sample of 2'-deoxy-5'-FDI **84** with an immobilised PNP (EC 2.4.2.1, *E. coli*). The generated product was subsequently treated with a commercial phytase enzyme (EC 3.1.3.8, *Aspergillus ficuum*) to remove the 1-phosphate group of 2-deoxy-5-FDRP **82**. The sample was then re-analysed by ^{19}F NMR and all of the 2-deoxy-5-FDRP **82** had converted to the free sugar 2-deoxy-5-FDR **83**.

The fact that 2'-deoxy-5'-FDA **59** cannot support the CFE biosynthesis of the fluorinated secondary metabolites fluoroacetate **8** and 4-fluorothreonine **47** suggests that a 2-OH group on the ribose ring is essential for further metabolism of the fluorinated sugar phosphate intermediate, 5-FDRP **81**. Overall, the results obtained are summarised in Scheme 2.6.

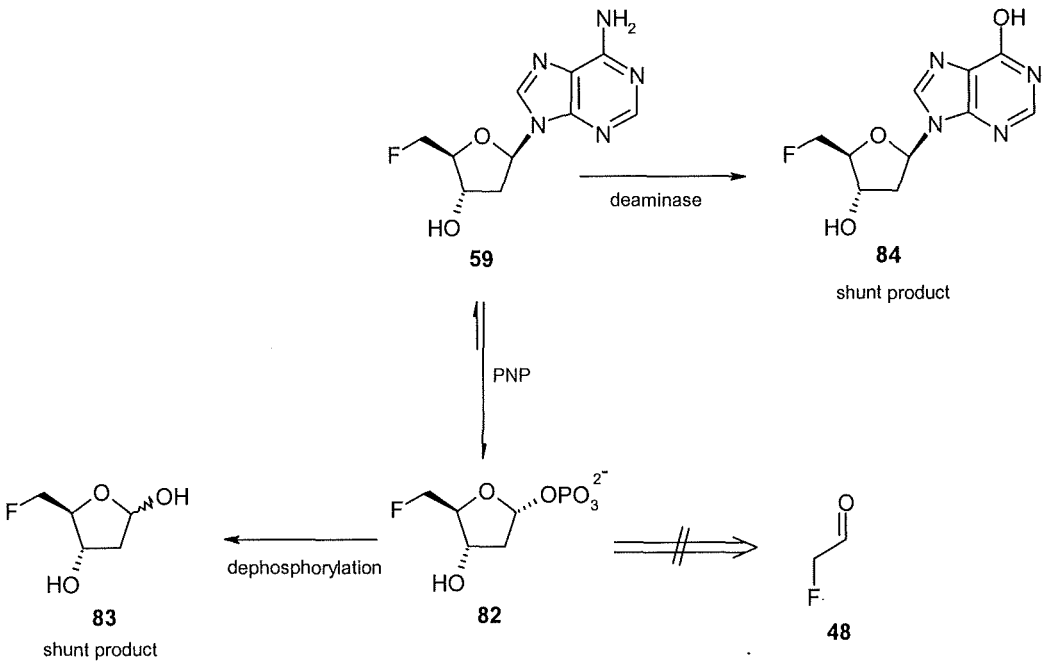

Scheme 2.6 Summary of 2'-deoxy-5'-FDA **59** biotransformation in CFE's of *S. cattleya*

With the presence of a PNP in *S. cattleya* now established the next objective was to purify the enzyme and these results are discussed in due course. Firstly however a general review on PNP enzymes is presented.

2.2.5 Purine nucleoside phosphorylase (PNP)

Purine nucleoside phosphorylases (PNP's) catalyse the reversible phosphorolysis between inorganic phosphate and the glycosidic bond of purine ribo- and deoxyribo-nucleosides and their analogues.[120] This phosphorolysis generates the free purine and a (deoxy) ribose-1-phosphate sugar. These enzymes are perhaps the most thoroughly studied members of the nucleoside phosphorylase (NP-1) family. The biochemical significance of glycosidic bond cleavage in purines by the phosphorolytic mechanism is most apparent in the purine salvage pathway, which make use of nucleobases and nucleosides as precursors in the production of nucleotides.[121,122] Previous studies have shown that there are two distinct classes of purine nucleoside phosphorylases namely NP-1 and NP-2.[123] Members of the

NP-I class are structurally either homotrimers or homohexamers made up of subunits of ~31 kDa and ~26 kDa respectively. Enzymes belonging to the NP-I family can be further classified according to their substrate specificity and amino-acid sequences. Trimeric PNPs specific for guanine and hypoxanthine (2'-deoxy) ribonucleosides are present in mammalian species. The hexameric PNPs, accept a broader range of substrates including adenine, guanine and hypoxanthine (2'-deoxy) ribonucleosides. These are mainly prevalent in bacterial species, although *Escherichia coli*,[123] *Bacillus subtilis*,[124] and *B. stearothermophilus*[125] appear to have both trimeric and hexameric forms. Other members of the NP-1 family include uridine phosphorylase (UP; EC 2.2.2.3) and 5'-deoxy-5-methylthioadenosine phosphorylase (MTAP; EC 2.4.2.28). UP has been shown to be specific for uridine nucleosides although it also accepts its 2'-deoxy analogues.[126] The enzyme functions as a hexamer with identical subunits corresponding to a molecular mass of approx. 27.5 kDa. MTAP, which is specific for the purine nucleoside analogue 5'-deoxy-5'-methylthioadenosine, is known to function mainly in a trimeric form with identical subunits of approx. 30 kDa. MTAP has been isolated and characterised from bacterial and mammalian species.[127,128,129] Members of the NP-II family are those enzymes that display a dimeric quaternary structure. Members of this family accept both thymidine and uridine in lower organisms,[111] but are specific for thymidine in higher species, including humans.[111]

2.3 Purification of a PNP from *S. cattleya*

2.3.1 Assay for PNP activity in *S. cattleya*

In order to purify the PNP enzyme from *S. cattleya* CFE, a suitable enzyme assay was required. Due to the strong chromophores of 5'-FDA **54** and adenine **75**, a UV-HPLC

method was used to assay for PNP activity in *S. cattleya*. The method was based on the assay outlined in Section 5.1.17, and is used throughout this section when assaying for PNP activity. It was found that during the early stages, purification of the PNP activity was confounded by the fact that 5'-FDI **55** and hypoxanthine **79** were also generated due to the simultaneous presence of the deaminase activity as previously discussed. Therefore, in the initial stages, purification was assayed by monitoring the levels of hypoxanthine **79**, adenine **75**, 5'-FDI **55** and 5'-FDA **54** in the same HPLC chromatogram (Figure 2.7).

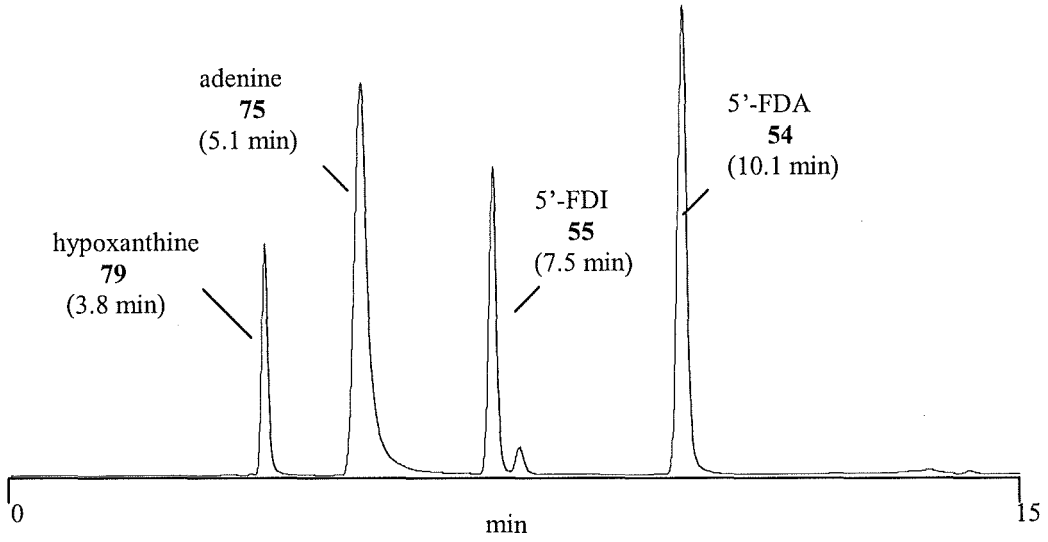

Figure 2.7 HPLC chromatogram of hypoxanthine **79**, adenine **75**, 5'-FDI **55** and 5'-FDA **54** elution respectively.

2.3.2 Step 1: Ammonium sulfate precipitation

In the first stage of the PNP purification, the crude cell-free extract (~4 mg / ml) was subjected to ammonium sulfate precipitation to salt out the desired protein. It was shown that addition of $(NH_4)_2SO_4$ to the CFE at concentrations of 35-50 % contained the desired PNP activity. No PNP activity was detected in any of the other fractions. The protein pellet could be used directly for further purification or alternatively stored at -80 °C.

The assay was performed by incubating this partially purified protein extract (100 μl) with 5'-FDA **54** (1 mM) in phosphate buffer (50 mM, pH 6.8) for 7 hrs at 37 °C. The sample was then heated to 100 °C for 3 min and the precipitated protein removed by centrifugation. For HPLC analysis, the supernatant (20 μl) was automatically injected in duplicates onto a reverse phase C18 column (Figure 2.8).

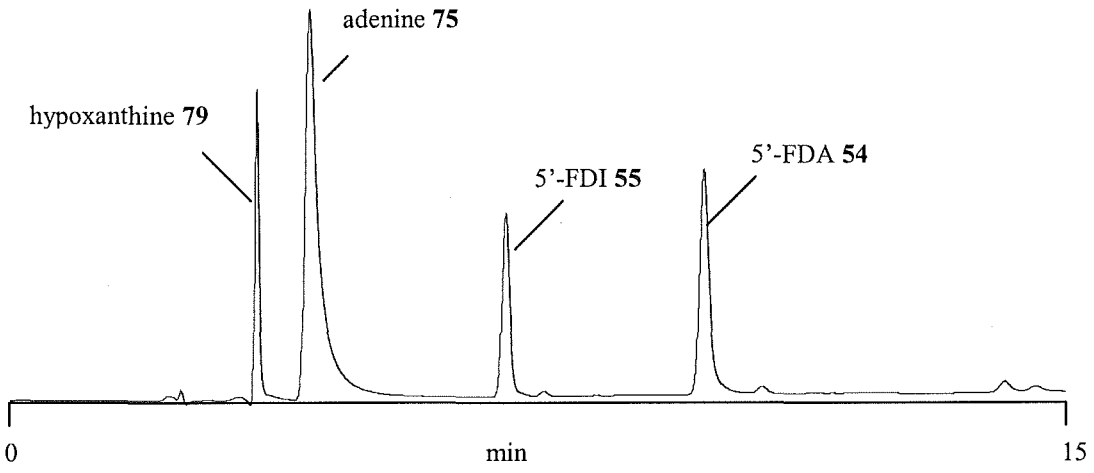

Figure 2.8 PNP assay: HPLC showing the products of a partially purified fraction incubated with 5'-FDA **54** at 37 °C for 7 hrs.

The assay shows that during the initial purification stages, in addition to the PNP activity, the accumulation of the shunt products 5'-FDI **55** and hypoxanthine **79** also indicate the presence of deaminase activity in the extract.

2.3.3 Step 2: Hydrophobic interaction chromatography

The second stage of the PNP purification involved passing the protein down a phenyl HP, (40 ml) column. Separation involves exploiting a hydrophobic attraction between the stationary phase and the protein. The stationary phase consists of small non-polar phenyl groups attached to a hydrophilic polymer backbone. The sample is loaded in a buffer

containing a high concentration of a non-denaturing salt (e.g. $(NH_4)_2SO_4$)). The proteins are then eluted as the concentration of the salt in the buffer is decreased.

Accordingly, the (Phenyl HP, 40 ml) column was equilibrated with phosphate buffer (50 mM, pH 6.8), supplemented with 1 M $(NH_4)_2SO_4$. Since the protein sample contained $(NH_4)_2SO_4$, prior treatment of the sample wasn't necessary. The protein pellet was re-dissolved in the starting buffer (5 ml, ~21 mg / ml) and filtered through a 0.45 µm filter to remove any particulate matter. The filtrate was applied by injection (5 ml) to the equilibrated phenyl HP column. The column was washed with 2 column volumes of the equilibrated starting buffer (flow rate of 2 ml / min) and subsequently eluted over a stepwise gradient from 1 M to 0 M $(NH_4)_2SO_4$ at a continuous flow rate of 2 ml / min. A typical chromatogram for such an analysis is shown in Figure 2.9.

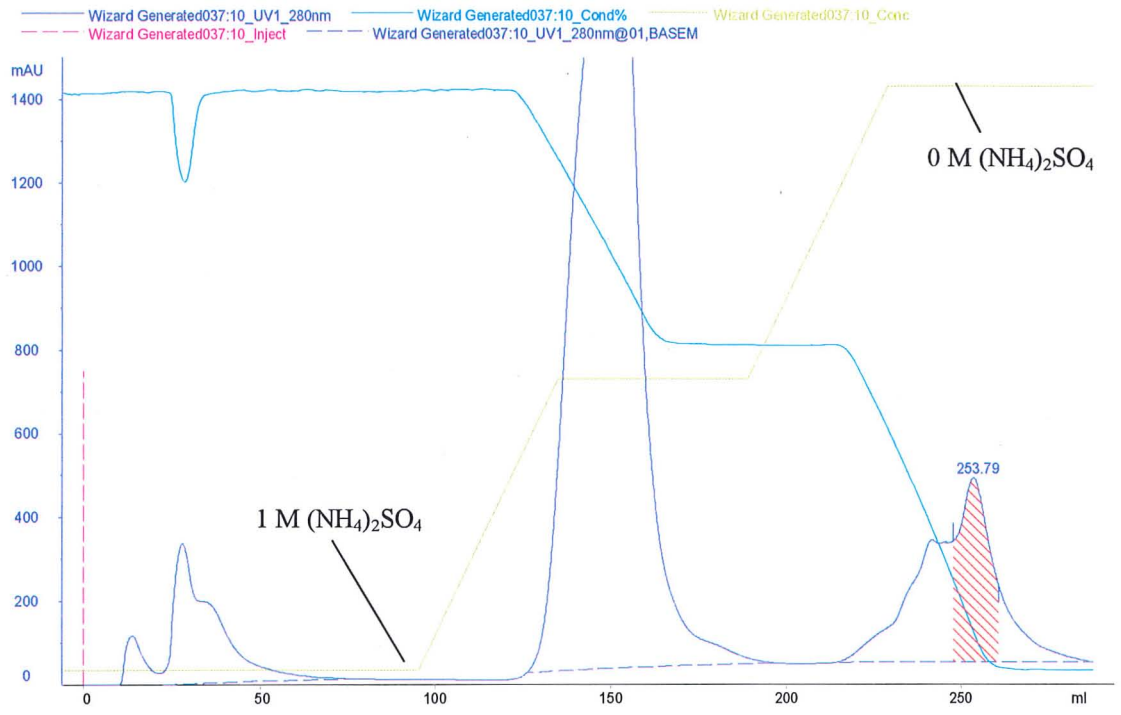

Figure 2.9 Phenyl HP (40 ml) chromatogram obtained after second stage purification.

The elution profile monitored at 280 nm in Figure 2.9 shows several protein peaks eluting at various stages during the purification protocol. The eluted fractions (4 ml) were assayed

for PNP activity by incubation of the eluent (100 μl) with 5'-FDA **54** (1 mM) at 37 °C for 7 hrs. PNP active fractions were shown to elute at the end of the gradient (highlighted area) indicating a high affinity of the enzyme towards the hydrophobic resin. The average volume which contained PNP activity was 12 ml with a protein concentration of ~0.5 mg / ml. No activity was detected in any of the other peaks. A substantial amount of protein did not bind to the column under the described conditions showing the removal of protein contaminants. However, the majority of protein was shown to elute from the column during the stepwise gradient at a concentration of phosphate buffer (50 mM, pH 6.8), supplemented with 0.4 M $(NH_4)_2SO_4$. Overall, the purification using hydrophobic interaction chromatography removed a substantial amount of undesired protein, and was an effective protocol.

2.3.4 Step 3: Ion exchange chromatography

The partially purified extract from Section 2.3.3 was subjected to anion exchange chromatography. This method is based on the binding of charged proteins to oppositely charged groups attached to an insoluble matrix. It follows that to bind a protein to an anion exchange column; the pH of the mobile phase must be above its pI in order to carry a net negative charge. Protein elution is achieved by a gradient of increasing salt (e.g NaCl) concentration. The fractions containing the PNP activity after Step 2 purification were pooled together (12 ml) and concentrated to (2 ml) by centrifugation. The concentrated protein was then passed through a desalting column (HiTrap™ desalting, 5 ml, Amersham) and re-concentrated to ~2 ml by the same method.

A strong anion exchange column (Q, 5 ml, Amersham Biosciences) was equilibrated with tris buffer (50 mM, pH 7.2) and loaded with the desalted protein sample (2 ml) containing

the PNP activity. The column was then eluted using a stepwise salt gradient to tris buffer (50 mM, pH 7.2) supplemented with 1 M KCl over 50 ml at a flow rate of 2 ml / min. The chromatogram in Figure 2.10 shows several protein peaks eluting at various stages during the protocol.

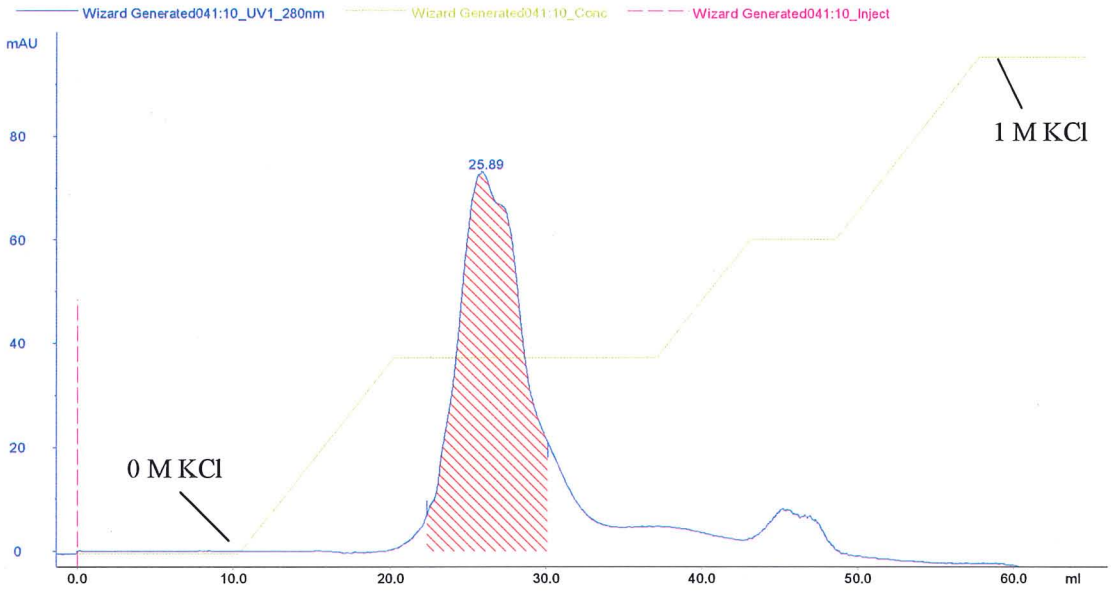

Figure 2.10 Anion exchange chromatogram, (Q column, 5 ml). The highlighted area represents PNP activity.

The resultant chromatogram shows several peaks eluting during the application of the stepwise gradient. Incubation and analysis of each fraction for PNP activity indicated the presence of active fractions eluting after 250 mM KCl gradient (highlighted area). The volume which contained the activity was ~8 ml with a protein concentration of ~ 0.3 mg / ml. No PNP activity was detected in any of the other protein fractions. It is evident that there is no base line separation between the observed peaks surrounding the active PNP fractions indicating other proteins are still present.

2.3.5 PNP analysis by SDS PAGE

The partial purification of the PNP enzyme during each of the purification steps (1-3) was monitored by SDS-PAGE. Figure 2.11 shows the protein purity progressing through the three purification steps.

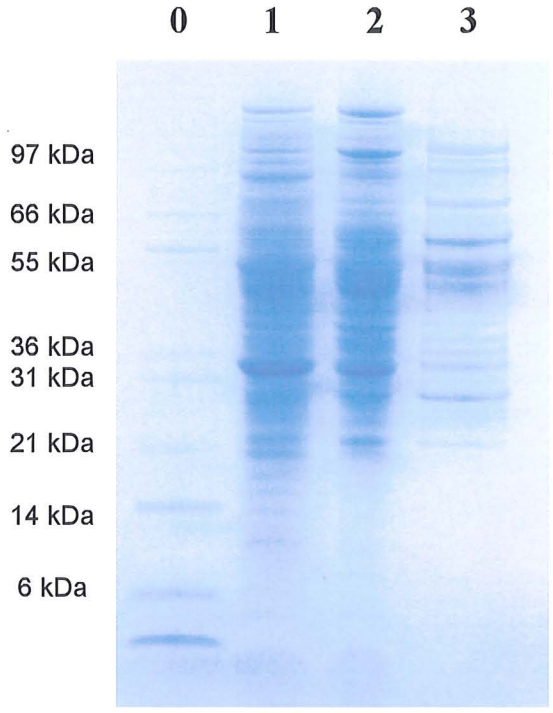

Figure 2.11 SDS PAGE gel (4-12 % acrylamide) showing pooled active protein fractions containing PNP activity during each purification step. Lanes: **0** molecular markers **1,** ammonium sulfate precipitation (35-50 %); **2,** hydrophobic interaction chromatography, **3,** anion exchange chromatography.

2.3.6 Production of 5-FDRP from the partially purified PNP

The partially purified PNP (100 µl, 0.5 mg / ml) solution was supplemented with 5'-FDA **54** (1 mM) in phosphate buffer (10 mM, pH 6.8) for 16 hrs at 37 °C. The sample was then heated to 100 °C for 3 min and the precipitated protein removed by centrifugation. Analysis of the supernatant by HPLC confirmed the phosphorolytic cleavage of 5'-FDA **54**

due to the presence of adenine **75**. Subsequently, the resulting supernatant was lyophilised and analysed by GC/MS after *N*-methyl-N-(trimethylsilyl)trifluoroacetamide (MSTFA) treatment which was carried out (Dr. J. Hamilton, University of Belfast). The mass spectrum obtained from GC/MS analysis is shown in Figure 2.12.

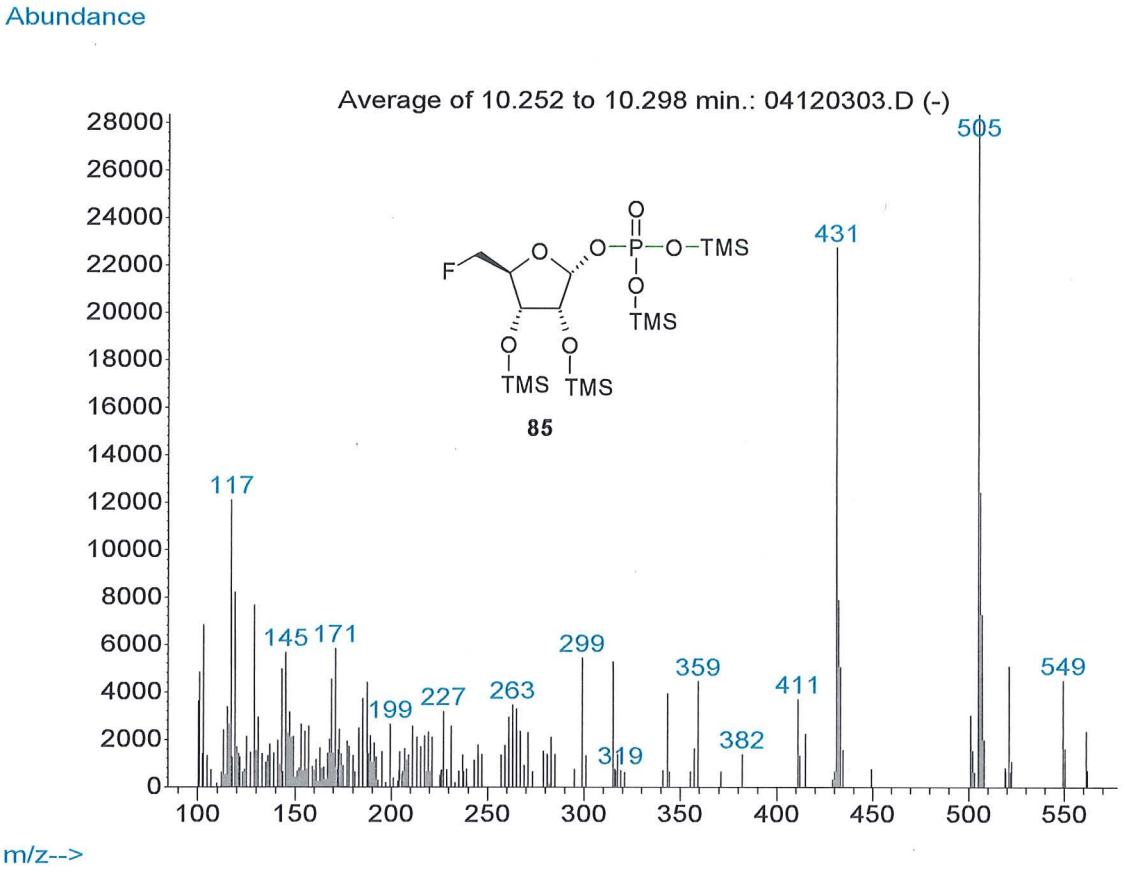

Figure 2.12 GC-MS spectrum of MSTFA derivative of 5-FDRP **85** chemical ionization (CI). Ion fragment m/*z* 505 is from (M^+- CH_3).

The resultant mass spectrum exhibits the *m/z* 505 ion which indicates the loss of CH_3 from the persilyl derivative of 5-FDRP **85**. Several of the other signals can be attributed to other ion fragments of the derivatised sample. This result indicates the presence of 5-FDRP **81** after the incubation of 5'-FDA **54** with partially purified PNP. Further analysis to support the observed result, was obtained by ESI-MS of a non derivatised sample of 5-FDRP **81**. This is shown in Figure 2.13.

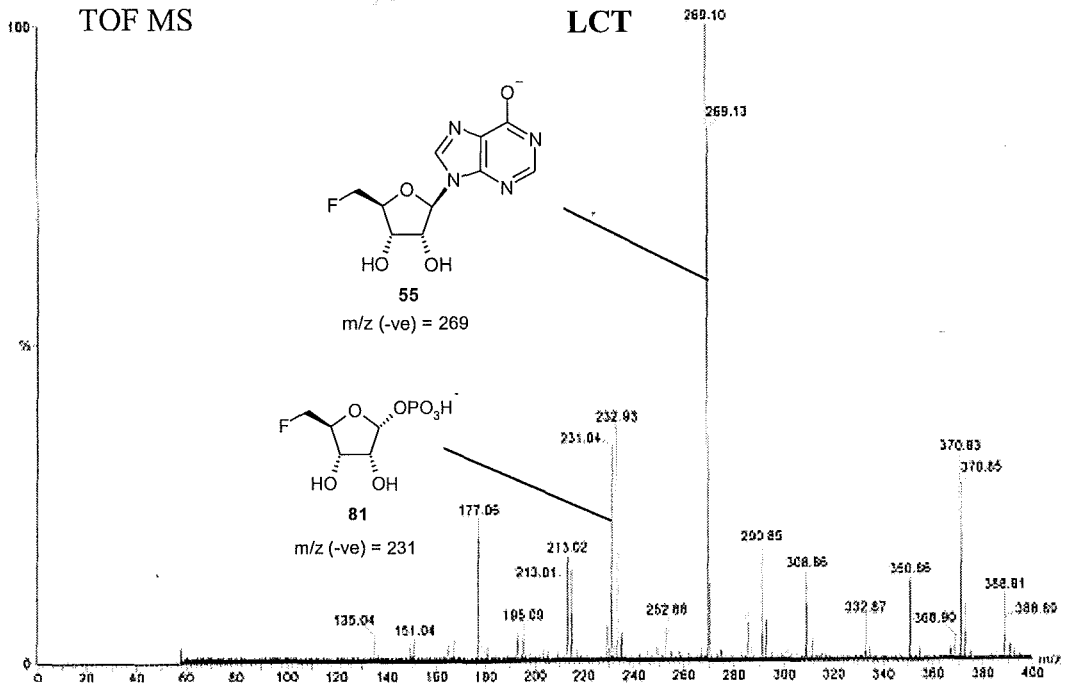

Figure 2.13 ESI-MS (-ve) spectrum of 5-FDRP **81** (M-H) and 5'-FDI **55** (M-H).

The analysis by ESI-MS shows an *m/z* signal at 231 in -ve mode. The mass of 5-FDRP **81** is 232, and therefore the *m/z* 231 ion is consistent with the mono anion. The strong *m/z* signal at 269 is assigned to [5'-FDI-H]$^-$ **55**. This result clearly shows the simultaneous presence of the deaminase activity in the partially purified PNP extract after hydrophobic interaction chromatography. However, these activities separate after anion exchange chromatography. Overall, this analysis supports the observed result from GC-MS, further confirming production of 5-FDRP **81** from 5'-FDA **54** by this enzyme.

2.3.7 Monitoring the PNP reaction by ^{19}F NMR

In order to study the PNP biotransformation of 5'-FDA **54** to 5-FDRP **81** in real time, a ^{19}F NMR time course experiment was carried out in an NMR tube. Accordingly, partially purified PNP (500 μl, ~0.5 mg / ml) in phosphate buffer (50 mM, pH 6.8) was taken

directly after anion exchange chromatography and was supplemented with 5'-FDA **54** (100 μl, 18.7 mM). The progress of the reaction was monitored by recording $^{19}F\{^{1}H\}$ NMR (470 MHz) spectra at one hour intervals over 8 hrs at 25 °C. Figure 2.14 shows the stacked ^{19}F NMR time course resulting from the biotransformation.

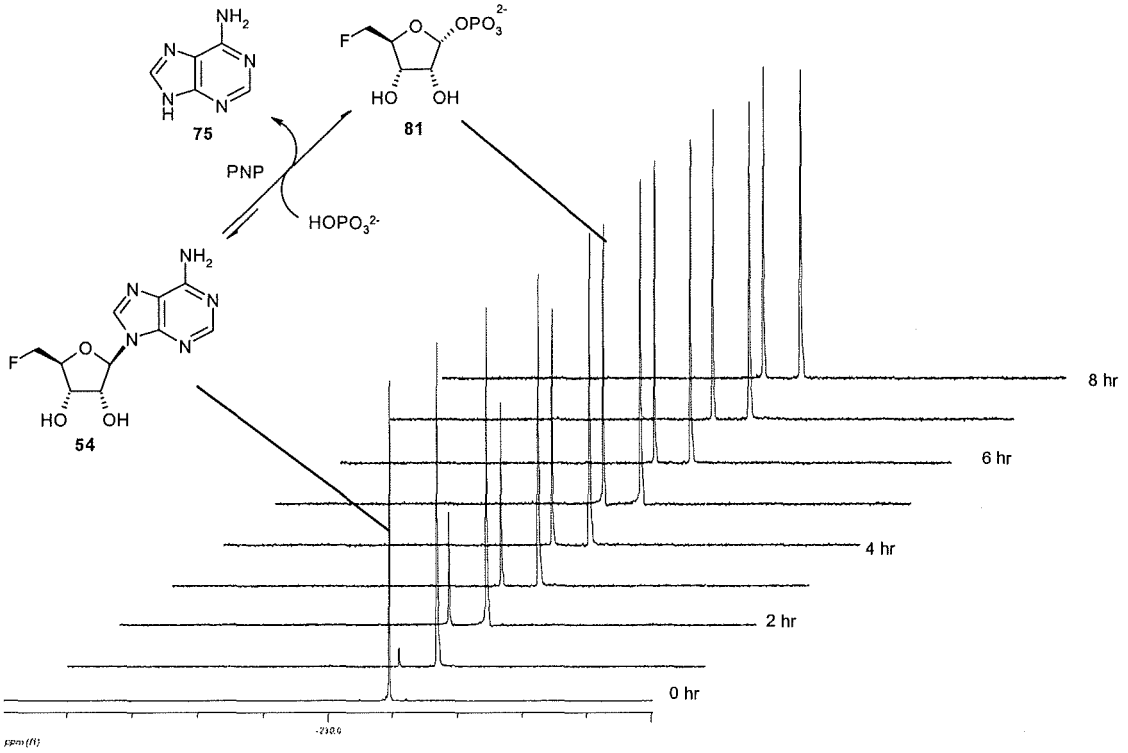

Figure 2.14 ^{19}F $\{^{1}H\}$ NMR time course, recorded hourly for 8 hrs, of the partially purified PNP extract incubated with 5'-FDA **54** at 25 °C.[106]

The resultant $^{19}F\{^{1}H\}$ NMR shows a product signal at -230.75 ppm appearing after just 1 hr of incubation. ESI-MS analysis showed this signal corresponds to 5-FDRP **81**, with a steady increase in 5-FDRP **81** formation over a 5 hr period. The signal begins to level off after 5 hrs, possibly due to the reversibility of the PNP reaction. HPLC analysis showed no deaminase activity was observed from the partially purified PNP extract indicating its removal after anion exchange chromatography. Overall, the NMR data are consistent with the previously observed results from HPLC and MS.

2.3.8 Substrate specificity of the partially purified PNP

There has been a lot of interest in exploring PNP substrate specificity and developing PNP enzymes as biocatalysts for the regio- and stereo-selective synthesis of purine nucleosides.[130] However, the number of nucleosides generated is limited due to the relatively narrow substrate specificity of PNP's.[131] These enzymes are specific for purine nucleosides in the β-configuration and exhibit a strong preference for ribosyl-containing nucleosides relative to the corresponding analogues containing the arabinose, xylose or lyxose stereoisomers.[132] Having a partially purified PNP from *S. cattleya* which acts on a novel substrate, it was of some interest to explore the specificity of this PNP relative to those previously described.

The substrate specificity of the PNP was evaluated using a range of substrate analogues. Firstly, the enzyme was partially purified by anion exchange chromatography as outlined in Section 2.3.4. This protein extract (100 μl, 0.3 mg / ml) was incubated with a range of different nucleoside analogues at a final conc. of 1 mM in phosphate buffer (50 mM, pH 6.8) for 16 hrs at 37 °C. After this time, the sample was heated to 100 °C for 3 min and the precipitated protein was removed by centrifugation. Control experiments were also carried out in the absence of protein, in the absence of the purine nucleoside, and also in the absence of phosphate in the buffer (50 mM, pH 6.8). For the HPLC analyses, 20 μl of the clear supernatant was injected directly onto the C18 column. In order to assess whether the individual nucleosides acted as substrates, detection of the appropriate purine provided an indication that phosphorolyic cleavage had occurred. The nucleosides were either prepared by S. L. Cobb[118] or could be purchased commercially. The various nucleoside analogues were modified at five different sites designated R1 to R5 (Scheme 2.7). The results are highlighted in Table 2.1 and the Table indicates the range of nucleosides that were tested

as potential substrates. Positive substrate activity is denoted with a (+), and no activity with (-).

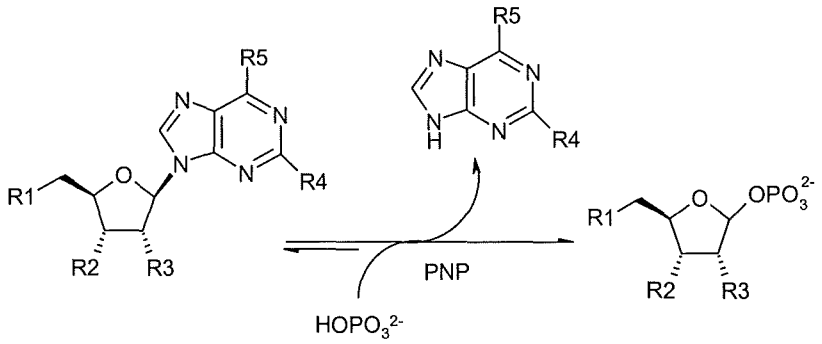

Scheme 2.7 Schematic representation of PNP activity and substrate analogues (see Table 2.1).

		R1	R2	R3	R4	R5	Substrate
*5'-fluoro-5'-deoxyadenosine	**54**	F	OH	OH	H	NH_2	+
5'-fluoro-5'-deoxyinosine	**55**	F	OH	OH	H	OH	-
*2,5 dideoxy-5'-fluoroadenosine	**59**	F	OH	H	H	NH_2	+
*2-amino-5'-fluoro-5'-deoxyadenosine	**91**	F	OH	OH	NH_2	NH_2	+
*5'-chloro-5'-deoxyadenosine	**88**	Cl	OH	OH	H	NH_2	+
*2,5-dideoxy-5'-chloroadenosine	**86**	Cl	OH	H	H	NH_2	+
2-chloroadenosine	**96**	OH	OH	OH	Cl	NH_2	+
*2-amino-5'-chloro-5'-deoxyadenosine	**97**	Cl	OH	OH	NH_2	NH_2	+
*5'-bromo-5'-deoxyadenosine	**89**	Br	OH	OH	H	NH_2	+
adenosine	**71**	OH	OH	OH	H	NH_2	+
2-deoxyadenosine	**87**	OH	OH	H	H	NH_2	+
*3'-deoxyadenosine	**99**	OH	H	OH	H	NH_2	-
*5'-deoxyadenosine	**90**	H	OH	OH	H	NH_2	+
*2',5'-dideoxyadenosine	**98**	OH	OH	H	H	NH_2	+
2-aminoadenosine	**94**	OH	OH	OH	NH_2	NH_2	+
2-amino-2-deoxyadenosine	**95**	OH	OH	H	NH_2	NH_2	+
adenosine monophosphate	**92**	PO_4^{2-}	OH	OH	H	NH_2	-
5'-thiomethyl-5'-deoxyadenosine	**76**	MeS	OH	OH	H	NH_2	+
*5'-acetyl-5'-deoxyademosine	**93**	OAc	OH	OH	H	NH_2	-
inosine	**72**	OH	OH	OH	H	OH	-

Table 2.1 Substrate specificity of the PNP for various nucleoside analogues; (+) indicates a substrate and (-) indicates no detectable activity. * Prepared by S. L. Cobb.[118]

The results from Table 2.1 show that the partially purified PNP did not accept either of the 6-oxopurine ribonucleosides, 5'-FDI **55** and inosine **72** as substrates. As discussed earlier,

5'-FDI **55** was shown to be metabolically inert in a CFE of *S. cattleya*, consistent with the result observed here. The inability of this enzyme to use 6-oxopurine nucleosides as substrates suggests that it shares a close resemblance to that of an MTAP.[133,134] With nucleosides containing the 2'-deoxyribofuranose moiety such as compounds **59**, **86** and **87,** excellent activity was observed by HPLC. Clearly this PNP prefers a ribofuranosyl or 2'-deoxyribofuranosyl group in the β configuration, consistent with other such enzymes.[110] The PNP from *S .cattleya* appears to be particularly permissive in terms of the substituents allowed at the C-5' position of the ribose ring, accepting the nucleosides **71**, **88**, **89**, **90** and **76**. The acceptance of OH, Cl, Br, H and MeS at this position indicates that the active site pocket receiving these residues is not particularly specific for fluorine. The various size of these substituents (e.g Br, MeS) suggests a large binding pocket. However, bulkier groups such as those on nucleosides **92** and **93**, which contain a charged phosphate and an acetyl group respectively at C-5' show no phosphorolytic cleavage. Nucleoside analogues such as **91**, **94**, **95, 96** and **97** which are modified with NH_2 and Cl at the C-2 position of the purine ring show phosphorolytic cleavage. This observation opens up the possibility of exploring the synthesis of nucleosides such as the prodrug, 9-β-D-arabinofuranosyl-2-fluoroadenine (F-dAdo) **100** by biotransformation.

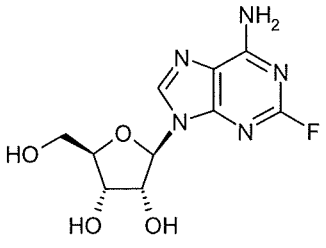

100

This compound is used in cancer treatment that utilises gene therapy to liberate the cytotoxic base 2-fluoroadenine.[135,136] In conclusion, these studies have shown that the substrate specificity of the partially purified PNP from *S. cattleya* has a significant

similarity to that of a bacterial MTAP. The wide variation of C-5' substituent tolerated, indicates that this enzyme is not particularly specific for the fluorinated substrate 5'-FDA **54**.

2.3.9 Reversibility of the PNP

It is well documented that PNP enzymes catalyse reversible C-N glycosidic bond formation to generate nucleoside bases from their corresponding purine base and α-ribose-1-phosphate.[132] In order to explore the reversibility of the PNP from *S. cattleya*, a coupled enzyme assay was utilised which consisted of the adenosine deaminase (*Aspergillus species*, EC 3.5.4.3) and two PNP enzymes, one from a commercial source and the other from *S. cattleya*. The experiments were carried out by first preparing a sample of 5-FDRP **81** from 5'-FDA **54** using the commercial adenosine deaminase and a bacterial PNP (*E. coli*, EC 2.4.2.1) (Section 5.1.9). It was anticipated that the addition of the partially purified PNP extract from *S. cattleya* to this reaction, supplemented with adenine **75** would generate the nucleoside 5'-FDA **54**. Scheme 2.8 outlines the proposed route to explore the reversibility of the PNP.

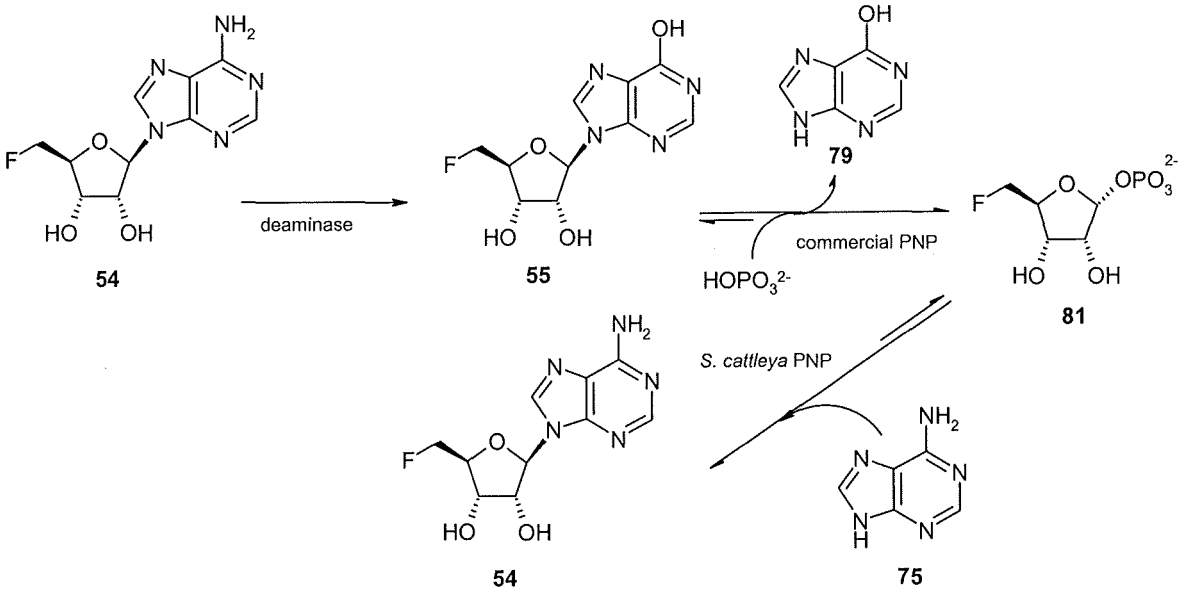

Scheme 2.8 Coupled enzyme assay exploring the reversibility of the PNP from *S. cattleya*.

Analytical HPLC was used to monitor the progress of each biotransformation step during the course of this assay. 5'-FDA **54** (18.5 mM) was incubated with adenosine deaminase for 16 hrs at 37 °C. The resulting HPLC chromatogram shown in Figure 2.15(**a**) indicated 100 % conversion to the product 5'-FDI **55**. The enzymatically synthesised 5'-FDI **55** (18.5 mM) was supplemented with an immobilised bacterial PNP from *E. coli* (gift from Galaxo Smith Kline) and incubated for 16 hrs at 37 °C.

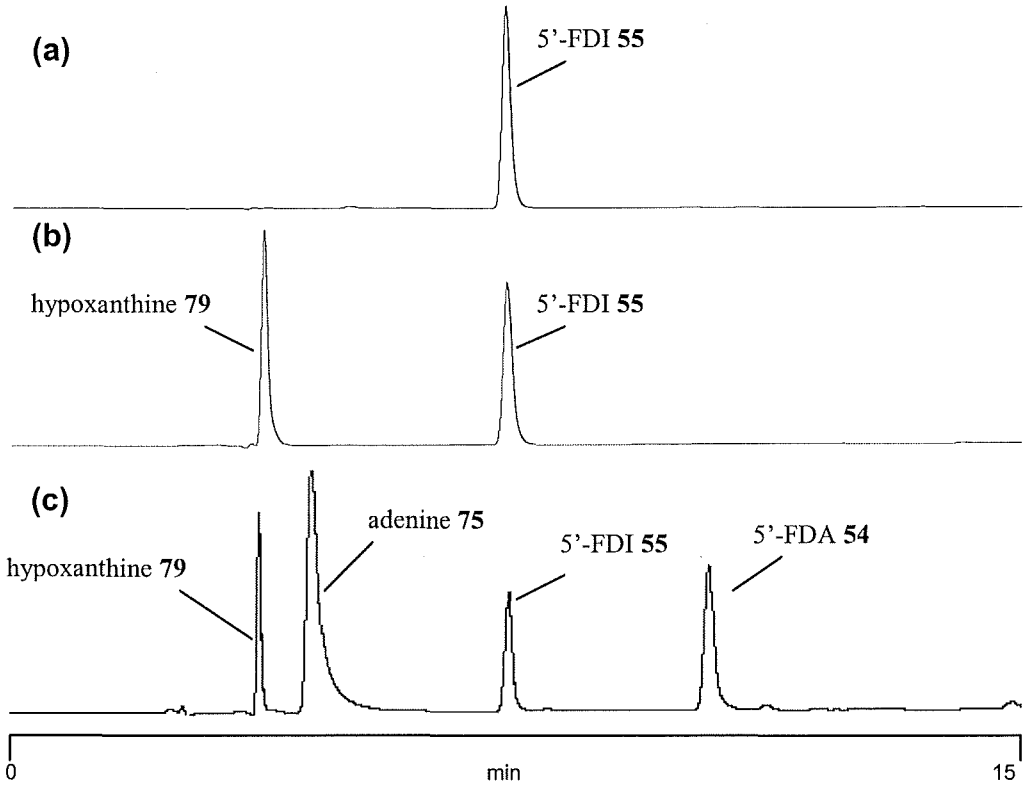

Figure 2.15 HPLC chromatogram showing (**a**), 5'-FDA **54** incubated with adenosine deaminase for 16 hrs at 37 °C. (**b**), incubation of an immobilised PNP to the enzymatically prepared 5'-FDI **55** for 16 hrs at 37 °C. (**c**), incubation of PNP from *S. cattleya* with 5-FDRP **81** (+ 5'-FDI **55**) and adenine **75**.

The resulting HPLC trace in Figure 2.15(**b**) shows the phosphorolytic reaction yielding a ~40 % conversion to hypoxanthine **79** (+5-FDRP **81**). With this established, the 5-FDRP **81** product was subjected to the final step which involved the addition of the partially

purified PNP (100 μl, 0.3 mg / ml) from *S. cattleya* to 5-FDRP **81** and adenine **75** (3.7 mM). The reaction was incubated for 16 hrs at 37 °C. The resulting chromatogram in Figure 2.15(**c**) clearly shows the presence of a fourth peak which was identified as 5'-FDA **54**. This result was reinforced by ^{19}F NMR spectroscopy and ES-MS, which showed that the PNP reaction is reversible.

Having demonstrated that the *S. cattleya* PNP is reversible it became interesting to explore the reversibility of the enzyme using purine analogues. Accordingly, a series of experiments was conducted by exploiting the assay outlined above. The analogues and results are shown in Table 2.2. Each of the purine bases (3.7 mM) was incubated with 5-FDRP **81** in the presence of the partially purified PNP. Analytical HPLC was used to monitor the reaction and determine the presence of newly formed nucleosides.

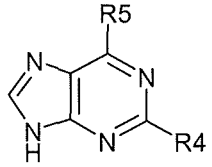

		R4	R5	Substrate
adenine	**75**	H	NH_2	+
hypoxanthine	**79**	H	OH	-
6-methylpurine	**102**	H	CH_3	-
6-chloropurine	**103**	H	Cl	-
2-amino-6-purinethiol	**104**	NH_2	SH	-
2,6-diaminopurine	**101**	NH_2	NH_2	+
2-amino-6-chloropurine	**106**	NH_2	Cl	-
2,6-dichloropurine	**107**	Cl	Cl	-
purine	**105**	H	H	-

Table 2.2 Substrate specificity of the PNP from *S. cattleya* with 5-FDRP **81**.

The results show that only the purine bases adenine **75** and 2,6-diaminopurine **101** were accepted as substrates. These observations were verified by co-injection experiments using

synthetic standards. The purine analogues **102**, **103**, **104**, **105** which were all substituted at C-6, with CH_3, Cl, SH and H respectively, were not substrates. This result emphasises the importance of the NH_2 group at C-6 of the purine ring for activity. Overall, the generation of novel halogenated purine analogues was not possible due to the substrate constraints encountered with the PNP from *S. cattleya*.

2.3.10 Generation of SAM analogues using the fluorinase and PNP in reverse

It was shown in Section 1.6.2 that the fluorinase operates in reverse, generating SAM **53** and inorganic fluoride from 5'-FDA **54** supplemented with L-methionine **56**. It was particularly interesting that the enzyme will also utilise 2'-deoxynucleoside substrates, which enables biotransformations to novel 2-deoxy-SAM **60** analogues. With this established, it was considered that the substrate specificity of the fluorinase be further explored in the reverse direction by generating halo-nucleoside substrate analogues using the PNP from *S. cattleya*. This would in turn, generate potential SAM **53** analogues. One such application of structural analogues of SAM **53**, with modifications in the amino acid, sugar, or base portions of the molecule is their use as either inhibitors and / or substrates for the study of SAM-dependent methyltransferases.[137] In order to explore the generation of SAM **53** analogues; a coupled enzymatic reaction was used which exploited the reversible reactions of the PNP and the fluorinase from *S. cattleya*.

A series of halogenated nucleosides was first prepared by exploiting the method outlined in Section 2.3.9. The newly synthesised halogenated nucleosides could be tested as fluorinase substrates by incubating the enzyme with the halogenated nucleoside and L-methionine **56**. Scheme 2.9 outlines the strategy taken for the generation of the modified SAM **53** analogues by exploiting the reverse reaction. [2-]

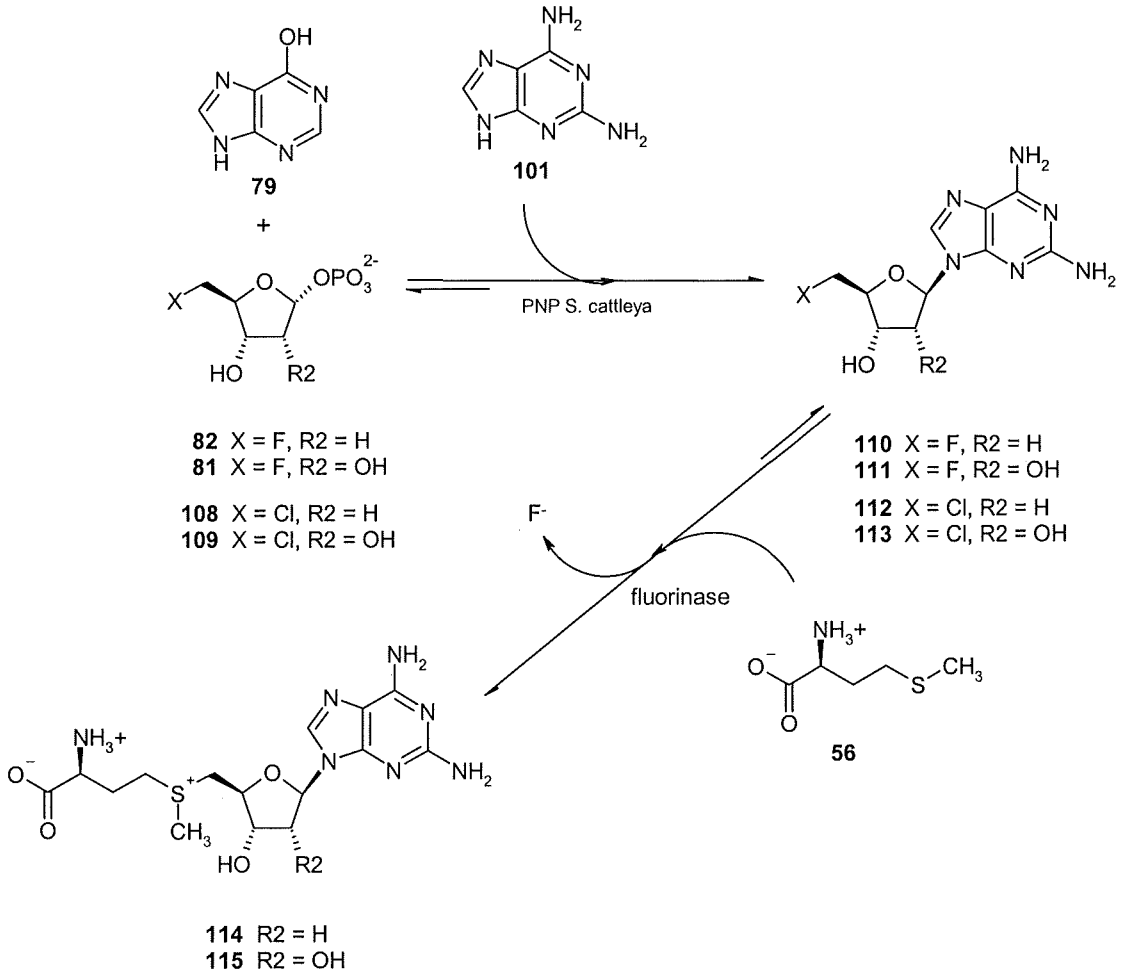

Scheme 2.9 Coupled enzymatic synthesis for the preparation of SAM **53** analogues using both partially purified PNP and the fluorinase in reverse from *S. cattleya*.

Accordingly, the generated halo-nucleoside was supplemented with the fluorinase (100μl, 10 mg / ml) and L-methionine **56** (10 mM), and incubated for 16 hrs at 37 °C. After this time, the sample was denatured by heating to 100 °C for 3 min and the precipitated protein was removed by centrifugation. Analysis of the supernatant by HPLC showed that it was possible to generate 2-amino-2-deoxy SAM **114** and 2-amino SAM **115** analogues from the corresponding halogenated (chlorinated or fluorinated) nucleoside.

In addition to HPLC analysis, ESI-MS along with co-injection experiments using synthetic standards confirmed the presence of the generated SAM **53** analogues. An example of such an analysis is shown in Figure 2.16, which shows the formation of 2-amino-SAM **115** from the corresponding nucleoside, 2-amino-5'-FDA **111** using the coupled enzymatic reaction. The ES-MS analysis confirmed an *m/z* of 414 $(M-H)^-$ corresponding to 2-amino-SAM **115** which supports the observed HPLC results.

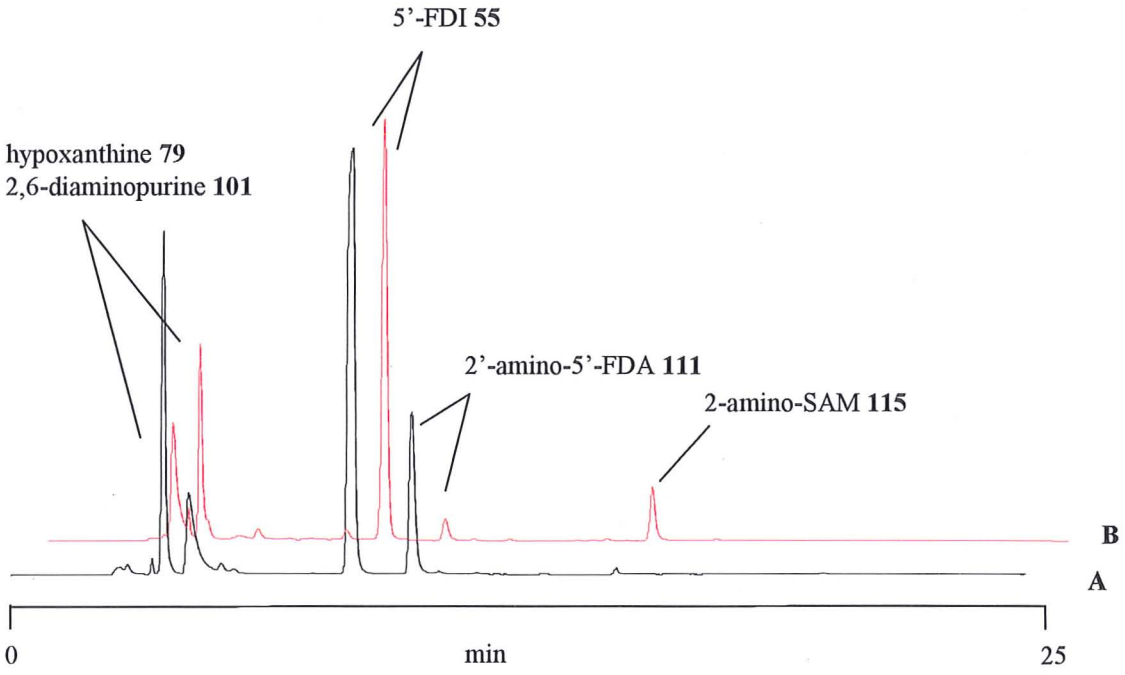

Figure 2.16 HPLC traces showing **(A)** (5-FDRP **81,** 5'-FDI **55**) mixture incubated with 2,6-diaminopurine **101** with partially purified PNP for 16 hrs at 37 °C. **(B)** Supplemented with L-methionine **56** in the presence of the fluorinase for 16 hrs at 37 °C.

This was only a preliminary study. Further investigation is needed to exploit this coupled enzyme method to generate other SAM **53** analogues. One possibility is to use the *E. coli* PNP which is known to have broader substrate specificity, accepting both 6-amino and 6-oxopurine nucleosides.[136] This could generate more potential nucleoside substrates for the fluorinase, and subsequent access to novel SAM analogues.

2.4 Fluorometabolite gene cluster in *S. cattleya*

The search for the genes encoding enzymes responsible for natural fluorine-containing metabolites has been a key challenge over the last few years. Recently, the cloning[93] of the fluorinase gene (*flA*) in collaboration with Dr Joe Spencer and Dr Fanglu Huang at the University of Cambridge has led to the DNA sequencing of a further 11 putative open reading frames (ORFs) adjacent to *flA*. Sequence similarities/identities indicate that several of these genes may be involved in fluorometabolite biosynthesis in *S. cattleya*. Of particular interest is the gene *flB* located immediately upstream of *flA* which encodes a protein of 299 amino acids and has a high degree of sequence similarity to a purine nucleoside phosphorylase (PNP) (see Section 2.4.1). Therefore, it is likely that the first two genes of the fluorometabolite pathway are together on the chromosome in *S .cattleya*. The *flB* gene and its product are discussed in the next section. Figure 2.17 shows the cluster of genes centred around the *flA* gene, all of which have been tentatively assigned a function based on known protein sequences.

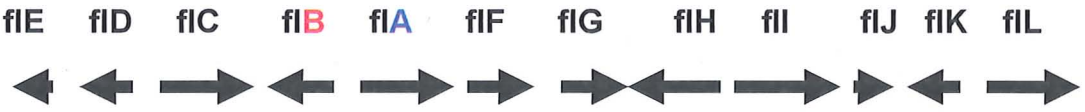

ORF	Length aa	Putative function
flE	222	DNA binding regulatory protein
flD	216	Dehalogenase/Phosphatase
flC	397	MFS permease
flB	299	PNP
flA	299	fluorinase
flF	185	DNA binding regulatory protein
flG	234	DNA binding regulatory protein
flH	467	Na^+/H^+ antiporter
fll	489	Homocysteine lyase
flJ	131	DNA binding protein
flK	139	Thioesterase/acyltransferase
flL	225	DNA binding regulatory protein

Figure 2.17 ORFs and map of the *fl* locus with tentative functions assigned.

It is noteworthy that the genes encoding the already purified fluoroacetaldehyde dehydrogenase and threonine transaldolase enzymes, which are involved in the latter stages of the fluorometabolite pathway, are absent from this gene cluster. The genes encoding these enzymes must therefore be part of another unidentified locus on the chromosome.

2.4.1 PNP sequence analysis

A database search using the BLAST program revealed that the putative PNP encoded within the *fl* cluster belongs to a family of 5'-methylthioadenosine phosphorylases (MTAPs). MTAP is known to be a key component in the L-methionine salvage pathway as previously discussed. Its function is to metabolise 5'-methylthioadenosine (MTA) **76** in the methionine salvage pathway (see Section 3.1).[113, 114]

Analysis of the sequence similarity between FlB and several homologues showed a high degree of identity with MTAPs. For example, this putative PNP shows a 53 % identity and 68 % sequence similarity to a putative MTAP from *G. metallireducens*. This putative PNP is similar to putative MTAP's present in Actinomycetes such as *S. coelicolor* and *S. avermitilis*, (52 % and 50 % identity respectively). Figure 2.18 illustrates the sequence alignment of FlB and its orthologues.

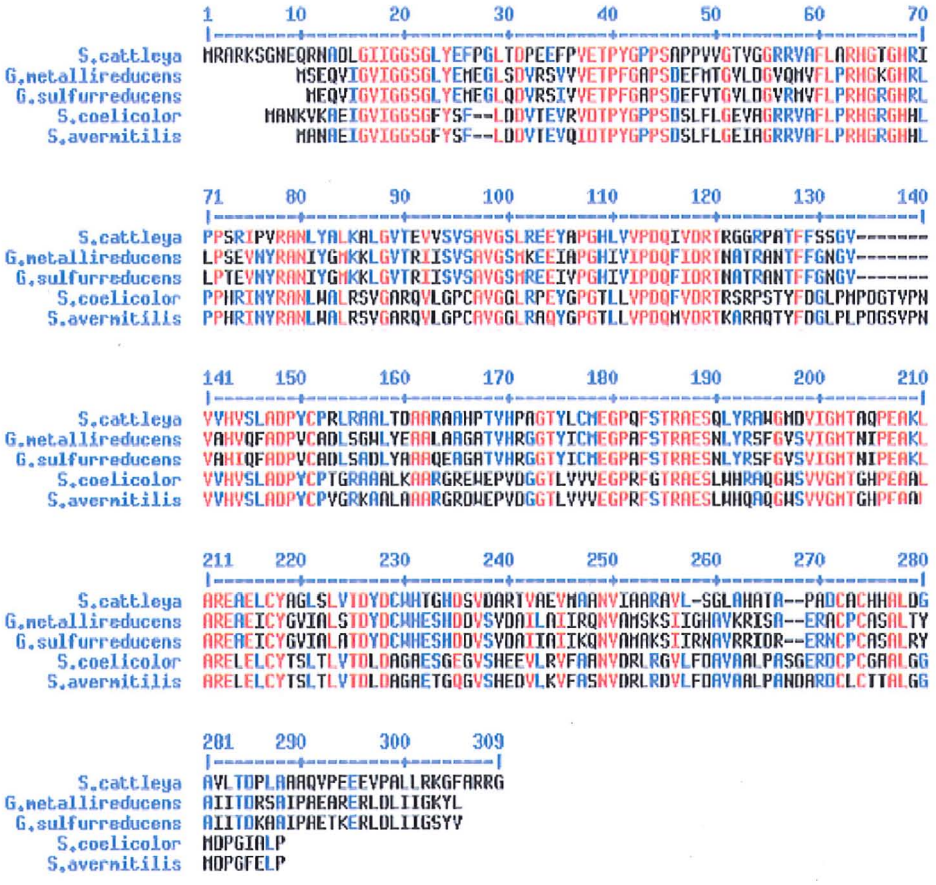

Figure 2.18 Sequence alignment of FlB with putative PNP's from bacteria. Residues that are highly conserved appear in red, and those weakly conserved in blue.

The *flB* gene was cloned into the pET28a(+) plasmid with an N-terminal His-Tag at the University of Cambridge, and the gene was over-expressed. The purified enzyme was able to catalyse the phosphorolytic cleavage of 5'-FDA **54** to adenine **75** and 5-FDRP **81** in an identical manner to the partially purified PNP from wild type in *S. cattleya.* This analysis, along with the location of the *flB* gene adjacent to the *flA* gene clearly suggests the involvement of this PNP in fluorometabolite biosynthesis. Although this protein was successfully overexpressed, it is largely insoluble. It became an objective in St Andrews to obtain the pET 28a(+) construct containing the *flB* gene to try and increase the solubility of the desired protein.

2.5 Expression and purification of a PNP from *S. cattleya*

2.5.1 Protein expression trials

For expression of the PNP, the pET28a(+) plasmid containing the *flB* gene was used to transform competent *E. coli* host cells (Section 5.1.27.2). Small scale expression trials (10 ml) were first performed in order to determine optimum conditions. The transformed *E. coli* host cells were selected on antibiotic-containing LB agar plates. Single colonies were picked and grown in 10 ml of growth medium at 37 °C and shaken at 200 rpm for ~12 hrs. After this time, aliquots (100 μl) were used to inoculate fresh growth medium (10 ml) for the overexpression trials. Expression was induced using various IPTG concentrations once the cell density had reached an OD_{600} of ~ 0.5. During the protein expression trials, numerous variables were altered in order to try and optimise *in vivo* expression of soluble protein. These variables are discussed below.

The following induction temperatures were used to try to limit the insoluble aggregation of the desired protein; 30 °C, 25 °C, 18 °C, 16 °C, 12 °C and 10 °C. Reducing the temperature is a general strategy employed for the solubilisation of proteins.[138] This can be explained by a number of important factors, including, a slower rate of protein synthesis and changes in the folding kinetics of the polypeptide chain.

Another important strategy that has shown success in production of high amounts of active proteins is the use of different growth media including e.g growth additives such as NaCl.[139] Additionally, glucose which is present in most rich media is shown to repress induction of the lac promoter by lactose.[140] For these reasons, the following media were used; Luria-Bertani (LB) medium, tryptone phosphate medium, terrific broth and Overnight Express™ Autoinduction System 1 (Novagen).

Inducing with lower concentrations of IPTG has also shown success in increasing protein solubility.[141] This approach can be explained by a reduction in translation rates which leads

to an increased chance of protein folding into a native state. Accordingly, the following IPTG concentrations were used; none (leaky expression); 0.1 mM, 0.2 mM, 0.4 mM, 0.6 mM, 0.8 mM and 1 mM.

The choice of expression host can significantly increase the activity and amount of target protein present in the soluble fraction. The following strains were used; BL21(DE3), BL21Star™, BL21(DE3)pLysS, BL21(DE3)pLysE, Rosetta(DE3) and C43(DE3). All of these variables were tested and protein production was analysed by SDS-PAGE.

For SDS-PAGE analysis, cells were first harvested by centrifugation (14,000 rpm / 5 min) and the cell pellet was re-suspended in buffer (20 mM Tris-HCl, pH 7.5). The resultant re-suspended cell pellet was disrupted by ultrasonication, at 60 % duty cycle for 10 sec and the cell debris removed by centrifugation (14,000 rpm / 5 min). The insoluble fraction, along with the soluble and non-induced sample was analysed.

The results showed that under most of the conditions tested, high expression levels of PNP resulted, however, the majority of the protein was found in the insoluble cell fraction as judged by SDS-PAGE (Mw: ~36 kDa) and trypsin digest MALDI-TOF mass spectrometry. The results presented in Figure 2.19(**a**) show three of the specialised host strains used to try and improve soluble expression of the PNP, however, in each case, the majority of the desired protein formed insoluble aggregates. Among these, the *E. coli* mutant strain C43(DE3) which has contributed significantly to soluble expression of difficult recombinant proteins,[142] also proved ineffective. The results in Figure 2.19(**b**) show the Overnight Express™ Autoinduction System which is optimised for tight expression, control and induction at high cell density also resulted in low levels of soluble PNP over various induction temperatures and lengths of incubation. This again is observed in the insoluble protein fraction.

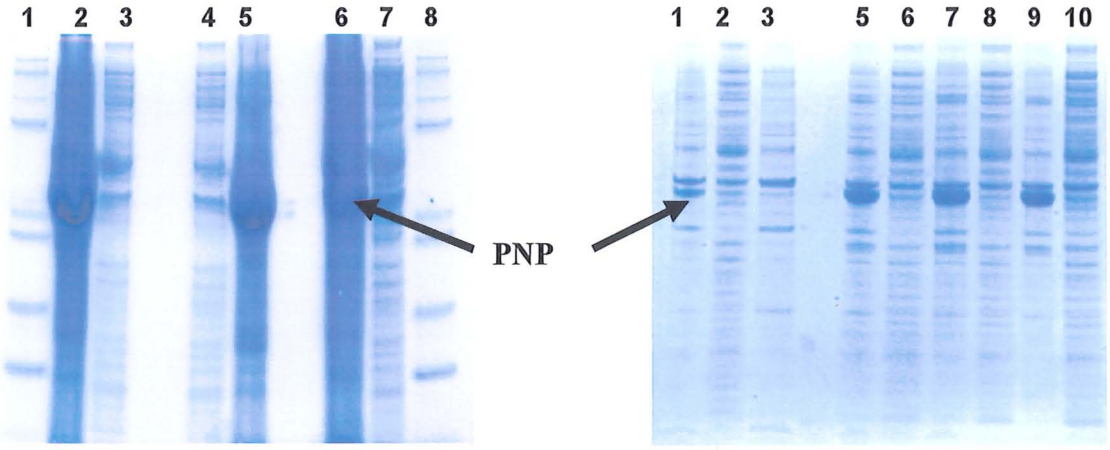

Figure 2.19 **(a)** SDS-PAGE showing expression trials of the PNP using three different expression hosts, BL21(DE3), Rosetta 2(DE3) and C43(DE3). Lanes **1**; SDS markers, **2**; BL21(DE3) Insoluble fraction, **3**; Soluble fraction, **4**; Rosetta2(DE3) Soluble fraction, **5**; Insoluble fraction, **6**; C43(DE3) Insoluble fraction, **7**; Soluble fraction, **8**; SDS markers.

(b) SDS-PAGE showing Overnight Express™ Autoinduction System induced at 16 °C. Lanes **1**; insoluble fraction, 22 hr, **2**, soluble fraction, 22 hr, **3**, soluble fraction, 25 hr, **5**, insoluble fraction, 27 hr, **6**, soluble fraction, 27 hr, **7**, insoluble fraction, 29 hr, **8**, soluble fraction, 29 hr, **9**, insoluble fraction, 31 hr, **10**, soluble fraction, 31 hr.

The expression trials that relied on leaky protein expression rather than IPTG induction to gain soluble protein were also unsuccessful in generating soluble protein. Additionally, *E. coli* strains that prevent leaky expression, such as BL21(DE3)pLysS and BL21(DE3)pLysE did not yield high levels of soluble protein. Induction temperature trials between 10 °C - 37 °C, did result in an improvement in soluble protein expression, particularly at 10 °C. The over-expressed protein is unlikely to be toxic to the bacteria as the expression did not prevent cell growth, as judged by the increase in OD_{600} during protein expression.

In summary, although only low levels of soluble PNP protein could be obtained, particularly from low induction temperatures, it was considered that large scale protein

expression would yield reasonable soluble protein concentrations for further purification. Therefore, conditions were optimised after these trials, and expression was scaled up to 500 ml cultures using BL21(DE3). Section 5.1.27.3(**b**) outlines the protocol for larger scale expression which resulted in ~13.5 g of cells from 5 L, with a total soluble protein of approximately 412 mg.

2.5.2 Purification of overexpressed PNP

PNP was purified using a three step purification protocol involving a metal chelate ($NiSO_4$ charged resin, fast flow sepharose, Amersham Biosciences) and gel filtration (Superdex 200, 60 x 16, Amersham Biosciences) chromatography. The protocol that was used is outlined in Section 5.1.27.3(**c**). The metal chelating column purified the N-terminal Histag protein which resulted in ~30 mg protein after a 250 mM imidazole elution. The resultant HisTag protein was cleaved with thrombin by incubation for 20 hrs at 4 ^{o}C and the resulting protein was reapplied to the nickel column for further purification. This resulted in approximately 4 mg protein. Figure 2.20 shows an SDS-PAGE gel highlighting various stages during PNP purification.

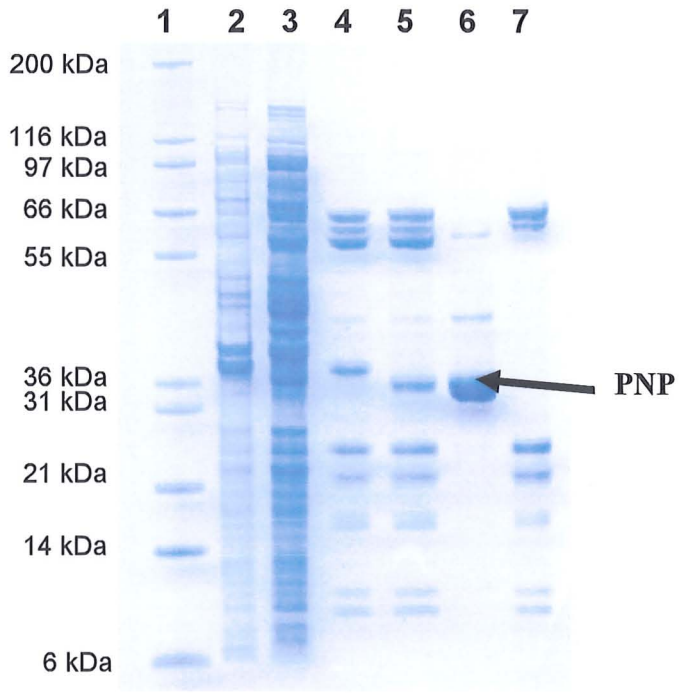

Figure 2.20 SDS-PAGE showing the protein after various stages during the purification of the PNP. **1**; molecular markers, **2;** insoluble fraction, **3**; soluble fraction, **4**; 250 mM imidazole elution, **5**; thrombin cleavage, **6**; 30 mM imidazole elution (2^{nd} nickel column), **7**; 250 mM imidazole elution (2^{nd} nickel column).

The final step in the purification protocol used a Superdex 200, (60 x 16, Amersham Biosciences) gel filtration column, which was pre-equilibrated with tris buffer (50 mM, pH 7.5) containing 0.3 M NaCl. Fractions containing PNP were pooled and concentrated to give a total of 3 mg of purified PNP in 1 ml of tris buffer. The resulting SDS-PAGE gel and ES-MS of the purified protein are shown in Figure 2.21.

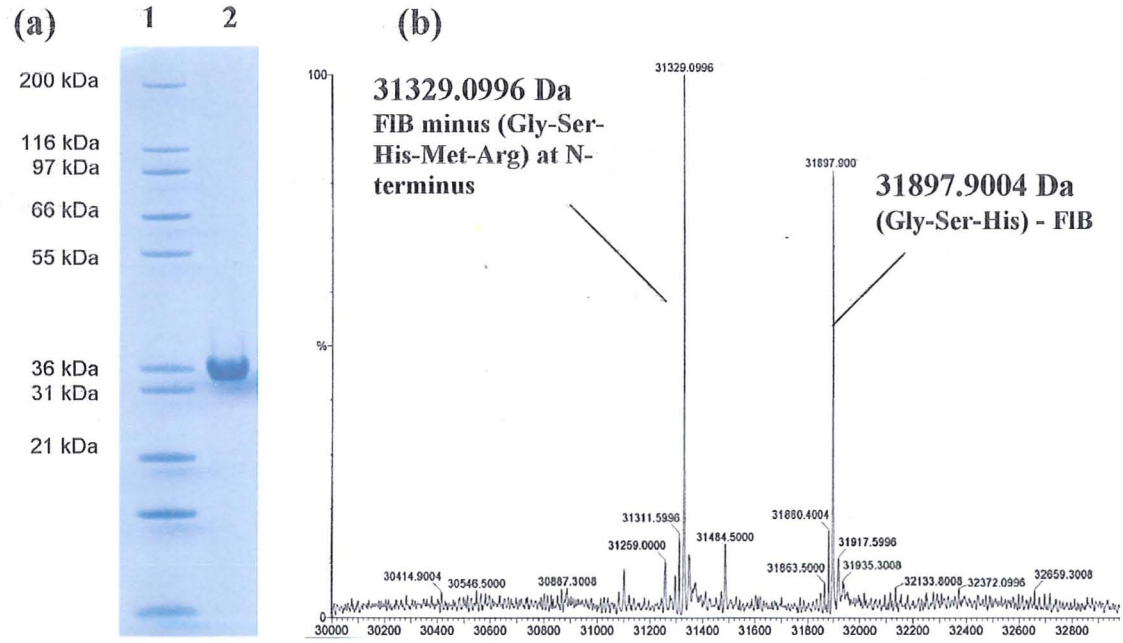

Figure 2.21 **(a)** SDS-PAGE showing purified FlB after gel filtration. Lanes **1**; molecular markers, **2**; gel filtration purification **(b)** ES-MS spectrum showing cleaved PNP.

The SDS-PAGE gel shows the PNP purified to homogeneity, showing an estimated mass of 33 kDa by comparison with standards. An accurate mass of the purified recombinant (Gly-Ser-His)-PNP protein was determined by ESI-MS to be 31,897 Da. This is in very close agreement to the calculated value of 31,894 Da from the gene sequence. The native mass of the enzyme was determined using a HiLoad 16/60 Superdex 200 gel filtration column which was calibrated using the reference proteins in Section 5.1.22. The native mass is approximately 80-90 kDa indicating that the enzyme is probably a homotrimer.

The method described in Section 5.1.17 was used to assay the purified PNP protein by incubating 5'-FDA **54** (1 mM) with 100 µg of purified PNP in phosphate buffer (10 mM, pH 6.8) for 30 min at 37 °C. After this time, the protein was denatured at 100 °C for 3 min and the precipitated protein was removed by centrifugation. Control experiments were carried out in the absence of 5'-FDA **54** and phosphate buffer (10 mM, pH 6.8), and also in

the absence of purified FlB. The reaction was followed by HPLC analysis of the supernatant (20 μl) by monitoring for adenine **75** release (Figure 2.22(**a**)). Further analysis was carried out by ^{19}F NMR spectroscopy after incubation of 5'-FDA **54** (5 mM) with 200 μg of FlB in phosphate buffer (10 mM, pH 6.8) and incubating for 7 hrs at 37 °C (Figure 2.22(**b**)). Additionally, ES-MS analysis was performed on the product; ES-MS, 5-FDRP **81** *m/z* 231 $(M-H)^-$.

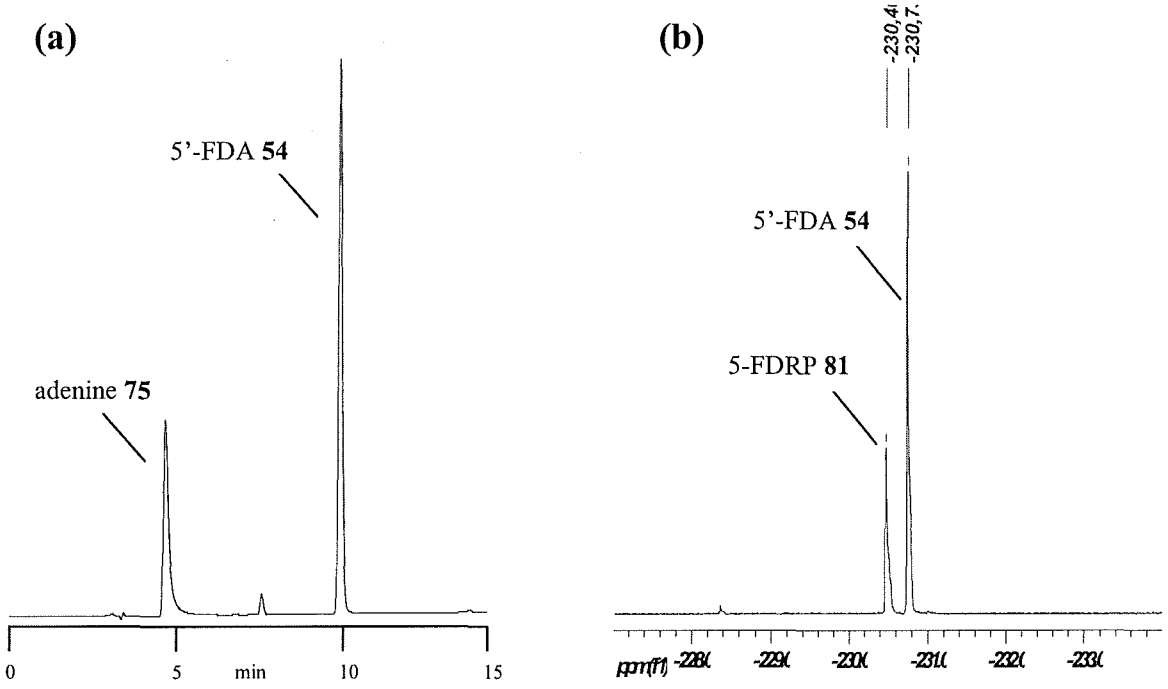

Figure 2.22 **(a)** HPLC chromatogram and **(b)**, ^{19}F $\{^1H\}$ NMR spectrum of purified FlB incubated with 5'-FDA **54** in phosphate buffer (10 mM, pH 6.8).

The successful over-expression and purification of the PNP has led to sufficient protein to carry out initial crystallisation trials. This work is ongoing in collaboration with Professor J. Naismith, University of St Andrews.

2.6 Conclusion

It has been shown that in *S. cattleya*, a purine nucleoside phosphorylase (PNP) is present which is able to catalyse the reversible phosphorolysis of the glycosidic bond of 5'-FDA **54** to 5-FDRP **81**. Investigations using a CFE have shown that the incubation of 5-FDRP **81** by an enzymatic preparation led to the accumulation of fluoroacetate **8** and 4-fluorothreonine **47**. The identity of this enzyme activity has led to a partially purified PNP from *S. cattleya* after ammonium sulfate precipitation, hydrophobic interaction chromatography and ion exchange chromatography respectively.

A study with this partially purified PNP has revealed a narrow substrate specificity and a profile which shares a close similarity to bacterial 5'-methylthioadenosine phosphorylases (MTAP's). The coupling of the fluorinase and the PNP to generate SAM **53** analogues has been achieved, and this may have utility for the preparation of novel SAM **53** analogues.

In collaboration with Dr Joe Spencer (University of Cambridge), a gene cluster encoding enzymes responsible for fluorometabolite biosynthesis in *S. cattleya* has been identified by sequencing out from the *fl*A (fluorinase) gene. The *flB* gene encoding a putative purine nucleoside phosphorylase (PNP) was identified adjacent to the fluorinase (*fl*A) gene. The catalytic behaviour is identical to that purified *de novo*, and its location adjacent to the *flA* gene indicates that it is involved in fluorometabolite biosynthesis. Over-expression and purification of the PNP has been achieved and initial crystallisation trials are underway.

3 Identification of an isomerase activity on the fluorometabolite pathway in *S. cattleya*

The metabolic conversion of 5-FDRP **81** to fluoroacetaldehyde **48** in fluorometabolite biosynthesis remains to be characterised at a biochemical level. The results described in this chapter show that 5-fluoro-5-deoxy-D-ribulose-1-phosphate (5-FDRibP) **121** is the intermediate formed after 5-FDRP **81** on the fluorometabolite pathway. The enzyme responsible for this transformation is shown to be a 5-fluoro-5-deoxy-D-ribose-1-phosphate isomerase. The biotransformation of FDRibP **121** to fluoroacetaldehyde **48** is unclear; however, biochemical evidence is presented which suggests that the diastereoisomer of **121**, 5-fluoro-5-deoxy-D-xylulose-1-phosphate (5-FDXyuP) **126** is the remaining unidentified metabolite. In order to gain an insight into the potential biosynthetic pathway for the metabolism of 5-FDRP **81**, the methionine salvage pathway is revisited.

3.1 L-Methionine salvage pathway

It was shown in Section 2.1.1 that MTA **76** is metabolised to 5-MTRP **78** by two independent routes.[113] The first involves the action of a PNP activity to yield 5-MTRP **78** from MTA **76**. The second route involves hydrolysis of MTA **76** by a nucleosidase activity to yield MTR **77** which is subsequently phosphorylated by the action of a kinase to give MTRP **78**. The next transformation involves formation of 5-methylthio-5-deoxy-D-ribulose-1-phosphate (MTRibP) **116** *via* an isomerase activity. This was first unravelled by Abeles and co-workers in *K. pneumoniae*.[143-147] Recently, the genes involved in this transformation and subsequent steps have been discovered in *B. subtilis*.[115] Within this

gene cluster is the gene for MTRP isomerase,[148] which has a protein sequence similar to that of a eukaryotic initiation factor eIF-2B.[149,150] Scheme 3.1 outlines the recycling of methionine in *Bacillus subtilis*.[115]

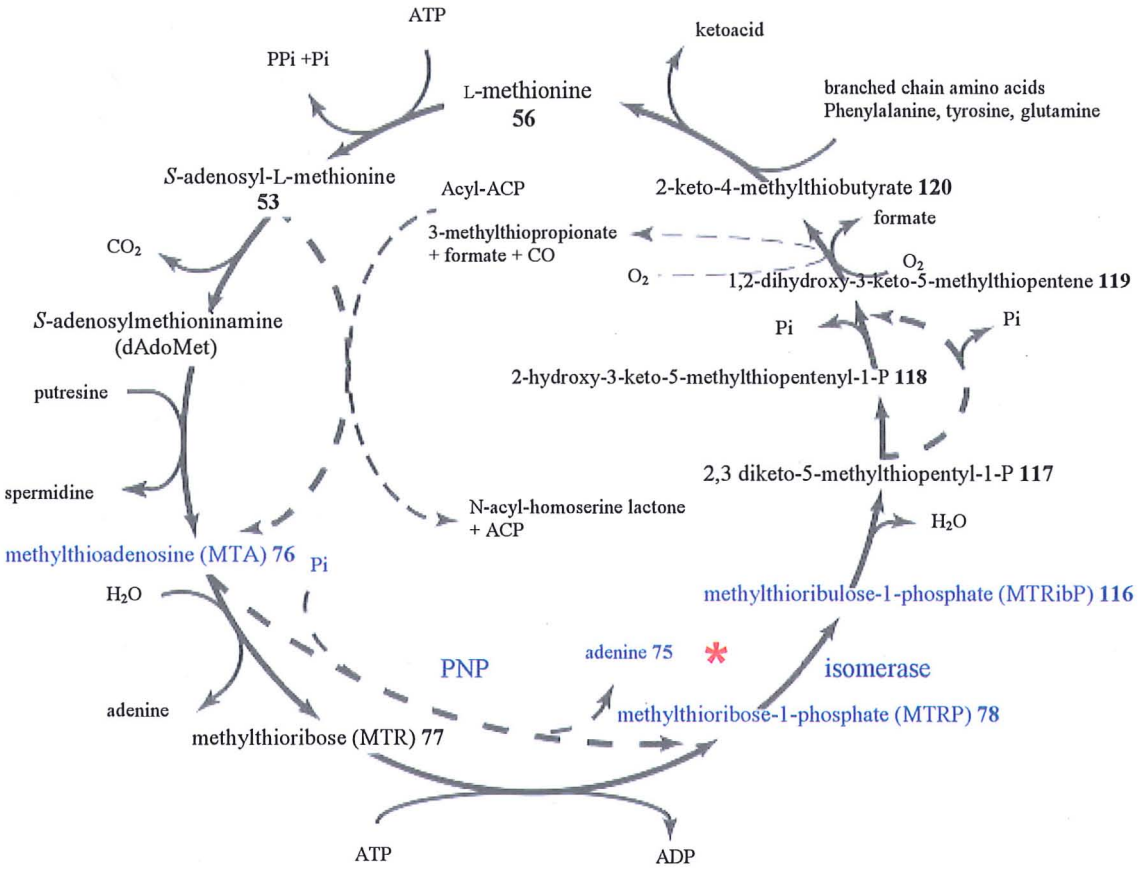

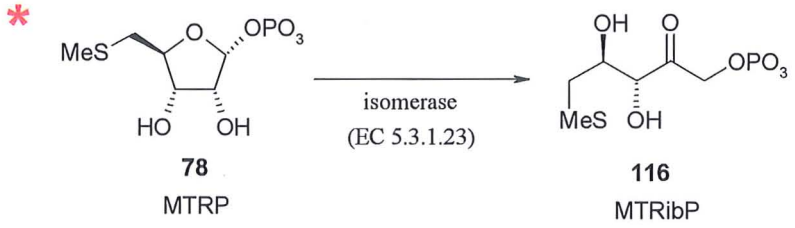

Scheme 3.1 L-Methionine salvage pathway: Intermediates and enzymes in blue outline a proposed pathway analogous to fluorometabolite biosynthesis in *S. cattleya*.

Several enzymes responsible for the transformation of MTRibP **116** to L-methionine **56** have been identified. The first of these involves the dehydration of MTRibP **116** catalysed

by a dehydratase to yield the diketone product 2,3-diketo-5-methylthiopentyl-1-phosphate (DK-MTP-1-P) **117**. This enzyme is shown to belong to a large cluster of proteins that form Class II aldolases. Amongst this cluster is L-ribulose-5-phosphate-4-epimerase which emphasises the importance of the ribulose backbone for recognition by enzymes of this class. DK-MTP-1-P **117** is converted to 2-hydroxy-3-keto-5-methylthiopentene (DHK-MTPene) **119** *via* the intermediate 2-hydroxy-3-keto-5-methylthiopentenyl-1-phosphate (HK-MTPenyl-1-P) **118**, by an enolase/phosphatase. The final two steps in the L-methionine salvage pathway appear to be ubiquitous to all organisms that grow in the presence of dioxygen. The first involves the enzymatic oxidation of DHK-MTPene **119** by an aci-reductone dioxygenase enzyme to yield 2-keto-4-methylthiobutyrate (KMTB) **120**. The final step involves the transamination of KMTB **120** to L-methionine **56** *via* an aminotransferase. For example, in *K. pneumoniae* this enzyme generates L-methionine **56** from KMTB **120** and tyrosine from its ketoacid precursor.[115]

.

3.1.1 5-Methylthio-5-deoxy-D-ribose-1-phosphate isomerase

A sequence alignment of the MTRP isomerase from *B. subtilis* with related protein sequences suggests that it belongs to a family of eukaryotic initiation factors, EIF-2B.[114] Members of EIF-2B function as important regulators of protein translation initiation. In eukaryotic translation, the initiation factor is involved in GTP/GDP exchange and is a member of GTP-dependent regulators.[151] Analysis of the sequence similarity between the MTRP isomerase from *B. subtilis* and related protein sequences from *Streptomyces coelicolor, Streptomyces avermitilis* and *Sacchromyces cerevisiae* (Ypr118W) are shown in Figure 3.1.

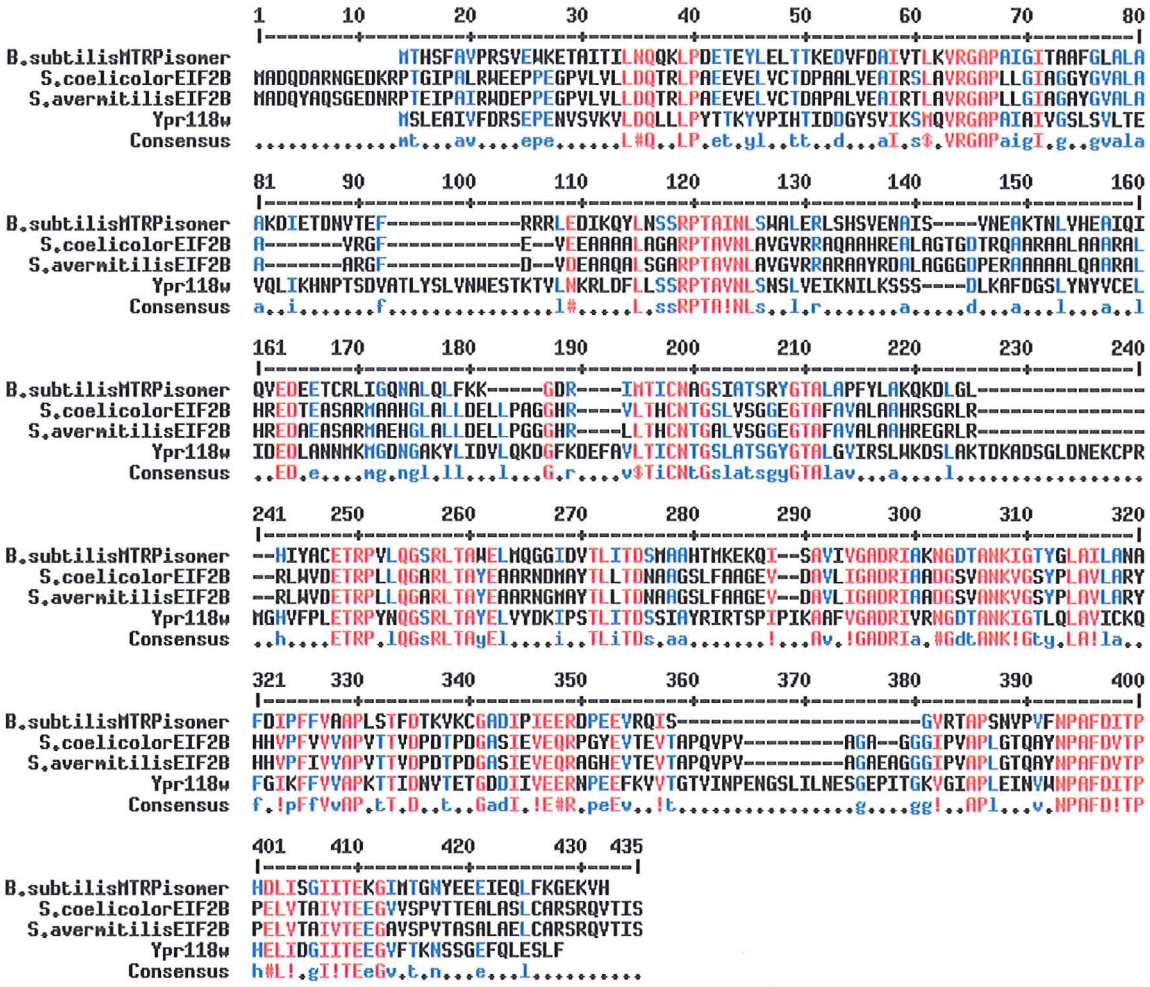

Figure 3.1 MTRP isomerase sequence alignments. Residues that are highly conserved appear in red, and those weakly conserved in blue.

This highlights a high degree of conserved residues between genes from the *Streptomyces* species assigned as putative translation initiation factor EIF-2B subunits based on sequence homology, and the *B. subtilis* MTRibP isomerase. For example, the *S. coelicolor* EIF-2B shows a 32 % identity and 52 % similarity to MTRP isomerase from *B. subtilis*. This observation tentatively suggests that the identified proteins are related to MTRibP isomerases. Recently, the crystal structure of a protein (Ypr118w) from *Saccharomyces cerevisiae*,[152] showed to be a MTRP isomerase related to regulatory E1F-2B subunits. This enzyme is the yeast ortholog of the MTRP isomerase from *B. subtilis* with a reported

sequence similarity of 37 %. Another recent report outlines the crystallisation and preliminary structure analysis of a MTRP isomerase from *Bacillus subtilis*.[153]

3.2 The metabolism of 5'-FDA in a CFE of *S. cattleya*

In order to elucidate the remaining fluorinated intermediates on the biosynthetic pathway to fluoroacetaldehyde **48**, the biotransformation of 5-FDA **54** to fluoroacetate **8** was examined in real time in CFE's of *S. cattleya*. Accordingly, an active CFE (500 μl) was supplemented with 5'-FDA **54** (100 μl, 18.6 mM) at 37 °C and the progress of the biotransformation was followed by ^{19}F NMR at one hour intervals over a period of 9 hrs. The resulting ^{19}F NMR time course is shown in Figure 3.2, which clearly shows a number of organo-fluorine compounds generated from 5'-FDA **54**. The secondary metabolites fluoroacetate **8** (-216.94 ppm) and 4-fluorothreonine **47** (-231.56 ppm) are shown, indicating that the CFE retains all of its biosynthetic activities. The fluorine signal emerging after 6 hrs at -224.44 ppm has previously been identified as fluoroethanol **69**, which accumulates from the action of an adventitious alcohol dehydrogenase activity in *S. cattleya* acting on fluoroacetaldehyde **48**. Expansion of the ^{19}F NMR spectrum after 4 hr incubation reveals a further four organo-fluorine compounds. The presence of 5-FDRP **81** (-230.80 ppm) and 5'-FDI **55** (-230.88 ppm) are clear due to PNP and deaminase activities respectively (see Section 2.2). The absence of 5'-FDA **54** (-230.92 ppm) highlights its rapid conversion due to the simultaneous action of the previously mentioned enzymes. The precursor to the fluorinated secondary metabolites, fluoroacetaldehyde **48** (231.04 ppm), is also apparent after four hours from its transformation by the unknown steps after 5-FDRP **81**. The remaining two organofluorine signals at -231.35 ppm and -228.21 ppm corresponding to intermediates **A** and **B** remain to be characterised. It is therefore

conceivable that these two unidentified intermediates are the remaining fluoro-metabolites between 5-FDRP **81** and fluoroacetaldehyde **48**.

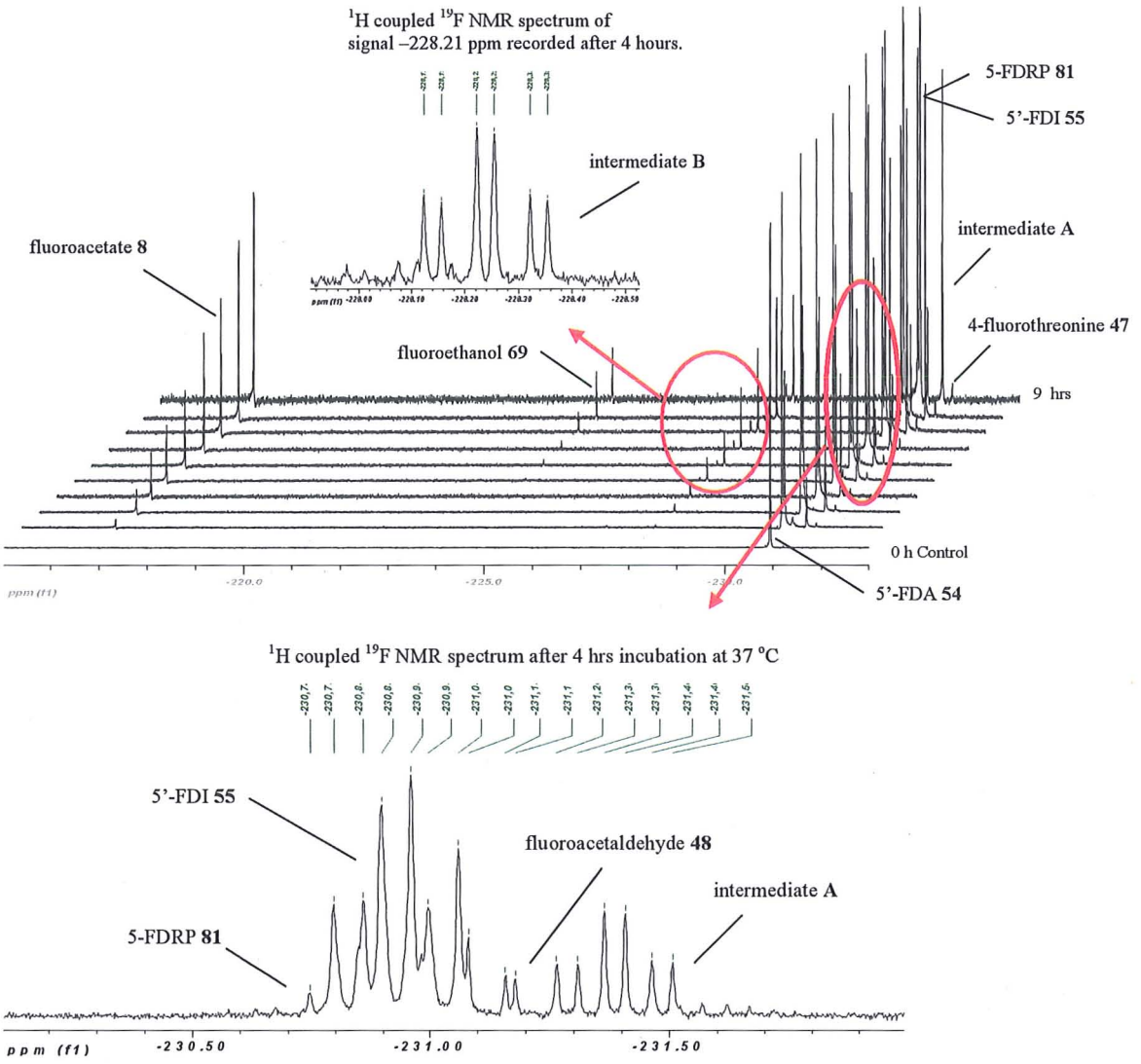

Figure 3.2 ^{19}F {^{1}H} NMR spectra time course spectra of 5'-FDA **54** incubated in a CFE of *S. cattleya*.

Expansion is ^{1}H coupled ^{19}F NMR spectrum, showing region -230.10 ppm to -232.00 ppm.

From the ^{19}F NMR spectra time course in Figure 3.2 the transformation of 5-FDRP **81** to the next intermediate remains elusive. No direct relationship could be established between 5-FDRP **81** and the two unidentified intermediates. However, from the results in Section 2.2.3 it was clear that the remaining intermediates are metabolised after overnight

incubation of a CFE with 5'-FDA **54**. This shows that both unidentified organo-fluorine signals are not shunt products on the pathway.

In order to study the transformation of 5-FDRP **81** to the next intermediate more closely, an experiment was conducted which involved the use of a less concentrated CFE (0.1 g cells / ml versus 0.2 g cells / ml). ^{19}F NMR spectra were recorded in real time, after the incubation of an active CFE (500 μl, 0.1 g cells / ml) with a synthetic sample of 5'-FDA **54** (100 μl, 18.6 mM) at hourly intervals for five hrs at 37 °C. The resultant ^{19}F NMR spectra time course is shown in Figure 3.3.

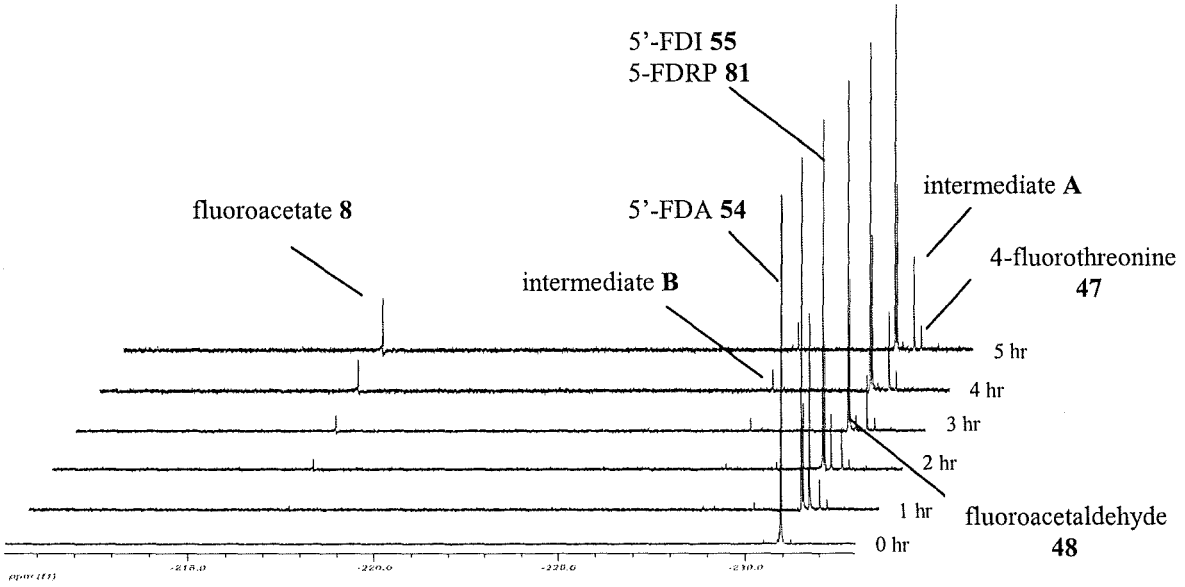

Figure 3.3 ^{19}F {^{1}H} NMR spectra time course of a CFE incubated with 5'-FDA **54**

The biotransformation of 5'-FDA **54** to 5-FDRP **81** and 5'-FDI **55** is clear after 1 hr due to the simultaneous activity of the PNP and deaminase respectively. The transformation of 5-FDRP **81** is shown to proceed to intermediate **A** (-231.34 ppm) which appears after 2 hrs of incubation and accumulates over time. It is unclear if intermediate **A** proceeds directly to **B** in this ^{19}F NMR time course. The intermediate fluoroacetaldehyde **48** is transient during the time course making it difficult to deduce a direct relationship between

intermediate **A** and fluoroacetaldehyde **48**. Therefore, it was anticipated that a clearer insight to the downstream section of the pathway might be unravelled by the addition of 5-FDRP **81** to a CFE.

3. 3 The metabolism of 5-FDRP in a CFE of *S. cattleya*

A cell free biotransformation of 5-FDRP **81** was explored. Accordingly, 5-FDRP **81** (200 μl) was prepared by the method established in Section 5.1.9, and was incubated with a CFE (500 μl). ^{19}F NMR spectra were recorded at hourly intervals for six hrs at 37 °C. The resulting spectra are shown in Figure 3.4.

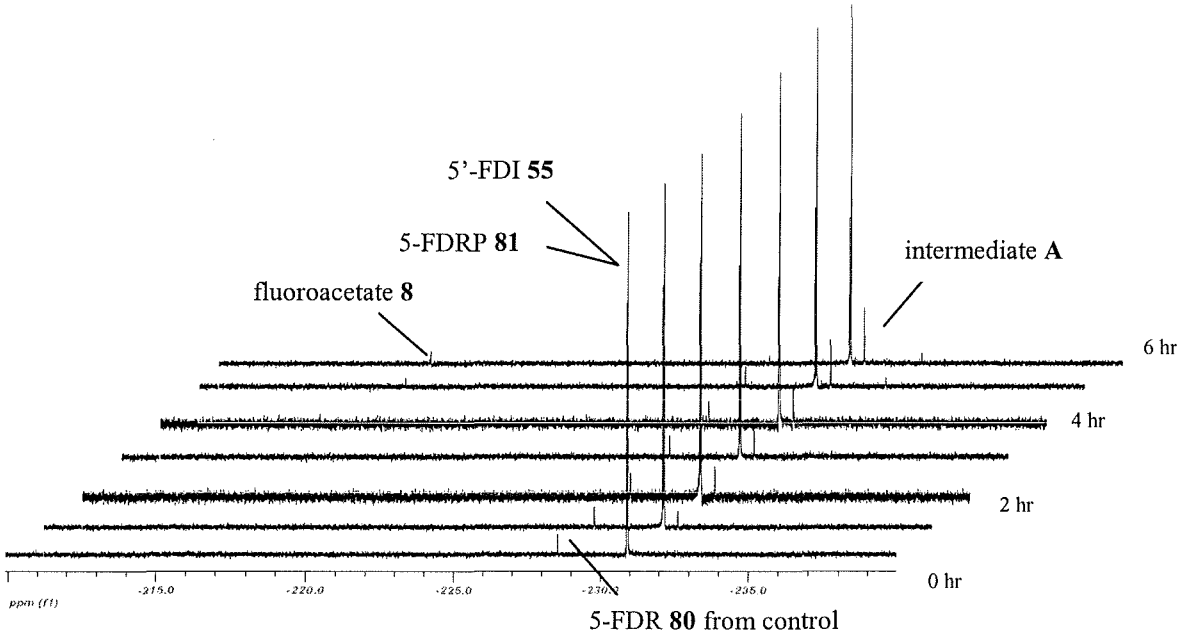

Figure 3.4 ^{19}F {^{1}H} NMR spectra time course of a CFE incubated with 5-FDRP **81**.

After one hour of incubation the emergence of an organo-fluorine signal at -231.30 ppm is apparent. This signal corresponds to intermediate **A** which was previously observed in Figure 3.2 and 3.3 in incubations with 5'-FDA **54**. During the time course the intensity of this signal increases. Although fluoroacetaldehyde **48** does not accumulate in this

experiment, presumably as it is transient, the formation of fluoroacetate **8** is apparent. No signal corresponding to intermediate **B** emerges suggesting that this compound is also transient in the experiment. Scheme 3.2 describes a working hypothesis of the metabolic fate of 5'-FDA **54** according to the CFE results so far.

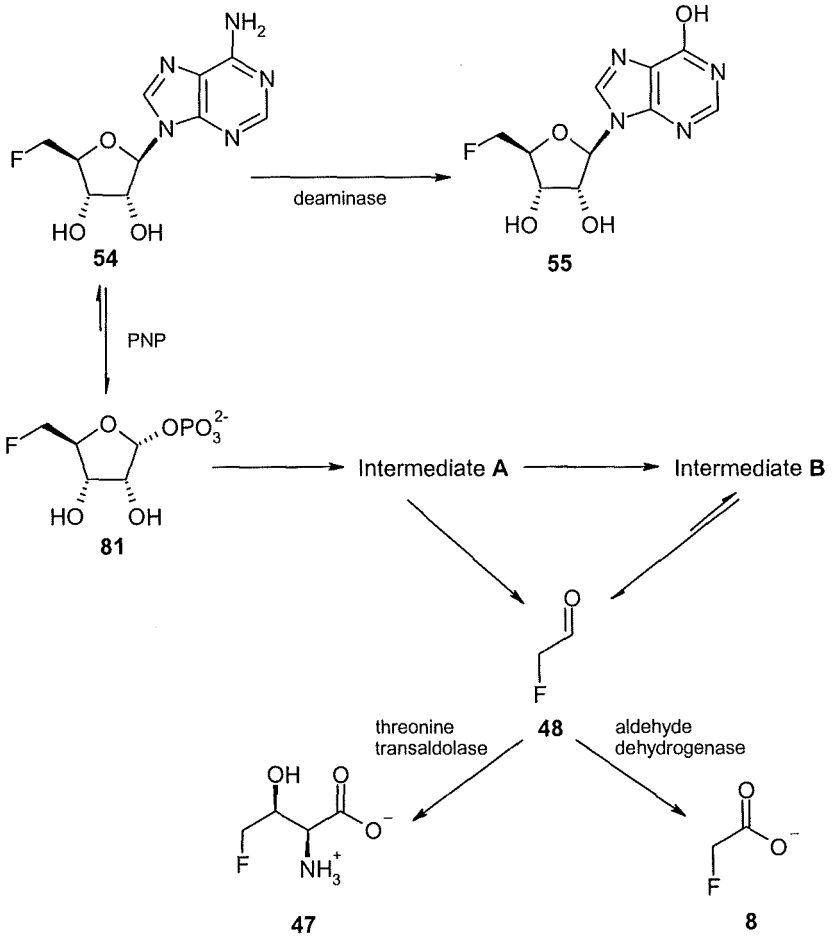

Scheme 3.2 Working hypothesis for the metabolic fate of 5'-FDA **54** from CFE studies.

The data suggest a direct transformation of intermediate **A** to **B**, and then **B** is metabolised to fluoroacetaldehyde **48**. Alternatively there is a transformation of intermediate **A** to fluoroacetaldehyde **48**, and then fluoroacetaldehyde **48** generates intermediate **B**. It is clearly important to identify intermediate **A** to begin to resolve these scenarios. An important strategy towards identifying the remaining intermediates involves blocking individual steps along the biosynthetic pathway to encourage the build up of intermediates. Therefore it was anticipated that the addition of various enzyme inhibitors such as EDTA

and iodoacetamide might selectively block key steps in the latter stages of the biotransformation.

3.3.1 Effect of iodoacetamide on the fluorometabolite production

It has previously been shown that iodoacetamide inhibited fluoroacetaldehyde dehydrogenase activity, preventing fluoroacetate **8** production in CFE's.[80,86] Iodoacetamide generally inhibits enzymes with free thiol groups. However it may inhibit other enzymes and result in the accumulation of **A** or **B**. Therefore, an active CFE (500 μl) was pre-incubated with iodoacetamide (final conc.10 mM) for 25 minutes at 37 °C. After this time, 5'-FDA **54** (100 μl, 18.6 mM) was added to the reaction and incubated for 7 hrs at 37 °C (Figure 3.5(ii)).

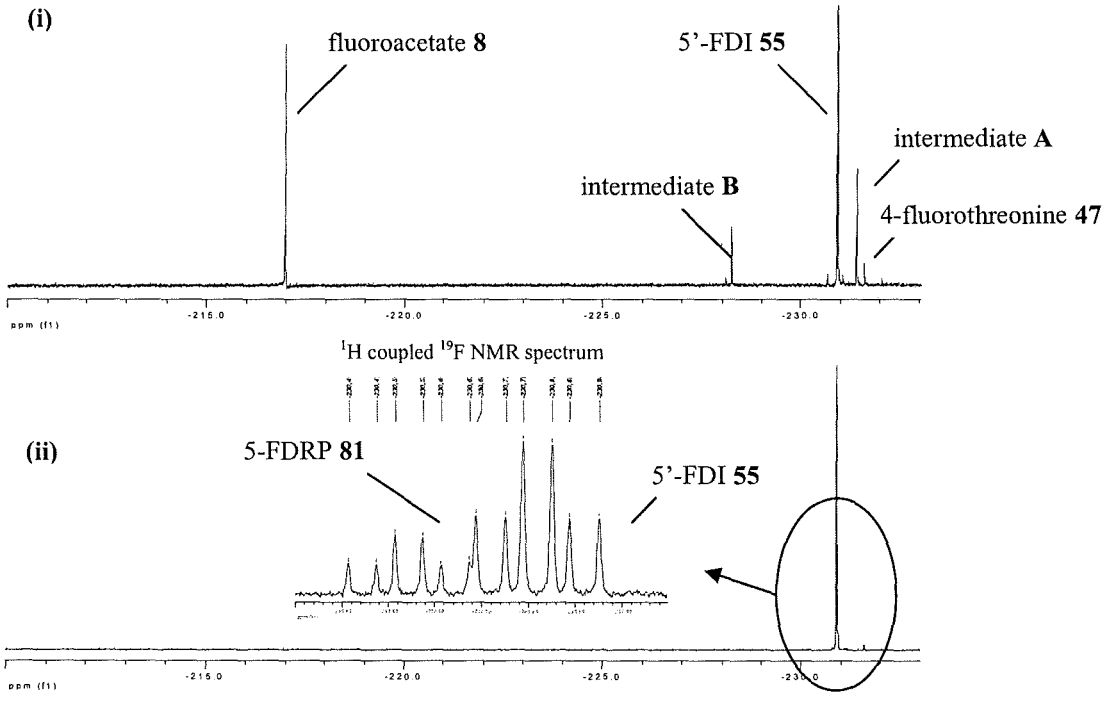

Figure 3.5 **(i)** ^{19}F $\{^1H\}$ NMR spectrum of 5'-FDA **54** incubated with CFE for 7 hrs at 37 °C. **(ii)** ^{19}F $\{^1H\}$ NMR spectrum of CFE incubated with 5'-FDA **54** for 7 hrs at 37 °C in the presence of iodoacetamide.

A control experiment, shown in Figure 3.5(i), indicates the production of fluoroacetate **8** and 4-fluorothreonine **47** indicating that the CFE retains all of the biosynthetic activities on the pathway. However, in the presence of iodoacetamide (Figure 3.5(ii)), fluoroacetate **8** (-216.97 ppm) and 4-fluorothreonine **47** (-231.61 ppm) no longer accumulate. Although the experiment arrested fluorometabolite production, there was no evidence of the accumulation of either **A** or **B** or fluoroacetaldehyde **48** (Figure 3.5(ii)). Both 5'-FDI **55** and 5-FDRP **81** also accumulated in this experiment. This was confirmed by HPLC analysis (Figure 3.6).

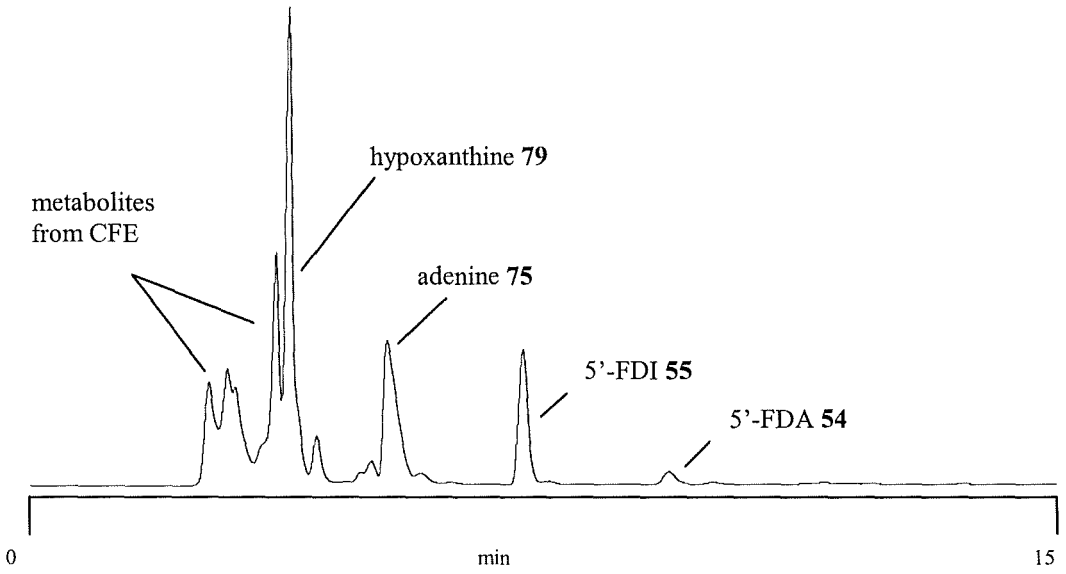

Figure 3.6 HPLC chromatogram of CFE incubated with 5'-FDA **54** for 5 hrs at 37 °C in the presence of iodoacetamide.

The presence of 5'-FDI **55** was confirmed by co-injection using a synthetic sample. The presence of adenine **75** and hypoxanthine **79** in the sample was also obvious by HPLC and their presence can be attributed to the simultaneous action of PNP and deaminase activities (Section 2.2). The remaining signal in the ^{19}F NMR spectrum corresponded to 5-FDRP **81**. To firmly establish this, the experiment was repeated with the addition of 5-FDRP **81** to a

CFE. Subsequent ^{19}F NMR analysis showed that the signal at -230.78 ppm (5-FDRP **81**) was reinforced.

Overall the results from this experiment show that the next enzyme responsible for the transformation of 5-FDRP **81** is inhibited by iodoacetamide, as 5-FDRP **81** accumulates.

3.3.2 Effect of EDTA on fluorometabolite production

EDTA chelates metal ions and generally inhibits metal requiring enzymes. An active CFE (500 μl) was pre-incubated with EDTA (final conc. 30 mM) for 25 minutes. After this time 5-FDRP **81** (150 μl) was added and the reaction incubated for 16 hrs at 37 °C. The resulting ^{19}F NMR spectrum is shown in Figure 3.7.

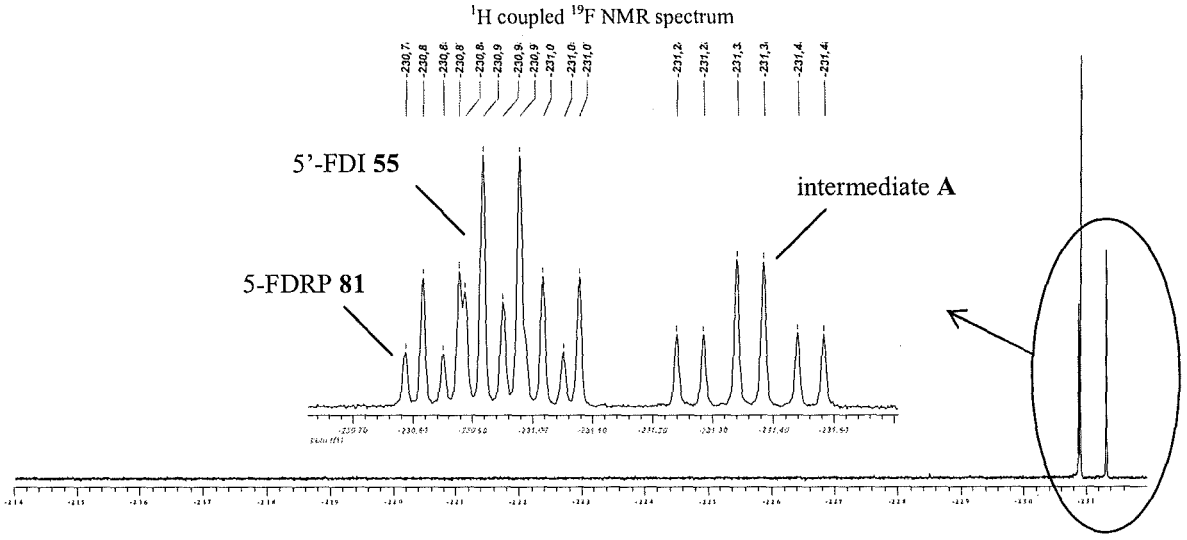

Figure 3.7 ^{19}F {^{1}H} NMR spectrum of (5'-FDI **55** + 5-FDRP **81**) incubated with CFE and EDTA for 16 hrs at 37 °C. Expansion is ^{1}H coupled ^{19}F NMR spectrum.

In the presence of EDTA, fluoroacetate **8** and 4-fluorothreonine **47** no longer accumulate. Although the experiment arrested secondary metabolite production, there was no evidence for the accumulation of fluoroacetaldehyde **48**. Three fluorine signals are apparent in Figure 3.7, two of these can be assigned to 5-FDRP **81** and 5'-FDI **55** based on previous

observations (Section 3.2). The third signal had the same chemical shift as intermediate **A**, identified in previous CFE experiments. Clearly this result suggests that EDTA inhibits the enzymes responsible for the biotransformation of intermediate **A** and that they require a metal ion as a cofactor. Intermediate **B** did not accumulate in this reaction. Scheme 3.3 summarises the developing hypothesis.

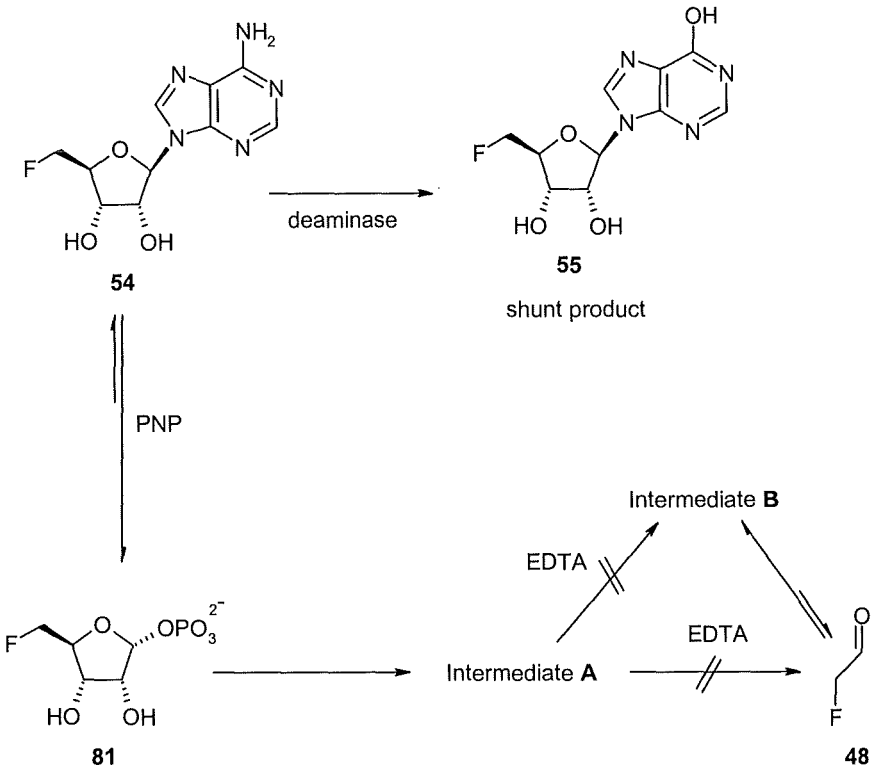

Scheme 3.3 Overview of EDTA effect on fluorometabolite production.

3.4 5-Fluoro-5-deoxy-D-ribulose-1-phosphate as a biosynthetic intermediate

If the transformation of 5-FDRP **81** to intermediate **A** proceeds along a similar line to that shown from the isomerisation of 5-MTRP **78** in the methionine salvage pathway (Section 3.1), then the product generated would be 5-fluoro-5-deoxy-D-ribulose-1-phosphate (5-

FDRibP) **121**. This is an attractive prospect as 5-FDRibP **121** is an ideal substrate for an aldolase (see Chapter 4). An aldolase could mediate a retro-aldol reaction to give fluoroacetaldehyde **48**, which has already been established as a biosynthetic intermediate. Scheme 3.4 illustrates the isomerisation catalysed by such a putative isomerase.

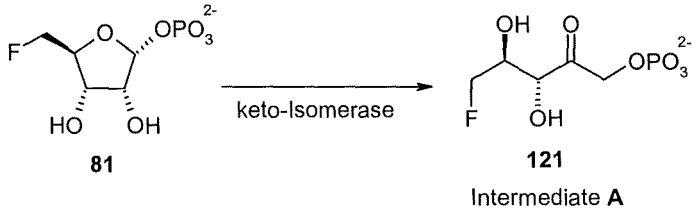

81 **121**

Intermediate **A**

Scheme 3.4 Proposed biotransformation of 5-FDRP **81** in *S. cattleya*.

3.4.1 Enzymatic preparation of 5-fluoro-5-deoxy-D-ribulose

Aldolases have been widely used to prepare a variety of modified carbohydrates, particularly ribuloses.[154] However, following the pioneering work by Bock and co-workers,[155] an alternative to the aldolase based method has involved xylose isomerase (EC 5.3.1.5).[156] 5'6-Aldofuranoses are isomerised to open-chain ketoses[157-159] and this enzyme has been shown to catalyse the isomerisation of various aldofuranoses such as D-erythrose, as well as homologous C-5 modified D-ribose derivatives. Ebner and co-workers[160] have shown that 5-FDR **80** is a substrate for the xylose isomerase (Scheme 3.5).

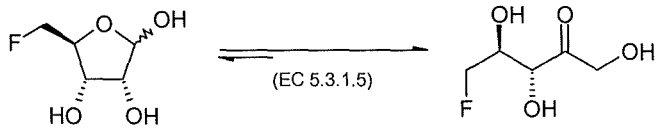

80 **122**

Scheme 3.5 Enzymatic reaction catalysed by xylose isomerase in presence of 5-FDR **80**.

The product 5-fluoro-5-deoxy-D-ribulose (5-FDRib) **122** is the de-phosphorylated analogue of 5-FDRibP **121**, our proposed biosynthetic intermediate. Therefore, it seemed appropriate to compare the product generated from the xylose isomerase reaction, 5-FDRib **122** with the de-phosphorylated intermediate **A** from *S. cattleya.* If both compounds are the same, this would provide proof of structure. The addition of a phosphatase to the accumulated intermediate **A** will result in the hydrolysis of the phosphate ester to give **122**. Scheme 3.6 outlines the experimental strategy.

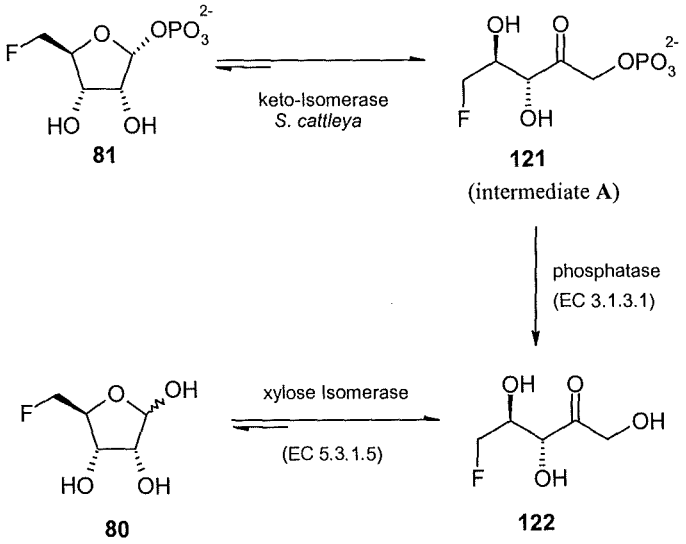

Scheme 3.6 Two complementary routes towards the synthesis of 5-FDRib **122**.

Xylose isomerase (EC 5.3.1.5 from *Streptomyces murinus*) was used for the production of 5-FDRib **122** from 5-FDR **80**. In order to perform the reaction, a synthetic sample of 5-FDR **80** prepared by Mayca Onega,[161] University of St Andrews, was obtained and incubated in the presence of xylose isomerase. A ^{19}F NMR time course experiment was conducted, in real time by incubation of 5-FDR **80** (final conc. 4.7 mM) with immobilised xylose isomerase and spectra recorded at hourly intervals for six hrs at 60 °C. The resulting ^{19}F NMR spectra are shown in a stacked format in Figure 3.8.

The results from the control experiment show the presence of the two anomers of 5-FDR **80**, (β-anomer -228.47) (td, $^{2}J_{F,H}$ 47.3 and $^{3}J_{F,H}$ 25.8), (α-anomer -230.78) (td, $^{2}J_{F,H}$ 47.3 and $^{3}J_{F,H}$ 27.3). Upon close inspection the depletion of these fluorine signals is obvious with the concomitant emergence of a third signal at -231.17 ppm (dt, $^{2}J_{F,H}$ 46.9 and $^{3}J_{F,H}$ 20.6). The identity of this signal is assumed to correspond to the isomer product, 5-FDRib **122**. Incubation times longer than 6 hrs did not result in further product formation, presumably due to the reversible xylose isomerase reaction reaching equilibrium.

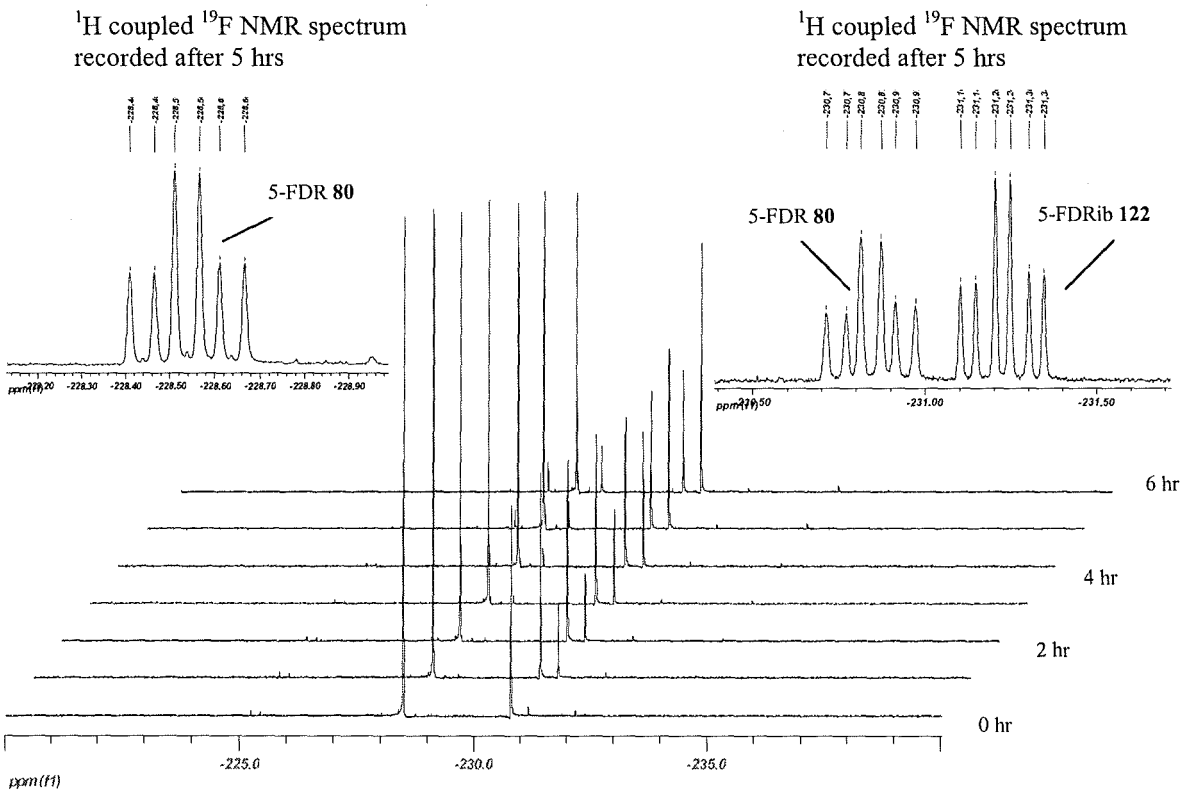

Figure 3.8 ^{19}F {^{1}H} NMR time course of 5-FDR **80** incubated with xylose isomerase. Expansions are ^{1}H coupled ^{19}F NMR spectra.

A second series of experiments involved the formation of intermediate **A** from *S. cattleya*. An experiment was conducted in which an active CFE (500 μl) was pre-incubated with EDTA (final conc. 30 mM) for 25 minutes. After this time, 5-FDRP **81** was added to the

pre-incubated sample and the reaction was monitored at hourly intervals again for 6 hrs at 37 °C (Figure 3.9).

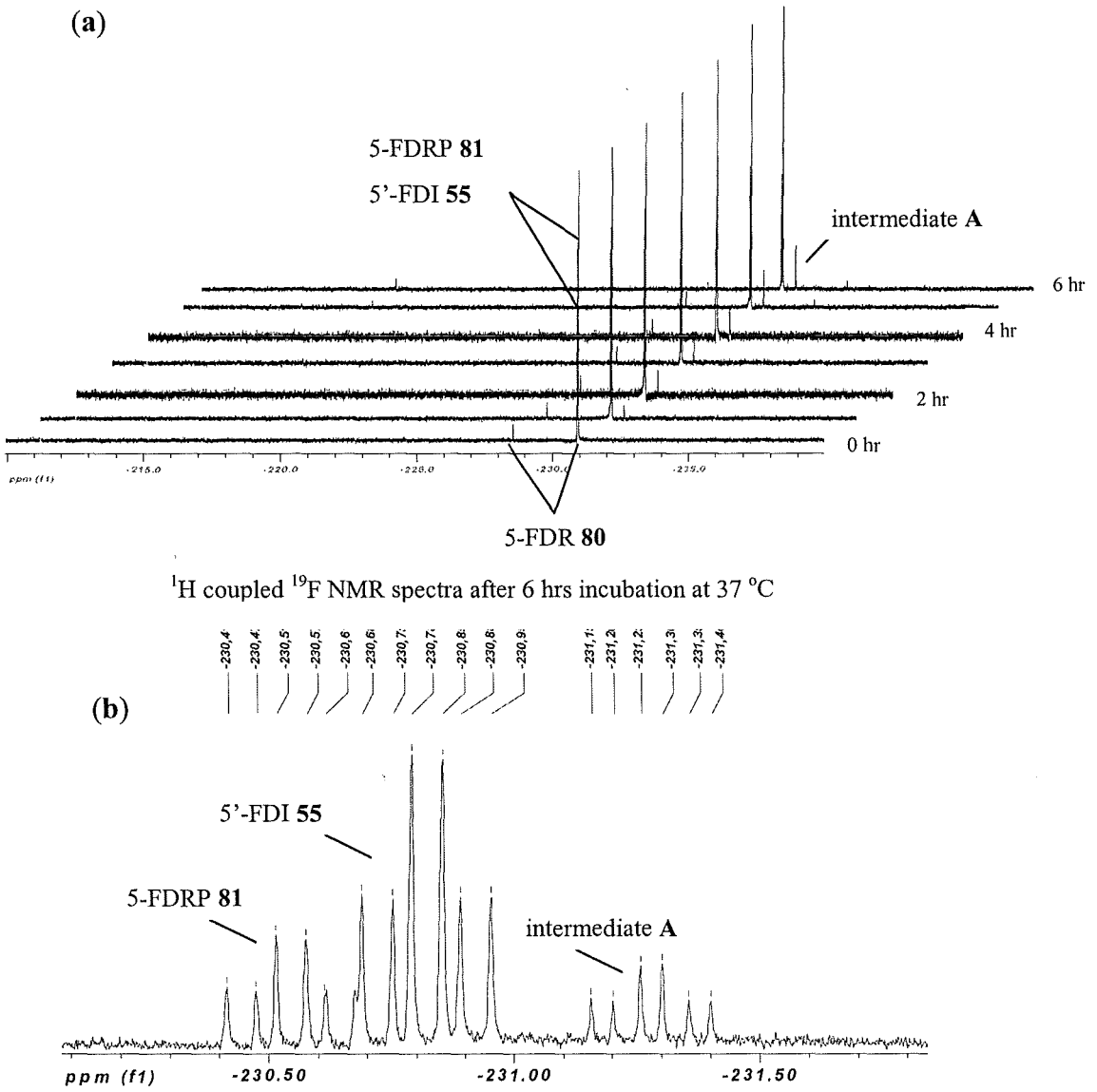

Figure 3.9 (**a**) ^{19}F {^{1}H} NMR time course of a CFE incubated with 5-FDRP **81** and EDTA. (**b**) ^{1}H coupled ^{19}F NMR spectrum after 6 hrs, expansion of region -230.10 ppm to -231.80 ppm.

The resulting stacked ^{19}F NMR spectrum shows the starting material 5-FDRP **81** and residual 5'-FDI **55**. A fluorine signal is apparent at -228.44 ppm in the control experiment which remains metabolically inert during the time course. The identity of this signal was

shown to be 5-FDR **80**, which is probably the result of an adventitious phosphatase activity present from the crude immobilised PNP. A third fluorine signal is shown to emerge after one hour incubation, with an increase in intensity over the 6 hrs. The signal corresponds to intermediate **A**.

Each of the resulting ^{19}F NMR samples from the time course in Figure 3.9 was supplemented with a phosphatase (EC 3.1.3.1, from bovine intestinal mucosa) (20 μl, 10 mg / ml) and incubated for a further 2 hrs at 37 °C. The results are presented in Figure 3.10.

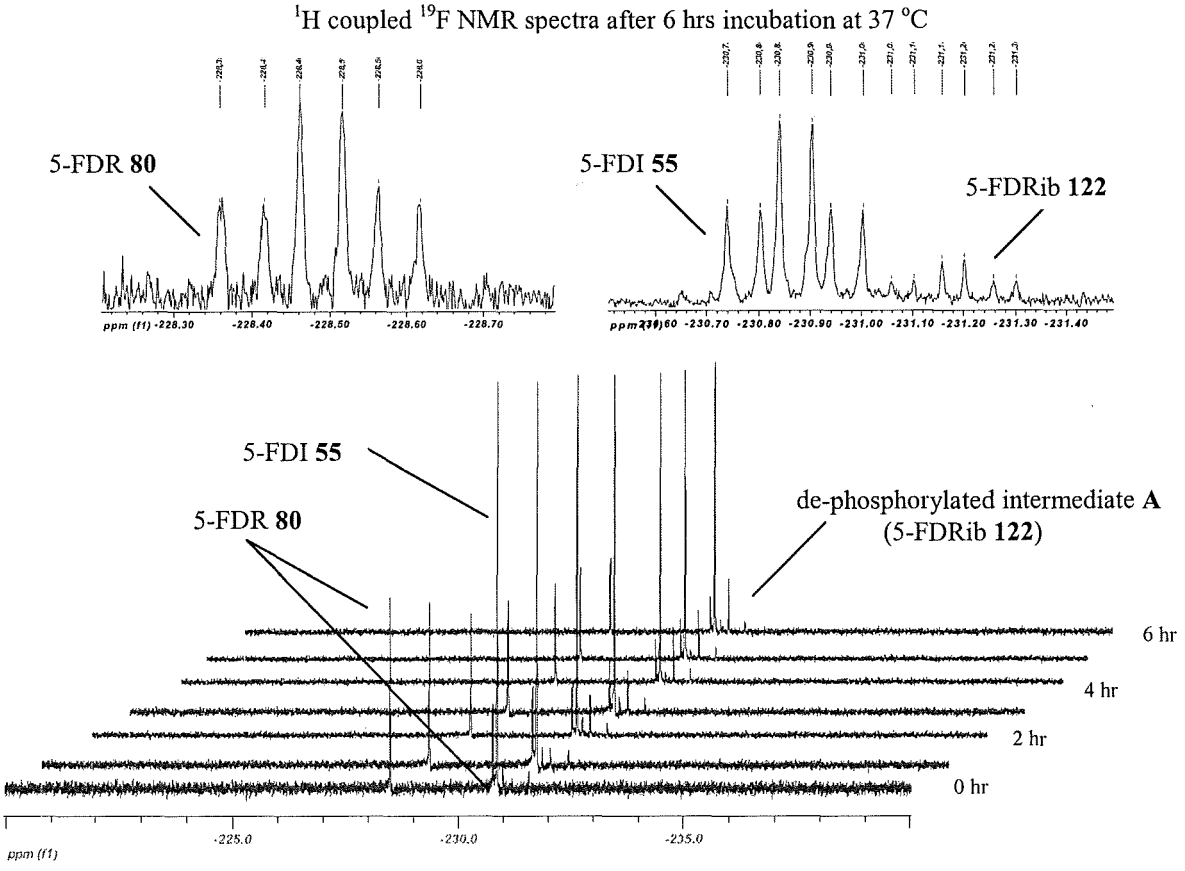

Figure 3.10 ^{19}F {^{1}H} NMR time course after addition of a phosphatase to the ^{19}F NMR samples from the time course in Figure 3.9. Expansions are ^{1}H coupled ^{19}F NMR spectra.

The two signals at -228.45 ppm (dt, $^{2}J_{F,H}$ 47.0 and $^{3}J_{F,H}$ 26.4) and -230.74 ppm (dt, $^{2}J_{F,H}$ 47.3 and $^{3}J_{F,H}$ 26.8) correspond to the two anomers of 5-FDR **80**. This can be explained by

the hydrolysis of the phosphate ester of unreacted 5-FDRP **81**. The addition of phosphatase also resulted in a small change in the chemical shift in the ^{19}F NMR signal from -231.32 ppm to -231.18 ppm consistent with the notion that intermediate **A** contained a phosphate group. To confirm this unambiguously the product of the xylose isomerase reaction; 5-FDRib **122** was added to the de-phosphorylated product obtained from the CFE's from Figure 3.10. The compounds were identical as judged by ^{19}F NMR as shown in Figure 3.11.

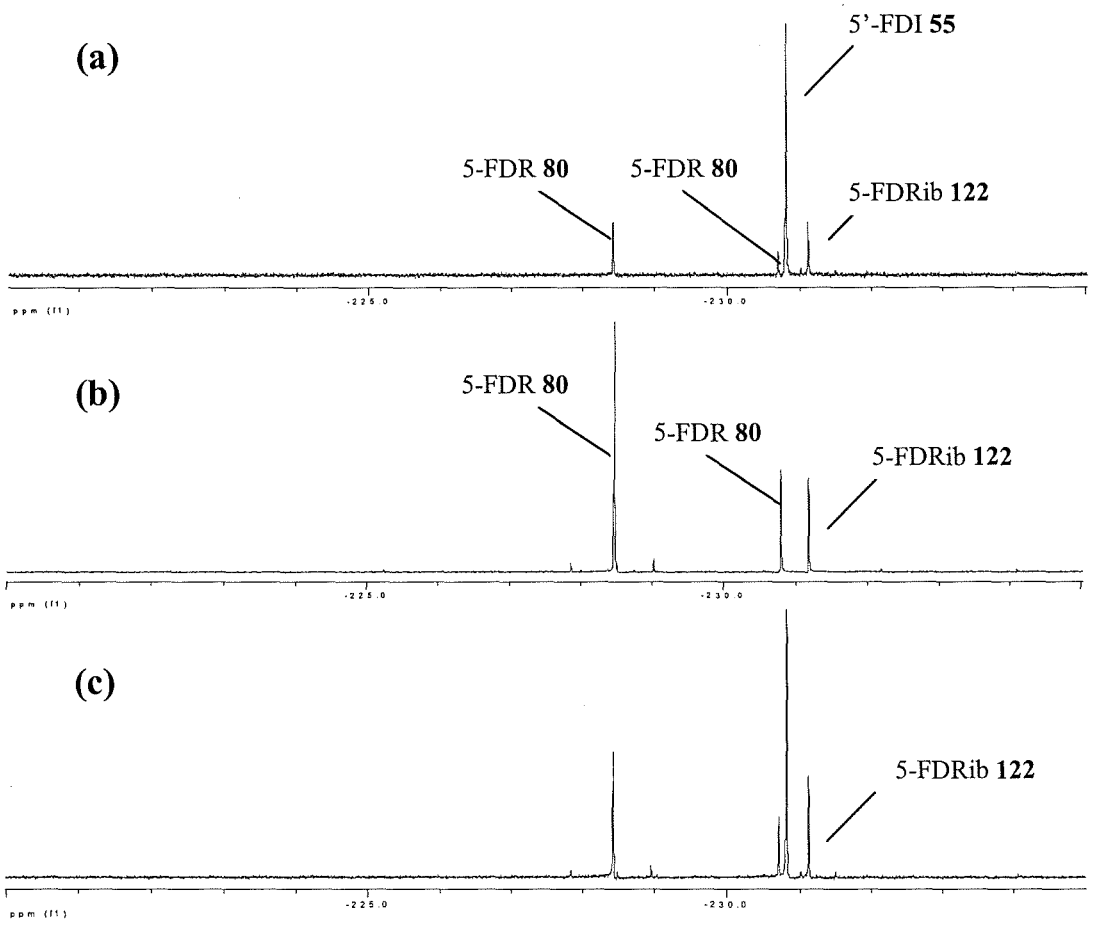

Figure 3.11 ^{19}F $\{^{1}H\}$ NMR spectra of **(a)** CFE incubated with 5-FDRP **81** and EDTA for 16 hrs at 37 °C, supplemented with phosphatase. **(b)** 5-FDR **80** incubated with xylose isomerase for 3 hrs at 60 °C. **(c)** Spectrum from **(a)** and **(b)** combined.

These results indicate that the de-phosphorylation product of intermediate **A** and the enzymatically prepared 5-FDRib **122** are identical. This reinforces the presence of an isomerase activity in *S. cattleya* which is responsible for the formation of the phosphorylated sugar, 5-FDRibP **121**.

3.4.2 The role of 5-fluoro-5-deoxy-D-ribulose

The role of 5-FDRib **122** was explored as a possible intermediate on the biosynthetic pathway in *S. cattleya*. It was of interest to establish if 5-FDRib **122**, a potential de-phosphorylated product of 5-FDRibP **121** could support the biosynthesis of fluoroacetate **8** and 4-fluorothreonine **47**. A chemo-enzymatic preparation of 5-FDRib **122** was carried out using xylose isomerase (Section 5.1.13) to obtain a sample for incubation studies. Due to the reversible nature of the xylose isomerase reaction, 5-FDR **80** was also present in the reaction product. However, from control experiments it is already established that 5-FDR **80** is metabolically inert in CFE's of *S. cattleya*. Accordingly, an active CFE (500 μl) was incubated with this 5-FDRib **122** (100 μl) preparation for 16 hrs at 37 °C (Figure 3.12).

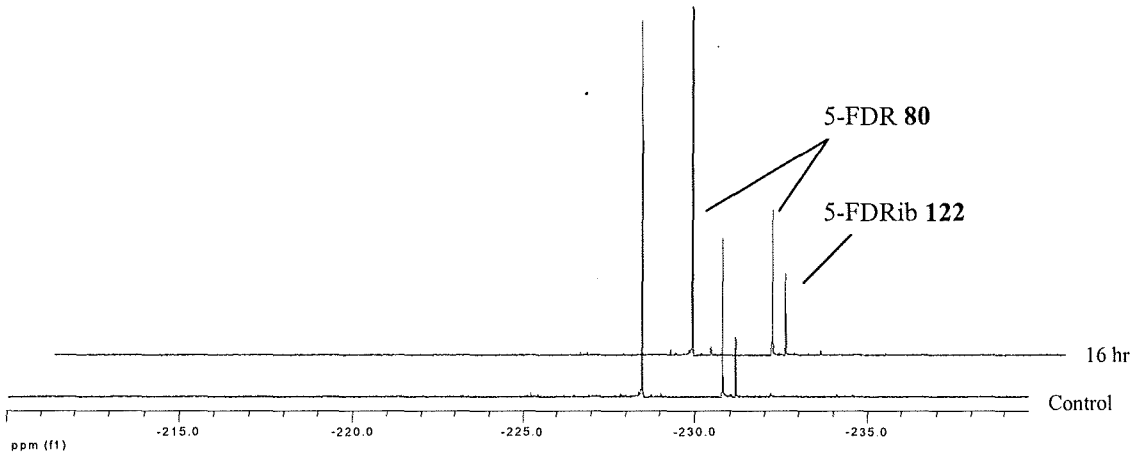

Figure 3.12 ^{19}F $\{^{1}H\}$ NMR spectrum of 5-FDRib **122** incubated in a CFE.

The resultant ^{19}F NMR spectrum shows the control experiment with three main organo-fluorine signals corresponding to the two anomers of 5-FDR **80** and the 5-FDRib **122** product. The subsequent experiment involving the addition of 5-FDRib **122** to a CFE showed no change. It is therefore concluded that 5-FDRib **122** does not support the biosynthesis of fluoroacetate **8** and 4-fluorothreonine **47**.

Overall, the results described in this section emphasize the importance of the phosphate group on 5-FDRibP **121** for fluorometabolite biosynthesis.

3.5 Purification of the isomerase

3.5.1 Assay for detection of isomerase activity

A ^{19}F NMR assay was employed to monitor the conversion of 5-FDRP **81** to 5-FDRibP **121** catalysed by the isomerase. The assay was based on the method outlined in Section 5.1.25, and was used at each purification stage.

3.5.2 Step 1: Ammonium sulfate precipitation

The first stage of protein purification after CFE generation, involved the addition of ammonium sulfate $(NH_4)_2SO_4$ to salt out the desired protein. It was previously shown to be an important step during PNP purification (Section 2.3.2), and was considered an attractive step to initiate isomerase purification. Four $(NH_4)_2SO_4$ cuts were used for precipitations (0-35 %, 35-50 %, 50-60 %, 60-80 %). After $(NH_4)_2SO_4$ addition to the CFE, the solution was left to stir for 20 min at 4 °C. After this time the precipitated protein was removed by centrifugation (14, 000 rpm / 20 min) and the supernatant used for the next $(NH_4)_2SO_4$ cut. Each of the $(NH_4)_2SO_4$ cuts was assayed in the following way.

Partially purified CFE (200 μl) was supplemented with 5-FDRP **81** prepared from the method outlined in Section 5.1.9 and incubated for 16 hrs at 37 °C. The resulting samples were analysed by ^{19}F NMR and can be seen in Figure 3.13.

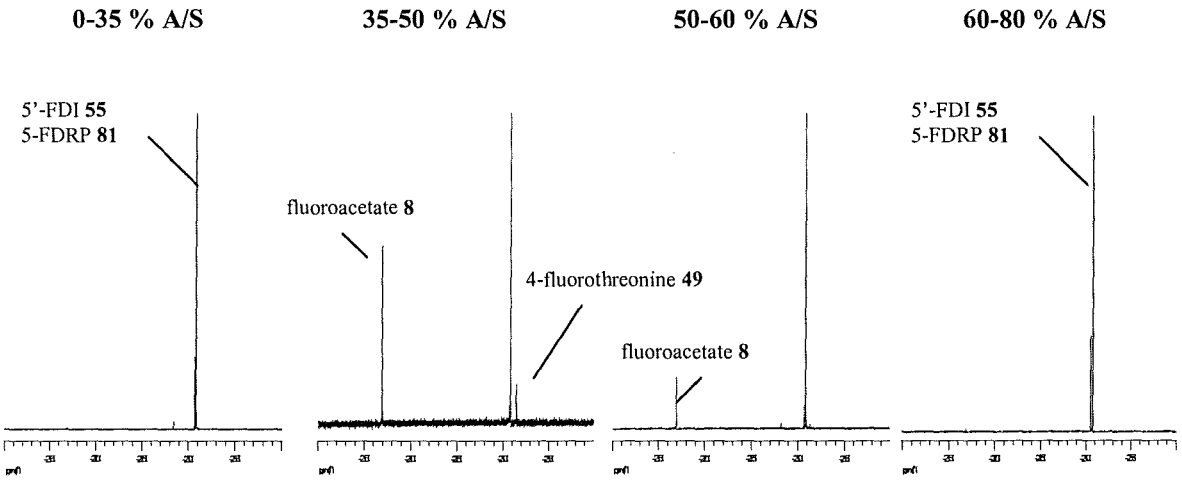

Figure 3.13 ^{19}F {^{1}H} NMR spectra of ammonium sulfate cuts incubated with 5-FDRP **81**.

The data shows that the 35-60 % cut contained all of the biosynthetic enzymes and cofactors to support fluoroacetate **8** and 4-fluorothreonine **47** biosynthesis. The isomerase activity is contained predominantly in the 35-50 % cut with a minor amount in the 50-60 % cut. No activity was detected in any of the other fractions, which only contained 5-FDRP **81** and 5'-FDI **55**. The transformation of 5-FDRP **81** to 5-FDRibP **121** could not be detected in real time; therefore, an experiment was conducted in a similar manner to that in Section 3.3.2 which involved the addition of EDTA. The 35-50 % cut (100 μl) was pre-incubated with EDTA for 25 min at 37 °C. After this time, the pre-incubated sample was supplemented with 5-FDRP **81** and incubated for 16 hrs at 37 °C. Analysis by ^{19}F NMR spectroscopy (Figure 3.14) shows the 35-50 % cut was able to support the synthesis of 5-FDRibP **121**. This indicates that the addition of a metal ion cofactor is not required for isomerase activity.

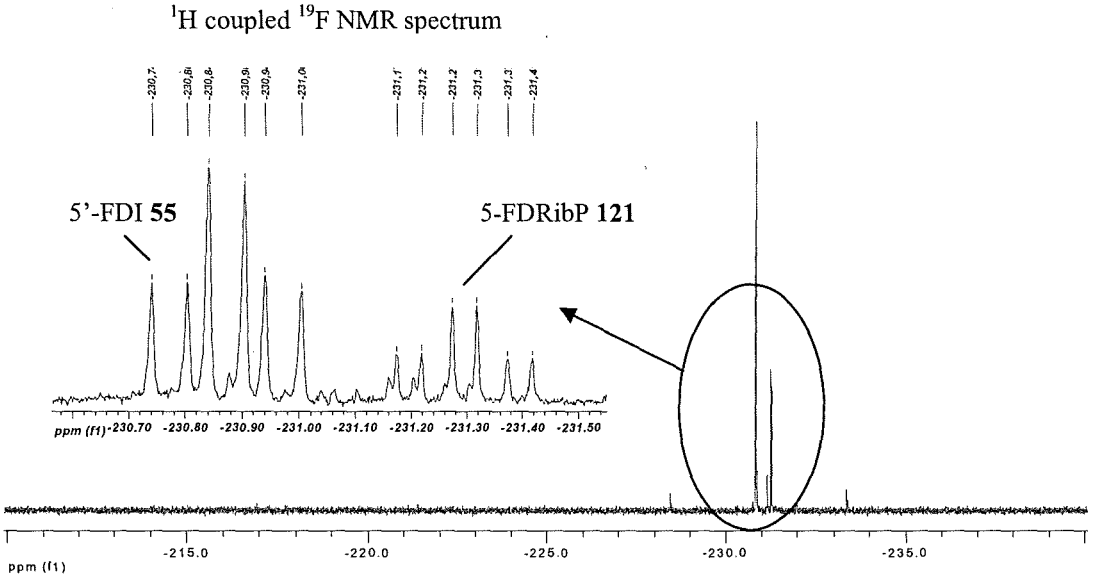

Figure 3.14 ^{19}F {^{1}H} NMR spectrum of 35-50% $(NH_4)_2SO_4$ cut incubated with 5-FDRP **81** and EDTA for 16 hrs at 37 °C.

The two organo-fluorine signals apparent in the resultant spectrum are assigned to 5'-FDI **55** and 5-FDRibP **121**. The presence of 5'-FDI **55** was additionally confirmed by HPLC and co-injection experiments using a synthetic sample.

3.5.3 Step 2: Hydrophobic interaction chromatography

It was shown in Section 2.3.3 that hydrophobic interaction chromatography proved to be a successful second step during PNP purification. The application of this technique towards isomerase purification was explored, based on the previous protocol. Consequently, a (Phenyl HP, 40 ml) column was equilibrated with phosphate buffer (50 mM, pH 6.8) supplemented with 1 M $(NH_4)_2SO_4$. The 35-50 % $(NH_4)_2SO_4$ precipitate was re-dissolved in equilibration buffer (6 ml, 20 mg / ml) and applied to the column and subsequently eluted according to Section 2.3.3. The resulting protein elution chromatogram is shown in Figure 3.15.

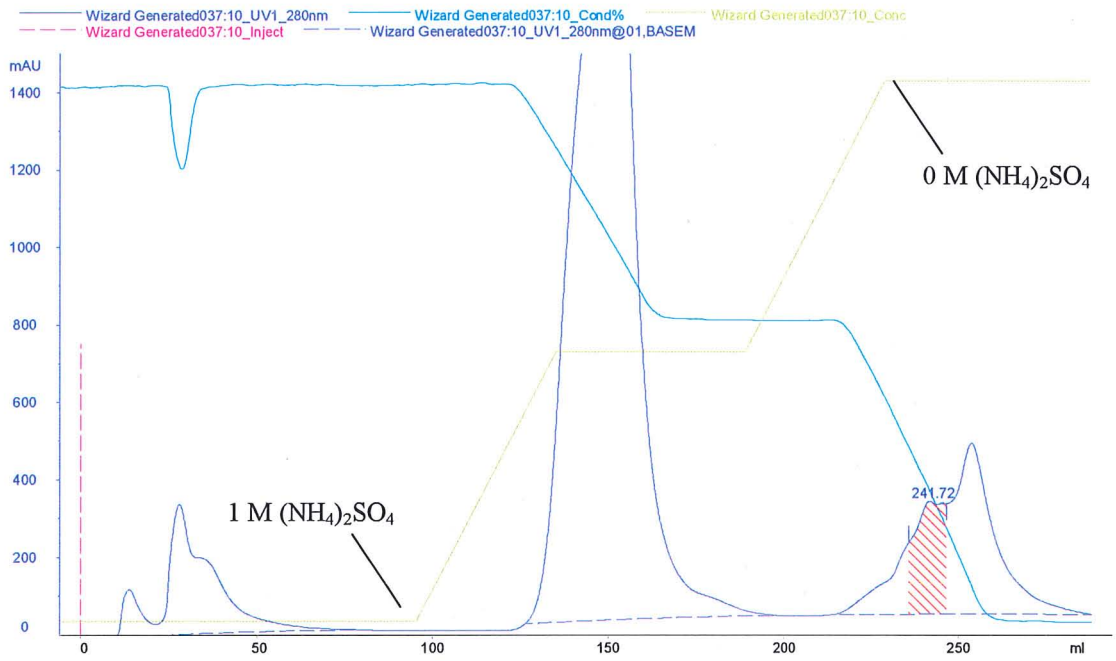

Figure 3.15 Step 2: Phenyl HP (40 ml) chromatogram obtained after a second stage purification.

The chromatogram shows several protein fractions eluting during the purification protocol. The eluted fractions were analysed by ^{19}F NMR spectroscopy after incubation of each fraction (200 µl) with 5-FDRP **81** (16 hrs at 37 °C). Isomerase activity was shown to elute at the end of the gradient (highlighted area), indicating a strong affinity to the resin. Overall, purification by hydrophobic interaction chromatography proved to be a successful technique as it removed a substantial amount of undesired protein.

3.5.4 Step 3: Size exclusion chromatography

For the next purification step, size exclusion chromatography was explored. This involves the separation of proteins according to molecular weight. Proteins that have a higher molecular weight are eluted faster than those with lower molecular weights. An advantage of using size exclusion at this stage is that the active isomerase fraction from the

hydrophobic interaction chromatography (HIC) only requires concentrating prior to injection.

The protein (2 ml, ~8 mg / ml) was applied to a pre-equilibrated Superdex 200 column at a flow rate of 1 ml / min. Figure 3.16 shows the resulting chromatogram obtained after purification by size exclusion chromatography.

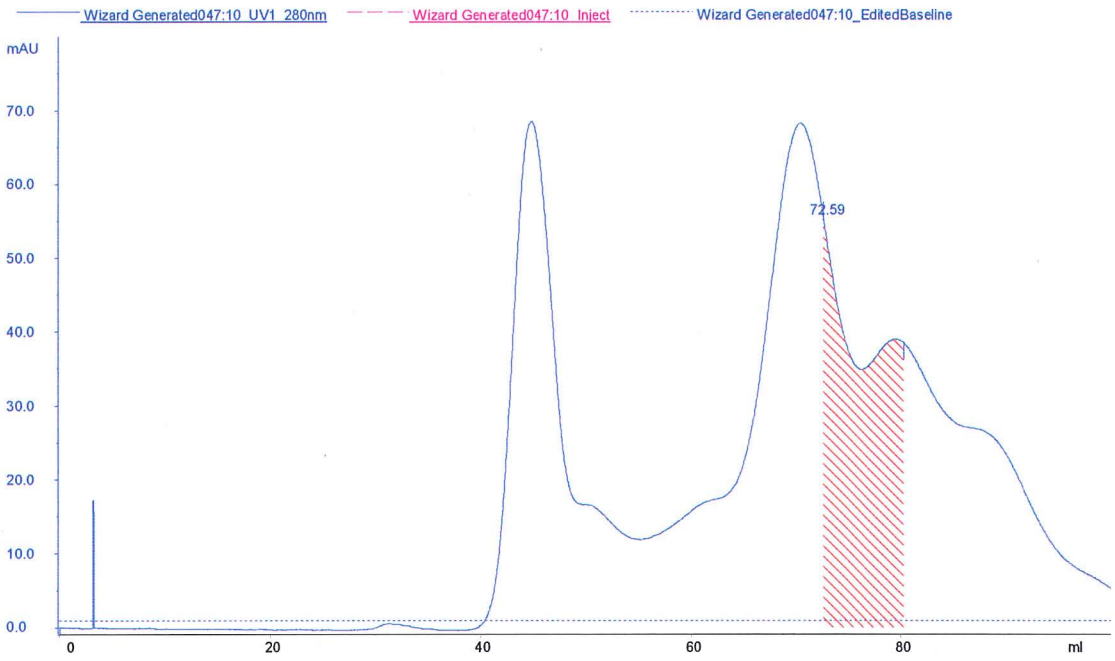

Figure 3.16 Step 3: Chromatogram obtained by size exclusion chromatography using a Superdex 200 column (120 ml) after injection of 2 ml sample from HIC purification.

Fractions were assayed for isomerase activity and the activity was found to elute between 72 - 80 ml (highlighted area) with a protein concentration of ~ 0.5 mg / ml. Although base line separation wasn't achieved, a substantial amount of undesired protein was removed. Further purification was clearly required to move towards a pure protein.

3.5.5 Step 4: Anion exchange chromatography

Anion exchange chromatography was now explored to purify the active fractions further following the protocol in Section 2.3.4 for PNP purification. The combined active fractions from step 3 (8 ml) were concentrated (2 ml) by centrifugation. The concentrated protein was then passed through a desalting column (HiTrap™ desalting, 5 ml) and re-concentrated to ~ 2 ml by the same method.

The 2 ml sample was loaded onto the strong anion exchange column (Q, 5 ml, Amersham Biosciences) pre-equilibrated with tris buffer (50 mM, pH 7.2). Elution was achieved by a stepwise gradient following the PNP protocol. The elution profile is shown in Figure 3.17.

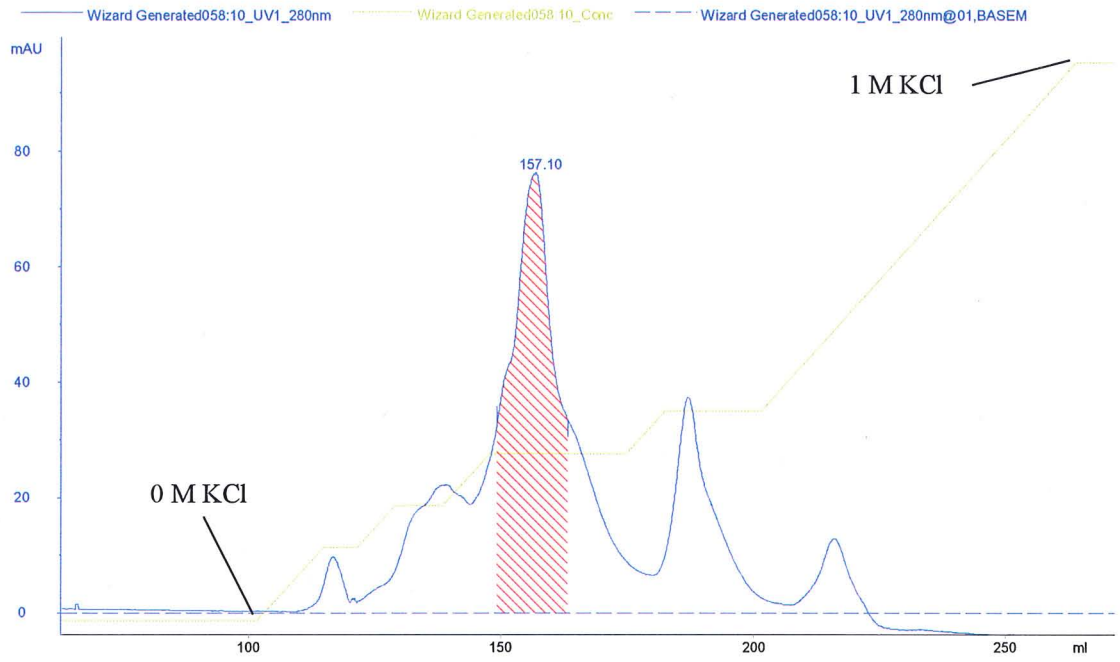

Figure 3.17 Step 4: Chromatogram obtained by anion exchange using a Q, 5 ml column after injection of (2 ml) from size exclusion purification.

Each fraction was assayed for isomerase activity using the assay outlined in Section 5.1.25. This showed that the desired activity eluted after 250 mM KCl addition with a total protein concentration of 1.5 mg / ml. It is clear from the trace in Figure 3.17 that further

purification is needed. Only a small proportion of undesired protein was removed in this step and it is evident that that the desired protein is not yet homogenous.

3.5.6 Isomerase analysis by SDS-PAGE

Each stage of the protein purification was monitored by SDS-PAGE and is shown in Figure 3.18.

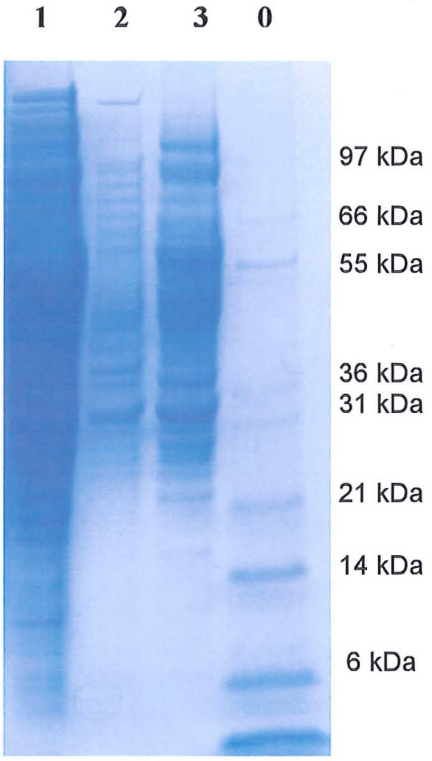

Figure 3.18 SDS PAGE gel (4-12% acrylamide) showing active protein fractions containing isomerase activity during each purification step. Lanes: **0,** molecular markers **1,** hydrophobic interaction chromatography, **2,** size exclusion chromatography, **3**, anion exchange chromatography.

In the end a partially purified fraction that was able to catalyse the isomerisation of 5-FDRP **81** to 5-FDRibP **121** was obtained.

3.6 Metabolic fate of 5-FDRibP in *S. cattleya*

This section details work that was carried out to investigate the subsequent metabolism of 5-fluoro-5-deoxy-D-ribulose-1-phosphate (5-FDRibP) **121** within *S. cattleya*. It was previously shown that intermediate **B** was formed in CFE incubations from 5'-FDA **54**. This led to two plausible routes to account for intermediate **B** formation, either from 5-FDRibP **121** or from fluoroacetaldehyde **48** (Scheme 3.7).

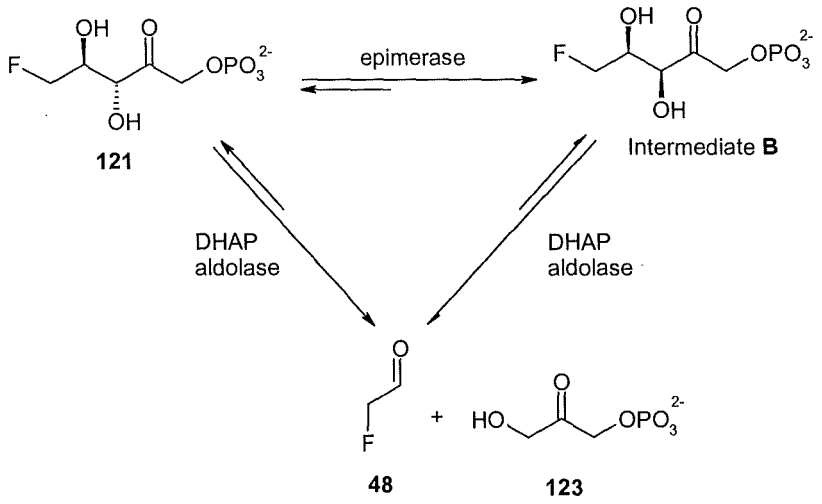

Scheme 3.7 Possible relationships between 5-FDRibP **121** and intermediate **B** in *S. cattleya*

Firstly, it is possible that 5-FDRibP **121** undergoes enzymatic epimerization to afford its diastereoisomer (intermediate **B**), which is then metabolised *via* a dihydroxyacetone phosphate dependent aldolase to give fluoroacetaldehyde **48**. The alternative pathway assumes that intermediate **B** is a shunt metabolite and not involved directly in the fluorometabolite pathway. In this case intermediate **B** is formed from fluoroacetaldehyde **48** by the action of an adventitious DHAP aldolase operating in the CFE. Although both routes are plausible, the identity of intermediate **B** as a diastereoisomer of 5-FDRibP **121** became a research focus.

3.6.1 Enzymatic preparation of 5-fluoro-5-deoxy-D-xylulose

Xylose isomerases exhibit a wide substrate tolerance and have been shown to catalyse the isomerisation of 5-fluoro-5-deoxy-D-xylose (5-FDX) **124** to 5-fluoro-5-deoxy-D-xylulose (5-FDXyu) **125** as shown in Scheme 3.8.[154]

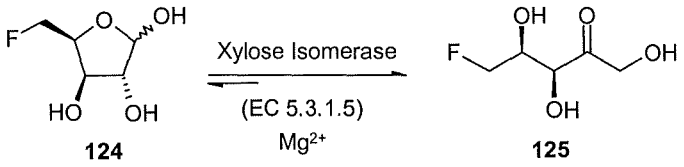

Scheme 3.8 Enzymatic reaction of xylose isomerase in the presence of 5-FDX **124**.

A synthetic sample of 5-FDX **124** was used (prepared by Mayca Onega, University of St Andrews)[161] as a substrate and was incubated with xylose isomerase (EC 5.3.1.5). A time course experiment was conducted following the reaction at hourly intervals for 5 hrs at 60 °C. The resulting ^{19}F NMR spectra are shown in Figure 3.19.

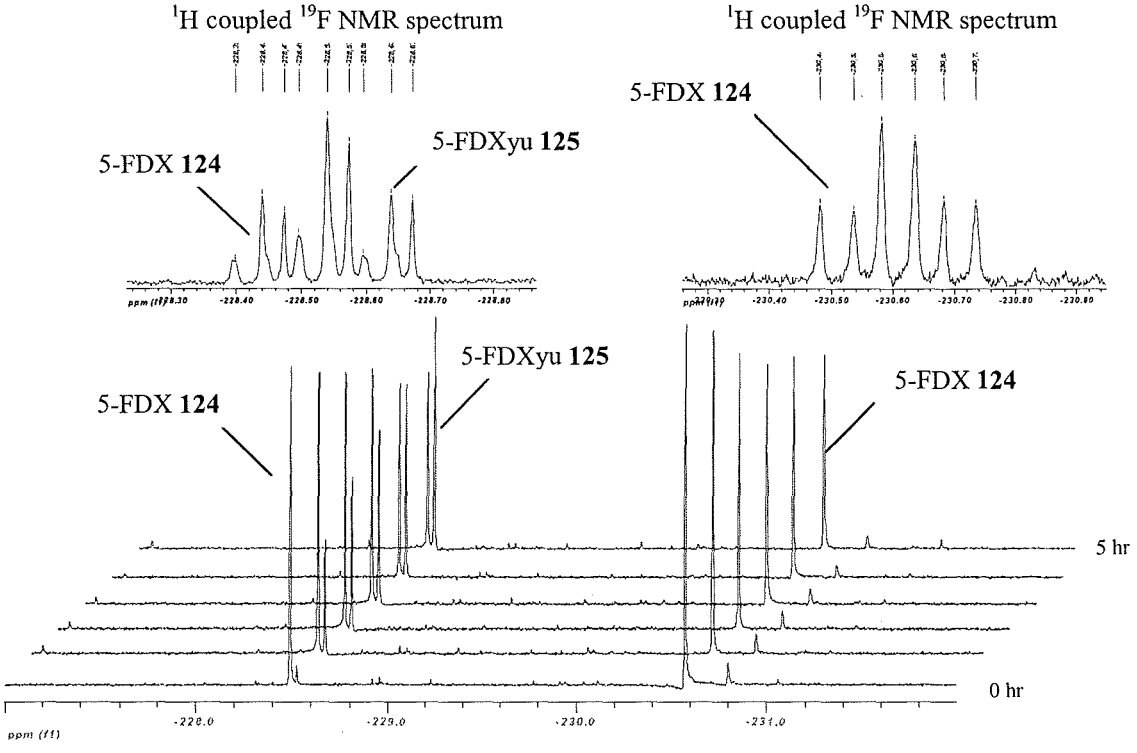

Figure 3.19 ^{19}F {^{1}H} NMR time course of xylose isomerase incubated with 5-FDX **124**.

The two fluorine signals at -228.49 ppm and -230.57 ppm represent the two anomers of 5-FDX **124**. A third organo-fluorine signal accumulates at -228.53 ppm (dt, $^{2}J_{F,H}$ 47.0 and $^{3}J_{F-H}$ 15.9) over the 5 hrs. This signal corresponds to the expected product 5-FDXyu **125**, as deduced by comparison with the literature.[154] It was envisaged that 5-FDXyu **125** could now be prepared in *S. cattleya* by phosphatase activity on intermediate **B**. Comparison with 5-FDXyu **125** from the xylose isomerase reaction would confirm its structure. Scheme 3.9 outlines the two routes taken to identify 5-fluoro-5-deoxy-D-xyulose-1-phosphate (5-FDXyuP) **126** as intermediate **B**.

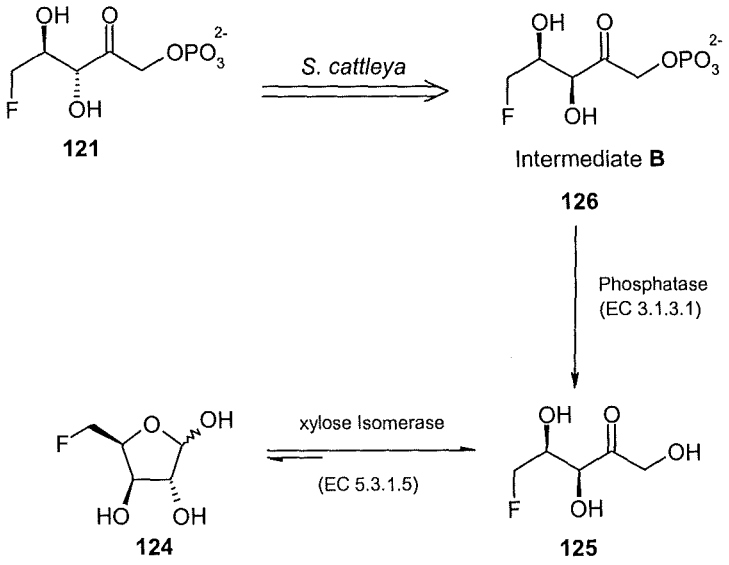

Scheme 3.9 Proposed routes towards the synthesis of 5-FDXyu **125**.

Accordingly, 5'-FDA **54** was incubated in a CFE for 8 hrs at 37 °C. After this time the sample was heated to 100 °C for 3 minutes and the precipitated protein removed by centrifugation. ^{19}F NMR analysis showed the presence of intermediate **B** (-228.22 ppm). A phosphatase from bovine intestinal mucosa was then added to the sample and the reaction was incubated for 2 hrs at 37 °C. The resulting ^{19}F NMR spectra showed a new signal at -228.49 ppm. The identity of the dephosphorylated product from *S. cattleya* was then confirmed by comparison with the reference sample of 5-FDXyu **125** produced

independently from 5-FDX **124** *via* the xylose isomerase protocol. ^{19}F NMR analysis of both reaction products showed signals with identical chemical shifts and coupling constants. To reinforce this result, the samples were admixed and again they were identical. In conclusion, it appears that intermediate **B** is the diastereoisomer of 5-FDRibP **121.**

3.6.2 The role of 5-fluoro-5-deoxy-D-xylulose

5-FDXyu **125** was explored as a biosynthetic intermediate on the fluorometabolite pathway. It was shown in Section 3.4.2 that 5-FDRib **122** remains metabolically inert in a CFE and is therefore unable to support secondary metabolite production. Having a chemo-enzymatic method for the synthesis of 5-FDXyu **125** it was of interest to see if this compound is metabolised in a CFE of *S. cattleya*. Consequently, 5-FDXyu **125**, prepared as described above, was incubated in a CFE of *S. cattleya.* This transformation was analysed by ^{19}F NMR spectroscopy, however there was no change and **125** was metabolically inert (Figure 3.20).

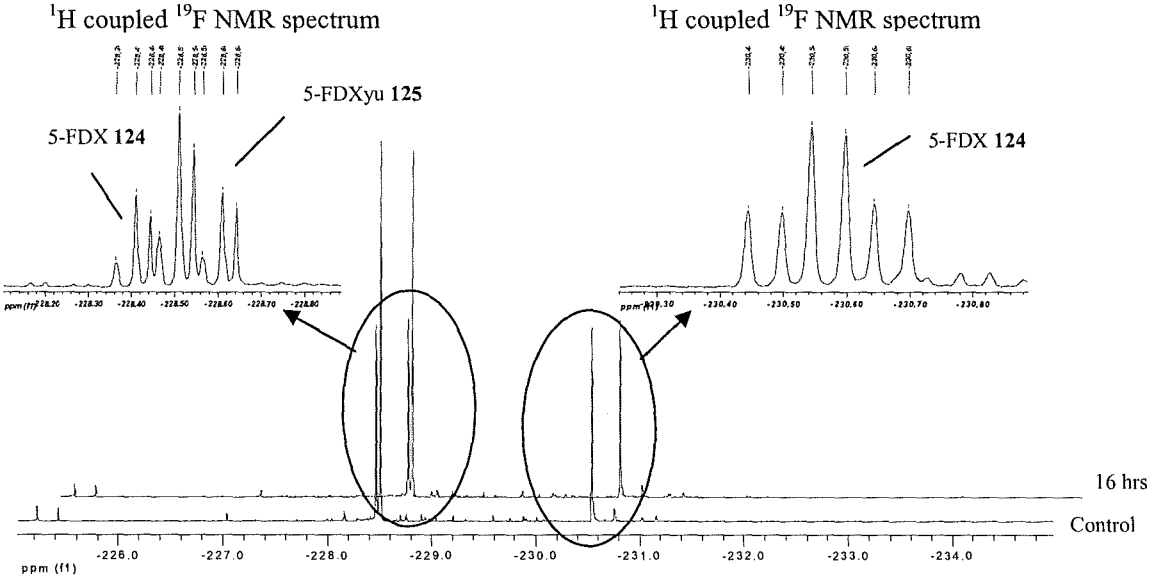

Figure 3.20 ^{19}F {^{1}H} NMR spectra of CFE incubated with 5-FDXyu **125** for 16 hrs at 37 °C. Expansions are ^{1}H coupled ^{19}F NMR spectra.

The result clearly demonstrates that the addition of 5-FDXyu **125** to a CFE resulted in no further fluorinated metabolites. The only signals present were those corresponding to the two anomers of 5-FDX **124** and 5-FDXyu **125** in the starting material. This reinforces that the phosphorylated sugars are required intermediates in fluorometabolite biosynthesis (see Chapter 4).

3.7 Conclusion

It has been revealed that in *S. cattleya*, a 5-fluoro-5-deoxy-D-ribose-1-phosphate isomerase in present which catalyses the transformation of 5-FDRP **81** to 5-fluoro-5-deoxy-D-ribulose-1-phosphate (5-FDRibP) **121**. The intermediate 5-FDRibP **121** was identified after comparison to a reference sample prepared by a chemo-enzymatic route using a xylose isomerase. Accordingly, the dephosphorylation of 5-FDRibP **121** from *S. cattleya* by the action of a commercial phosphatase gave the free sugar, which was correlated to a reference sample. These experiments reinforce 5-FDRibP **121** as an intermediate in fluorometabolite biosynthesis.

The identity of this isomerase from *S. cattleya* has led to a partially purified protein extract by ammonium sulfate precipitation, hydrophobic interaction chromatography, size exclusion chromatography and anion exchange chromatography.

The biotransformation of 5-FDRibP **121** to fluoroacetaldehyde **48** remains unclear. The experimental data presented in this chapter suggest two alternative pathways. Firstly, a direct transformation of 5-FDRibP **121** to intermediate **B,** and then **B** is metabolised to fluoroacetaldehyde **48**. The alternative pathway involves a direct transformation of 5-FDRibP **121** to fluoroacetaldehyde **48**, and then fluoroacetaldehyde **48** generates intermediate **B** in an adventitious reaction.

The identity of intermediate **B** was shown to be 5-fluoro-5-deoxy-D-xylulose-1-phosphate (5-FDXyuP) **126**, a diastereoisomer of 5-FDRibP **121**. Such sugars are well known products of dihydroxyacetone phosphate dependent aldolases and the reverse aldol reaction could clearly generate fluoroacetaldehyde **48**. This is discussed in Chapter 4.

4 DHAP aldolases from *S. cattleya*

This chapter describes the identification of two dihydroxyacetone phosphate (DHAP) dependent aldolases, one of which is involved in fluorometabolite biosynthesis in *S. cattleya* and generates fluoroacetaldehyde **48** from 5-fluoro-5-deoxy-D-ribulose-1-phosphate (5-FDRibP) **121**. The other, an L-fructose 1,6-bisphosphate aldolase (L-fruA) has been purified to homogeneity and appears to be responsible for the formation of 5-fluoro-5-deoxy-D-xylulose-1-phosphate (5-FDXyuP) **126**, a diastereoisomer of **121**, that is not an intermediate on the pathway. By way of introduction, a short review of DHAP aldolases is given below.

4. 1 Dihydroxyacetone phosphate (DHAP) dependent aldolases

DHAP dependent aldolases catalyse the reversible aldol reaction of DHAP **123** and an aldehyde acceptor. There are four possible stereochemical outcomes all of which are catalysed by different enzymes and the four DHAP dependent aldolases have enjoyed a significant level of interest in biotransformations because of their capacity to construct two stereogenic centres in one reaction.[162-166] Scheme 4.1 illustrates these stereochemical outcomes. All four of these aldolases possess a high specificity for DHAP **123**, but show tolerance for a variety of different aldehyde electrophiles.

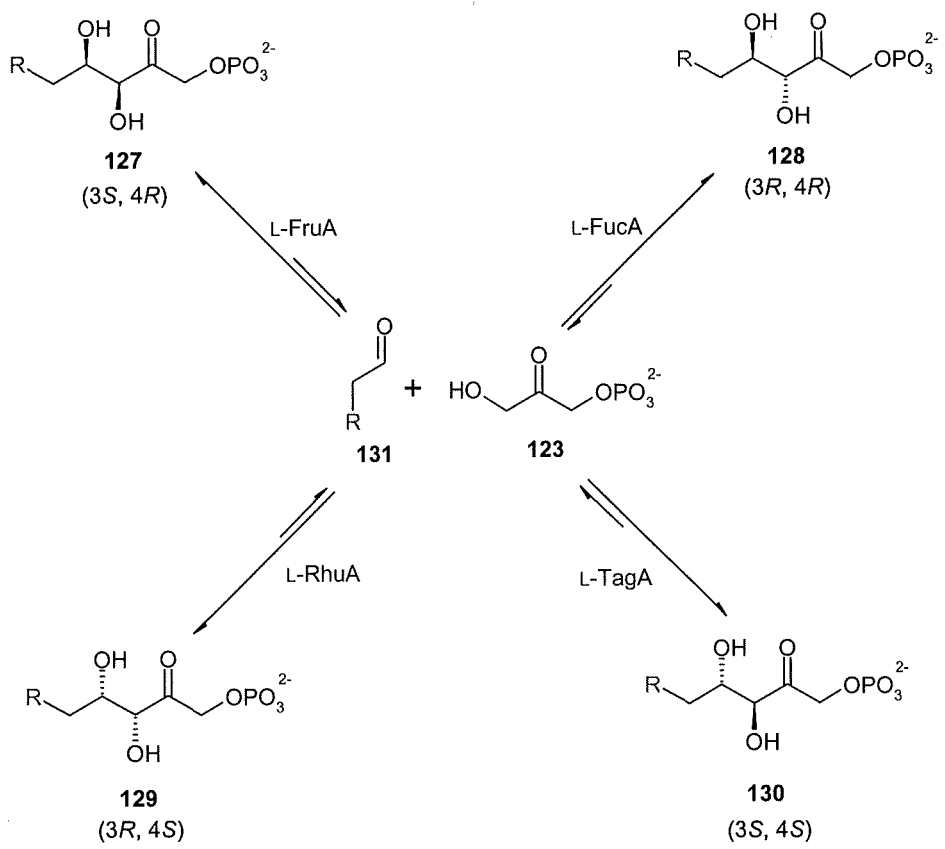

Scheme 4.1 L-Fuculose-1-phosphate aldolase (L-FucA) (E.C. 4.1.2.17), L-Rhamnulose-1-phosphate aldolase (L-RhuA) (E.C. 4.1.2.19), L-Tagatose 1,6-bisphosphate aldolase (L-TagA) (E.C. 4.1.2.40) and L-Fructose 1,6-bisphosphate aldolase (L-FruA) (E.C. 4.1.2.13).[167,168]

DHAP dependent aldolases are either Class I or Class II depending on their mechanism, although they catalyse identical reactions.[168] Class I aldolases form a Schiff-base intermediate.[169] These aldolases are generally homotetrameric enzymes found in eukaryotes or higher organisms, although Class I aldolases have been reported in prokaryotes.[170] The generally accepted catalytic reaction of Class I aldolases, proceed *via* the formation of an iminium intermediate between a lysyl group at the active site and the carbonyl of DHAP **123**.[171,172] A general mechanism for the Class I fructose 1,6-bisphosphate aldolase is shown in Scheme 4.2.

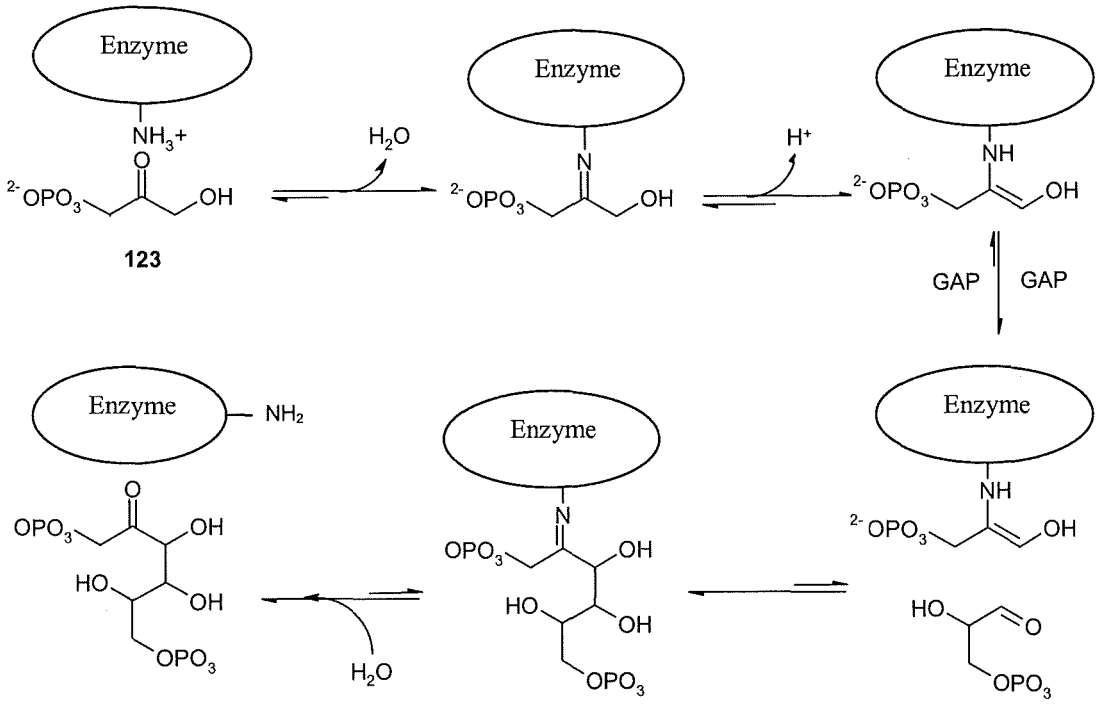

Scheme 4.2 General mechanism for Class I L-fructose 1,6-bisphosphate aldolase (L-FruA).[169]

Class II DHAP dependent aldolases are generally found in prokaryotes and lower eukaryotic organisms such as yeast, fungi and algae.[173] These enzymes are homodimeric and require a divalent metal ion, usually Zn^{2+} as an essential Lewis acid cofactor. They are inhibited by chelating compounds such as EDTA which sequester the Zn^{2+}.[174] The mechanism of the Class II enzymes which is highlighted in Scheme 4.3 is less well understood than that of the Class I enzymes.[175] Scheme 4.3 shows an L-fuculose-1-phosphate aldolase (L-FucA) which catalyses the condensation of L-lactaldehyde **132** and DHAP **123**.

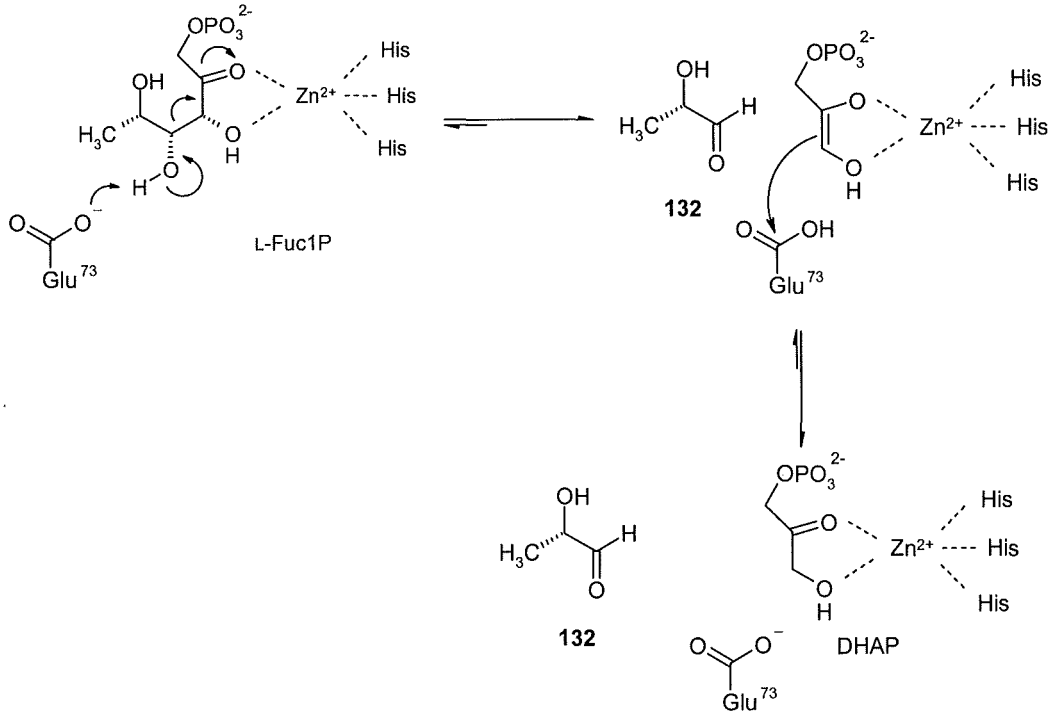

Scheme 4.3 Mechanism of the Class II DHAP dependent aldolase.[176]

4.2 Stereospecificity of two DHAP aldolases using fluoroacetaldehyde as the substrate

Chapter 3 discussed the identification of two diastereoisomers, 5-FDRibP **121** (Compound **A**) and 5-FDXyuP **126** (Compound **B**). Previous knowledge of the stereochemical course of DHAP aldolases with non fluorinated substrates indicate that L-FucA generates the (3*R*, 4*R*) stereoisomer **128**.[176-178] This would be the anticipated stereochemistry of **121**, the product from the isomerase reaction in *S. cattleya* as shown in Section 3.4. Compound **B** (**126**), the other diastereoisomer identified equates to the stereoisomer with the (3*S*, 4*R*) **127** configuration,[179] generated by L-FruA. Therefore, both aldolases could be present in the cell free extract (CFE). Scheme 4.4 outlines the predicted stereoselectivity of the two aldolases from the CFE using fluoroacetaldehyde **48** as a substrate.

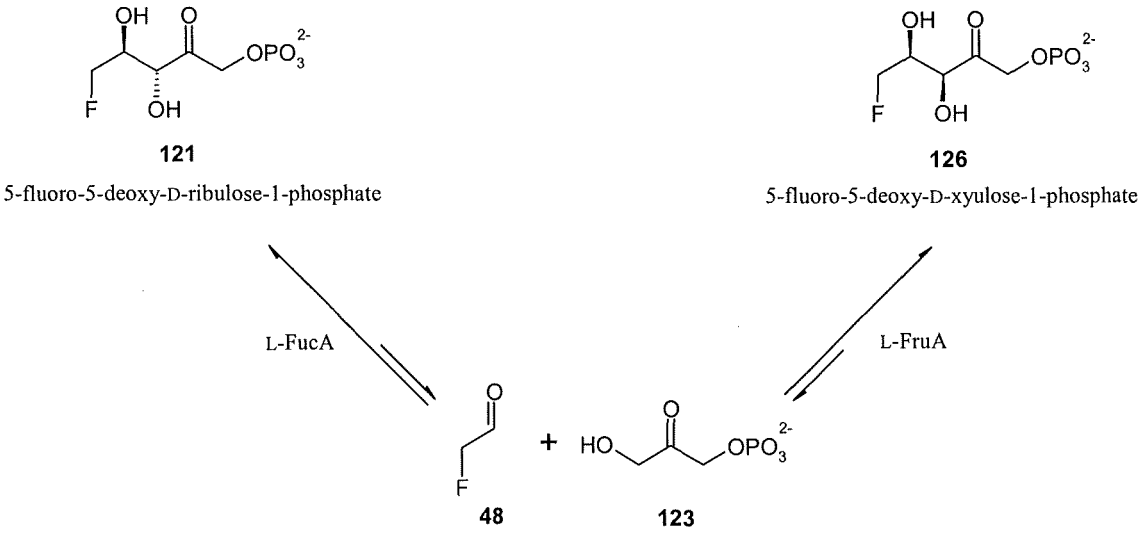

Scheme 4.4 The stereochemical relationships of the two predicted aldolases in the *S. cattleya* CFE.

4.2.1 The role of an L-fuculose-1-phosphate aldolase (L-FucA) on the fluorometabolite pathway in *S. cattleya*

L-FucA, the enzyme that would give the predicted stereoisomer, 5-FDRibP **121** is not commercially available. However, a pTrcHis C plasmid containing the Class I L-FucA gene from *E. coli* was available from LGC PromoChem. This enzyme was overproduced and purified according to the protocol outlined in Section 5.1.28. The product of this aldol reaction, 5-FDRibP **121** could be compared to the assigned 5-FDRibP **121** from *S. cattleya*. The aldol reaction was carried out in phosphate buffer (700 μl, 50 mM, pH 6.8) containing fluoroacetaldehyde **48** (20 mM + residual fluoroethanol **69**) and DHAP **123** (10 mM). The reaction was initiated by the addition of L-FucA (200 μl, 0.4 mg / ml) and incubated at 37 ^{o}C for 1 hr. The sample was denatured by heating to 100 ^{o}C for 3 min and the precipitated protein removed by centrifugation. The clear supernatant was supplemented with 100 μl of D_2O and analysed by ^{19}F NMR. A typical ^{19}F NMR spectrum of the resultant product is shown in Figure 4.1.

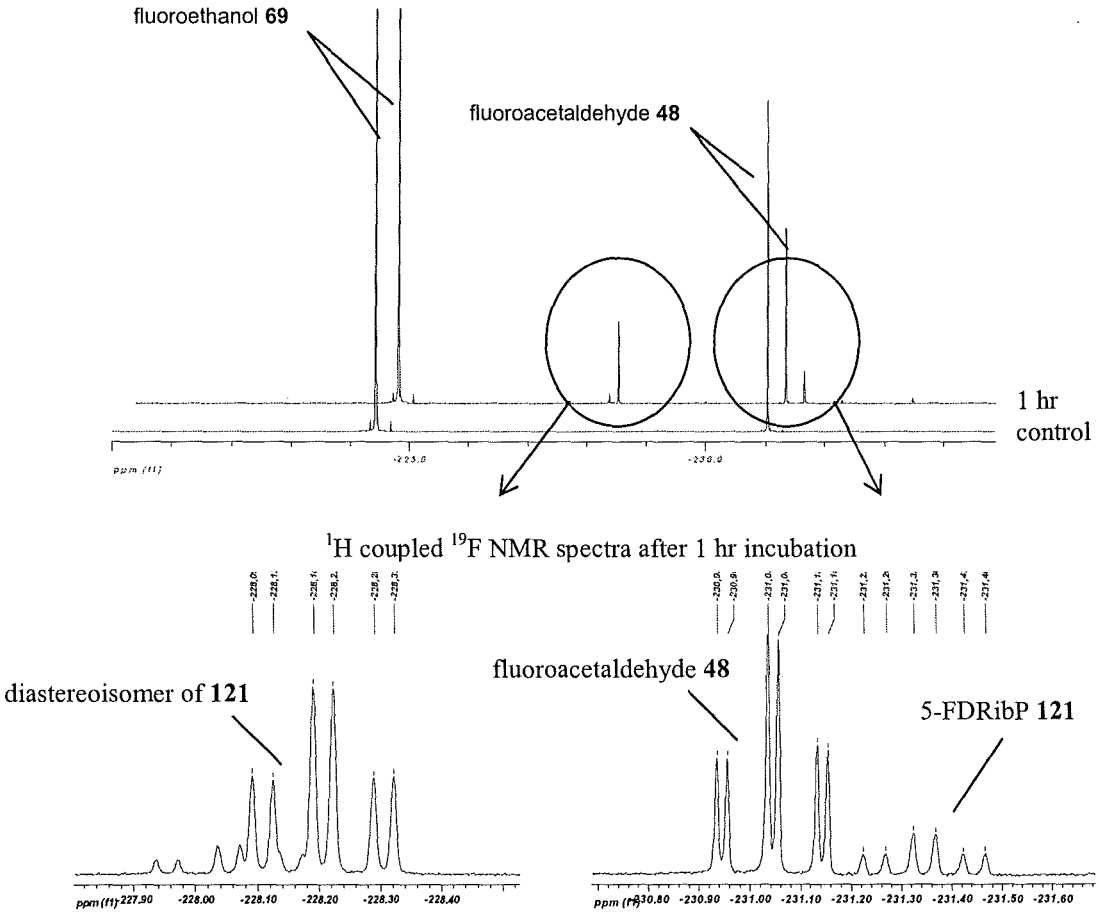

Figure 4.1 ^{19}F {^{1}H} NMR spectra showing DHAP **123** (10 mM) and fluoroacetaldehyde **48** (20 mM) incubated with L-FucA for 1 hr at 37 °C.

^{19}F NMR analysis of the aldol reaction with L-FucA showed the presence of fluoroacetaldehyde **48** and residual fluoroethanol **69**. However, two new ^{19}F NMR signals were observed at -228.21 ppm (dt, $^2J_{F,H}$ 47.0 Hz $^3J_{F,H}$ and 16.0 Hz) and –231.34 ppm, (dt, $^2J_{F,H}$ 47.0 and $^3J_{F,H}$ 16.0) which were absent from the control. The major -228.21 ppm signal was not anticipated during this reaction, however, it is possible that this signal corresponds to a diastereoisomer of **121**. The chemical shift and coupling constants for the minor signal at -231.34 ppm clearly correlate to 5-FDRibP **121**. To support this, as before

(Section 3.4), an experiment was performed, whereby the product was converted to the free sugar by the action of a phytase (EC 3.1.3.8, from *Aspergillus ficuum*).

Accordingly, the product was lyophilised to remove the majority of residual fluoroacetaldehyde **48** and fluoroethanol **69**. The lyophilised sample was then incubated in 700 μl phosphate buffer (50 mM, pH 6.8) and treated with the phytase. This resulted in a small shift in the fluorine signal from -231.34 ppm to -231.12 ppm, consistent with *in vitro* phosphate hydrolysis. The organo-fluorine signal at -231.12 ppm was then correlated to 5-FDRib **122** by comparison with a reference sample. This was prepared from a synthetic sample of 5-FDR **80** by the action of xylose isomerase (see Section 5.1.13). Scheme 4.5 outlines the correlation strategy leading to 5-FDRib **122,** by these two different routes.

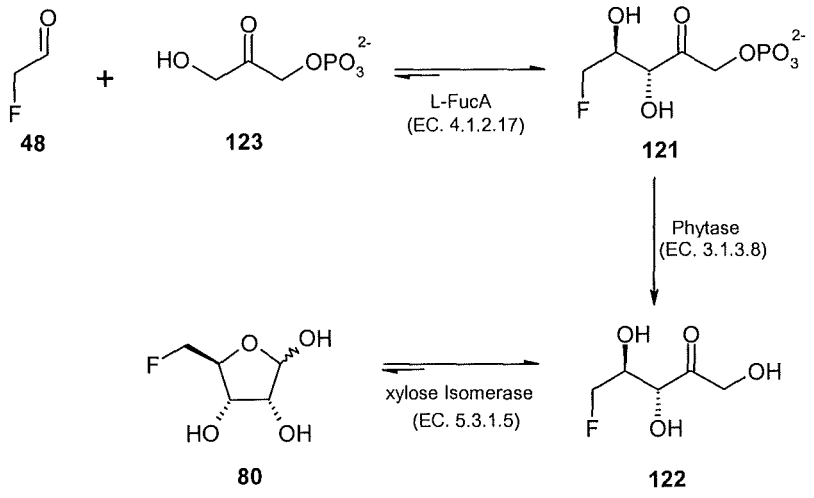

Scheme 4.5 Working hypothesis leading to the formation of 5-FDRib **122**

^{19}F NMR analysis of both enzymatic routes showed the presence of a signal at -231.12 ppm (dt, $^{2}J_{F,H}$ 46.9 and $^{3}J_{F,H}$ 20.6) (Figure 4.2 (**a**) and (**b**)). The samples were admixed and re-analysed by ^{19}F NMR spectroscopy. The results confirmed that both signals were identical; indicating that 5-FDRib **122** is a common fluorinated product from both routes.

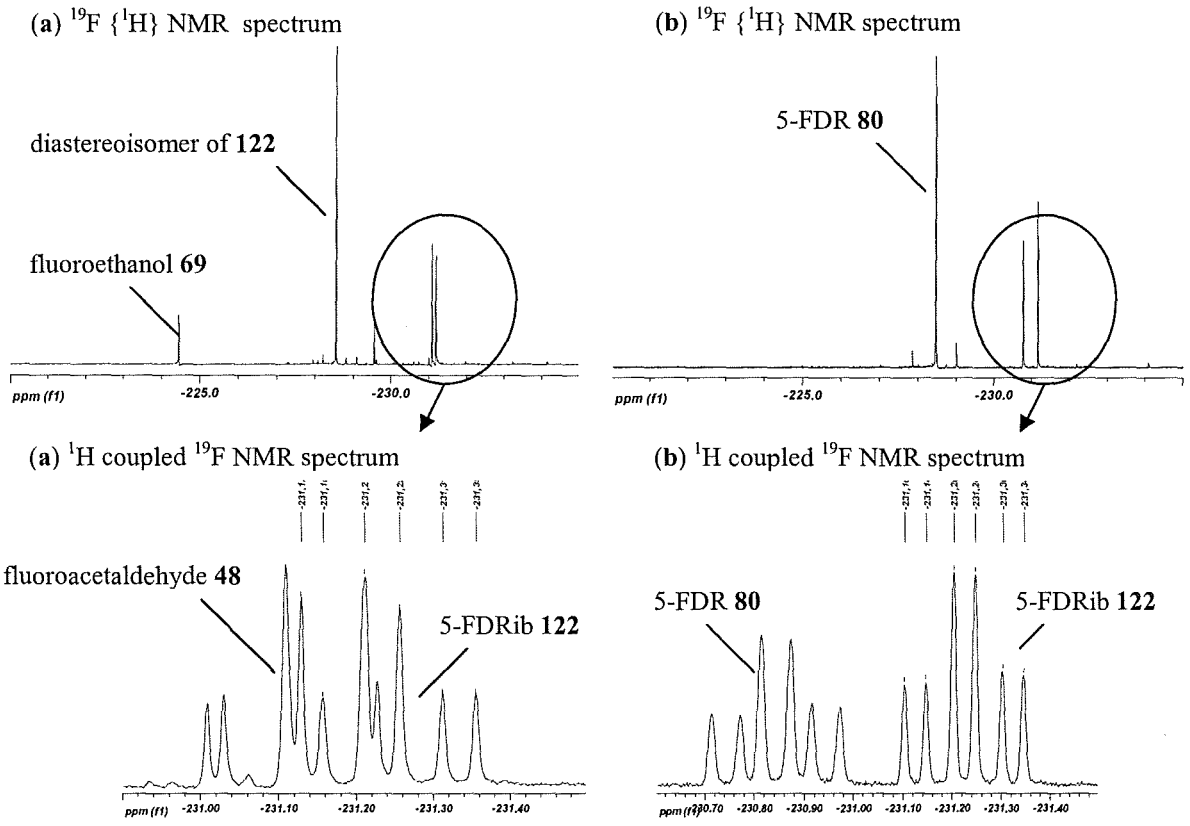

Figure 4.2 ^{19}F NMR spectra of (**a**), L-FucA incubated with DHAP **123** and fluoroacetaldehyde **48** in the presence of a phytase enzyme and (**b**), xylose isomerase incubated with 5-FDR **80**.

These experiments suggest that the L-FucA aldolase from *E. coli* is not stereoselective. The identity of the major isomer is possibly a diastereoisomer of **121** (or its enantiomer). The minor product appears to be, 5-FDRibP **121**, the stereoisomer relevant to the fluorometabolite pathway.

The next objective was to examine further if this L-FucA produced 5-FDRibP **121** matched the *S. cattleya* product and was not for example an enantiomer (Section 3.4). A comparison of the chemical shift and splitting pattern (by ^{19}F NMR spectroscopy) of 5-FDRibP **121** prepared using the over-expressed L-FucA aldolase with the identified metabolite 5-FDRibP **121** from the fluorometabolite pathway in *S. cattleya* showed both fluorine signals to be identical. To show that they are the same enantiomer, an experiment was conducted whereby commercial L-FucA was added to a pre-incubated CFE, which contained 5-

FDRibP **121**. A reduction of the fluorine signal (-231.34 pm) assigned to **121**, with an increase in fluoroacetaldehyde **48** was envisaged.

Therefore, a CFE of *S. cattleya* was incubated with 5'-FDA **54** for 6 hrs at 37 °C. The resultant denatured sample was analysed by ^{19}F NMR which showed the CFE retained all of its biosynthetic activities. (Figure 4.3, Spectrum (**a**)). L-FucA (100 μl, 0.2 mg / ml) was then added to the sample recorded in Spectrum (**a**) and incubated for 1 hr at 37 °C. The resulting ^{19}F NMR spectrum is shown in Spectrum (**b**), Figure 4.3.

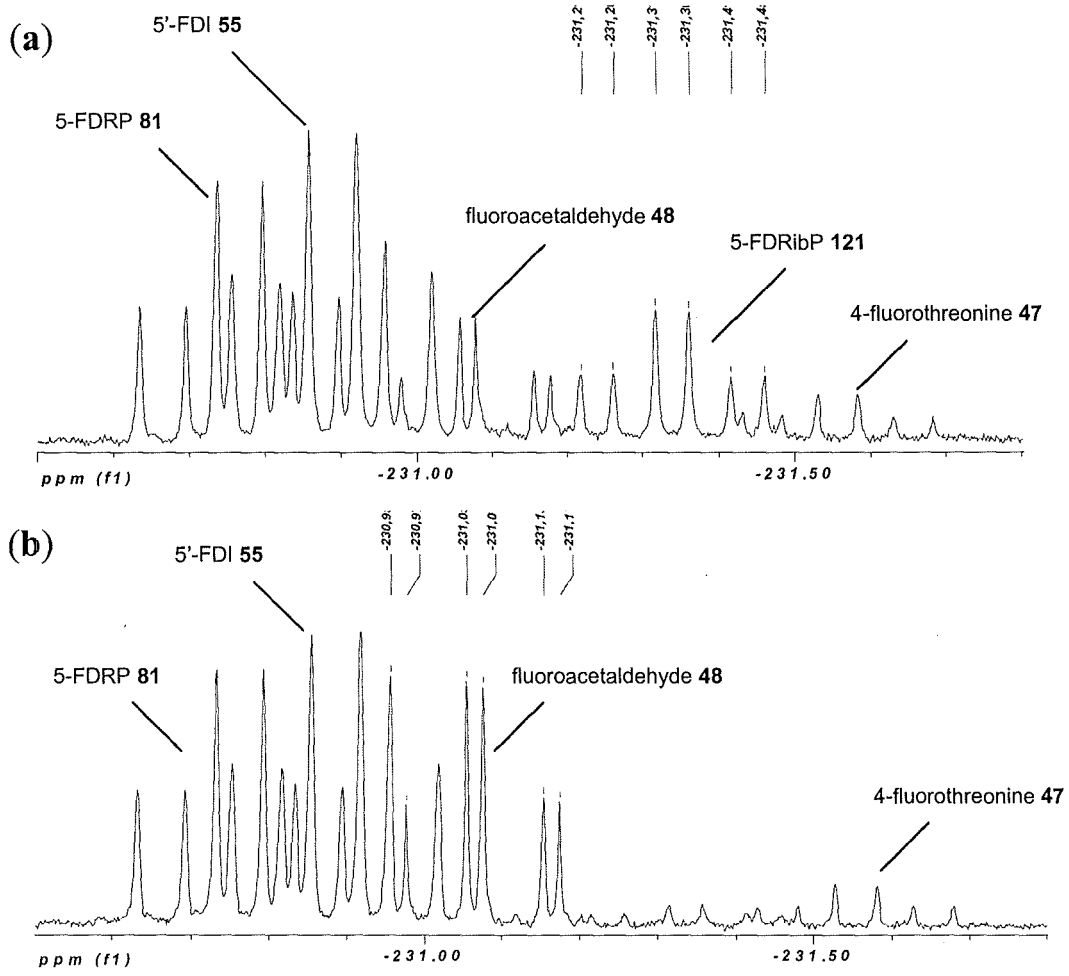

Figure 4.3 ^{1}H coupled ^{19}F NMR spectra (expansion of region -230.5 ppm to -231.8 ppm) containing CFE incubated with 5'-FDA **54** for 6 hrs at 37 °C (Spectrum **a**), and incubation with L-FucA for 1 hr at 37 °C. (Spectrum **b**).

Spectrum (**a**) shows a ^{19}F NMR expansion illustrating most of the fluorinated intermediates on the biosynthetic pathway. After treatment with L-FucA (Spectra (**b**)), it is evident that 5-FDRibP **121** (-231.34 ppm) is significantly diminished and that fluoroacetaldehyde **48** (-231.08 ppm) levels have increased, consistent with L-FucA accepting the *S. cattleya* product as a substrate.

4.2.2 The role of an L-fructose 1,6-bisphosphate aldolase (L-FruA) on the fluorometabolite pathway in *S. cattleya*

It appeared appropriate now to explore the presence of a L-FruA aldolase in CFE's of *S. cattleya*, which would catalyse the formation of compound **B**, assigned as 5-FDXyuP **126**. A commercial Class I L-FruA from rabbit muscle was used to prepare a reference sample of 5-FDXyuP **126**. Accordingly, the aldol reaction was carried out in phosphate buffer (700 μl, 50 mM, pH 6.8) containing fluoroacetaldehyde **48** (20 mM + residual fluoroethanol **69**) and DHAP **123** (10 mM). The reaction was initiated by the addition of L-FruA (20 μl, 2 mg / ml) and incubated at 37 ^{o}C for 1 hr. The sample was then denatured by heating to 100 ^{o}C for 3 min and the precipitated protein removed by centrifugation. The clear supernatant was supplemented with 100 μl of D_2O and analysed by ^{19}F NMR. A typical ^{19}F NMR spectrum of the resultant product is shown in Figure 4.4.

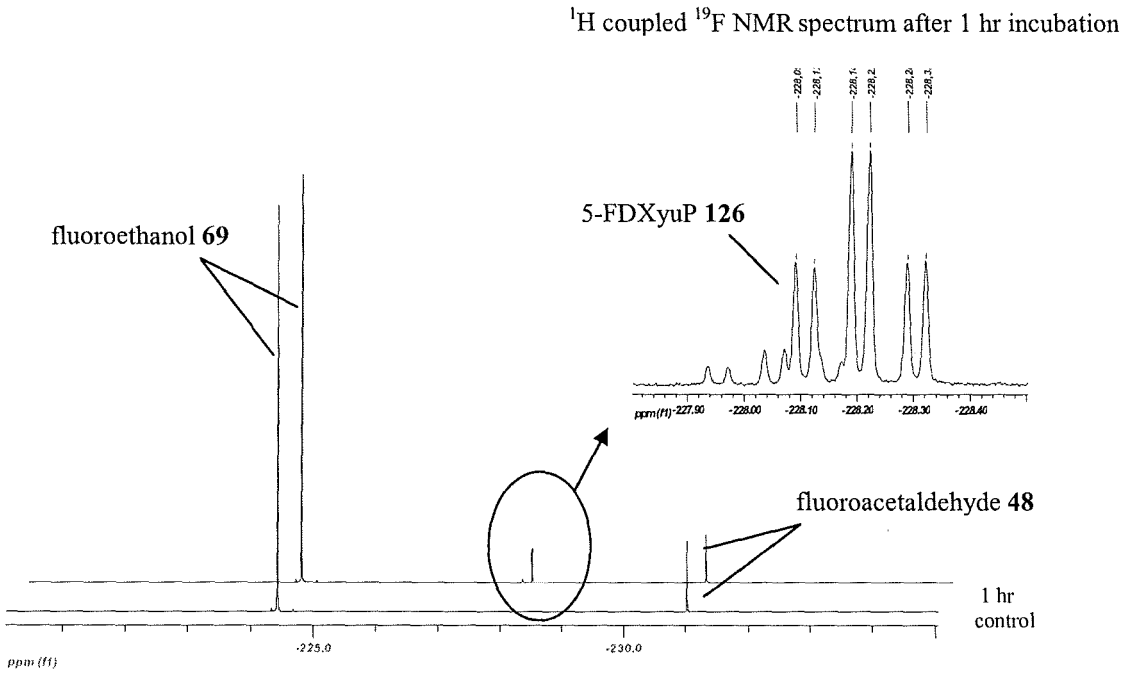

Figure 4.4 ^{19}F {^{1}H} NMR analysis of L-FruA incubated with DHAP **123** (10 mM) and fluoroacetaldehyde **48** (20 mM) for 1 hr at 37 °C. Fluoroethanol **69** is a contaminant of **48**.

The resulting ^{19}F NMR spectrum clearly indicates the presence of a new fluorine signal at -228.20 ppm (dt, $^{2}J_{F,H}$ 46.2 Hz $^{3}J_{F,H}$ and 15.3 Hz). A control reaction in the absence of the enzyme, showed only starting material indicating that the new fluorine signal is formed in the presence of L-FruA. The peak at -228.20 ppm was assumed to be the product of the aldolase catalyzed reaction, 5-FDXyuP **126**. It was possible to convert this product to the free sugar by the action of a phytase. Accordingly, the product of the L-FruA reaction was lyophilised to remove the majority of residual fluoroacetaldehyde **48** (and fluoroethanol **69**). A small amount of the lyophilised sample was then treated with the commercial phytase (*Aspergillus ficuum*, EC 3.1.3.8) (10 μl, 10 mg / ml) for 1 hr at 37 °C. This resulted in a small shift in the fluorine signal from -228.20 ppm to -228.53 ppm. This product was then compared to the ^{19}F NMR signal of a reference sample of 5-FDXyu **125** prepared by the xylose isomerase reaction (see Section 5.1.14). Scheme 4.6 outlines the two complementary enzymatic routes leading to the formation of 5-FDXyu **125**.

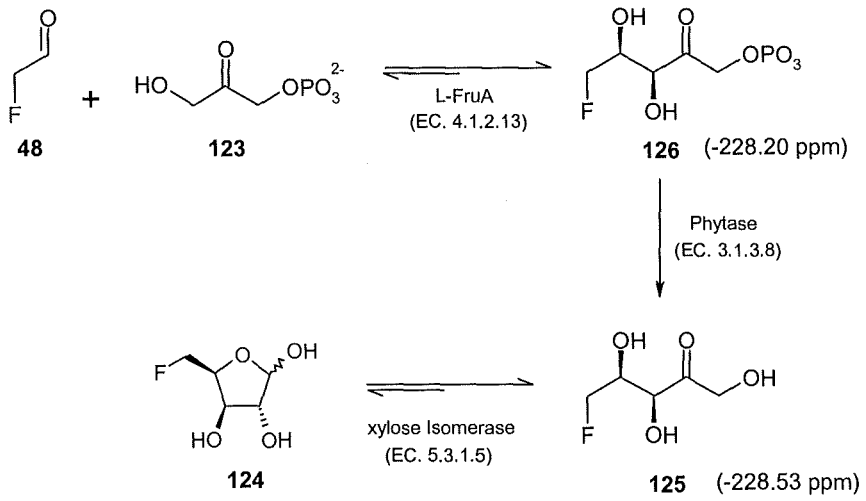

Scheme 4.6 Two complementary methods for the formation of 5-FDXyu **125**.

The products of both enzymatic routes were identical by ^{19}F NMR (-228.53 ppm, td, $^{2}J_{F,H}$ 46.2 Hz and $^{3}J_{F,H}$ 15.3 Hz) (Figure 4.5 (**a** and **b**)). This was also shown by admixing both samples. Of course this experiment does not formally rule out the possibility that opposite enantiomers were generated as products; however that outcome would be inconsistent with previous knowledge of the stereochemical course of these reactions with non fluorinated substrates.[167]

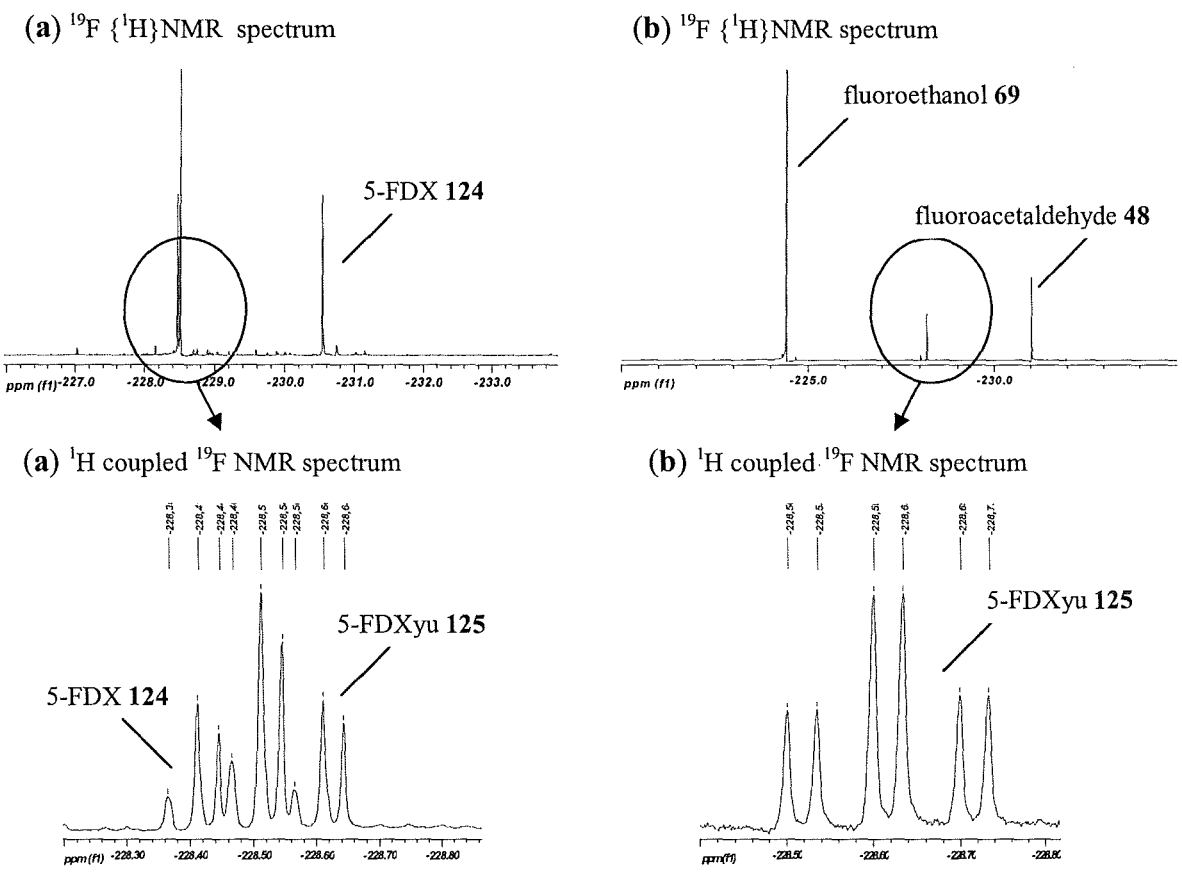

Figure 4.5 ^{19}F NMR spectra of (**a**), the xylose isomerase reaction product with 5-FDX **124** for 3 hr at 60 °C and (**b**), L-FruA incubated with DHAP **123** and fluoroacetaldehyde **48** for 1 hr at 37 °C, and supplemented with a phytase enzyme (10 μl, 10 mg / ml) for 1 hr at 37 °C.

A Class II L-FruA aldolase from *Bacillus stearothermophilus* (courtesy of Professor Littlechild, University of Exeter) was assayed under similar conditions to that outlined in Figure 4.4, except Zn^{2+} (1 mM) was added to the reaction. This experiment was carried out to explore further the stereoselectivity of the L-FruA reaction. The ^{19}F NMR spectrum reinforced the results in Figure 4.4, showing a single organo-fluorine signal at -228.20 ppm corresponding to 5-FDXyuP **126**. In summary, Class I and II L-FruA aldolases generated a common product consistent with the production of 5-FDXyuP **126** after incubation with fluoroacetaldehyde **48** and DHAP **123.**

The next objective was to examine if this L-FruA product 5-FDXyuP **126** matched compound **B** in *S. cattleya.* A comparison of chemical shifts and admixing of both samples showed identical fluorine signals. To further support this observation, an experiment was conducted whereby commercial Class I L-FruA was added to a pre-incubated CFE, which contained compound **B** (5-FDXyuP **126**). A reduction of compound **B** and an increase in fluoroacetaldehyde **48,** in a similar manner to that shown in the previous section, was envisaged.

Accordingly, an active CFE (500 μl) was incubated with synthetic 5'-FDA **54** (10 mM) for 6 hrs at 37 °C. After this time, the CFE was denatured by heating to 100 °C for 3 min and the precipitated protein centrifuged. The supernatant was supplemented with 100 μl of D_2O and analysed by ^{19}F NMR which showed a number of organo-fluorine signals (Spectra (**a**), Figure 4.6) including compound **B**. The second experiment consisted of the addition of L-FruA to the denatured sample recorded in Spectrum (**a**) which was incubated for 2 hrs at 37 °C and subsequently analysed by ^{19}F NMR. (Spectrum (**b**), Figure 4.6).

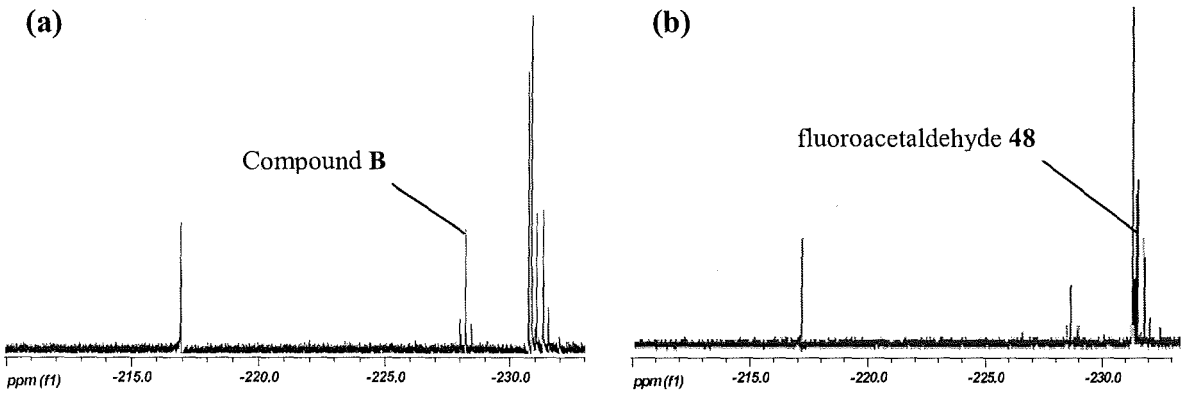

Figure 4.6 ^{19}F {^{1}H} NMR spectra of (**a**), CFE incubated with 5'-FDA **54** for 6 hrs at 37 °C and (**b**), incubation of sample recorded in Spectrum (**a**) with L-FruA (2 mg) for 2 hrs at 37 °C.

The resulting ^{19}F NMR spectrum in Figure 4.6(**a**) shows all of the fluorinated metabolites on the pathway including fluoroacetate **8** (-216.92 ppm) and 4-fluorothreonine **47** (-231.54

ppm). The two major signals belong to 5-FDRP **81** (-230.79 ppm) and 5'-FDI **55** (-230.87 ppm). 5'-FDA **54** is not observed, indicating that it is completely metabolised by the simultaneous actions of PNP and deaminase activities. Fluoroacetaldehyde **48** (-231.03 ppm) and 5-FDRibP **121** (-231.33 ppm) are clearly apparent. The organo-fluorine signal at -228.21 ppm corresponds to Compound **B** (5-FDXyuP **126**). The ^{19}F NMR spectrum recorded in Figure 4.6(**b**) shows the subsequent addition of the Class I L-FruA. Comparison of both samples clearly illustrates that the addition of L-FruA resulted in the consumption of the fluorine signal corresponding to compound **B**, with a corresponding increase in fluoroacetaldehyde **48** production. This confirms that compound **B** and 5-FDXyuP **126** are one and the same.

An experiment was conducted to further support this observation. This consisted of adding enzymatically prepared 5-FDXyuP **126** to the *S. cattleya* CFE for 16 hrs at 37 °C. Analysis of the product by ^{19}F NMR showed the transformation of 5-FDXyuP **126** to fluoroacetaldehyde **48**, emphasizing the presence of an L-FruA operating in *S. cattleya*.

L-FruA is an enzyme of primary metabolism,[169] and therefore, there is some ambiguity about its role on this pathway. All activities are released in the CFE, and probably compound **B** (5-FDXyuP**126**) is not a relevant intermediate in the fully constructed cells.

4.2.3 Monitoring both aldolase activities in *S. cattleya* by ^{19}F NMR

In order to study both aldolase reactions in real time, a time course experiment was performed in which a CFE (500 μl) of *S. cattleya* was incubated with DHAP **123** (10 mM) and fluoroacetaldehyde **48** (20 mM containing residual fluoroethanol **69**). Figure 4.7 shows ^{19}F NMR spectra recorded every 2 hours for an 8 hr period (at 37 °C). The signal at -216.93 ppm which corresponds to fluoroacetate **8** is most obvious and arises due to the

aldehyde dehydrogenase which oxidises fluoroacetaldehyde **48** to fluoroacetate **8**. 4-Fluorothreonine **47** is also apparent at -231.51 ppm. The signals at -224.42 ppm and -231.04 ppm belong to fluoroethanol **69** and fluoroacetaldehyde **48** respectively. The two aldol products **121** and **126** at -228.20 ppm and -231.34 ppm are apparent after 2 hrs of incubation. Both of these signals begin to diminish over the 8 hr period showing the reversible nature of aldol reactions.

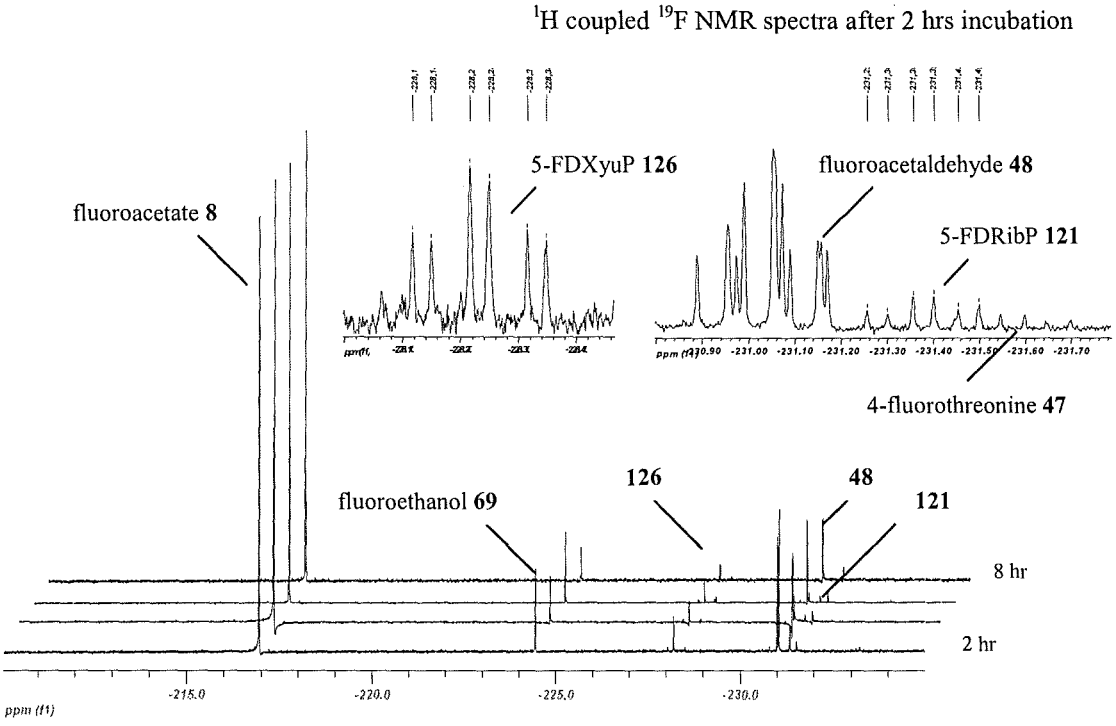

Figure 4.7 ^{19}F {^{1}H} NMR spectra time course of cell-free extract incubated with DHAP **123** and fluoroacetaldehyde **48**. Expansions are ^{1}H coupled ^{19}F NMR spectra.

In conclusion, the results described in the last three sections suggest the action of L-FucA and L-FruA activities in CFE's of *S. cattleya*. The relationships between both aldolases and intermediates are shown in Scheme 4.7, based on the experiments and results conducted so far. The earlier idea that **121** and **126** are linked by an epimerase is now less relevant in the light of these experiments.

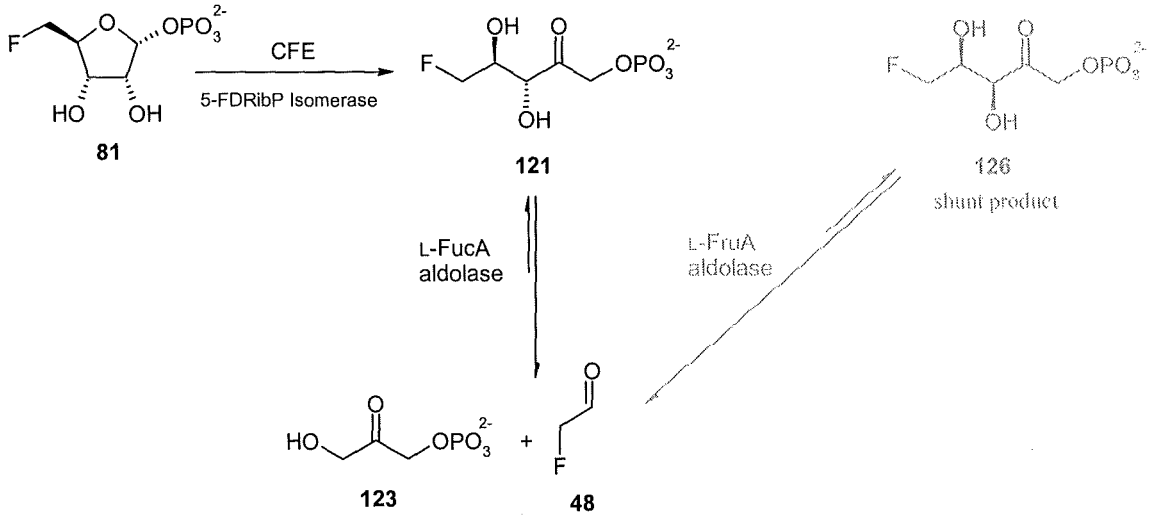

Scheme 4.7 Working hypothesis of the metabolic fate of 5-FDRP **81**.

4.2.4 Effect of EDTA on DHAP dependent aldolase activity in *S. cattleya*

Having established both aldolase products in the CFE, the next objective was to determine whether the enzymes that process them are Class I or II aldolases. A key experiment for determination of Class II activity involves the addition of EDTA to sequester divalent metal ions. A CFE (500 μl) was pre-incubated with EDTA (final conc. 30 mM) for 25 min at 37 °C. After this time, DHAP **123** (10 mM) and fluoroacetaldehyde **48** (20 mM) were added to the reaction which was incubated for a further 2 hrs at 37 °C. Figure 4.8 shows the resultant ^{19}F NMR spectrum.

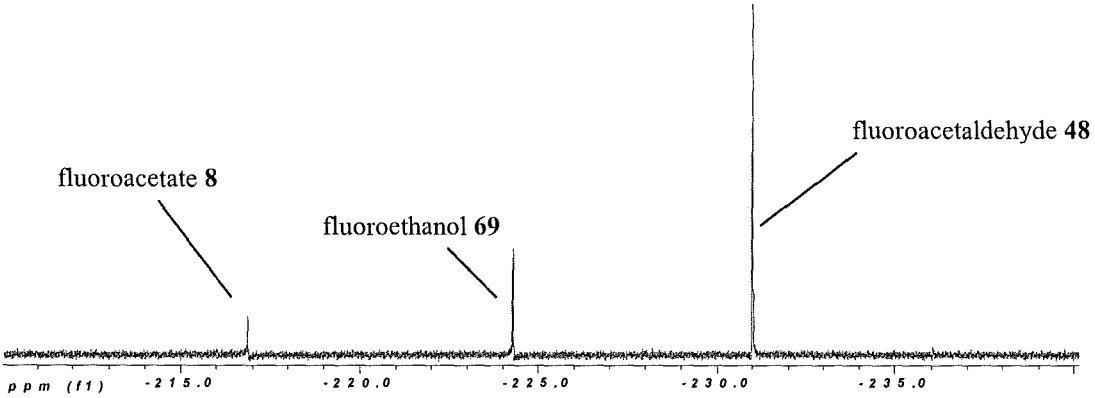

Figure 4.8 ^{19}F {^{1}H} NMR spectrum showing the CFE incubated with DHAP **123** and fluoroacetaldehyde **48** for 2 hrs at 37 °C in the presence of EDTA.

It is clear from the spectrum and under controlled conditions that the addition of EDTA resulted in complete inhibition of aldolase activity. There are no ^{19}F NMR signals corresponding to 5-FDRibP **121** (-231.34 ppm) or 5-FDXyuP **126** (-228.21 ppm). This result clearly supports the action of Class II aldolases in *S. cattleya*. This observation is also reinforced by the results generated in Section 3.3.2, which showed that the addition of EDTA to a CFE incubated with 5-FDRP **81** resulted in the accumulation of 5-FDRibP **121**. A ^{19}F NMR time course of this experiment is shown in Figure 4.9.

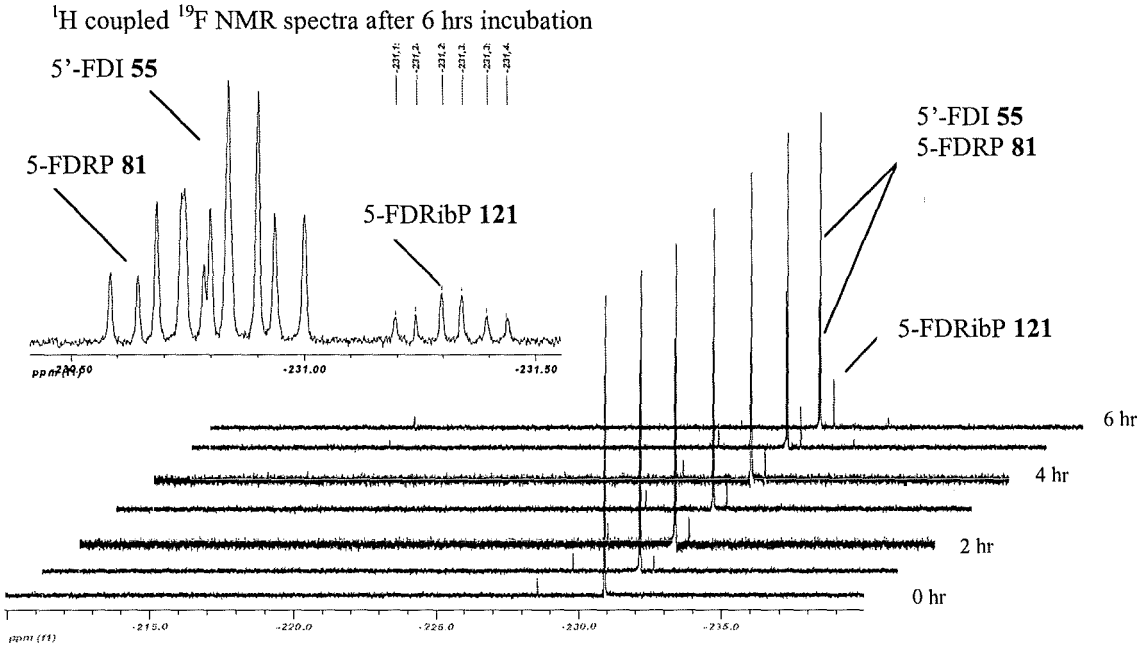

Figure 4.9 ^{19}F {1H} NMR time course recorded every hour for 8 hrs showing a CFE (500 μl) incubated with (5-FDRP **81**+5'-FDI **55**) and supplemented with EDTA.

It is clear from the ^{19}F NMR spectra in Figure 4.9 that 5-FDRibP **121** accumulates and that there is no fluoroacetaldehyde **48** indicating inhibition of the aldolase by the addition of EDTA. A further experiment was conducted to show the conversion of 5-FDRibP **121** to fluoroacetaldehyde **48** by L-FucA. This involved preparing a partially purified protein extract containing PNP and isomerase activity (Section 2.3 and 3.5) from *S. cattleya*, which was supplemented with 5'-FDA **54**. This allowed the direct transformation of 5'-

FDA **54** to 5-FDRibP **121**. Addition of over-expressed Class I L-FucA to this product promoted its conversion to fluoroacetaldehyde **48**. The experimental details were as follows. An ammonium sulfate cut (35-50 %) of the CFE was incubated with 5'-FDA **54** for 5 hrs at 37 °C and subsequently analysed by ^{19}F NMR. The resulting ^{19}F NMR spectrum is shown in Figure 4.10(**a**). The Class I L-FucA was added to this sample (Figure 4.10(**a**)) for 1 hr at 37 °C. The result is shown in Figure 4.10(**b**). The ^{19}F NMR spectrum in Figure 4.10(**c**) shows an increase in fluoroacetaldehyde **48** and can be compared to the sample from Figure 4.10(**b**) which has a lower level of fluoroacetaldehyde **48**.

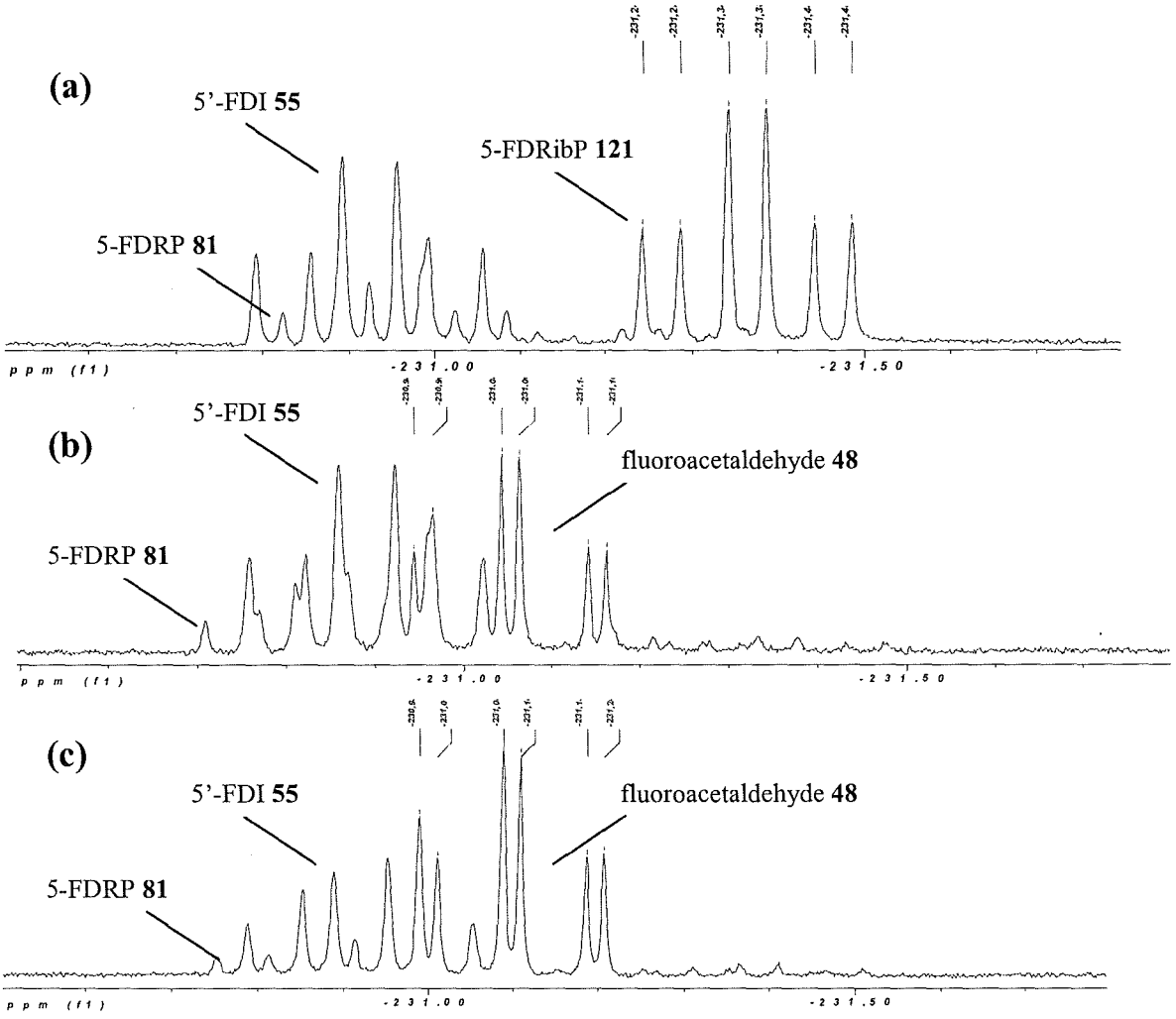

Figure 4.10 ^{1}H coupled ^{19}F NMR spectra of **(a)**, 5'-FDA **54** incubated in a partially purified CFE for 5 hrs at 37 °C. **(b)**, Supplemented with L-FucA and incubated for 16 hrs at 37 °C. **(c)**, Co-injection with **48**.

The ^{19}F NMR spectrum in Figure 4.10(**a**) shows three fluorinated compounds. Two of these correspond to 5'-FDI **55** and 5-FDRP **81**. No signal for 5'-FDA **54** was observed indicating its rapid metabolism (PNP and deaminase) as discussed in Section 3.2. The third compound is 5-FDRibP **121** arising from the transformation of 5-FDRP **81** *via* isomerase activity. The spectrum in Figure 4.10(**b**) is the product after addition of the over-expressed Class I L-FucA to the sample in Figure 4.10(**a**). It is clear that 5-FDRibP **121** is completely consumed with a subsequent increase in fluoroacetaldehyde **48** production. To confirm the transformation of **121** to **48**, Figure 4.10(**c**) shows a co-injection experiment with the addition of a synthetic sample of fluoroacetaldehyde **48** to the sample in Figure 4.10(**b**).

With the presence of Class II aldolases in *S. cattleya* now established, it became an objective to purify these enzymes. Progress towards this is discussed in the next section.

4.3 Purification of a DHAP dependent aldolase

4.3.1 Assay for the detection of DHAP aldolase activity

In order to purify aldolase enzymes, an appropriate assay was required. Unfortunately 5-FDRibP **121** and 5-FDXyuP **126** are not commercially available. However, due to the reversibility of the aldol reaction, a ^{19}F NMR assay was established for the detection of aldolase activity by the incubation of DHAP **123** and fluoroacetaldehyde **48**. Although NMR is a time consuming assay method, the formation of the products 5-FDRibP **121** and 5-FDXyuP **126** proved to be a sufficient assay to guide DHAP aldolase purification. The method described below has been used throughout the protein purification protocol when assaying for aldolase activity.

For the analysis of **121** and **126** by ^{19}F NMR, protein fractions (200 μl) were incubated with fluoroacetaldehyde **48** (20 mM), DHAP **123** (10 mM) and Zn^{2+} (1 mM) for 16 hrs at 37 °C. The sample was heated to 100 °C for 3 min and the precipitated protein was removed by centrifugation. The supernatant was lyophilised to remove the majority of residual fluoroacetaldehyde **48** and fluoroethanol **69**. It was possible to detect both stereoisomers by this method (Figure 4.11).

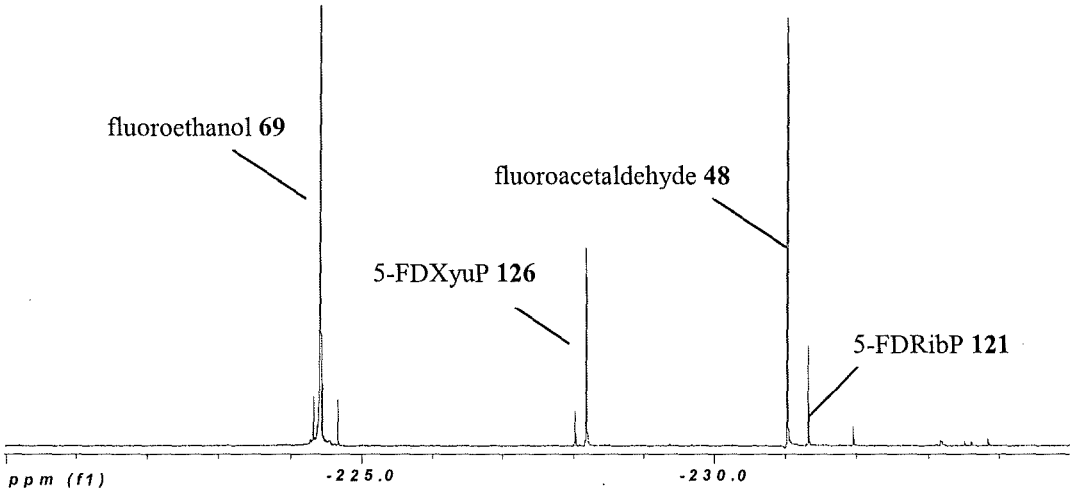

Figure 4.11 Aldolase assay: ^{19}F {^{1}H} NMR showing a CFE incubated with fluoroacetaldehyde **48** (20 mM) and DHAP **123** (10 mM) for 16 hrs at 37 °C.

4.3.2 Aldolase purification by ammonium sulfate precipitation

The CFE was subjected to ammonium sulfate precipitation to salt out the desired protein. This was previously shown in Section 2.3.2 and 3.5.2 to be a critical step during the purification of PNP and isomerase activities, therefore a similar approach was taken for aldolase purification. A total of three ammonium sulfate cuts were assayed (0-35 %, 35-50 %, 50-100 %) by the ^{19}F NMR method outlined earlier. The resultant ^{19}F NMR spectra are illustrated in Figure 4.12

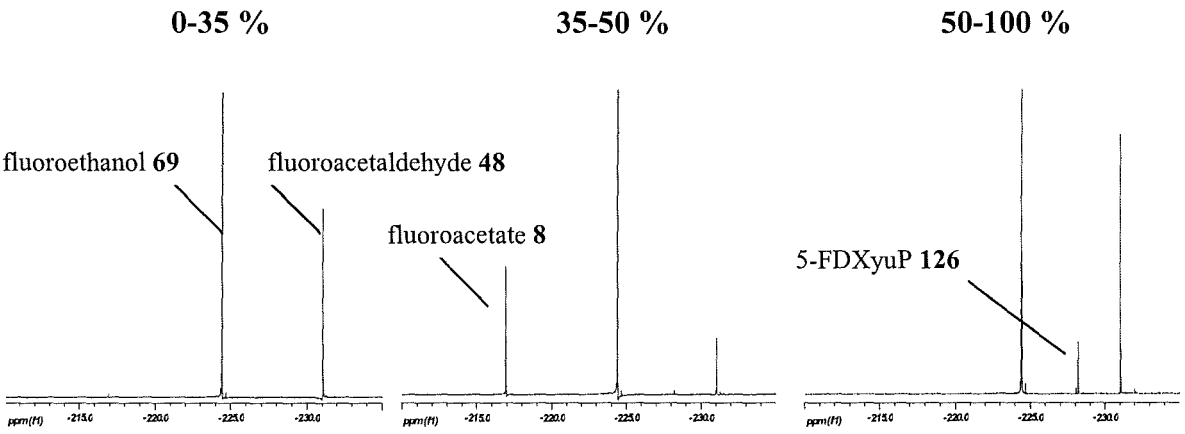

Figure 4.12 ^{19}F $\{^{1}H\}$ NMR spectra of the ammonium sulfate cuts after the incubation with fluoroacetaldehyde **48** (20 mM) and DHAP **123** (10 mM) for 16 hrs at 37 °C.

The results show that only the 50-100 % ammonium sulfate cut had aldolase activity. Interestingly, only diastereoisomer 5-FDXyuP **126** accumulated without 5-FDRibP **121** in any of the other cuts. Therefore, at this stage it would appear that L-FucA aldolase activity has been lost. Further purification using ammonium sulfate precipitation revealed that the addition of $(NH_4)_2SO_4$ at concentrations between 60-80 % contained the majority of the aldolase activity.

4.3.3 Aldolase purification by hydrophobic interaction chromatography

The next stage of purification involved hydrophobic interaction chromatography. A Phenyl HP (40 ml) column was equilibrated with phosphate buffer (50 mM, pH 6.8) containing 1M $(NH_4)_2SO_4$. The resulting protein pellet after ammonium sulfate precipitation (Section 4.3.2) was redissolved in buffer at a final concentration of ~12 mg / ml (5 ml). The sample was injected in duplicate volumes onto the equilibrated Phenyl HP column. The column was washed at 2 ml / min for three column volumes and subsequently eluted over a stepwise gradient from 1 M to 0 M $(NH_4)_2SO_4$ at a continuous flow rate of 2 ml / min. The resulting chromatogram is shown in Figure 4.13.

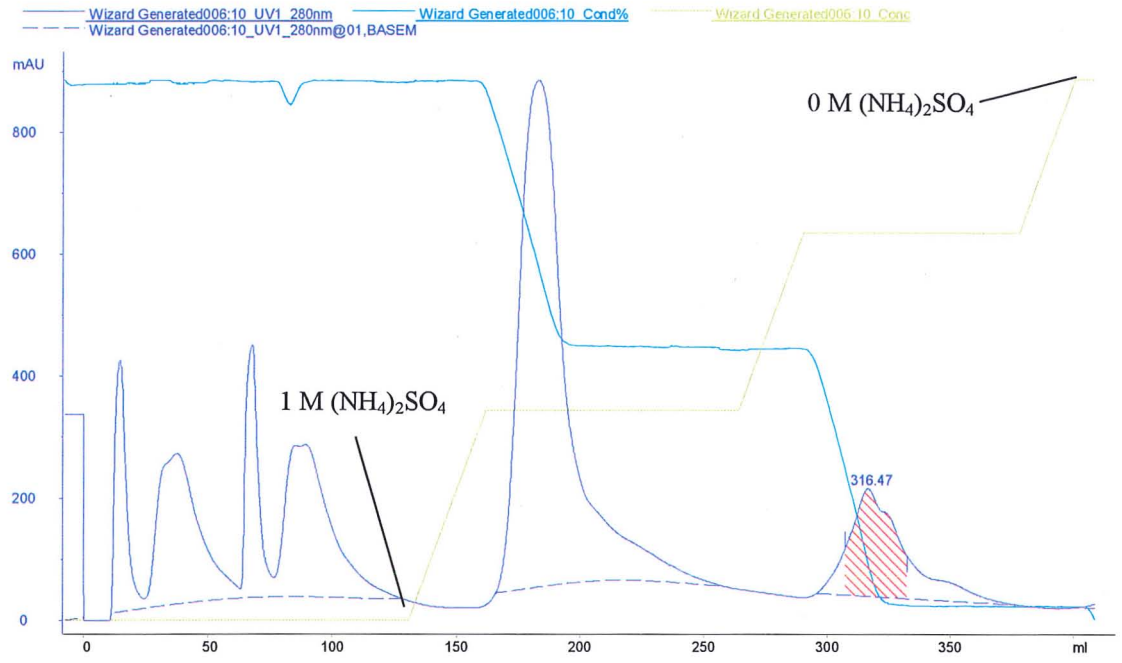

Figure 4.13 Chromatogram obtained after Phenyl HP (40 ml) column elution of the ammonium sulfate (60-80 %) fraction.

The application of hydrophobic interaction chromatography proved successful as it removed a substantial amount of unwanted protein. The elution profile in Figure 4.13 shows unwanted protein eluting at the start of the chromatogram. During the stepwise gradient elution the majority of protein eluted after 0.6 M $(NH_4)_2SO_4$, a concentration that was maintained to elute the unwanted protein. The gradient was applied for a further 30 ml to a concentration of 0.3 M $(NH_4)_2SO_4$ and held until the protein peaks eluted. The majority of aldolase activity was contained within the highlighted protein peaks in Figure 4.13.

4.3.4 Aldolase purification by size exclusion chromatography

The active fractions from the hydrophobic HP column (14 ml) were concentrated (2 ml) and injected onto a size exclusion column (Superdex 200, 60 x 16, Amersham Biotech)

which was pre-equilibrated with phosphate buffer (50 mM, pH 6.8) containing 0.3 M KCl. For protein elution, a flow rate of 1 ml / min was used and the eluent collected in 2 ml fractions. The results from the chromatogram in Figure 4.14 show the presence of several protein peaks.

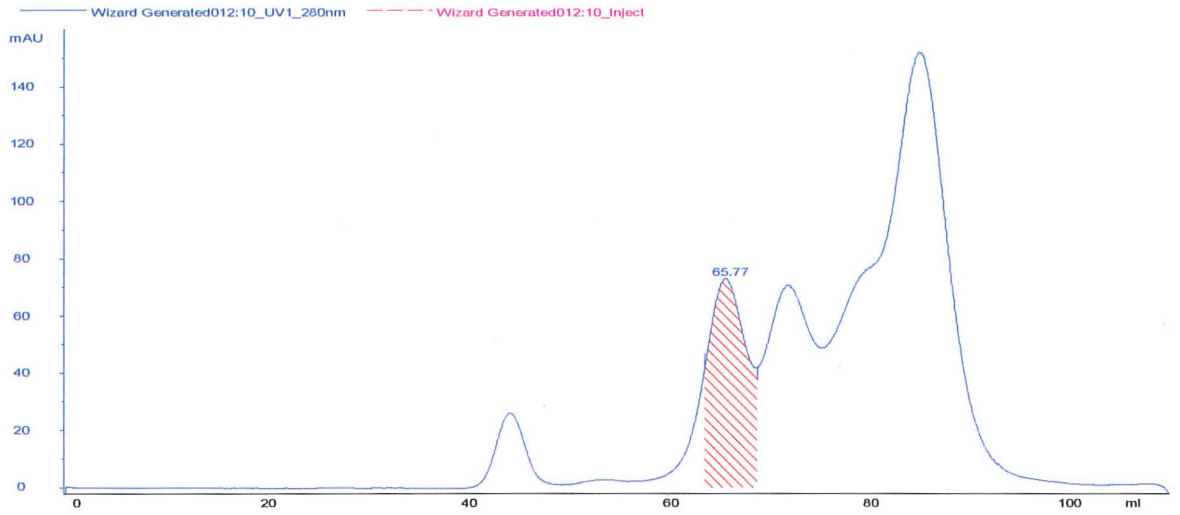

Figure 4.14 Chromatogram obtained by size exclusion using a Superdex 200 column (120 ml) after injection of 2 ml sample from HIC purification.

The collected fractions were assayed for aldolase activity, and activity was found in the highlighted peak, eluting between 60 and 72 ml.

Size exclusion chromatography removed a substantial amount of unwanted protein. However, there is no baseline separation between the protein peaks indicating that the protein is not homogenous. Further protein purification was needed in order to improve the level of purity.

4.3.5 Aldolase purification by anion exchange chromatography

The next stage of purification involved anion exchange chromatography. The active fractions from the size exclusion step (12 ml) were concentrated (2 ml) and desalted using a desalting column (HiTrap™ desalting, 5 ml, Amersham) and were then re-concentrated

(~ 2 ml). The sample was applied to a strong anion exchange column (15Q, 5 ml) equilibrated with tris buffer (50 mM, pH 7.2). A solvent gradient was applied from 100 % tris buffer (50 mM, pH 7.2) to 100 % tris buffer (50 mM, pH 7.2) containing 1 M KCl over 80 ml at a flow rate of 2 ml / min. The initial results showed one main peak eluting after 300 mM KCl along with a few minor peaks. The majority of the aldolase activity was found to be contained within the major peak. Conditions were optimised in order to remove the majority of the minor contaminants by employing a step wise gradient. To achieve this, the gradient was maintained after 300 mM KCl elution for a further 10 min in order to completely elute the desired protein. After this time, the gradient was applied in a step wise fashion in order to completely elute the remainder of the undesired proteins. Fractions (4 ml) were collected and assayed according to the procedure outlined in Section 4.3.1. The highlighted area in the chromatogram in Figure 4.15 shows active aldolase activity.

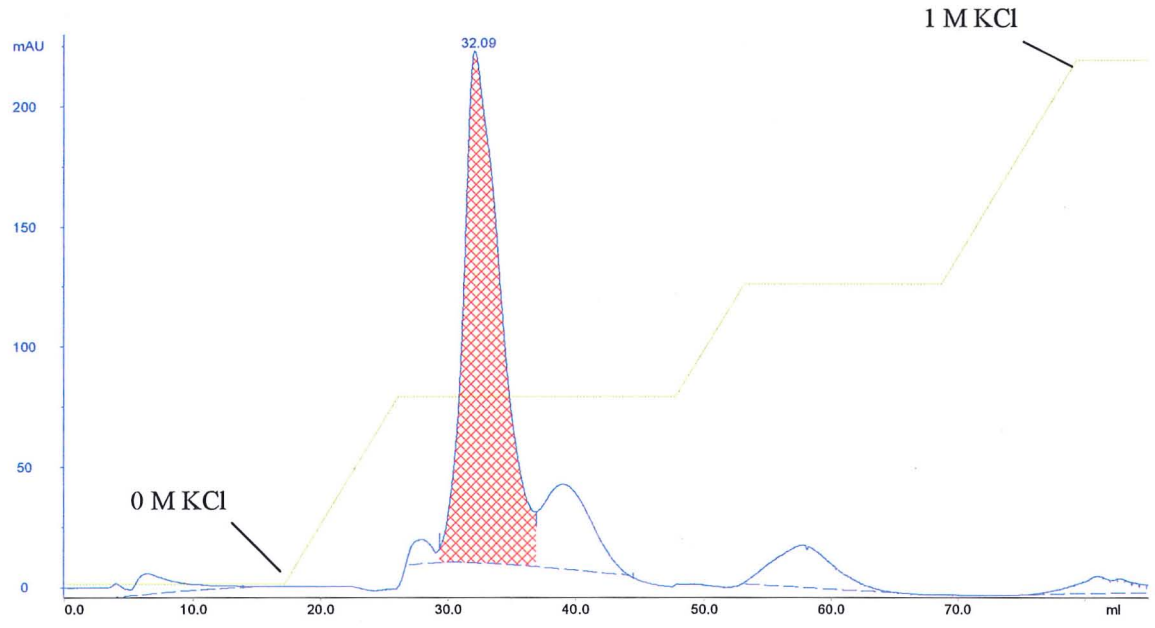

Figure 4.15 Chromatogram obtained using a 15Q anion (5 ml) column after injection of 2 ml protein sample from size exclusion. The highlighted area shows the active aldolase fraction.

A total protein concentration of 0.2 mg / ml was achieved from the protein purification protocol.

4.3.6 Analysis of DHAP aldolase purification by SDS-PAGE

The aldolase purity after each purification step was monitored by SDS PAGE where it became clear that one major band with a molecular subunit mass of approximately 40 kDa became increasingly prominent. Figure 4.16 shows the SDS PAGE analysis of the various fractions and indicates that the L-FruA has been purified to homogeneity.

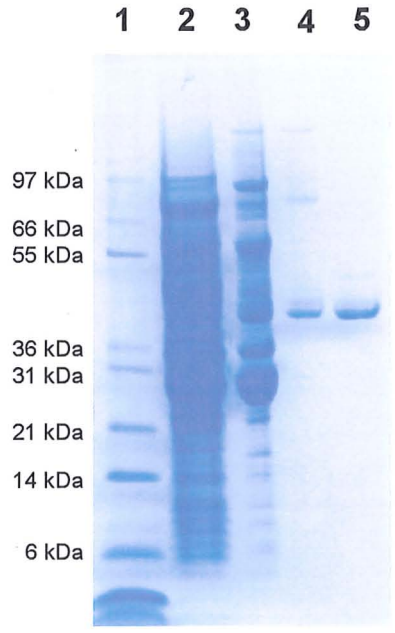

Figure 4.16 SDS PAGE gel (4-12 % acrylamide) showing active protein fractions containing DHAP aldolase activity during each purification step. Lanes: **1** molecular markers, .**2**, ammonium sulfate precipitation (60-80 %); **3**, hydrophobic interaction chromatography; **4**, size exclusion chromatography; **5**, anion exchange chromatography.

4.3.7 Measuring the molecular mass of the aldolase

The monomeric subunit of the fully purified aldolase analysed by SDS-PAGE showed a subunit mass of approximately 40 kDa by comparison with molecular weight markers.

The native mass of the enzyme was determined using a HiLoad 16/60 Superdex 200 size exclusion column. The column was calibrated with the following marker proteins; apoferritin [443 kDa], amylase [200 kDa], albumin [66 kDa] and cytochrome C [12.4 kDa]. Passing the purified DHAP aldolase down the same pre-equilibrated column revealed a native molecular mass of approximately 160 kDa, indicating that the enzyme is a homotetramer.

4.3.8 Effect of various metal ions on aldolase activity

A putative L-FruA has been purified to homogeneity from *S. cattleya*. The enzyme requires Zn^{2+} as a cofactor. The effect of other metal ions on its activity was investigated by conducting an assay using a partially purified aldolase fraction (100 μl, 1.5 mg / ml) obtained after size exclusion chromatography. In order to remove any metal ions already present in this fraction, EDTA (10 mM) was added and the protein stirred for 20 min at 4 ^{o}C. After this time, the sample was dialysed against 4 L of tris buffer (50 mM, pH 7.2) for 16 hrs at 4 ^{o}C. The dialysed sample was then assayed after addition of various divalent metal ions including Zn^{2+}, Mg^{2+}, Mn^{2+}, Co^{2+}, Ni^{2+}, Fe^{2+} and Ca^{2+}. The resulting ^{19}F NMR spectra showed aldolase activity with each of the metal ions added. Additionally, monovalent metal ions such as Na^{+}, K^{+}, resulted in no activity under the described conditions.

4.3.9 Sequence analysis of the aldolase

The purified protein was treated with trypsin. After the trypsic digest a small peptide (2059 Da) was isolated and the amino acid sequence was determined to be; –Phe-Ala-Tyr-Pro-Ala-Ile-Asn-Val-Thr-Ser-Ser-Gln-Thr-Leu-His-Ala-Ala-LeuArg-. A database search using NCBI BLAST showed a homology to a fructose 1,6-bisphosphate aldolase (L-FruA) from

Streptomyces galbus.[180] This match to a L-FruA is consistent with the stereochemical course of this enzyme which generates 5-FDXyuP **126** rather than 5-FDRibP **121**.

N-terminus amino acid sequence analysis of the purified L-FruA using Edman degradation showed that the first 20 amino acids (determined using an Applied Biosystems Procise 491 sequencing instrument) were; -Pro-Ile-Ala-Thr-Pro-Glu-Ile-Tyr-X-Glu-Met-Leu-Asp-Arg-Ala-Lys-Ala-Gly-Lys-Phe. The results in Figure 4.17 show a sequence alignment using MultiAlin of the first 20 N-terminus amino acids of L-FruA from *S. cattleya* related to homologues.

Figure 4.17 Sequence alignment of the first 20 N-terminal amino acids of L-FruA from *S. cattleya* with bacterial homologues. Residues that are highly conserved are in red. Weakly conserved residues are in blue.

Sequence analysis clearly suggests that the aldolase from *S. cattleya* is an L-FruA which catalyses the formation of 5-FDXyuP **126**. This may be an enzyme of primary metabolism.[181] The L-FucA aldolase remains to be purified. In the early stages of the purification such an activity was not apparent. Perhaps this can be rationalised by a high level of dehydrogenase activity present during ammonium sulfate precipitation (35-50 %) which would prevent the reverse aldol reaction to 5-FDRibP **121**. This observation is supported by the results in Section 3.5.2 which showed a 35-50 % ammonium sulfate cut containing all of the biosynthetic enzymes to support fluoroacetate **8** and 4-fluorothreonine **47** biosynthesis. Although the second aldolase has not been purified, putative L-FucA

genes have been identified in other streptomycetes such as *S. coelicolor* and *S. avermitilis*. The main function of this enzyme is the involvement in the L-fucose[182] and D-arabinose pathways.[183]

The metabolic relationships and enzymes involved in the biosynthesis of fluoroacetate **8** and 4-fluorothreonine **47** in *S. cattleya* that have been discussed throughout Chapters 2, 3 and 4 are summarised in Scheme 4.8.

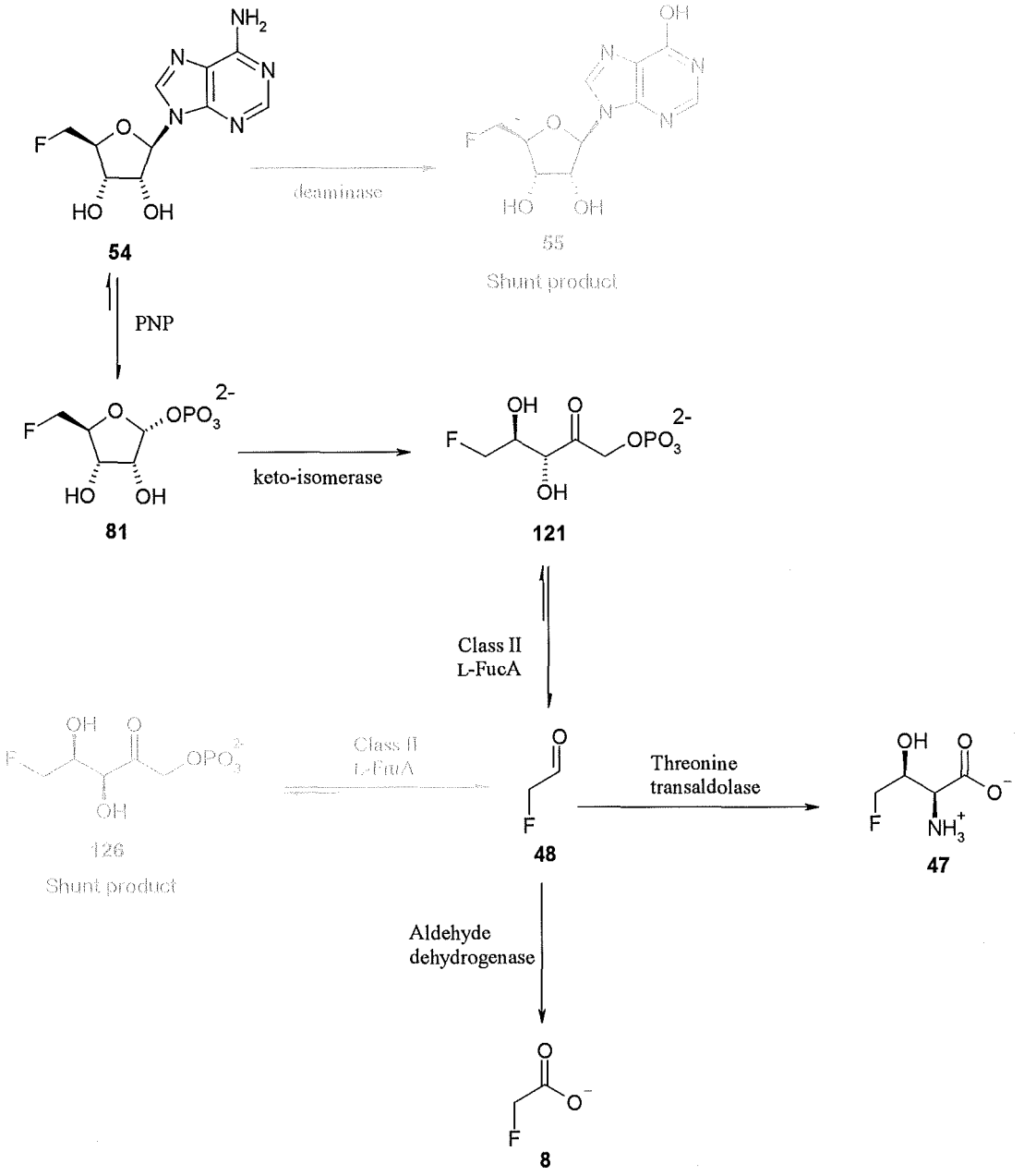

Scheme 4.8 Overview of the possible routes taken by 5'-FDA **54** towards the biosynthesis of fluoroacetate **8** and 4-fluorothreonine **47**.

4.4 Conclusion

It has been shown that two DHAP dependent aldolases are present on the fluorometabolite pathway in *S. cattleya*. One of these aldolases has been identified as a putative L-FucA which catalyses a retro-aldol reaction of 5-FDRibP **121** to fluoroacetaldehyde **48** and DHAP **123**. This enzyme is shown to be a Class II aldolase which requires a divalent metal ion for catalytic activity, and it is inhibited by the chelating agent EDTA.

A second aldolase was shown to be L-FruA which catalyses an aldol reaction between DHAP **123** and fluoroacetaldehyde **48** to generate 5-FDXyuP **126**. This enzyme is also a Class II aldolase, requiring a divalent metal ion such as Zn^{2+}, Mg^{2+}, Mn^{2+}, Co^{2+}, Ni^{2+}, Fe^{2+} and Ca^{2+} for catalytic activity. This enzyme was purified to homogeneity using standard chromatography techniques. Analysis by SDS-PAGE showed a monomeric subunit mass of approximately 40 kDa, and a native mass of 160 kDa was observed by gel filtration. This L-FruA had high sequence similarity in selected regions to other bacterial L-FruA's.

The action of this enzyme of primary metabolism in CFE's is probably adventitious. Our current hypothesis assumes that 5-FDXyuP **126** (Compound **B**) is a shunt product generated during fluoroacetaldehyde **48** production. The L-FucA aldolase, most relevant to fluorometabolite biosynthesis remains to be purified.

5 Experimental

5.1 Biochemical experimental

5.1.1 General methods

All commercial reagents, chemicals or enzymes were purchased from Sigma Biochemicals, Berry and Associates (U.S.A), and Fluka unless otherwise stated. The following commercial enzymes were used. 5'-Adenylic acid deaminase (EC 3.5.4.6, from *Aspergillus species*, A 1907, 0.11 units / mg), phytase (EC 3.1.3.8, from *Aspergillus ficuum*, P 9792, 3.5 units / mg), phosphatase (EC 3.1.3.1, from bovine intestinal mucosa, ammonium sulfate suspension, P-5521, 2,000-4000 DEA units / mg), fructose 1, 6-bisphosphate aldolase (EC 4.1.2.13, from rabbit muscle, lyophilized powder, A 2714, 10 units / mg), xylose isomerase (EC 5.3.1.5, Sweetzyme T, from *Streptomyces murinus*, G-4166, 350 units / mg) and immobilised crude PNP (*E. coli*, donated by GlaxoSmithKline, EC 2.4.2.1). The L-fuculose-1-phosphate gene was obtained as a pTrcHis C construct (ATCC number 86984) purchased from Promochem. The gene was over-expressed in *E. coli* and purified by nickel chromatography (see Section 5.1.28). The competent cells BL21(DE3), C43(DE3), BL21Star™, BL21(DE3)pLysS, BL21(DE3)pLysE and Rosetta2(DE3) were purchased from invitrogen in vials containing 50 µl aliquots.

^{19}F NMR analyses were performed on Bruker vance 500 MHz (operating at 470 MHz) or Varian unity 500 MHz (operating at 470 MHz) spectrometers. All ^{19}F NMR spectroscopy was carried out using D_2O (~ 10 %) as an internal reference. Chemical shifts are given in ppm and coupling constants (*J*) are given in Hertz (Hz). Spectral coupling patterns are designated as follows; d: doublet and t: triplet. High performance liquid chromatography

(HPLC) analyses were carried out using a solvent delivery system (230 Prostar) with an analytical C_{18} column (see Section 5.1.17). Electro-spray mass spectrometry (ES-MS) was performed on a Micromass LCT time of flight instrument. Gas chromatography mass spectrometry (GC-MS) was carried out by Dr. J. T. G. Hamilton at the Queen's University of Belfast.

HPLC was carried out using a Varian prostar system containing a solvent delivery system (230, ProStar) and equipped with a dual wavelength UV-Vis detector (325, ProStar) and a ProStar 400 autosampler. For analytical purposes, a Hypersil 5 μm C-18 column (250 x 10 mm, Phenomenex) was used. Typical flow rates were 1 ml / min and sample volumes were 100-200 μl in which 20 μl was automatically injected. All solvents were HPLC grade and filtered prior to use. The mobile phases consisted of two solvents, **A**, 50 mM KH_2PO_4: acetonitrile (95:5) and solvent **B**, 50 mM KH_2PO_4: acetonitrile (80:20). Runs were monitored at 254 nm by gradient elution over 30 min from 0 % B to 100 % B.

All microbiological work was carried out in a Gallenkamp flowhood under sterile conditions unless stated otherwise. Glassware, media and consumables were sterilised by autoclaving. Cell cultures were incubated at 28 °C in a Gallenkemp orbital incubator. Centrifugation (>1000 μl) was carried out either on a Beckman JA 14 instrument at 14,000 rpm, a JA 25.5 at 20,000 rpm or a JLA 9.1 at 9,100 rpm. For micro-centrifugation (20-1000 µl), an Eppendorf 5415C centrifuge was used. Cell-free extracts (CFE's) were prepared by disrupting the cells by sonication using Sonics & Materials Inc., Vibra Cell. Aqueous solutions were prepared using Ultra-pure water generated by a USF elga maxima water supply system.

5.1.2 Growth and maintenance of *S. cattleya* on agar

Streptomyces cattleya NRRL 8057 was originally supplied by Prof. D. B. Harper at the Queens University of Belfast, Microbial Biochemistry Section, Food Science Department, Belfast. Cultures were maintained on agar plates containing soybean flour (2 % w/v), mannitol (2 % w/v), agar (1.5 % w/v) and tap water. The plates were incubated at 30 °C for 28 days or until sporulation could be detected. The resultant static cultures were stored at 4 °C for future use.

5.1.3 Culture medium and growth conditions of *S. cattleya*[78]

Streptomyces cattleya seed and batch cultures were grown in conical flasks (500 ml) containing chemically defined medium (90 ml). The medium was prepared as follows. Sterile ultra-pure water (450 ml) was added to ion solution (150 ml), filtered carbon solution (75 ml), (see Section 5.1.4), sterile phosphate buffer (75 ml, 150 mM, pH 7.0) and sterile potassium fluoride (3 ml, 0.5 M). The seed cultures were prepared by transferring spores from a static culture as described above, and added to a conical flask (500 ml) containing chemically defined medium (90 ml). After incubation for 6 days at 28 °C on an orbital shaker (180 rpm), an aliquot (0.3 ml) of spores was used to inoculate the batch cultures. The batch cultures were incubated at 28 °C, on an orbital shaker at 180 rpm for 6-8 days.

5.1.4 Media procedure for growing *S. cattleya*

Ion solution

The following reagents were added to ultra-pure water (900 ml).

NH_4Cl	6.75 g
NaCl	2.25 g
$MgSO_4.7H_2O$	2.25 g
$CaCO_3$	1.13 g
$FeSO_4.7H_2O$	0.113 g
$CoCl_2.6H_2O$	0.045 g
$ZnSO_4.7H_2O$	0.045 g.

The solution was sterilised by autoclaving prior to use.

Carbon source solution

The following reagents were added to ultra-pure water (900 ml).

Glycerol (45 g)

monosodium glutamate (22.5 g)

myo-inositol (1.8 g)

para-aminobenzoic acid (450 µl of freshly prepared solution 1 mg / ml)

The solution was sterilised by filtration into pre-sterilised Schott bottles.

5.1.5 Preparation of resting cell cultures of *S. cattleya*

After 6 days of growth, cells were harvested by centrifugation (9,100 rpm / 25 min) and the resulting pellet was washed three times with phosphate buffer (50 mM, pH 6.8). After the

final wash, the bacterial pellet was stored at –80 °C or could be used directly for cell free extract (CFE) preparation.

5.1.6 Preparation of cell free extract (CFE) of *S. cattleya*

CFE was prepared in two ways; firstly by re-suspending 0.1 g cells / ml of phosphate buffer (50 mM, pH 6.8) and left to stir for 20 minutes at 4 °C. The cells were then sonicated 6-10 times at 60 cycles for 1 min. After sonication, the cells were centrifuged at (14,000 rpm / 20 min) and the resultant cell pellet was discarded and the supernatant retained as a CFE. For experiments on the biosynthesis of fluorinated metabolites, a CFE was prepared under parallel conditions except by re-suspending 0.2 g of cells / ml of phosphate buffer (50 mM, pH 6.8).

5.1.7 Assay to determine biosynthetic activity in a CFE of *S. cattleya*

CFE (500 μl) was incubated with 5'-FDA **54** (100 μl, 18.6 mM) in phosphate buffer (50 mM, pH 6.8) for 16 hrs at 37 °C. The sample was subsequently heated at 100 °C for 3 min and the denatured protein micro-centrifuged at (14,000 rpm, 5 min). The protein pellet was discarded and the supernatant retained for analysis by ^{19}F NMR spectroscopy (470 MHz, 10 % D_2O). The production of fluoroacetate **8**, -216.97 (t, $^2J_{F,H}$ 48.2) and 4-fluorothreonine **47** -231.60 (t, $^2J_{F,H}$ 46.8) confirmed the CFE retained all its biosynthetic activities. Reference compounds of fluoroacetate **8** and 4-fluorothreonine **47** confirmed this unambiguously. Control experiments were conducted under the same conditions except

using a denatured CFE. This showed that 5'-FDA **54** is stable over an incubation period of 16 hrs at 37 °C.

5.1.8 Incubation of 5-fluoro-5-deoxy-D-ribose (5-FDR) in a CFE of *S. cattleya*

Synthetic 5-FDR **80** was prepared as a reference compound by S. L. Cobb,[118] University of St Andrews. 5-FDR **80** (100 μl, 32.9 mM) was incubated with an active CFE (500 μl) in phosphate buffer (50 mM pH 6.8) for 16 hrs at 37 °C. After this time the protein was denatured by heating to 100 °C for 3 min and the precipitated protein removed by micro-centrifugation (14,000 rpm / 5 min). D_2O (100 μl) was added to the supernatant and the sample analysed by ^{19}F NMR. δ_F (470 MHz, 10% D_2O) 5-FDR **80** β-anomer -228. 55 (ddd, $^2J_{F,H}$ 47.0 and $^3J_{F,H}$ 26.4) and α-anomer -230.86 (ddd, $^2J_{F,H}$ 46.9 and $^3J_{F,H}$ 26.3). Control experiments were carried out under similar conditions except using a denatured CFE. Analysis by ^{19}F NMR concluded that 5-FDR **80** is chemically stable after 16 hrs at 37 °C.

5.1.9 Chemo-enzymatic preparation of 5-fluoro-5-deoxy-D-ribose -1-phosphate (5-FDRP)

5'-FDA **54** (18.6 mM) and adenosine deaminase (2 mg) were suspended in phosphate buffer (50 mM, pH 6.8) in a total volume of 1 ml for 16 hrs at 37 °C. After incubation the sample was heated to 100 °C for 3 min and the denatured protein removed from the solution by micro-centrifugation (14,000 rpm / 15 min). Analysis by HPLC showed 100 % bioconversion to 5'-FDI **55**. The supernatant sample was incubated with immobilised PNP

(2 mg resin) and incubated at 37 °C for a further 16 hrs. After this time the sample was denatured at 100 °C for 3 min and the precipitated protein removed by micro-centrifugation (14,000 rpm / 5 min). The sample was analysed by ^{19}F NMR spectroscopy and HPLC (UV detection); δ_F (470 MHz; 10 % D_2O) (5-FDRP **81**, ~ 40 %) -230.75 (dt, $^2J_{F,H}$ 47.3 and $^3J_{F,H}$ 28.3) and (5'-FDI **55**, ~ 60 %) -230.85 (dt, $^2J_{F,H}$ 47.0 and $^3J_{F,H}$ 28.9). HPLC (UV, λ = 254 nm) analysis indicated the production of hypoxanthine **79** and the presence of unreacted 5'-FDI **55**.

An aliquot (500 µl) was lyophilised and treated with MSTFA prior to GC-MS analysis; ***m/z*** 505 (16%), 382 (11), 353 (14), 300 (24), 299 (100) and 147 (20). ES-MS (-ve) analysis; 5-FDRP **81** *m/z* 231 $(M-H)^-$, 5'-FDI **55** *m/z* 269 $(M-H)^-$.

5.1.9.1 Incubation of 5-FDRP with a CFE of *S. cattleya*

5-FDRP **81** was prepared according to Section 5.1.9. The sample contained ~60 % 5'-FDI **55**. Control experiments showed that 5'-FDI **55** is not metabolised in a CFE of *S. cattleya.* Also incubation of a denatured CFE with 5-FDRP **81** at 37 °C for 16 hrs showed no chemical breakdown. 5-FDRP **81** (200 µl) was incubated with a CFE (500 µl) in phosphate buffer (50 mM, pH 6.8) for 16 hrs at 37 °C. After the incubation period the protein was denatured (100 °C / 3 min) and removed by centrifugation (14,000 rpm / 5 min). D_2O (100 µl) was added to the supernatant, which was then analysed by ^{19}F NMR. The identities of the new fluorinated products were confirmed by co-injection with reference compounds. δ_F (470 MHz, 10 % D_2O) fluoroacetate **8**, -216.96 (t, $^2J_{F,H}$ 48.3), 5'-FDI **55**, -230.85 (dt, $^2J_{F,H}$ 46.9 and $^3J_{F,H}$ 26.9) and 4-fluorothreonine **47**, -231.58 (t, $^2J_{F,H}$ 46.8). HPLC (UV) analysis showed the presence of hypoxanthine **79** and 5'-FDI **55**.

5.1.10 Incubation of 2-deoxy-5'-FDA in a CFE of *S. cattleya*

Synthetic 2-deoxy-5'-FDA **59** was prepared by S. L. Cobb,[118] University of St Andrews. 2-deoxy-5'-FDA **59** (100 μl, 18.6 mM) was incubated with a CFE (500 μl) for 16 hrs at 37 °C. After this time the sample was denatured at 100 °C for 3 min and subsequently micro-centrifuged at (14,000 rpm, 5 min). The supernatant was analysed by ^{19}F NMR. δ_F (470 MHz, 10 % D_2O), 2-deoxy-5-FDR **83**, -227.81 (dt, $^2J_{F,H}$ 47.0 and $^3J_{F,H}$ 22.9), 2'-deoxy-5'-FDI **84**, -230.60 (dt, $^2J_{F,H}$ 47.0 and $^3J_{F,H}$ 26.4). HPLC analysis showed the presence of 2-deoxy-5'-FDI **84** and hypoxanthine which was confirmed by co-injection experiments using synthetic standards. Control experiments were carried out under parallel conditions using a denatured CFE. ^{19}F NMR and HPLC analysis showed no chemical degradation of 2-deoxy-5'-FDA **59** over the same time period.

5.1.11 Effect of iodoacetamide on fluorometabolite production

Experiment 1: A CFE (490 μl) was pre-incubated with iodoacetamide (10 μl, 0.5 M) for 25 min at 37 °C. After this time 5'-FDA **54** (100 μl, 18.6 mM) was added to the pre-incubated CFE and the incubation continued for 16 hrs at 37 °C. After this time the sample was denatured at 100 °C for 3 min and the precipitated protein removed by micro-centrifugation (14, 000 rpm / 5 min). The supernatant was analysed by ^{19}F NMR. δ_F (470 MHz, 10 % D_2O), 5'-FDI **55** 230.91 (dt, $^2J_{F,H}$ 47.0 and $^3J_{F,H}$ 28.9) and 5-FDRP **81** -230.87 (dt, $^2J_{F,H}$ 47.0 and $^3J_{F,H}$ 28.7). HPLC (UV) analysis indicated the presence of 5'-FDI **55** and hypoxanthine **79**.

Experiment 2: A CFE (490 μl) was pre-incubated with iodoacetamide (10 μl, 0.5 M) for 25 min at 37 °C. The addition of 5-FDRP **81** (200 μl) containing an excess of 5'-FDI **55** was added to the pre-incubated CFE for 16 hrs at 37 °C. The resulting sample was then denatured at 100 °C for 3 min and the precipitated protein micro-centrifuged (14,000 rpm / 5 min). The supernatant was analysed by ^{19}F NMR. δ_F (470 MHz, 10% D_2O), 5'-FDI **55** -230.90 (dt, $^2J_{F,H}$ 47.0 and $^3J_{F,H}$ 28.7) and 5-FDRP **81** -230.86 (dt, $^2J_{F,H}$ 46.9 and $^3J_{F,H}$ 28.6). HPLC analysis indicated the presence of 5'-FDI **55** and hypoxanthine **79**.

5.1.12 Effect of EDTA on fluorometabolite production

Experiment 1: A CFE (500 μl) was pre-incubated with EDTA (final conc. 30 mM) for 25 min at 37 °C. 5'-FDA **54** (100 μl, 18.6 mM) was then added and the incubation was continued for 16 hrs at 37 °C. After this time the sample was denatured at 100 °C for 3 min and the denatured protein removed by micro-centrifugation (14,000 rpm, 5 min). The supernatant was analysed by ^{19}F NMR. δ_F (470 MHz, 10% D_2O), 5'-FDI **55** -230.83 (dt, $^2J_{F,H}$ 47.0 and $^3J_{F,H}$ 29.8), 5-FDRP **81** -230.76 (dt, $^2J_{F,H}$ 47.3 and $^3J_{F,H}$ 28.3) and 5-FDRibP **121** -231.28 (dt, $^2J_{F,H}$ 46.8 and $^3J_{F,H}$ 20.6). HPLC analysis indicated the presence of 5'-FDI **55** and hypoxanthine **79**. This was confirmed by co-injection experiments using synthetic standards. No 5'-FDA **54** was observed under these conditions.

Experiment 2: A CFE (500 μl) was pre-incubated with EDTA at a final concentration of 30 mM for 25 min at 37 °C. 5-FDRP **81** (200 μl) was then added and the incubation continued for 16 hrs at 37 °C. After this time the sample was denatured at 100 °C for 3 min and the denatured protein removed by micro-centrifugation (14,000 rpm, 5 min). The supernatant was analysed by ^{19}F NMR. δ_F (470 MHz, 10% D_2O), 5'-FDI **55** -230.85 (dt,

$^{2}J_{F,H}$ 47.0 and $^{3}J_{F,H}$ 29.8), 5-FDRP **81** -230.80 (dt, $^{2}J_{F,H}$ 47.3 and $^{3}J_{F,H}$ 28.3) and 5-FDRibP **121** -231.30 (dt, $^{2}J_{F,H}$ 47.0 and $^{3}J_{F,H}$ 20.7). HPLC analysis indicated the presence of 5'-FDI **55** and hypoxanthine **79**. This was confirmed by co-injection experiments using synthetic standards.

5.1.13 Chemoenzymatic preparation and CFE incubation of 5-fluoro-5-deoxy-D- ribulose (5-FDRib)

Experiment 1: Synthetic 5-FDR **80** was prepared by Mayca. Onega,[2] University of St Andrews. Immobilised xylose isomerase (3 mg) was incubated with 5-FDR **80** (100 μl, 32.9 mM) in a total volume of 700 μl containing phosphate buffer (50 mM, pH 6.8) for 4 hours at 60 °C. After incubation, the enzyme was denatured at 100 °C for 3 min and micro-centrifuged at (14.000 rpm / 5 min). The supernatant was analysed by ^{19}F NMR. δ_F (470 MHz, 10% D_2O) 5-FDR **80**, α anomer -230.78 (dt, $^{2}J_{F,H}$ 46.9 and $^{3}J_{F,H}$ 26.3), 5-FDR **80**, β anomer -228.47 (dt, $^{2}J_{F,H}$ 47.0 and $^{3}J_{F,H}$ 26.4) and 5-fluoro-5-deoxy-D-ribulose **122**, -231.17 (dt, $^{2}J_{F,H}$ 47.0 and $^{3}J_{F,H}$ 20.6).

Control experiments were carried out in the absence of xylose isomerase which indicated that 5-FDR **80** was chemically inert over the time period.

Experiment 2: 5-FDRib **122** (100 μl) containing an excess of 5-FDR **80** (Experiment 1) was incubated with a CFE (500 μl) for 16 hrs at 37 °C. After this time the sample was denatured at 100 °C for 3 min and the precipitated protein removed by micro-centrifugation (14, 000 rpm / 5 min). The supernatant was analysed by ^{19}F NMR. δ_F (470 MHz, 10% D_2O) 5-FDR **80**, α anomer -230.80 (dt, $^{2}J_{F,H}$ 47.3 and $^{3}J_{F,H}$ 27.3), 5-FDR **80**, β

anomer -228.50 (dt, $^{2}J_{F,H}$ 47.3 and $^{3}J_{F,H}$ 25.8) and 5-FDRib **122**, -231.18 (dt, $^{2}J_{F,H}$ 47.0 and $^{3}J_{F,H}$ 20.7).

5.1.14 Chemoenzymatic preparation and CFE incubation of 5-fluoro-5-deoxy-D- xyulose (5-FDXyu)

Experiment 1: Synthetic 5-fluoro-5-deoxy-D-xylose (5-FDX) **124** was prepared by Mayca Onega,[161] University of St Andrews. A synthetic sample of 5-FDX **124** (100 μl, 32.9 mM) was incubated with immobilised xylose isomerase (3 mg) in a total volume of 700 μl containing phosphate buffer (50 mM, pH 6.8) for 4 hrs at 60 °C. After incubation, the enzyme was denatured at 100 °C for 3 min and the precipitate micro-centrifuged at (14,000 rpm / 5 min). D_2O (100 μl) was added to the supernatant, which was then analysed by ^{19}F NMR. δ_F (470 MHz, 10 % D_2O) 5-FDX **124**, -228.46 (dt, $^{2}J_{F,H}$ 47.0 and $^{3}J_{F,H}$ 22.9), 5-FDX **124**, -230.54 (dt, $^{2}J_{F,H}$ 47.0 and $^{3}J_{F,H}$ 25.2) and 5-fluoro-5-deoxy-D-xyulose **125**, -228.50 (dt, $^{2}J_{F,H}$ 47.0 and $^{3}J_{F,H}$ 16.0).

Control experiments were performed in the absence of xylose isomerase which indicated that 5-FDX **124** remains chemically inert to degradation over the 16 hrs incubation at 37 °C.

Experiment 2: Enzymatically prepared 5-fluoro-5-deoxy-D-xyulose (5-FDXyu) **125** (100 μl) was incubated with a CFE (500 μl) for 16 hrs at 37 °C. After incubation, the sample was denatured at 100 °C for 3 min and finally micro-centrifuged at (14,000 rpm / 5 min) to remove the denatured precipitate. Addition of D_2O (100 μl) to the supernatant was then analysed by ^{19}F NMR spectroscopy, δ_F (470 MHz, 10 % D_2O), 5-FDX **124**, -228.47 (dt, $^{2}J_{F,H}$ 46.9 and $^{3}J_{F,H}$ 21.8), 5-FDX **124**, -230.55 (dt, $^{2}J_{F,H}$ 47.0 and $^{3}J_{F,H}$ 24.0), 5-FDXyu **125**, -228.51 (dt, $^{2}J_{F,H}$ 46.9 and $^{3}J_{F,H}$ 15.9).

5.1.15 Preparation of 5-fluoro-5-deoxy-D-ribulose-1-phosphate (5-FDRibP)

Fluoroacetaldehyde* **48** was prepared by S. L. Cobb,[118] University of St Andrews. A typical protocol for preparing 5-FDRibP **121** is as follows. Fluoroacetaldehyde **48** (30 μl, 140 mM) and DHAP **123** (70 μl, 55 mM) were incubated with L-FucA (200 μl, 0.4 mg / ml) in a total volume of 700 μl with phosphate buffer (50 mM, pH 6.8) for 1 hr at 37 °C. After this time the sample was denatured at 100 °C for 3 min and the precipitated enzyme removed by micro-centrifugation (14,000 rpm / 5 min). The resulting supernatant was lyophilised to remove the residual fluoroacetaldehyde **48** and fluoroethanol **69** present. The lyophilised sample was re-suspended in H_2O (700 μl) and analysed by ^{19}F NMR. δ_F (470 MHz, 10 % D_2O), (5-fluoro-5-deoxy-D-ribulose-1-phosphate **121**, 30 %), -231.34 (dt, $^2J_{F,H}$ 47.0 and $^3J_{F,H}$ 20.7), (diastereoisomer of **121**, 70 %), -228.21 (dt, $^2J_{F,H}$ 46.2 and $^3J_{F,H}$ 15.3).

Control experiments were carried under the same conditions in the absence of L-FucA. The product was subsequently analysed by ^{19}F NMR. δ_F (470 MHz, 10 % D_2O), fluoroacetaldehyde **48** -231.04 ppm and fluoroethanol **69** -224.50 ppm.

* The preparation of fluoroacetaldehyde **48** contained an excess of fluoroethanol **69**.

5.1.16 Preparation of 5-fluoro-5-deoxy-D-xyulose-1-phosphate (5-FDXyuP)

A similar procedure to Section 5.1.15 was adopted for the preparation of 5-FDXyuP. Therefore, fluoroacetaldehyde **48** (30 μl, 20 mM) and DHAP **123** (70 μl, 10 mM) were

incubated with L-FruA (20 μl, 2 mg / ml) in phosphate buffer (580 μl, 50 mM, pH 6.8) for 16 hrs at 37 °C. After this time the sample was denatured at 100 °C for 3 min and the precipitated protein removed by micro-centrifugation (14,000 rpm / 5 min). The supernatant was subsequently lyophilised to remove the majority of residual fluoroethanol **69** and fluoroacetaldehyde **48**. The freeze-dried sample was re-suspended in H_2O (700 μl) and analysed by ^{19}F NMR. δ_F (470 MHz, 10 % D_2O) 5-FDXyuP **126** -228.20 (dt, $^2J_{F,H}$ 46.2 and $^3J_{F,H}$ 15.3).

Control experiments were carried under the same conditions in the absence of L-FruA. The product was analysed by ^{19}F NMR. δ_F (470 MHz, 10 % D_2O), fluoroacetaldehyde **48** -231.03 ppm and fluoroethanol **69** -224.51 ppm.

5.1.17 Protein purification by ammonium sulfate precipitation

A CFE was prepared according to Section 5.1.6. According to the volume of the supernatant, ammonium sulfate was slowly added to the desired % saturation level (see Table 5.1). After all the ammonium sulfate was dissolved by stirring for 20 minutes at 4 °C, the precipitated solution was centrifuged for 20 minutes at 14,000 rpm and the supernatant either discarded or kept for further precipitation. The protein pellet could then be used directly or kept at –80 °C.

Final concentration of ammonium sulfate, % saturation at 0°C

Initial concentration of ammonium sulfate, % saturation at 0 °C	20	25	30	35	40	45	50	55	60	65	70	75	80	85	90	95	100
	g solid ammonium sulfate to add to 100 ml of solution																
0	10.7	13.6	16.6	19.7	22.2	26.2	29.5	33.1	36.6	40.4	44.2	48.3	52.3	56.7	61.1	65.9	70.7
5	8.0	10.9	13.9	16.8	20.0	23.2	26.6	30.0	33.6	37.3	41.1	45.0	49.1	53.3	57.8	62.4	67.1
10	5.4	8.2	11.1	14.4	17.1	20.3	23.6	27.0	30.5	34.2	37.9	41.8	45.8	50.0	54.4	58.9	63.6
15	2.6	5.5	8.3	11.3	14.3	17.4	20.7	24.0	27.5	31.0	34.8	38.6	42.6	46.6	51.0	55.5	60.0
20	0	2.7	5.6	8.4	11.5	14.5	17.7	21.0	24.4	28.0	31.6	35.4	39.2	43.3	47.6	51.9	56.5
25		0	2.7	5.7	8.5	11.7	14.8	18.2	21.4	24.8	28.4	32.1	36.0	40.1	44.2	48.5	52.9
30			0	2.8	5.7	8.7	11.9	15.0	18.4	21.7	25.3	28.9	32.8	36.7	40.8	45.1	49.5
35				0	2.8	5.8	8.8	12.0	15.3	18.7	22.1	25.8	29.5	33.4	37.4	41.6	45.9
40					0	2.9	5.9	9.0	12.2	15.5	19.0	22.5	26.2	30.0	34.0	38.1	42.4
45						0	2.9	6.0	9.1	12.5	15.8	19.3	22.9	26.7	30.6	34.7	38.8
50							0	3.0	6.1	9.3	12.7	16.1	19.7	23.3	27.2	31.2	35.3
55								0	3	6.2	9.4	12.9	16.3	20.0	23.8	27.7	31.7
60									0	3.1	6.3	9.6	13.1	16.6	20.4	24.2	28.3
65										0	3.1	6.4	9.8	13.4	17.0	20.8	24.7
70											0	3.2	6.6	10.0	13.6	17.3	21.2
75												0	3.2	6.7	10.2	13.9	17.6
80													0	3.3	6.8	10.4	14.1
85														0	3.4	6.9	10.6
90															0	3.4	7.1
95																0	3.5
100																	0

Table 5.1 Ammonium sulfate table showing grams of ammonium sulfate added to 100 ml of solution.[184]

5.1.18 SDS-Polyacrylamide gel electrophoresis (SDS-PAGE)

SDS-PAGE was performed on an Invitrogen XCell *SureLock*^{TM} mini-cell apparatus connected to an Amersham Pharmacia biotech EPS 301 power supply operating at a constant current of 125 mA for 40 minutes. NuPAGE^{TM} Bis-Tris 10 well gels were used which contained either 10 % or 4-12 % of acrylamide.

5.1.19 Sample preparation for SDS-PAGE

The protein sample was prepared as follows. To 20 μl of a protein sample was added 5 μl of NuPAGE^{R} LDS sample buffer under denaturing conditions. The solution was heated to 100 ^{o}C for 3 min and subsequently 10-20 μl was added to the sample wells of the pre-cast NuPAGE^{TM} Bis-Tris gel. Protein markers (Mark 12 ^{TM} standards, Invitrogen life technologies) used were; myosin [200 kDa], β-galactosidase [116 kDa], phosphorylase B [97.4 kDa], BSA [66 kDa], glutamic dehydrogenase [55 kDa], lactate dehydrogenase [36.5 kDa], carbonic anhydrase [31 kDa], trypsin inhibitor [21.5 kDa], lysozyme [14.4 kDa], aprotinin [6 kDa].

5.1.19.1 Staining and destaining of SDS gels

After each SDS-PAGE run, the gel was stained by soaking in a solution of Coomassie blue G250 dye for 30-60 min. After this time the gel was destained overnight in destain solution with constant agitation to remove any unbound dye. The composition of both stains was as follows,

Stain solution		**Destain solution**	
Coomassie blue G250	2.0 g	Methanol	400 ml
Methanol	400 ml	Glacial acetic acid	70 ml
Glacial acetic acid	70 ml	Ultra pure water	530 ml
Ultra pure water	530 ml		

5.1.20 Protein concentration determination

Protein concentrations were determined using a Bradford assay, (Bradford solution, Sigma Chemicals). In a microcuvette, the protein solution (50 μl) was added to Bradford reagent (1500 μl) and thoroughly mixed. After 5 minutes the absorbance was read at λ max = 595. The result was compared to a standard curve using BSA from known concentrations (Figure 5.1).

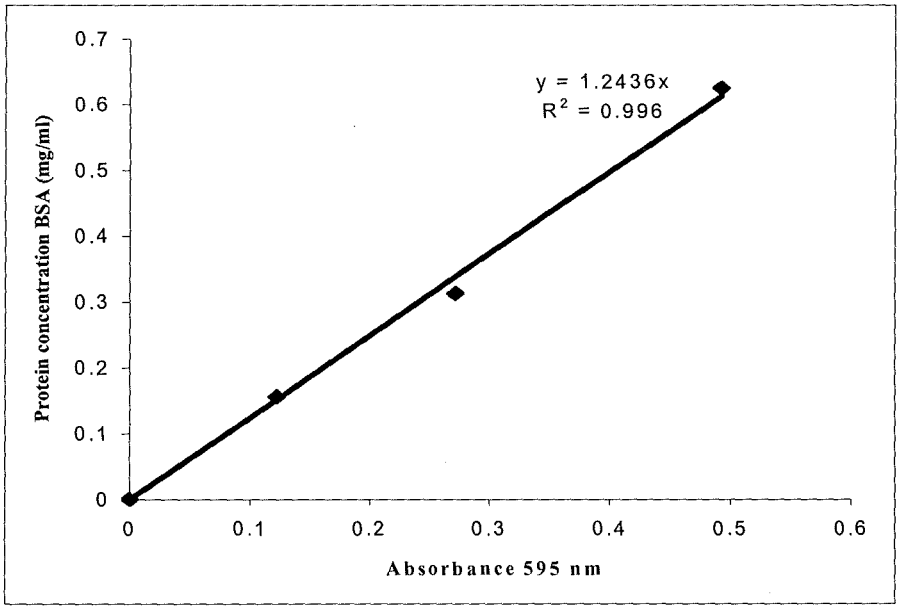

Figure 5.1 Protein concentration determinations from a standard curve

5.1.21 Fast protein liquid chromatography (FPLC)

Protein purification was carried out on an ACTA basic system at room temperature. The following techniques were employed; size exclusion chromatography using a High load 16/60 Superdex 200 (Amersham Biosciences), hydrophobic interaction chromatography (HIC) using Phenyl Sepharose HP, 40 ml bed volume (Amersham Biosciences), anion exchange using a Q, 10 ml bed volume (Amersham Biosciences), anion exchange, ANX

sepharose 4 FF, 1 ml bed volume (Amersham Biosciences), DEAE sepharose FF, 20 ml bed volume (Amersham Biosciences), hydroxyapetite type I and II, 5 ml bed volume (BioRad) and cation exchange 15S, 10 ml bed volume (Amersham Biosciences). Typical flow rates were between 1 ml / min and 5 ml / min.

5.1.22 Calibration of native protein masses by size exclusion chromatography

The molecular weight of native proteins was measured by size exclusion chromatography using a HiLoad 16/60 Superdex 200, (Amersham Biosciences). The column was equilibrated with phosphate buffer (50 mM, pH 6.8) and calibrated with the following reference proteins; apoferritin (443 kDa), amylase (200 kDa), albumin (66 kDa), and cytochrome C (12.4 kDa). The void volume (V_o) of 44.0 ml was determined using blue dextran. The calibration curve of the relative elution volumes (log (V_e/V_o) against the molecular weights (log MW) of the reference proteins is shown in Figure 5.2.

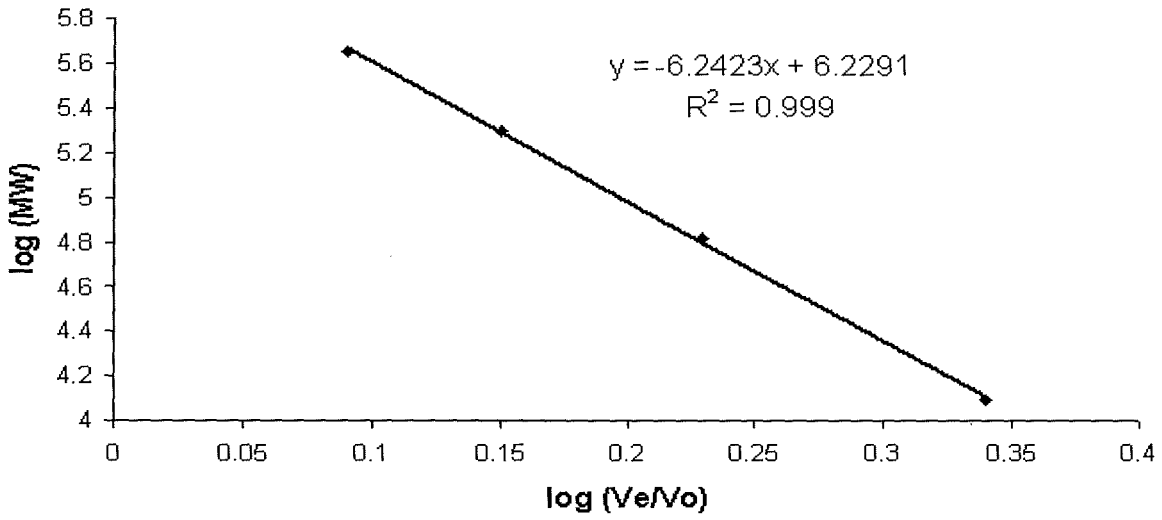

Figure 5.2 Calibration curve of molecular weight proteins from HiLoad 16/60 Superdex 200.

5.1.23 Partial purification of a PNP from *S. cattleya*

CFE (150 ml, ~4 mg / ml) was prepared as described under Section 5.1.6 and ammonium sulfate precipitation was carried out as described in Section 5.1.18. The protein pellet 35-50 % was dissolved in phosphate buffer (5 ml, 50 mM, pH 6.8) containing 1 M $(NH_4)_2SO_4$ at a final concentration of ~21 mg / ml. Prior to further purification, the re-suspended protein pellet was filtered through a 0.45 μm HT Tuffryn^R membrane filter.

To assay for PNP activity, 100 μl of CFE or the partially purified fractions were incubated with 5'-FDA **54** (final conc. 1 mM) for 16 hrs at 37 °C. After this time the sample was denatured at 100 °C for 3 min and subsequently micro-centrifuged at (14,000 rpm / 5 min). The clear supernatant (100 μl) was used directly for HPLC analysis.

5.1.23.1 Step 2: Hydrophobic interaction chromatography (HIC)

The dissolved pellet (5 ml) was injected onto a 40 ml Phenyl sepharose HP column (Amersham Biosciences) equilibrated with 2 column volumes of phosphate buffer (50 mM, pH 6.8) containing 1 M $(NH_4)_2SO_4$. The column was washed with a further two column volumes of this buffer and subsequently eluted by applying a step wise gradient at 2 ml / min from 1 M to 0 M $(NH_4)_2SO_4$. PNP activity eluted at the end of the gradient which was collected manually (12 ml, ~0.5 mg / ml).

5.1.23.2 Step 3: Ion exchange chromatography (IEC)

The eluent (~12 ml) from HIC was concentrated to 2 ml using a 10 kDa Amicon^R Ultra-15 centrifugal concentrator. The concentrated protein was then subjected to desalting using a HiTrap^{TM} desalting column, (5 ml) and finally re-concentrated to ~2 ml by the same method. The concentrated protein sample (2 ml) was applied to an anion exchange column (Q, 5 ml sepharose) which was pre-equilibrated with five column volumes of tris buffer (50 mM, pH 7.2). The loaded protein sample was washed with two column volumes and subsequently eluted using a step wise gradient of tris buffer (50 mM, pH 7.2) containing 1 M KCl at a flow rate of 2 ml / min. The peak containing the activity eluted after a gradient elution of 250 mM KCl, ~8 ml (0.3 mg / ml).

5.1.24 Substrate specificity of PNP from *S. cattleya*

PNP substrate specificity was assayed as follows. Partially purified PNP (100 μl, 0.3 mg / ml) after step 3, anion exchange chromatography (see Section 5.1.23.2) was incubated with each nucleoside analogue (10 μl, 11 mM) (see Table 5.2) for 16 hrs at 37 °C.

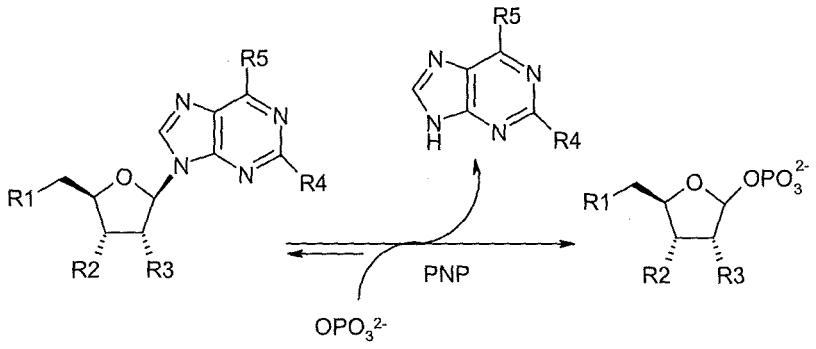

Nucleosides		R1	R2	R3	R4	R5	RT (min)	Substrate
*5'-fluoro-5'-deoxyadenosine	**54**	F	OH	OH	H	NH_2	10.1	+
5'-fluoro-5'-deoxyinosine	**55**	F	OH	OH	H	OH	7.5	-
*2,5 dideoxy-5'-fluoroadenosine	**59**	F	OH	H	H	NH_2	10.7	+
*2-amino-5'-fluoro-5'-deoxyadenosine	**91**	F	OH	OH	NH_2	NH_2	9.5	+
*5'-chloro-5'-deoxyadenosine	**88**	Cl	OH	OH	H	NH_2	12.7	+
*2,5-dideoxy-5'-chloroadenosine	**86**	Cl	OH	H	H	NH_2	13.8	+
2-chloroadenosine	**96**	OH	OH	OH	Cl	NH_2	12.1	+
*2-amino-5'-chloro-5'-deoxyadenosine	**97**	Cl	OH	OH	NH_2	NH_2	11.9	+
*5'-bromo-5'-deoxyadenosine	**89**	Br	OH	OH	H	NH_2	15.2	+
adenosine	**71**	OH	OH	OH	H	NH_2	7.4	+
2-deoxyadenosine	**87**	OH	OH	H	H	NH_2	7.8	+
*3'-deoxyadenosine	**99**	OH	H	OH	H	NH_2	8.2	-
*5'-deoxyadenosine	**90**	H	OH	OH	H	NH_2	9.6	+
*2',5'-dideoxyadenosine	**98**	OH	OH	H	H	NH_2	10.4	+
2-aminoadenosine	**94**	OH	OH	OH	NH_2	NH_2	7.0	+
2-amino-2-deoxyadenosine	**95**	OH	OH	H	NH_2	NH_2	7.7	+
adenosine monophosphate	**92**	OPO_3	OH	OH	H	NH_2	3.5	-
5'-thiomethyl-5'-deoxyadenosine	**76**	MeS	OH	OH	H	NH_2	15.0	+
*5'-acetyl-5'-deoxyademosine	**93**	OAc	OH	OH	H	NH_2	14.0	-
inosine	**72**	OH	OH	OH	H	OH	5.3	-

RT = average retention times (min) * Prepared by S. L. Cobb.[118]

Table 5.2 Substrate specificity of the PNP for various nucleoside analogues; (+) indicates a substrate and (-) indicates no detectable activity.

After this time the sample was denatured at 100 °C for 3 min and the precipitated protein removed by micro-centrifugation at (14,000 rpm / 5 min). An aliquot (20 μl) was

subjected to HPLC analysis. Table 2.1 shows a (+) sign indicating phosphorolytic cleavage with the generation of the "free" base. Co-injection experiments with the corresponding bases confirmed this unambiguously. A (-) sign indicates no enzyme activity.

Control experiments were carried out under analogous conditions using a denatured protein extract. This indicated that all compounds were stable and resistant to chemical degradation unless the PNP was active.

5.1.24.1 Reversibility of the PNP

Experiment 1: 5'-FDI **55** (18.5 mM) was incubated with immobilised PNP (2 mg resin) in a total volume of 1 ml containing phosphate buffer (50 mM, pH 6.8) for 16 hrs at 37 °C. After this time the sample was denatured at 100 °C for 3 min and the precipitated enzyme removed by micro-centrifugation (14,000 rpm / 5 min). The supernatant was analysed by ^{19}F NMR δ_F (470 MHz; 10 % D_2O) (5-FDRP **81**, ~40 %) -230.78 (dt, $^2J_{F,H}$ 47.3 and $^3J_{F,H}$ 28.3) and (5'-FDI **55,** ~60 %) -230.85 (dt, $^2J_{F,H}$ 47.0 and $^3J_{F,H}$ 28.9). HPLC analysis showed production of hypoxanthine **79** and unreacted 5'-FDI **55**.

Experiment 2: Partially purified PNP (100 μl, 0.3 mg / ml) from *S. cattleya* was supplemented with 5-FDRP **81** (100 μl) prepared from experiment 1 and incubated with each purine base (3.7 mM) for 16 hrs at 37 °C. After this time the sample was denatured at 100 °C for 3 min and the precipitated protein removed by micro-centrifugation (14,000 rpm / 5 min). An aliquot, (20 μl) of the supernatant was analysed by HPLC. Table 5.3 shows a (+) sign indicating the generation of a nucleoside analogue. Co-injection

experiments with the corresponding nucleoside confirmed this unambiguously. A (-) sign indicates no PNP activity.

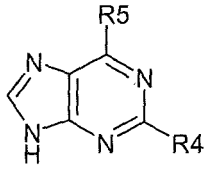

Purine bases		R4	R5	RT (min)	Substrate
adenine	**75**	H	NH_2	5.2	+
hypoxanthine	**81**	H	OH	3.8	-
6-methylpurine	**102**	H	CH_3	7.4	-
6-chloropurine	**103**	H	Cl	8.2	-
2-amino-6-purinethiol	**104**	NH_2	SH	5.6	-
2,6-diaminopurine	**101**	NH_2	NH_2	4.8	+
2-amino-6-chloropurine	**106**	NH_2	Cl	7.8	-
2,6-dichloropurine	**107**	Cl	Cl	17.8	-
purine	**105**	H	H	5.2	-

Table 5.3 Substrate specificity of the PNP from *S. cattleya* with 5-FDRP **81**.

5.1.24.2 Generation of SAM analogues using the fluorinase in the reverse direction

Preparation of 2-amino-SAM

Experiment 1: Partially purified PNP from *S. cattleya* (100 µl, 0.3 mg / ml) was incubated with 5-FDRP **81** (100 µl) and 2-aminoadenine **101** (final conc. 3.7 mM) for 16 hrs at 37 °C. After incubation the sample was heated (100 °C / 3 min) and the denatured protein removed by centrifugation (14,000 rpm / 15 min). HPLC analysis with a reference

compound indicated the production of 2-amino-5-FDA **111**. ES-MS also indicated the production of 2-amino-5'-FDA **111**; *m/z* 284 $(M + H)^+$.

Experiment 2: 2-amino-5-FDA **111** (100 μl) was incubated with the fluorinase (200 μl, 10 mg / ml) and L-methionine **56** (10 mM) at 37 °C for 16 hrs. The product was heated (100 °C / 3 min) and the denatured protein removed by centrifugation (14,000 rpm / 15 min). HPLC analysis indicated the production of a new compound with a retention time of 15.5 min. The compound was collected and lyophilised and the resultant powder dissolved in 1 ml of MeCN (1 ml) for ES-MS analysis; 2-amino-SAM **115**; *m/z* 414 $(M+H)^+$, 100 %) and 313 $(M + H, - C_4H_8NO_2)^+$.

5.1.25 Partial purification of an isomerase from *S. cattleya*

CFE (150 μl) was prepared according to Section 5.1.6 and ammonium sulfate precipitation was carried out as described in Section 5.1.18. The protein pellet 35-50 % was dissolved in phosphate buffer (50 mM, pH 6.8) supplemented with 1 M $(NH_4)_2SO_4$ in a total volume of 6 ml with a protein concentration of ~20 mg / ml. Prior to further purification the re-dissolved protein pellet was filtered through a 0.45 μm HT Tuffryn® membrane filter. Partially purified fractions (200 μl) were incubated with 5-FDRP **81** (100 μl) for 16 hrs at 37 °C to assay for isomerase activity. After this time the sample was denatured at 100 °C for 3 min and the precipitated protein removed by centrifugation (14,000 rpm / 5 min). The supernatant was retained and assayed by ^{19}F NMR for isomerase activity; δ_F (470 MHz, 10% D_2O), 5'-FDI **55** -230.84 (dt, $^2J_{F,H}$ 47.0 and $^3J_{F,H}$ 28.9), 5-FDRP **81** -230.77 (dt, $^2J_{F,H}$ 47.3 and $^3J_{F,H}$ 28.3) and 5-FDRibP **121** -231.32 (dt, $^2J_{F,H}$ 47.0 and $^3J_{F,H}$ 20.7).

5.1.25.1 Step 2: Hydrophobic interaction chromatography (HIC)

The dissolved protein pellet (6 ml) was injected onto a 40 ml Phenyl sepharose HP column equilibrated with 2 column volumes of phosphate buffer (50 mM, pH 6.8) containing 1 M $(NH_4)_2SO_4$. The column was washed with a further two column volumes and subsequently eluted by applying a step wise gradient at 2 ml / min from 1 M to 0 M $(NH_4)_2SO_4$. The isomerase eluted at the end of the gradient adjacent to the PNP fraction (Section 5.1.23.1) and was collected manually (12 ml, 1.3 mg / ml).

5.1.25.2 Step 3: Size exclusion chromatography

The eluent (~ 12 ml) from the Phenyl sepharose HP column was concentrated to 2 ml using a 10 kDa Amicon® Ultra-15 centrifugal concentrator. The concentrated protein was loaded onto a 16/60 Superdex 200 gel filtration column equilibrated with tris buffer (50 mM, pH 7.2) supplemented with 0.3 M KCl at a constant flow rate of 1 ml / min. Protein elution was carried out isocratically over 180 ml. Isomerase activity eluted between 72-80 ml with a protein concentration of 0.5 mg / ml.

5.1.25.3 Step 4: Ion exchange chromatography (IEC)

The eluent (8 ml) from the size exclusion column was concentrated to 2 ml using a 10 kDa Amicon® Ultra-15 centrifugal concentrator. The concentrated protein was then desalted using a HiTrap™ desalting column (5 ml) to remove KCl. The sample was then re-concentrated to ~2 ml by the same method.

The concentrated protein sample (2 ml) was applied to an anion exchange column (Q, 5 ml sepharose) which was pre-equilibrated with five column volumes of tris buffer (50 mM,

pH 7.2). The loaded protein sample was washed with two column volumes and subsequently eluted using a step wise gradient of tris buffer (50 mM, pH 7.2) containing 1 M KCl at a flow rate of 2 ml / min. The peak containing isomerase activity eluted after a gradient of 250 mM KCl with a total protein concentration of 1.5 mg / ml.

5.1.26 Purification of fructose-1,6-bisphosphate aldolase

Cell-free extract (150 ml) was prepared as described under Section 5.1.6 and ammonium sulfate precipitation was carried out as described under Section 5.1.18. The protein pellet (60-80 %) was dissolved in phosphate buffer (50 mM, pH 6.8) containing 1 M $(NH_4)_2SO_4$. Prior to further purification the re-suspended protein pellet was filtered through a 0.45 μm HT Tuffryn® membrane filter. Aldolase activity was assayed according to the following procedure. The partially purified aldolase fractions (200 μl) were incubated with fluoroacetaldehyde **48** (30 μl, 20 mM) and DHAP **123** (70 μl, 10 mM) with the addition of Zn^{2+} (1 mM) for 16 hrs at 37 °C. After this time the protein was denatured at 100 °C for 3 min and the precipitate removed by centrifugation (14,000 rpm / 5 min). Analysis by ^{19}F NMR showed; δ_F (470 MHz, 10 % D_2O), fluoroacetaldehyde **48**, -231.05 (dt, $^2J_{F,H}$ 46.5 and $^3J_{F,H}$ 9.8), fluoroethanol **69** -224.51, 5-FDXyuP **126**, -228.18 (dt, $^2J_{F,H}$ 46.5 and $^3J_{F,H}$ 15.3).

5.1.26.1 Step 2: Hydrophobic interaction chromatography

The dissolved pellet (5 ml, 12 mg / ml) from Section 5.1.26 was injected directly onto a 40 ml Phenyl sepharose HP column equilibrated with phosphate buffer (50 mM, pH 6.8) containing 1 M $(NH_4)_2SO_4$. The column was washed with two column volumes of the

same buffer and was then loaded with the re-suspended protein pellet in duplicates. The column was washed with phosphate buffer (40 ml, 50 mM pH 6.8) containing 1 M $(NH_4)_2SO_4$. and eluted using a stepwise gradient over 80 ml at a flow rate of 2 ml / min from 1 M to 0 M $(NH_4)_2SO_4$. The aldolase eluted after 70 % of phosphate buffer containing 1 M $(NH_4)_2SO_4$.

5.1.26.2 Step 3: Size exclusion chromatography

The eluent (~ 14 ml) from a Phenyl sepharose HP column was concentrated to 2 ml using a 10 kDa Amicon® Ultra-15 centrifugal concentrator. The concentrated protein was loaded onto a 16/60 Superdex 200 gel filtration column equilibrated with phosphate buffer (50 mM, pH 6.8) at a flow rate of 1 ml / min. Protein elution was carried out isocratically over 180 ml. The aldolase was shown to elute between 62-72 ml with an average protein concentration of 0.5 mg / ml.

5.1.26.3 Step 4: Ion exchange chromatography (IEC)

The eluent (~16 ml) from size exclusion chromatography was concentrated to 2 ml using a 10 kDa Amicon® Ultra-15 centrifugal concentrator. The concentrated protein sample was applied to a 10 ml source 15 Q column which was equilibrated with tris buffer (50 mM, pH 7.2). The loaded protein sample was washed with 20 ml of the same buffer at 2 ml / min. Elution of the enzyme was carried out over a linear gradient to 1 M KCl. The desired protein eluted after 300 mM KCl addition, and the final protein concentration of the purified protein was 2 ml, 0.2 mg / ml.

5.1.26.4 Effect of various metal ions on class II L-FruA activity

After ammonium sulfate precipitation the partially purified L-FruA (6 ml, 15 mg / ml) was incubated with EDTA (final conc. 10 mM) for 20 min at 4 °C. The sample was then dialysed using dialysis tubing (MW 10 kDa cut off) against 4 L of phosphate buffer (50 mM, pH 6.8) overnight at 4 °C. The dialysed sample was assayed against the following divalent metal ions Zn^{2+}, Mg^{2+}, Mn^{2+}, Co^{2+}, Ni^{2+}, Fe^{2+}, Ca^{2+} and monovalent metal ions, Na^{+}. Accordingly, partially purified aldolase (100 μl, 1.5 mg / ml) was incubated with fluoroacetaldehyde **48** (30 μl, 20 mM) and DHAP **123** (70 μl, 10 mM) in the presence of each metal ion (final conc. 1 mM) for 16 hrs at 37 °C. After this time the sample was denatured at 100 °C for 3 min and was subsequently centrifuged (14,000 rpm / 5 min). The supernatant was supplemented with D_2O (100 μl) and analysed by ^{19}F NMR spectroscopy.

5.1.27 Purine nucleoside phosphorylase (PNP) overexpression and purification

5.1.27.1 Expression vector

The pET28a(+) construct (supplied by Dr Joe Spencer, University of Cambridge), carries an N-terminal His Tag® / thrombin / T7 Tag® configuration plus an optional C-terminal His Tag sequence. It also encodes a gene for kanamycin resistance. As with all pET expression systems, target gene expression is induced by IPTG via a T7 promoter. The presence of this promoter requires a T7 RNA polymerase whose expression is induced by IPTG (Figure 5.3).

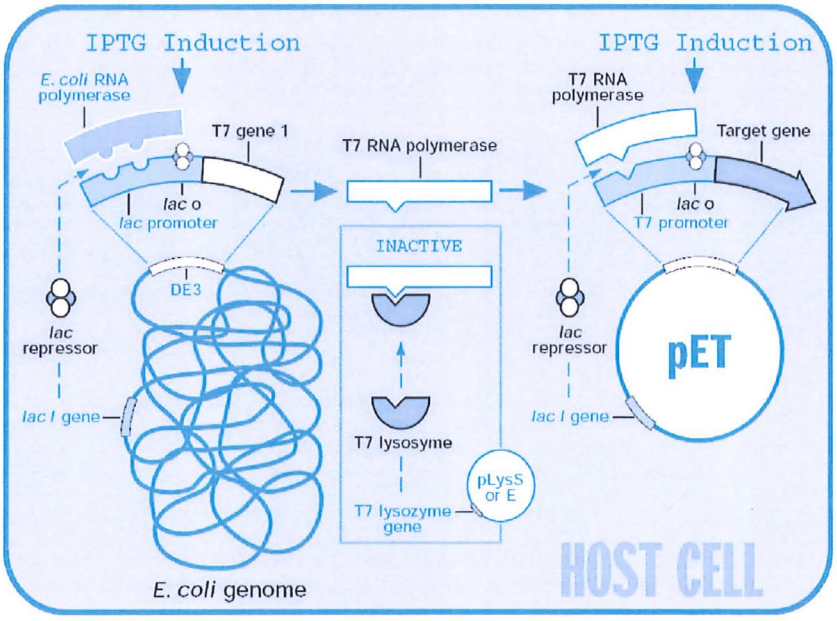

Figure 5.3 Protein expression from pET vectors (taken from Novagen catalogue 2002-2003, p. 88).

5.1.27.2 Transformation of competent cells with pET28a(+) construct

Chemically competent *E. coli* cells were purchased from invitrogen. The competent cells were in vials containing 50 µl aliquots. To transform these cells, each 50 µl aliquot was placed on ice and allowed to thaw for 2-5 min, while gently mixing to evenly re-suspend the cells. After thawing, addition of 1 µl (200 ng) of plasmid DNA was added directly to each aliquot, stirring gently and returning the vial on ice. The vial was incubated for a further 5 min. Heat shock was performed by heating the vials for exactly 30 sec in a 42 °C water bath. The vials were then placed on ice for 2 min. SOC medium (250 µl) was added to each vial on ice. The vials were then incubated at 37 °C while shaking at 250 rpm for 60 min. An aliquot (60 µl) of the transformed cells was added to the agar plates containing the antibiotic kanamycin, and evenly distributed using a plate spreader. (Note: Prior to spreading, the agar plates were pre-incubated at 37 °C). The plates were then incubated at 37 °C for 16 hrs.

5.1.27.3 Expression of *flB* and purification of FlB

(a) Expression trials

Single colonies were picked and grown up in LB (10 ml) containing 50 μg / ml of kanamycin at 37 °C for ~16 hrs on an orbital shaker (200 rpm). After this time, aliquots (100 μl) were used to inoculate fresh growth media (10 ml) for the over-expression trials. The fresh inoculated LB containing kanamycin was incubated at 37 °C for a further 4 hrs. Once the cell density reached OD_{600} = 0.6, expression was induced with IPTG. The following variables were altered to optimise expression of soluble PNP from the pET 28a(+) construct.

Temperature	30 °C, 25 °C, 18 °C, 16 °C, 12 °C and 10 °C.
Growth Media	Luria-Bertani, Tryptone phosphate, Terrific Broth and Overnight Express™ Autoinduction System 1 (Novogen).
Host strain	BL21(DE3), BL21Star™, BL21(DE3)pLysS, BL21(DE3)pLysE, Rosetta(DE3) and C43(DE3).
IPTG conc.	0.1 mM, 0.2 mM, 0.4 mM, 0.6 mM, 0.8 mM and 1 mM.
Expression times	1-42 hrs.

For each expression trial, samples (1 ml) were taken at various intervals for analysis. Cells were harvested by centrifugation (14,000 rpm / 5 min) and the resulting pellet was re-suspended in tris buffer (1 ml, 50 mM, pH 6.8) and the re-suspended cells were then lysed by sonication at 60 cycles for 20 sec. After sonication, the cells were centrifuged (14,000 rpm / 20 min) and the resultant cell pellet and the supernatant were retained as the insoluble and soluble fractions respectively for SDS-PAGE analysis.

(b) Large scale expression of flB

Single colonies were picked and grown up in LB (30 ml) containing 50 μg / ml kanamycin at 37 °C for ~16 hrs on an orbital shaker (200 rpm). After this time, aliquots (5 ml) were used to inoculate fresh LB medium (500 ml) using 6 x 2 L baffled flasks. The inoculated flasks were incubated at 37 °C for 4-6 hours on an orbital shaker (200 rpm) at or until an $O.D_{600}$ = 0.6 was reached. After this time the flasks were placed on ice for several minutes with subsequent addition of IPTG (final conc. 0.2 mM) to each flask. The flasks were then incubated at 10 °C for 30-36 hrs. After this time the cells were harvested by centrifugation (9,000 rpm / 20 min) and the resulting pellet was either stored at -80 °C or used directly for protein purification.

(c) Purification of flB

Cells (0.1 g) were resuspended in 1 ml of buffer A consisting of tris buffer (50 mM, pH 6.8) supplemented with 10 mM imidazole. The resulting solution was left to stir for 30 min at 4 °C. After this time, cells were disrupted by sonication, ten times at 60 % duty cycle for 60 seconds depending on the volume. Cell debris was removed by centrifugation at (9,100 rpm / 25 min) and the clear supernatant was retained as cell-free extract (CFE). Purification was carried out on a $NiSO_4$ charged resin on a fast flow sepharose column using the following buffers.

Buffer **A**	Buffer **B**	Buffer **C**
0.3 M NaCl	0.3 M NaCl	0.3 M NaCl
10 mM imidazole	30 mM imidazole	250 mM imidazole
20 mM tris pH 7.5	20 mM tris pH 7.5	20 mM tris pH 7.5

The sample was loaded onto the column at a constant flow rate of 1 ml / min pre-equilbrated with buffer **A**. After this time the column was washed with several column volumes of Buffer **B** to remove any undesired proteins. The desired protein was then eluted by applying Buffer **C**.

5.1.28 L-Fuculose-1-phosphate aldolase (L-FucA) over-expression and purification

.Expression

The following protocol was prepared by Dr Hai Deng, University of St Andrews. The pTrcHis C plasmid containing the fuculose-1-phosphate aldolase gene was purchased as a transformed *E. coli* stock (LGC Promochem). Gene expression was achieved by addition of cell stock (20 μl) containing 50 % glycerol to LB (20 ml) containing 0.05 % (100 mg / ml) ampicillin and incubated at 37 ^{o}C for 16 hrs. Aliquots (2.5 ml) were transferred to each 6 x 2 L flasks containing LB (750 ml) and incubate at 37 ^{o}C for 4 hours or until an O.D 0.6 was reached. After this time the cells were harvested by centrifugation at 9,100 rpm / 20 min, the supernatant discarded and the cell pellet was either stored at -80 ^{o}C or used directly for further protein purification.

Purification

Cells (0.1 g) were resuspended in Buffer A containing tris buffer (1 ml, 50 mM, pH 6.8) supplemented with 10 mM imidazole and stirred for 30 min at 4 ^{o}C. After this time the solution was sonicated six times at 60 cycles for one minute each. The cell debris was

removed by centrifugation at (9,100 rpm / 25 min) and the supernatant retained as a CFE. Purification was carried out on a $NiSO_4$ charged resin, fast flow sepharose column using the following buffers.

Buffer **A**	Buffer **B**	Buffer **C**
0.3 M NaCl	0.3 M NaCl	0.3 M NaCl
10 mM imidazole	30 mM imidazole	250 mM imidazole
20 mM tris pH 7.5	20 mM tris pH 7.5	20 mM tris pH 7.5

The column was first pre-equilibrated with several column volumes of Buffer **A** at a constant flow rate of 2 ml / min. After this time the protein sample was loaded onto the column and was washed with several column volumes of Buffer A to remove endogenous proteins. Elution with Buffer **B** for a further 4 column volumes was followed by elution with buffer **C** (Figure 5.1).

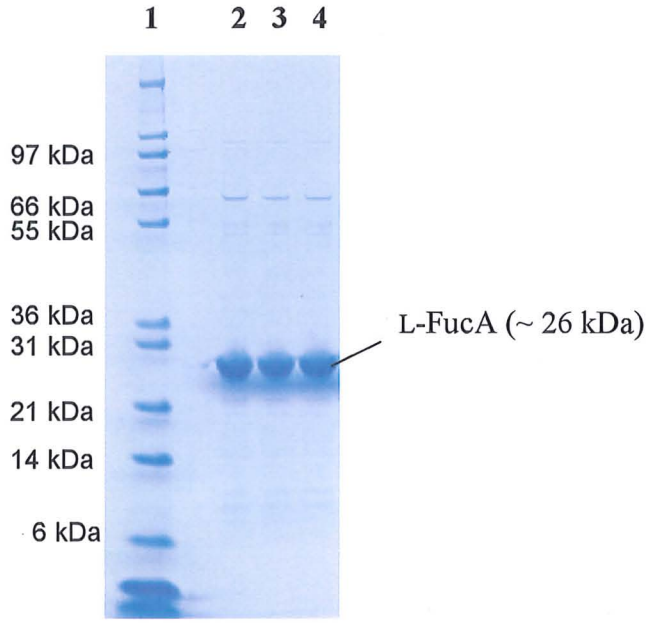

Figure 5.1 SDS PAGE gel analysis of L-FucA after nickel purification. Lanes **1**; SDS markers, (Mark 12 ™ standards, Invitrogen life technologies) used consisted of, myosin [200 kDa], β-galactosidase [116 kDa], phosphorylase B [97.4 kDa], BSA [66 kDa], glutamic dehydrogenase [55 kDa], lactate dehydrogenase [36.5 kDa], carbonic anhydrase [31 kDa], trypsin inhibitor [21.5 kDa], lysozyme [14.4 kDa], aprotinin [6 kDa], **2-4**, L-FucA after purification via Ni-NTA affinity chromatography.

References

1. J. R. Hanson, "*Natural Products, the Secondary Metabolites*", 1st Ed., Royal Society of Chemistry, 2003, pp 2.
2. Alan Crozier, "*Plant Secondary Metabolites in Diet and Health*", 1st Ed., Blackwell publishing, 2006, pp 1.
3. A. Rahman and P. L. Quesne, Ed., "*Natural Products Chemistry*," Vol. 3, Springer Verlag, Berlin, 1988, pp 10.
4. M. C. Wani, H. L. Taylor, M. E. Wall, P. Coggin and A. T. McPhail, *J. Am. Chem. Soc.*, 1971, **93**, 2325.
5. M. E. Wall and M. C. Wani, *Cancer Res.*, 1995, **55**, 753.
6. E. Van Geldre, A. Vergauwe and E. Van der Eeckhout, *Plant Mol. Biol.*, 1997, **33**, 199.
7. M. Hayashi, *Folia Pharmacol. Japon*, 1977, **73**, 205.
8. G. W. Gribble, *J. Chem. Educ.*, 2004, **81**, 1441.
9. M. Sancelme, S. Fabre and M. Prudhomme, *J. Antibiotics*, 1994, **47**, 792.
10. Y. Kan, B. Sakamoto, T. Fujita and H. Nagai, *J. Nat. Prod.*, 2000, **63**, 1599.
11. N. Sitachitta, B. L. Marquez, R. T. Williamson, J. Rossi, M. A. Roberts, W. H. Gerwick, V. A. Nguyen and C. L. Wills, *Tetrahedron*, 2000, **56**, 9103.
12. M. Sanada, T. Miyano, S. Iwadare, J. M. Williamson, B. H. Arison, J. L. Smith, A. W. Douglas, J. M. Liesch and E. Inamine, *J. Antibiotics*, 1986, **39**, 259.
13. R. S. Beissner, W. J. Guilford, R. M. Coates and L. P. Hager, *Biochemistry*, 1981, **20**, 3724.
14. P. Messerschmidt, L. Prade and R. Wever, *Biol. Chem.*, 1997, **378**, 309.

15. M. Sundaramoorthy, J. Terner and T. L. Poulos, *Chem. Biol.*, 1998, **5**, 461.

16. P. D. Shaw and L. P. Hager, *J. Biol. Chem.*, 1959, **234**, 2565.

17. L. P. Hager, D. R. Morris, F. S. Brown and H. Eberwein, *J. Biol. Chem.*, 1966, **241,** 1769.

18. S. L. Neidleman and J. Geigert, "*Biohalogenation: Principles, Basic roles and Applications*," 1986, p 46, Chicester: Ellis Horwood.

19. H. Vilter, *Phytochemistry*, 1984, **23**, 1387.

20. M. Almeida, S. Filipe, M. Humanes, M. F. Maia, R. Melo, N. Severino, J. A. L. da Silva, J. J. R. F. da Silva and R. Wever, *Phytochemistry*, 2001, **57**, 633.

21. K.-H. van Peé, *Ann. Rev. Microbiol.*, 1996, **50**, 375.

22. M. Picard, J. Gross, E. Lubbert, S. Tolzer, S. Krauss, K.-H. van Peé and A. Berkessel, *Angew. Chem. Int. Ed.*, 1997, **36**, 1196.

23. B. Hofmann, S. Tolzer, I. Pelletier, J. Altenbuchner, K. –H. van Peé and H. J. Hecht, *J. Mol. Biol.*, 1998, **279**, 889.

24. T. Dairi, T. Nakano, K. Aisaka, R. Katsumata and M. Hasegawa, *Biosci. Biotech. Biochem.*, 1995, **59**, 1099.

25. S. Kirner, P. E. Hammer, D. S. Hill, A. Altmann, I. Weislo, L. J. Lanahan, K. –H. van Peé and J. M. Ligon, *J. Bacteriol.*, 1998, **180**, 1939.

26. D. H. Williams and B. Bardsley, *Angew. Chem. Int. Ed.*, 1999, **38**, 1172.

27. J. Ahlert, E. Shepard, N. Lomovskaya, E. Zazopoulos, A. Staffa, B. O. Bachmann, K. Huang, L. Fonstein, A. Czisny, R. E. Whitwam, C. M. Farnet and J. S. Thorson, *Science*, 2002, **297**, 1173.

28. O. Puk, P. Huber, D. Bischoff, J. Recktenwald, G. Jung, R. D. Submuth, K. –H. van Peé, W. Wohlleben and S. Pelzer, *Chem. Biol.*, 2002, **9**, 225.

29. P. C. Dorrestein, E. Yeh, S. Garneau-Tsodikova, N. L. Kelleher and C. T. Walsh,

Proc. Natl. Acad. Sci. U.S.A., 2005, **102**, 13843.

30. S. Keller, T. Wage, K. Hohaus, M. Holzer, E. Eichhorn and K.-H. van Peé, *Angew. Chem. Int. Ed.*, 2000, **39**, 2300.

31. D. M. Zeigler, *Drug Metab. Rev.*, 2002, **34**, 503.

32. C. J. Dong, S. Flecks, S. Unversucht, C. Haupt, K.-H. van Peé and J. H. Naismith, *Science*, **309**, 2216.

33. E. Yeh, S. Garneau and C. T. Walsh, *Proc. Natl. Acad. Sci.* U.S.A., 2005, **102**, 3960.

34. C. Sanchez, I. A. Butovich, A. F. Brana, J. Rohr, C. Mendez and J. A. Salas, *Chem. Biol.*, 2002, **9**, 519.

35. J. Hartung, *Angew. Chem. Int. Ed.*, 1999, **38**, 1209.

36. F. H. Vaillancourt, J. Yin and C. T. Walsh, *Proc. Natl. Acad. Sci.* U.S.A., 2005, **102**, 10111.

37. F. H. Vaillancourt, E. Yeh, D. A. Vosburg, S. E. O'Connor and C. T. Walsh, *Nature*, **436**, 1191.

38. E. L. Hegg and L. Jr Que, *Eur. J. Biochem.*, 1997, **250**, 625.

39. K. D. Koehntop, J. P. Emerson and L. Jr Que, *J. Biol. Inorg. Chem.*, 2005, **10**, 87.

40. J. C. Price, E. W. Barr, B. Tirupati, J. M. Jr. Bollinger and C. Krebs, *Biochemistry*, 2003, **42**, 7497.

41. J. U. Rohde, J.–H. In, M. H. Lim, W. W. Brennessel, M. R. Bukowski, A. Stubna, E. Munck, W. Nam and L. Que Jr, *Science*, 2003, **299**, 1037.

42. H. J. M. Bowen, '*Trace elements in biochemistry*', Academic Press, London and New York, 1966, p 10.

43. E. A. Paul and P. M. Huang, in '*Hand book of environmental chemistry*', Vol 1, part A, Springer Verlag, Berlin, 1980, p 69.

44. B. E. Smart, *'Molecular structure and energetics'*, Ed., J. L. Leibman and A. Greenberg, VCH Publishers Inc., Deerfield Park, Florida, 1986, Vol 3, p. 141.

45. C. Walsh, *Adv. in Enzymology*, 1982, **55**, 197.

46. J. S. C Marais, *Onderstepoort J. Vet. Sci. Anim. Ind.*, 1943, **18**, 203.

47. J. S. C Marais, *Onderstepoort J. Vet. Sci. Anim. Ind.*, 1944, **20**, 67.

48. B. Vickery, M. L. Vickery and J. T. Ashu, *Phytochemistry*, 1973, **12**, 145.

49. D. O'Hagan, R. Perry, J. M. Lock, J. J. M. Meyer, L. Dasaradhi, J. T. G. Hamilton and D. B. Harper, *Phytochemistry*, 1993, **33**, 1043.

50. B. Vickery and M. L. Vickery, *Phytochemistry,* 1972, **11**, 1905.

51. R. A. Peters, R. W. Wakelin, P. Buffa and L. C. Thomas, *Proc. Roy. Soc. B*, 1953, **40**, 497.

52. C. J. Lovelace, G. W. Miller and G. W. Welkie, *Atmos. Environ.*, 1968, **2**, 187.

53. M. H. Yu and G. W. Miller, *Environ. Sci. Technol.*, 1970, **4**, 492.

54. H. Luable, M. C Kennedy, M. H Emptage, H. Beinert and C. D. Stout, *Proc. Natl. Acad. Sci.* U.S.A., 1996, **93**, 13699.

55. E. Kun, E. Kirsten and M. L. Sharma, *Dev. Bioener. Biomemb.*, 1978, **2**, 285.

56. R. A. Peters and M. Shorthouse, *Nature*, 1967, **216**, 80.

57. R. A. Peters and M. Shorthouse, *Nature*, 1971, **231**, 123.

58. R. A. Peters and R. J. Hall, *Biochem. Pharmacol.*, 1959, **2**, 25.

59. P. F. V. Ward, R. J. Hall and R. A. Peters, *Nature*, 1964, **201**, 611.

60 R. A. Peters, R. J. Hall, P. F. V. Ward and N. Sheppard, *Biochem. J.*, 1960, **77**, 17.

61. J. T. G. Hamilton and D. B. Harper, *Phytochemistry*, 1997, **44**, 1129.

62. T. Higa, J. Tanaka, A. Kitamura, T. Koyama, M. Takahashi and T. Uchia, *Pure Appl. Chem.*, 1994, **66**, 2227.

63. X.-H. Xu, G.-M. Yao, Y.-M. Li, J.-H. Lu, C.-J. Lin, X. Wang and C-H. Kong, *J. Nat. Prod.*, 2003, **66**, 285.

64. D. Robert, P. Edward and H. Charle, *J. Am. Chem. Soc.*, 1957, **79**, 4559.

65. S. Ozaki, Y. Watanabe, T. Hoshiko, H. Mizuno, K. Ishirawa and H. Mori, *Chem. Pharm. Bull.*, 1984, **32**, 733.

66. R. Ignoffo, *J. Am. Health-Syst. Pharm.*, 1999, **56**, 2417.

67. S. O. Thomas, V. L. Singleton, J. A. Lowery, R. W. Sharpe, L. M. Pruess, J. N. Porter, J. H. Mowat and N. Bohonas, *Antibiotics Ann.*, 1957, 716.

68. C. W. Waller, J. B. Patrick, W. Fulmor and W. E. Meyer, *J. Am. Chem. Soc.*, 1957 **79**, 1011.

69. G. O. Morton, J. E. Lancaster, G. E. Van Lear, W. Fulmor and W. E. Meyer, *J. Am. Chem. Soc.*, 1969, **91**, 1535.

70. I. D. Jenkins, J. P. H. Verheyden and J. G. Moffatt, *J. Am. Chem. Soc.,* 1976, **98**, 3346.

71. A. R. Maguire, W.-d. Meng, S. M. Roberts and A. J. Willetts, *J. Chem. Soc., Perkin Trans.*, **1**, 1993, 1795.

72. J. M. Williamson, E. Inamine, K. E. Wilson, A. W. Douglas, J. M. Liesch and G. Albers-Schonberg, *J. Biol. Chem.*, 1985, **260**, 4637.

73. G. Albers-Schonberg, B. H. Arison, O. D. Hensens, J. Hirshfield, K. Hoogsteen, E. A. Kaczka, R. E. Rhode, J. S. Kahan, F. M. Kahan, R. W. Ratcliffe, E. Wilson, L. J. Ruswinkle, R. B. Morin and B. G. Christensen, *J. Am. Chem. Soc.*, 1978, **100**, 6491.

74. R. Schoenheimer and D. Rittenberg, *J. Biol. Chem.*, 1935, **111**, 163.

75. D. B Cowie, E. T Bolton and N. K Sands, *J. Bacteriol.,* 1950, **60**, 233.

76. Roberts, R. B., P. H. Abelson, D. B. Cowie, E. T. Bolton, and R. J. Britten, 1955 Carnegie Inst. Wash. Publ. 607, Washington, D.C.

77. J. T. G. Hamilton, C. D. Murphy, A. R. Muhammad, D. O'Hagan and D. B. Harper, *J. Chem. Soc., Perkin Trans.,* **1**, 1998, 759.

78. K. A. Reid, J. T. G. Hamilton, R. D. Bowden, D. O'Hagan, L. Dasaradhi, M. R. Amin and D. B. Harper, *Microbiology*, 1995, **141**, 1385.

79. S. J. Moss, C. D. Murphy, J. T. G. Hamilton, W. C. McRoberts, D. O'Hagan, C. Schaffrath and D. B. Harper, *Chem. Commun.*, 2000, 2281.

80. C. D. Murphy, S. J. Moss and D. O'Hagan, *Appl. Environ. Microbiol.*, 2001, **67**, 4919.

81. C. D. Murphy, C. Schaffrath and D. O'Hagan, *Chemosphere,* 2003, **52**, 455.

82. C. D. Murphy, D. O'Hagan and C. Schaffrath, *Angew. Chem. Int. Ed.*, 2001, **40**, 4479.

83. I. Grgurina and F. Mariotti, *FEBS Lett.*, 1999, **462**, 151.

84. A. M. Wuosmaa and L. P. Hager, *Science*, 1990, **249**, 160.

85. D. L. Zechel, S. P. Reid, O. Nashiru, C. Mayer, D. Stoll, D. L. Jakeman, R. A. J. Warren and S. G. Withers, *J. Am. Chem. Soc.*, 2001, **123**, 4350.

86. C. Schaffrath, PhD thesis, '*Biosynthesis and enzymology of fluorometabolite production in Streptomyces cattleya*', University of St Andrews, 2002.

87. M. Flavin, H. Castro-Mendoza and S. Ochoa, *J. Biol. Chem.*, 1957, **229**, 981.

88. T. C. Chou and P. Talalay, *Biochemistry*, 1972, **11,** 1065.

89. C. Schaffrath, S. L. Cobb and D. O'Hagan, *Angew. Chem. Int. Ed.*, 2002, **41**, 3913.

90. S. L. Cobb, H. Deng, J. T. G. Hamilton, R. P. McGlinchey, D. O'Hagan and C. Schaffrath, *Bioorg. Chem.*, 2005, **33**, 393.

91. D. O'Hagan, C. Schaffrath, S. L. Cobb, J. T. G. Hamilton and C. D. Murphy, *Nature*, 2002, **416**, 279.

92. C. Schaffrath, H. Deng and D. O'Hagan, *FEBS Lett.*, 2003, **547**, 111.

93. C. J. Dong, F. Huang, H. Deng, C. Schaffrath, J. B. Spencer, D. O'Hagan and J. H. Naismith, *Nature*, 2004, **427**, 561.

94. A. M. Reeve, S. D. Breazeale and C. A. Townsend, *J. Biol. Chem.*, 1998, **273**, 30695.

95. A. K. Ghosh and Y. Wang, *J. Chem. Soc., Perkin Trans.* 1, 1999, 3597.

96. C. J. Dong, H. Deng, M. Dorward, C. Schaffrath, D. O'Hagan and J. H. Naismith, *Acta Crystallogr., Sect D: Biol. Crystallogr.*, 2003, **60**, 760.

97. D. O'Hagan, R. J. M. Goss, A. Meddour and J. Courtieu, *J. Am. Chem. Soc.*, 2003, **125**, 379.

98. C. D. Cadicamo, J. Courtieu, H. Deng, A. Meddour and D. O'Hagan, *ChemBioChem*, 2004, **5**, 685.

99. H. M. Senn, D. O'Hagan and W. Thiel, *J. Am. Chem. Soc.*, 2005, **127**, 13643.

100. H. Deng, S. L. Cobb, A. McEwan, R. P. McGlinchey, J. H. Naismith, D. O'Hagan, D. A. Robinson and J. B. Spencer, *Angew. Chem. Int. Ed.*, 2005 (in press).

101. M. M. Goodman. Automated Synthesis of Radiotracers for Positron Emission Tomography Applications, *Clinical Positron Emission Tomography (PET)*, K. F. Hubner, E. Buonocore, J. Collmann and G. W. Kabalka (Eds). Mosby-Year Book, Inc., St. Louis, MO, 1991; p110.

102. M. R. Kilbourn. *Fluorine-18 labelling of Radiopharmaceuticals*, National Academy Press: Washington, DC, 1990.

103. C. G. Kim, D. J. Yang, E. E. Kim, A. Chrif, L. R. Kuang, C. Li, W. Tansey, C. W. Lui, S. C. Li, S. Wallace and D. A. Podoloff, *J. Pharmaceutical Sci.*, 1996, **85**, 339.

104. Sz Lehel, G. Horvath, I. Boros, T. Marian and L. Tron, *J. Radioanalyst Nucl. Chem.*, 2002, **245**, 399.

105. L. Martarello, C. Schaffrath, H. Deng, A. D. Gee, A. Lockhart and D. O'Hagan, *J. Label Compd. Radiopharm.*, 2003, **46**, 1181.

106. S. L. Cobb, H. Deng, J. T. G. Hamilton, R. P. McGlinchey and D. O'Hagan, *Chem. Commun.*, 2004, 592.

107. H. G. E. Lloyd, A. Deussen, H. Wuppermann and J. Schrader, *Biochem. J.*, 1988, **252**, 489.

108. J. Barankiewiez and A. Cohen, *J. Biol. Chem.*, 1984, **259**, 15178.

109. J. L. Palmer and R. H. Abeles, *J. Biol. Chem.*, 1979, **254**, 1217.

110. I. I. Mathews, M. D. Erion and S. E. Ealick, *Biochemistry,* 1998, **37**, 15607.

111. M. J. Pugmire and S. E. Ealick, *Biochem. J.*, 2002, **361**, 1.

112. M. D. Erion, K. Takabayashi, H. B. Smith, J. Kessi, S. Wagner, S. Honger, S. L. Shames and S. E. Ealick, *Biochemistry*, 1997, **36**, 11725.

113. A. Sekowska and A. Danchin, *BMC Microbiology,* 2002, **2**, 8.

114. E. S. Furfine and R. H. Abeles, *J. Biol. Chem.*, 1988, **263**, 9598.

115. A. Sekowska, V. Denervaud, H. Ashida, K. Michoud, D. Haas, A. Yokota and A. Danchin, *BMC Microbiology*, 2004, **4**, 9.

116. J. D. Z. Feng and P. K. F. Yeung, *Therap. Drug Monit.*, 2000, **22**, 177.

117. E. Sottofattori, M. Anzaldi and L. O. T. Tonello, *J. Pharm. Biomed. Anal.*, 2001, **24**, 1143.

118. S. L. Cobb, Ph.D thesis, '*The origin and metabolism of 5'-FDA in Streptomyces cattleya*, University of St Andrews, 2004.

119. Q. Zhang and H.-W. Liu, *Bioorg. Med. Chem. Lett.*, 2001, **11**, 145.

120. E. M. Bennett, C. Li, P. W. Allen, W. B. Parker and S. E. Ealick, *J. Biol. Chem*, 2003, **278**, 47110.

121. J. Neuhard, *Utilization of performed pyrimidine bases and nucleosides. In metabolism of nucleotides, nucleosides, and nucleobases in microorganisms.* (A. Munch-Peterson, Ed.), 1983, pp. 95, Academic Press, London.

122. P. Nygaard, *Utilization of performed pyrimidine bases and nucleosides. In metabolism of nucleotides, nucleosides, and nucleobases in microorganisms.* (A. Munch-Peterson, Ed.), 1983, pp. 27, Academic Press, London.

123. C. Seeger, C. Poulsen and G. Dandanell, *J. Bacteriol.*, 1995, **177**, 5506.

124. S. Senesi, G. Falcone, U. Mura, F. Sgarrella and P. L. Ipata, *FEBS Lett.*,1976, **64**, 353.

125. N. Hori, M. Watanabe, Y. Yamazaki and Y. Nmikami, *Agric. Biol.*, 1989, **53**, 3219.

126. T. A. Krenitsky, J. W. Mellors and R. K. Barclay, *J. Biol. Chem*, 1965, **240**, 1281.

127. G. Cacciapuoti, M. Porcelli, C. Bertoldo, M. De Rosa and V. Zappia, *J. Biol. Chem.*, 1994, **269**, 24762.

128. F. D. Ragione, A. Oliva, V. Gragnaniello, G. L. Russo, R. Palumbo and V. Zappia, *J. Biol. Chem*, 1990, **265**, 6241.

129. A. J. Ferro, N. C. Wrobel and J. A. Nicolette, *Biochim. Biophys. Acta*, 1979, **570**, 65.

130. T. A. Krenitsky, G. W. Koszalka and J. V. Tuttle, 1981, *Biochemistry*, **20**, 3615.

131. A. Bzowska, E. Kulikowska and D. Shugar, *Z. Naturforsh.*, 1990, **45**, 59.

132. R. E. Parks Jr. and R. P. Agarwal, *The Enzymes,* 3rd Ed., (P. D. Boyer, ed.), 1972, Vol 7, pp 483, Academic Press, Inc., New York.

133. K. Fabianowska-Majewska, J. Duley, L. Fairbanks, A. Simmonds and T. Wasiak, *Acta Biochim Pol.*, 1994, **41**, 391.

134. V. Zappia, A. Oliva, G. Cacciapuoti, P. Galletti, G. Mignucci and M. Carteni-Farina, *Biochem. J.*, 1978, **175**, 1043.

135. T. M. Savarese, A. J. Cannistra, R.E. Parks Jr, J. A. Secrist III, A. T. Shortnacy and J. A. Montgomery, *Biochem. Pharmacol.*, 1987, **36**, 1881.

136. J. A. Secrist III, W. B. Parker, P. W. Allen, L. L. Bennett, Jr, W. R. Waud, J. W. Truss, A. T. Fowler, J. A. Montgomery, S. E. Ealick, A. H. Wells, G. Y. Gillespie, V. K. Gadi and E. J. Sorscher, *Nucleosides and Nucleotides*, 1999, **18**, 745.

137. R. T. Borchardt, Y. S. Wu, J. A. Huber and A. F. Wycpalek, *J. Med. Chem.*, 1976, **19**, 1104.

138. C. H. Schein and M. H. M. Noteborn, *Biotechnology (N Y)*, 1988, **6**, 291.

139. A. K. Chopra, A. R. Brasier, M. Des, X. J. Xu and J. W. Peterson, *Gene*, 1994, **144**, 81.

140. G. Georgiou and P. Valax, *Current Opinion Biotechnol.*, 1996, **7**, 190.

141. E. Winograd, M. A. Pulido and M. Wasserman, *Biotechniques*, 1993, **14**, 886.

142. B. Miroux and J. E. Walker, *J. Mol. Biol.*, 1996, **260**, 289.

143. P. C. Trackman and R. H. Abeles, *J. Biol. Chem.*, 1983, **258**, 6717.

144. L. Y. Ghoda, T. M. Savarese, D. L. Dexter, R. E. Parks, Jr., P. C. Trackman and R. Abeles, *J. Biol. Chem.*, 1984, **259**, 6715.

145. J. W. Wray and R. H. Abeles, *J. Biol. Chem.*, 1993, **268**, 21466.

146. R. Meyers, J. W. Wray, S. Fish and R. Abeles, *J. Biol. Chem.*, 1993, **268**, 24785.

147. J. W. Wray and R. H. Abeles, *J. Biol. Chem.*, 1995, **270**, 3147.

148. H. Ashida, Y. Saito, C. Kojima, K. Kobayashi, N. Ogasawara and A. Yokota, *Science*, 2003, **302**, 286.

149. N. T. Price, G. Francia, L. Hall and C. G. Proud, *Biochim. Biophys. Acta*, 1994, **1217**, 207.

150. A. M. Cigan, J. L. Bushman, T. R. Boal and A. G. Hinnebusch, *Proc. Natl. Acad. Sci.* U.S.A., 1993, **90**, 5350.

151. S. R. Kimball, *Int. J. Biochem. Cell Biol.*, 1999, **31**, 25.

152. M. Bumann, S. Djafarzadeh, A. E. Oberholzer, P. Bigler, M. Altmann, H. Trachsel and U. Baumann, *J. Biol. Chem.*, 2004, **279**, 37087.

153. H. Tamura, H. Matsumura, T. Inoue, H. Ashida, Y. Saito, A. Yokota and Y. Kai, *Acta Cryst.*, 2005, F**61**, 595.

154. P. Hadwiger, P. Mayr, B. Nidetzky, A. E. Stutz and A. Tauss, *Tetrahedron Asymm.*, 2000, **11**, 607.

155. K. Bock, M. Mendal, B. Meyer and L. Weibe, *Acta. Chim. Scand.*, 1983, **B 37**, 101.

156. A. de Raadt, C. W. Ekhart and A. E. Stutz, *Adv. Detailed React. Mechan.*, 1995, **4**, 175.

157. A. Berger, A. de Raadt, G. Gradnig, M. Grasser, H. Low and A.E. Stutz, *Tetrahedron Lett.*, 1992, **33**, 7125.

158. M. H. Fechter, A. E. Stutz and A. Tauss, *Curr. Org. Chem.*, 1999, **3**, 269.

159. M. H. Fechter and A. E. Stutz, *Carb. Research.*, 1999, **319**, 55.

160. M. Ebner and A. E. Stutz, *Carb. Research*, 1998, **305**, 331.

161. M. Onega, Ph.D Ist year report, '*Exploring the isomerase and aldolase activity in Streptomyces cattleya* University of St Andrews, 2005.

162. G. M. Whitesides and C. –H. Wong, *Angew. Chem. Int. Ed*, 1985, **25**, 617.

163. E. J. Toone, E. S. Simon, M. D. Bednarski and G. M. Whitesides, *Tetrahedron*, 1989, **45,** 5365.

164. P. G. Wang, W. Fitz and C. –H. Wong, *CHEMTECH*, 1995, 22.

165. H. J. M. Gijsen, L. Qiao, W. Fitz and C. –H. Wong, *Chem. Rev.*, 1996, **91**, 443.

166. W. –D. Fessner and C. Walter, *Angew. Chem. Int. Ed.*, 1992, **31**, 614.

167. R. Schoevaart, PhD thesis, "Applications of aldolases in organic synthesis," 2000, Delft University of Technology.

168. R. Schoevaart, F. van Rantwijk and R. Sheldon, *J. Org. Chem*, 2000, **65**, 6940.

169. W. J. Rutter, *Fed Proc*, 1964, **23**, 1248.

170. T. Gefflaut, C. Blonski, J. Perie and M. Willson, *Prog. Biophys. Molec. Biol.*, 1995, **63**, 301.

171. G. J. Thomson, G. J. Howlett, A. E. Ashcroft and A. Berry, *Biochem. J.*,1998, **331**, 437.

172. E. Lorentzen, B. Siebers, R. Hensel and E. Pohl, *Biochemistry*, 2005, **44**, 4222.

173. A. R. Platter, S. M. Zgiby, G. L. Thomson, S. Qamar, C. W. Wharton and A. Berry, *J. Mol. Biol.*, 1999, **285**, 843.

174. C. H. von der Osten, C. F. D. Barbas, C. H. Wong and A. J. Sinskey, *Mol. Microbiol.,* 1989, **3**, 1625.

175. A. C. Joerger, C. Gosse, W. D. Fessner and G. E. Schulz, *Biochemistry*, 2000, **39**, 6033.

176. W.D. Fessner, A. Schneider, H. Held, G. Sinerius, C. Walter, M. Hixon and J. V. Schloss, *Angew. Chem. Int. Ed.*, 1996, **35**, 2219.

177. W. D Fessner, G. Sinerius, A. Schneider, M. Dreyer, G. E. Schulz, J. Badia and J. Aguilar, *Angew. Chem. Int. Ed*, 1991, **30**, 555.

178. A. Ozaki, E. J. Toone, C. H. von der Osten, A. J. Sinskey and G. M. Whitesides, *J. Am. Chem. Soc.*, 1990, **112**, 4970.

179. M. D. Bednarski, E. S. Simon, N. Bischofberger, W-D. Fessner, M. J. Kim, W. Lees, T. Saito, H. Waldmann and G. M. Whitesides, *J. Am. Chem. Soc.*, 1989, **111**, 627.

180. U. D. Wehmeier, *FEMS Microbiol. Letters*, 2001, **197**, 53.

181. B. L. Horecker, O. Tsolas and C. Y. Lai, "The Enzymes," 3rd Ed, Vol 7, pp 213. Academic Press, New York.

182. M. A. Ghalambor and E. C. Heath, *J. Biol. Chem.*, 1962, **237**, 2427.

183. E. A. Elsinghorst and R. P. Mortlock, *J. Bacteriol.*, 1994, **176**, 7223.

184. R. K. Scopes, 'Protein Purification, Principles and Practice,' 3rd Ed., Springer, New York, 1994, p. 346.

Appendix

Publications

1. S. L. Cobb, H. Deng, J. T. G. Hamilton, R. P. McGlinchey and D. O'Hagan, *Chem. Commun.*, 2004, 592.

2. S. L Cobb, H. Deng, J. T. G. Hamilton, R. P. McGlinchey, D. O'Hagan and C. Schaffrath, *BioOrg. Chem,* 2005, **33,** 393.

3. H. Deng, S. L. Cobb, R. P. McGlinchey, A. R. McEwan, D. O'Hagan, J. Naismith, D. Robinson and J. Spencer, *Angew. Chem. Int. Ed.*, 2006, 45, 759.

4. H. Deng, S. L. Cobb, A. Gee, A. Lockhart, L. Martarello, R. P. McGlinchey, D. O'Hagan and M. Onega, *Chem. Commun.*, 2006, 652.

Awards and prizes

Oral presentation (1st prize), 2nd Organic Chemistry PhD symposium, 2nd June 2005
University of St Andrews.

Poster presentation (1st prize),Annual RSC Fluorine Subject, 1st-2nd September 2005
Group Postgraduate Meeting, University of Oxford.

Presentations

Poster presentation, Pro Bio Faraday, Biocatalysis for manufacture, Current Practice and Future Opportunities, University of Heriot-Watt. 5th-6th November 2003

Oral presentation, 4th RSC Fluorine Subject Group Postgraduate Meeting, University of Durham. 2nd-3rd September 2004

Poster presentation, Pro-Bio Faraday partnership, University of Warwick. 8th-9th November 2004

Poster presentation, 33rd RSC Scottish Organic Division Meeting, University of St Andrews. 20th December 2004

Oral presentation, Pro Bio Faraday biocatalysis research projects, Bradford. 21st-22nd July 2005

Oral presentation, ProBio Faraday Partnership Research Review Meeting, Bradford. 8th-9th June 2004

Oral presentation, 2nd Organic Chemistry PhD symposium, St Andrews University. 2nd June 2005

Poster presentation, RSC and BBSRC symposium on 'The Chemistry and Biology of Natural Product Biosynthesis II', University of Bristol. 15th July 2005

Poster presentation BIOTRANS 2005 –Delft, Netherlands 7th International Symposium on Biocatalysis and Biotransformations. 3-8th July 2005

Poster presentation, 5th Annual RSC Fluorine Subject Group Postgraduate Meeting, University of Oxford. 1-2nd September 2005

Conferences attended

RSC Bio-organic postgraduate symposium, St John's College,
University of Cambridge. 27th Nov 2002

31st Scottish Regional Perkin Division Meeting, Dundee University. 18th Dec 2002

Enzyme mechanism. A structural perspective, University of St Andrews. 12th-14th Jan 2003

14th Scottish Graduate Symposium on novel organic chemistry,
University of Aberdeen. 9th April 2003

3rd RSC Fluorine Subject Group Postgraduate Meeting,
University of St Andrews. 4th-5th Sept 2003

1st University of Glasgow/Organon Symposium on synthetic chemistry. 22nd Sept 2003

RSC Organic Division and Chemical Biology Forum,
University of Edinburgh. 31st October 2003

Pro Bio Faraday, Biocatalysis for manufacture, Current Practice and
Future Opportunities, University of Heriot-Watt. 5th-6th November 2003

32 rd Scottish Regional Perkin Meeting, University of Edinburgh 17th December 2003

Pro Bio Faraday biocatalysis research projects, Bradford. 8th-9th June 2004

4th RSC Fluorine Subject Group Postgraduate Meeting,
University of Durham. 2nd-3rd September 2004

14th International Isotope Society (UK group) symposium
Wellcome Genome Campus, Hinxton. 4th November 2004

Pro Bio Faraday Biocatalysis, University of Warwick. 8th-9th November 2004

33 rd Scottish Organic Division Meeting, University of St Andrews. 20th December 2004

Pro Bio Faraday biocatalysis research projects, Bradford. 21st-22nd July 2005

2nd Organic Chemistry PhD symposium, University of St Andrews. 2nd June 2005

RSC and BBSRC symposium,'The Chemistry and Biology of Natural Product

Biosynthesis II', Bristol. 15th July 2005

BIOTRANS 2005 –Delft, Netherlands, 7th International Symposium on Biocatalysis and Biotransformations. 3-8th July 2005

5th Annual RSC Fluorine Subject Group Postgraduate Meeting, University of Oxford. 1-2nd September 2005